Application of "annual" moraines to assess recent patterns and rates of ice-marginal retreat at Skálafellsjökull, SE Iceland

CHANDLER, BENJAMIN,MARC,PETER

How to cite:

CHANDLER, BENJAMIN,MARC,PETER (2015) *Application of "annual" moraines to assess recent patterns and rates of ice-marginal retreat at Skálafellsjökull, SE Iceland*, Durham theses, Durham University. Available at Durham E-Theses Online: http://etheses.dur.ac.uk/11046/

Application of “annual” moraines to assess recent patterns and rates of ice-marginal retreat at Skálafellsjökull, SE Iceland

Benjamin Marc Peter Chandler

Iceland is situated in a climatically sensitive area close to both atmospheric and oceanic polar fronts, thus representing an important location for understanding North Atlantic climatic change. Icelandic glaciers are particularly sensitive to climatic fluctuations on annual to decadal timescales, and have exhibited accelerating rates of ice-marginal retreat and mass loss during the past decade. Understanding these current rapid glacier fluctuations is crucial to placing current atmospheric warming and associated glacier retreat in a broader context.

This study uses the characteristics of recessional (“annual”) moraines and complementary climate data to examine patterns, rates and drivers of ice-marginal retreat that has occurred at Skálafellsjökull, SE Iceland since the 1930s. High-resolution glacial geomorphological mapping reveals suites of *minor moraines* across the glacier foreland, with the features displaying distinctive *sawtooth* planform geometries. Chronological investigations of the Skálafellsjökull moraines, which integrate remote sensing observations and lichenometry, indicate that minor moraines on the northern and central parts of the glacier foreland formed on an annual basis. Sedimentological investigations reveal that these *annual moraines* form through a range of ice-marginal processes, with push/squeeze mechanisms being dominate. The geomorphological, chronological and sedimentological data therefore indicate these moraines represent successive annual ice-frontal positions. Thus, these annual moraines provide a framework for exploring patterns, rates and drivers of ice-marginal retreat at Skálafellsjökull.

Annual ice-margin retreat rates (IMRRs), equivalent to annual moraine spacing, indicate prominent periods of glacier recession at Skálafellsjökull are coincident with those at other Icelandic outlet glaciers, as well as those identified at Greenlandic outlet glaciers. Analysis of IMRRs and climate data suggests summer air temperature, sea surface temperature and North Atlantic Oscillation have an influence on IMRRs at Skálafellsjökull, with the glacier appearing to be most sensitive to summer air temperature. Based on this analysis, it is hypothesised that sea surface temperature may drive air temperature changes in the North Atlantic region, which in turn forces IMRRs. The increase in SST over recent decades may link to atmospheric-driven variations in North Atlantic subpolar gyre dynamics. Further research on glacier change in the North Atlantic region, and the controls thereon, is nonetheless required to test this hypothesis.

Application of “annual” moraines to assess recent patterns and rates of ice-marginal retreat at Skálafellsjökull, SE Iceland

Benjamin Marc Peter Chandler

A thesis submitted in partial fulfilment of the requirements of the
University of Durham for the degree of Master of Science

Department of Geography
University of Durham

January 2015

CONTENTS

Chapter 1: Scientific rationale, aims and objectives

Chapter 2: Icelandic glacier fluctuations and sediment-landform products

Chapter 3: Location and setting of Skálafellsjökull

Chapter 4: Remote sensing and field-based techniques

Chapter 5: Moraine geomorphology, sedimentology and chronology

Chapter 6: Inter-annual variability in SE Iceland climate

Chapter 7: Significance of annual moraines at Skálafellsjökull

Chapter 8: Conclusions

LIST OF FIGURES

Chapter 1: Scientific rationale, aims and objectives

Chapter 2: Icelandic glacier fluctuations and sediment-landform products

Chapter 3: Location and setting of Skálafellsjökull

Chapter 4: Remote sensing and field-based techniques

Chapter 5: Moraine geomorphology, sedimentology and chronology

Chapter 6: Inter-annual variability in SE Iceland climate

Chapter 7: Significance of annual moraines at Skálafellsjökull

LIST OF TABLES

Chapter 2: Icelandic glacier fluctuations and sediment-landform products

Chapter 4: Remote sensing and field-based techniques

Chapter 5: Moraine geomorphology, sedimentology and chronology

Chapter 7: Significance of annual moraines at Skálafellsjökull

STATEMENT OF COPYRIGHT

I confirm that no part of the material presented in this thesis has previously been submitted by me or any other person for a degree in this or any other university. In all cases, where it is relevant, material from the work of others has been acknowledged.

Benjamin M.P. Chandler

Department of Geography
University of Durham

January 2015

ACKNOWLEDGEMENTS

There are several people whom I wish to acknowledge for their support and advice. Firstly, I would like to thank my supervisors, Dave Evans and Dave Roberts, for their valuable advice and thought-provoking discussions during the course of this research. Additionally, I am grateful for their patience during the writing-up process and constructive comments on earlier drafts of chapters from this thesis. Finally, thanks for the amusing anecdotes from fieldwork in Iceland and elsewhere!

I am particularly indebted to Marek Ewertowski, whose expertise in GIS and Remote Sensing were invaluable during this project. Marek introduced me to *Agisoft PhotoScan*, and kindly provided assistance during the processing of aerial photographs and GPS data. Additionally, Marek provided some helpful tips for the dGPS surveying. Sven Lukas (Queen Mary University of London) also provided valuable discussion on annual moraines and advice on sampling strategies.

Thanks must go to a number of people and organisations who kindly provided data utilised in this research. Oddur Sigurðsson (Icelandic Meteorological Office) kindly provided access to ice-front measurements, whilst Trausti Jónsson (also Icelandic Meteorological Office) assisted in the compilation of meteorological data. A high-resolution DEM of the Skálafellsjökull foreland and associated UAV imagery was kindly provided by Alex Clayton (University of Southampton), for which I am particularly grateful. Thanks are also due to the UK Meteorological Office and British Atmospheric Data Centre for granting access to the HadSST2 dataset.

The laboratory, technical, administrative and IT staff in the Department of Geography helped to make this project run as smoothly as possible. Chris Longley provided training in the utilisation of the dGPS, whilst Mervyn Brown and Frank Davies provided field equipment.

Fieldwork was an integral component of this research and would not have been possible without the assistance of a number of people. I am very grateful to Jonathan Chandler, Bertie Miles and Hannah Bickerdike for their assistance and companionship during fieldwork in Iceland. Regína Hreinsdóttir (National Park Warden, South Territory) granted permission to undertake fieldwork within the Vatnajökull National Park. Thanks are also due to Svandís Sigvaldadóttir for issuing a RANNÍS Research Declaration (Agreement 4/2014).

Fieldwork was supported by a Quaternary Research Association (QRA) New Research Workers' Award and Van Mildert College Principal's Award. Additionally, financial support for my studies was provided by a Van Mildert College Postgraduate Award, which is gratefully acknowledged. I am thankful to the generosity of Van Mildert Association members and friends of Van Mildert College, without which this funding would not be available.

To my colleagues in the Department, particularly my fellow inhabitants of "the dungeon" (the GIS lab), thanks for our coffee breaks, chats, discussions and rants throughout the year. Thanks also to the postgraduate community at Van Mildert College who made my year in Durham an enjoyable experience.

Finally, I would like to thank my family for all their support, encouragement and forbearance throughout this MSc research. I am particularly grateful to my father, Jonathan, who has been my trusted field assistant and proof-reader over a number of years. Thanks also for putting up with my glacial musings! To my Mum, Deborah, for her fortitude and those much needed boxes of flapjack. The intervention of my sister, Abigail, made this all possible and I am eternally grateful. Thank you to my brother, Samuel, for sharing my passion for Geography and maps. Last, but not least, thank you to my pets, Bobby, Bella, Bertie, Berry and George, for all the fun and games during my visits back home to Norfolk.

“It is man’s nature to wish to see and experience the things
that he has heard about and thus to learn whether the facts are as told or not”

– Konungs skuggsjá (King’s Mirror), 13th Century Norwegian text

CHAPTER 1

Scientific rationale, aims and objectives

1.1 Scientific rationale

The world's glaciers are now considered to be unequivocally losing mass in response to both atmospheric and oceanic warming by the Intergovernmental Panel on Climate Change (IPCC, 2007, 2013). This mass loss has contributed to global mean sea-level rise, with the majority of the recent cryospheric contribution accounted for by mass loss from glaciers and ice caps (~56% between 1993 and 2010: IPCC, 2013), rather than the large ice sheets in Greenland and Antarctica (Meier *et al*., 2007; Church *et al*., 2011; but see Rignot *et al*., 2011). Recent studies of glacier mass balance and ice-frontal positions of glaciers outside of Greenland and Antarctica have demonstrated accelerating rates of mass loss and ice-marginal retreat since the 1970s (Figure 1.1; Kaser *et al*., 2006; Cogley, 2009; Zemp *et al*., 2009; Jacob *et al*., 2012; Marzeion *et al*., 2012; Gardner *et al*., 2013; Stokes *et al*., 2013a; Carr *et al*., 2014). Moreover, their contribution to sea-level rise is likely to continue to increase in the 21st Century (Meier *et al*., 2007; Pfeffer *et al*., 2008; Bahr *et al*., 2009; Radić and Hock, 2011).

The response of glaciers to climate perturbations is complex, but it has been shown that temperate glaciers and small ice-caps are particularly sensitive indicators of climatic fluctuations (e.g. Nye, 1965; Rosqvist and Østrem, 1989; Oerlemans *et al*., 1998; Klok and Oerlemans, 2003). Previous studies have highlighted the importance of air temperature and precipitation in determining glacier fluctuations, particularly on decadal to centennial timescales (e.g. Oerlemans, 1989; Jóhannesson and Sigurðsson, 1998; Sigurðsson *et al*., 2007). Furthermore, studies of small-scale, annual ice-front fluctuations have demonstrated a temporal link between annual ice-margin retreat rates and climate variations (e.g. Bradwell, 2004a; Beedle *et al*., 2009; Lukas, 2012).

Iceland lies in a climatically important location in the North Atlantic, situated at the boundary between polar and mid-latitude atmospheric circulation cells and oceanic currents (Guðmundsson, 1997; Flowers *et al*., 2005; Bradwell *et al*., 2006; Geirsdóttir *et al*., 2009). As a consequence of Iceland's position between the warm Irminger and cold East Greenland and East Iceland ocean currents, Icelandic glaciers are highly sensitive climate indicators (Flowers *et al*., 2005; Sigurðsson *et al*., 2007). The temperate glaciers of Iceland are particularly sensitive to climatic fluctuations on an annual to decadal scale, and have exhibited rapid rates of ice-marginal retreat and mass loss during the past decade (e.g. Jóhannesson, 1986; Sigurðsson and Jónsson, 1995; Aðalgeirsdóttir *et al*., 2006; Sigurðsson *et al*., 2007; Björnsson and Pálsson, 2008; Björnsson *et al*., 2013; Bradwell *et al*., 2013; Mernild *et al*., 2014). An understanding of the rapid glacier fluctuations currently evident in Iceland is important to place the current period of atmospheric warming and associated glacier retreat in a broader context (Bradwell *et al*., 2013).

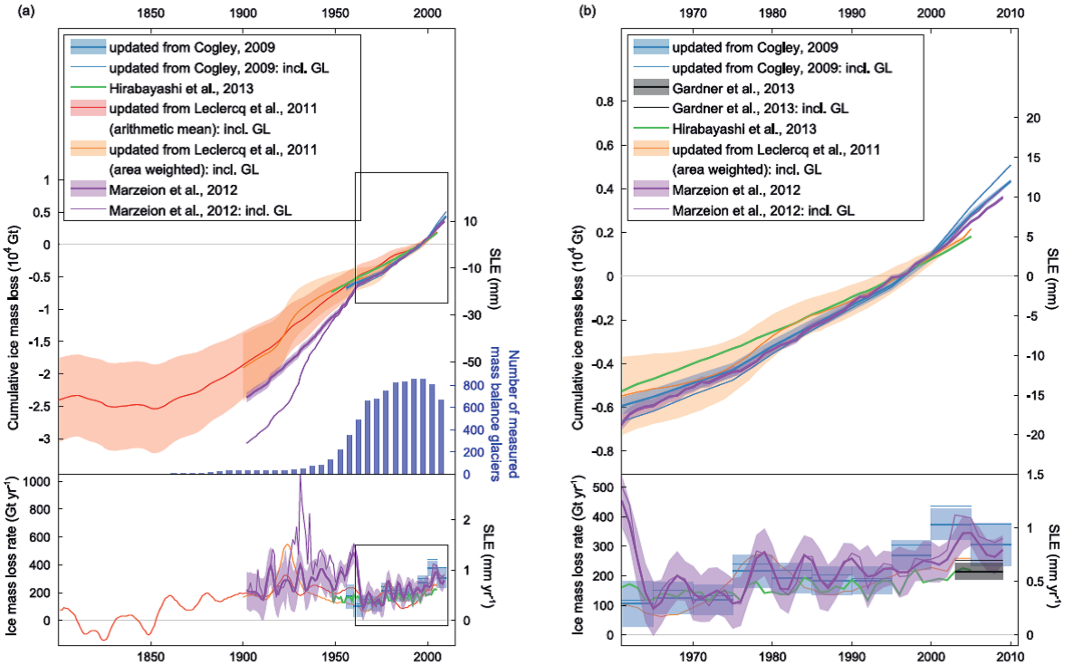

Figure 1.1: Global cumulative (top graphs) and annual (lower graphs) glacier mass change for (a) 1801–2010 and (b) 1961–2010. The cumulative estimates are all set to zero mean over 1986–2005. Estimates are based on glacier length variations (updated from Leclercq *et al*., 2011), from area-weighted extrapolations of individual directly and geodetically measured glacier mass budgets (updated from Cogley, 2009), and from modelling with atmospheric variables as input (Marzeion *et al*., 2012; Hirabayashi *et al*., 2013). Uncertainties are based on comprehensive error analyses in Cogley (2009) and Marzeion *et al*. (2012) and on assumptions about the representativeness of the sampled glaciers in Leclercq *et al*. (2011). Hirabayashi *et al*. (2013) give a bulk error estimate only. For clarity in the bottom panels, uncertainties are shown only for the Cogley and Marzeion curves excluding Greenland (GL). The blue bars (a, top) show the number of measured single-glacier mass balances per pentad in the updated Cogley (2009) time series. The mean 2003–2009 estimate of Gardner *et al*. (2013) is added to b, bottom. *Source:* IPCC (2013).

Monitoring of Icelandic glacier termini has been undertaken since the 1930s through a programme of regular ice-front measurements (Eyþórsson, 1931; Sigurðsson, 1998). Several studies have attempted to correlate glacier fluctuations that have occurred during this observational period with climate variations. Sigurðsson *et al*. (2007) demonstrated that observed ice-front variations of non-surge-type glaciers were in sympathy with major air temperature trends during the 20th Century. Jóhannesson and Sigurðsson (1998) and

Sigurðsson *et al*. (2007) inferred that the primary control on Icelandic glacier behaviour during the 20th Century was fluctuations in summer temperature. According to their analysis of mass-balance measurements, summer balance exhibited greater variations than the winter balance, indicating the importance of summer temperature in the annual mass-balance (Sigurðsson *et al*., 2007). Both Jóhannesson and Sigurðsson (1998) and Sigurðsson *et al.* (2007) attributed the rapid retreat of Icelandic glaciers during the period 1931 – 1960 to high summer temperatures, whilst the reversal of this retreat trend to glacier advance between 1965 and 1970 was attributed to climate cooling.

Recently, multidisciplinary investigations at Virkisjökull-Falljökull, a twin-lobed outlet glacier of Öræfajökull, SE Iceland, have shown increasing rates of glacier retreat, with the glacier undergoing a major change in glacier behaviour, switching from active retreat to passive downwasting and fault controlled ice-marginal collapse (Bradwell *et al*., 2013; Phillips *et al*., 2013, 2014). Using annual moraine spacing as a proxy for ice-margin retreat rate, Bradwell *et al*. (2013) showed that average ice-margin retreat rates during the 1930s and 1940s (28 m a^{-1}) were twice as high as during the period from 1990 to 2004 (14 m a^{-1}). Since 2005, however, ice-front measurements demonstrate that retreat rates have increased considerably (average: 35 m a^{-1}), with the last 5 years representing the greatest amount of ice-front retreat in any 5-year period since measurements began. Bradwell *et al*. (2013) proposed that this recent, rapid, ice-margin retreat and thinning in a decade of unusually warm summers has resulted in a glaciological threshold being breached, with subsequent large-scale stagnation of the glacier terminus (i.e. no forward movement). It is suggested that breaching this threshold has caused rapid non-uniform retreat and downwasting since 2005 through a system feedback between surface melting, glacier thinning, decreased driving stress and decreased forward motion.

Further structural glaciology investigations and continuous monitoring at Falljökull by Phillips *et al*. (2014) have established that, following breach of the dynamic threshold in 2004 – 2006, the icefall of Falljökull remained active: the lower reaches of the glacier were abandoned to stagnation and passive retreat processes whilst the upper part of the glacier continues to undergo forward motion. To accommodate this continued forward motion, the active glacier “margin” is undergoing intense deformation (folding and thrusting) and is consequently being thrust over the lower, immobile section of Falljökull which has become dynamically detached (Figure 1.2; Phillips *et al*., 2014). This structural response has allowed the glacier to rapidly re-equilibrate to changes in mass balance resulting from warmer summers in SE Iceland (*cf*. Guðmundsson, 2000; Jóhannesson *et al*., 2013). Further research is, however, required to attain greater understanding of contemporary Icelandic glacier change and the controls thereon. Such understanding will provide insights into the potential future response of Icelandic glaciers to climatic perturbations.

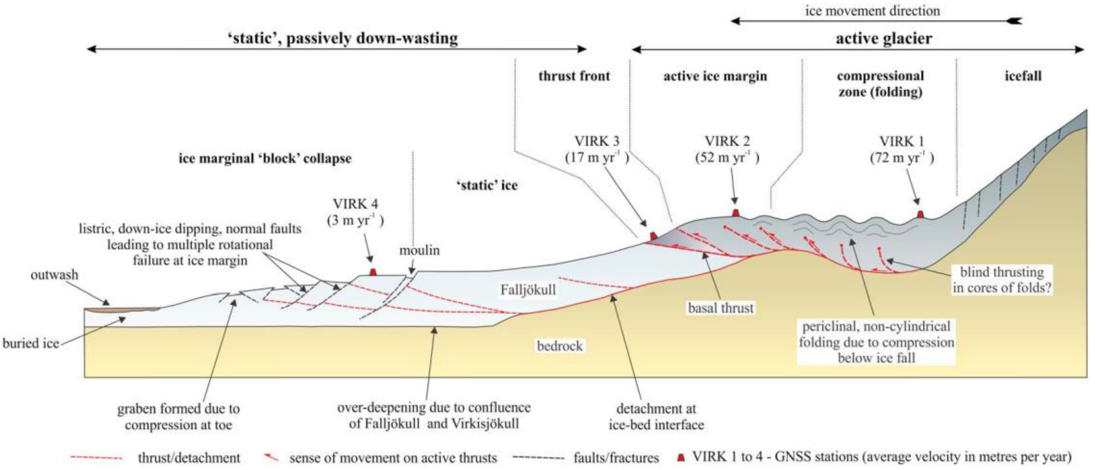

Figure 1.2: Schematic structural cross-section through Falljökull (not to scale) showing the main deformation structures controlling: (1) ice-marginal collapse; and (2) thrusting and folding of the active glacier "margin", which is accommodating continued forward motion of the upper, active part of the glacier as it overrides the stagnating lower reaches. The positions of GNSS stations are also shown, with average ice velocity calculated at these locations. Reproduced from Phillips *et al*. (2014).

Annual ice-marginal fluctuations at many Icelandic glaciers manifest in the form of "annual" moraines (e.g. Price, 1970; Sharp, 1984; Krüger, 1995; Evans and Twigg, 2002), a characteristic signature of the active temperate glacial landsystem (Evans, 2003a, 2005; Evans and Orton, 2014). Consequently, annual moraines afford the opportunity to link ice-marginal moraines to specific glaciological and climatic conditions (e.g. Lukas, 2012; Reinardy *et al*., 2013). Annual moraine formation occurs at the ice-margin during a period when forward ice-front movement exceeds the negligible ablation during the winter (Lukas, 2012; Bradwell *et al*., 2013). Long sequences of annual moraines form when ice-front recession during the summer (ablation season) outstrips advance during the winter (accumulation season) over the course of a number of years (Boulton 1986; Bennett 2001). Such long sequences potentially contain a seasonal signature of glacier response to climatic fluctuations, and have been associated with periods of elevated ablation-season temperature (Sharp, 1984; Krüger, 1995; Bradwell, 2004a; Beedle *et al*., 2009; Bradwell *et al*., 2013).

Given the potential of annual moraines as a terrestrial climate archive, detailed examination of the distribution, geomorphology and formation of annual moraines on the forelands of Icelandic glaciers could yield valuable insights into the nature of, and controls on, recent ice-marginal retreat. This study applies "annual" moraines on the foreland of Skálafellsjökull, SE Iceland as a geomorphological proxy to examine ice-marginal fluctuations of Skálafellsjökull that have occurred since the 1930s. Skálafellsjökull has been identified as a key study site owing to the availability of a long-archive of imagery, spanning the period 1945 to 2012, and the unusually-long sequence of recessional (“annual”) moraines on the glacier foreland. Remote sensing, geomorphological and sedimentological investigations of these “annual” moraines, combined with lichenometry surveys and interrogation of instrumental data, allow the significance of patterns and rates of recent ice-marginal retreat of Skálafellsjökull to be assessed.

1.2 Aims and objectives

The overarching aim of this research is to utilise the characteristics of recessional (“annual”) moraines and apply multiple methods to arrive at a holistic understanding of recent patterns and rates of ice-marginal retreat of Skálafellsjökull, wherein the potential factors controlling these ice-marginal fluctuations are assessed. Implicit within the research is a consideration of the concept of “annual” moraines and their applicability as climatic indicators. The following specific objectives are defined:

(1) to examine variations in the distribution and geomorphology of recessional moraines on the Skálafellsjökull foreland;
(2) to establish a chronological framework for the recessional moraines at Skálafellsjökull;
(3) to determine processes of moraine formation at the ice-margin and develop a conceptual model thereof;
(4) to assess patterns, rates and drivers of recent ice-marginal retreat at Skálafellsjökull; and
(5) to place the findings from Skálafellsjökull in the context of previous observations from Iceland and elsewhere.

1.3 Thesis structure

This thesis is divided into eight distinct chapters, each with their own specific purpose. In this chapter the rationale for undertaking this research has been outlined, and the overarching aim and specific objectives of this research have been defined. Chapter 2 provides a broader context for this study through a review of key literature, and explores four key areas: (1) the Little Ice Age and Little Ice Age Type Events (§2.1); (2) glacier fluctuations during the “observational” period (§2.2); (3) the active temperate glacial landsystem (§2.3); and (4) annual moraines as important sediment-landform archives (§2.4). The review of previous decadal- and annual-scale glacier fluctuations (§2.1 and §2.2) provides context for the moraine record and ice-marginal fluctuations explored in this study, whilst the discussion of the active temperate glacial landsystem demonstrates how annual moraines fit within the overall glacial landsystem. Annual moraines are reviewed in §2.4, with particular focus on their application as climatic indicators. The geographic, climatic and glaciological setting of Skálafellsjökull is then discussed in Chapter 3. Subsequently, Chapter 4 outlines the key remote sensing and field techniques applied in this research. In Chapter 5 the results of the geomorphological, sedimentological and chronological investigations are presented, providing a framework to explore patterns and rates of recent ice-marginal retreat at Skálafellsjökull, and the controls thereon. Inter-annual variability in SE Iceland climate is examined in Chapter 6, allowing the key potential drivers of ice-marginal retreat to be introduced. Chapter 7 synthesises the results presented in the previous chapter and explores four key themes: (1) annual moraine genetic processes; (2) influences on annual moraine geomorphology, wherein the interplay of topographic and glaciological factors is explored; (3) recent ice-marginal fluctuations and their climatic significance; and (4) the applicability of annual moraines in extracting climate signals. The final chapter (Chapter 8) then draws a series of conclusions based upon the results and analyses presented and discussed in this thesis.

CHAPTER 2

Icelandic glacier fluctuations and sediment-landform products

---

The aim of this chapter is to outline the conceptual framework for the research in this thesis, elaborating on and exemplifying key concepts introduced in Chapter 1. The first two sections of this chapter (Sections 2.1 and 2.2) consider the current state of our understanding of Icelandic glacier fluctuations at decadal and annual timescales. The review of decadal- and annual-scale Icelandic glacier fluctuations provides context for the Skálafellsjökull moraine record. Subsequently, the active temperate glacial landsystem is discussed in Section 2.3, with key constituent sediment-landform assemblages identified, thereby demonstrating the setting of "annual" moraines in the overall glacial landsystem. Section 2.4 examines the geomorphological and sedimentological characteristics of "annual" moraines and considers the applicability of this sediment-landform assemblage as a climate proxy. Highlighted within Section 2.4 is the importance of recognising and accounting for non-climatic factors that may influence "annual" moraine sequences.

2.1 The Little Ice Age and Little Ice Age Type Events

2.1.1 The Little Ice Age

The term *Little Ice Age* (LIA) is widely used to describe the cold period that followed the *Medieval Warm Period* (MWP), beginning in the late sixteenth century AD and lasting until *c*. 1900 AD (Guðmundsson, 1997; Grove, 2004; Ingólfsson *et al*., 2010). This period is recorded in historical records as a period of unusually high-variability, characterised by decadal-scale climate and mass balance fluctuations (Thórarinsson, 1943; Ogilvie, 1984, 1992; Ogilvie and Jónsson, 2001; Grove, 2004; Geirsdóttir *et al*., 2009). Despite this cooling period being variable and punctuated by mild intervals, warm conditions did not return to Iceland before the end of the 19th Century (Geirsdóttir *et al*., 2009). During the LIA, the most extensive and widespread Holocene glacier advances are believed to have occurred, with many of Iceland's glaciers reaching their Holocene maximum (e.g. Björnsson, 1979; Guðmundsson, 1997; Bradwell, 2001a, b; Bradwell, 2004b; Grove, 2004; Sigurðsson, 2005a; Björnsson and Pálsson, 2008; Ingólfsson *et al*., 2010; Larsen *et al*., 2011; Hannesdóttir *et al*., 2014). This is concordant with sea surface temperature reconstructions off North Iceland which demonstrate that the LIA is the coldest period since the Holocene Thermal Maximum (HTM; Sicre *et al*., 2008), which ended 5.0 cal ka BP (Guðmundsson, 1997; NGRIP members, 2004; Flowers *et al*., 2008; Ran *et al*., 2008).

The earliest scientific investigation of LIA glacier maxima was conducted by Thórarinsson (1936), who argued that the outermost moraines on the forelands of the Vatnajökull outlet glaciers were related to glaciation during historical time, and represented their maximum postglacial extent. Subsequent studies by Thórarinsson (1939, 1943, 1956, 1958, 1964, 1966), based on the integration of archival data, maps, contemporary accounts, field investigations and tephrochronology, suggested that Icelandic glaciers reached their maximum Holocene glacier extent in the second half of the 19th Century. Chronological techniques were expanded following the introduction of lichenometry as a relative dating method of moraines in Iceland (Jaksch, 1970, 1975). Lichenometric investigations, in some cases integrated with tephrochronology, suggest the large lobate outlet glaciers from the ice-caps in southern Iceland reached their maximum around AD 1890 (Gordon and Sharp, 1983; Snorrason, 1984, Maizels and Dugmore, 1985; Thompson and Jones, 1986; Thompson, 1988; Evans *et al*., 1999a). Although, the application of a size-frequency approach (*cf*. Caseldine, 1991; Bradwell, 2001a, b, 2004b, for further details) combined with tephrochronology, has prompted the proposition of a revised chronology for outlet glaciers of the Eyjafjallajökull, Mýrdalsjökull, Öræfajökull and Vatnajökull ice-caps, implying an earlier LIA maximum in the late 18th Century or early 19th Century (Kirkbride and Dugmore, 2001a, b; Bradwell, 2004b, Casely and Dugmore, 2004; McKinzey *et al*., 2004, 2005). In the northern and western parts of Iceland, glaciers advanced to their LIA maximum between *c*. AD 1750 and *c*. AD 1850 (e.g. Caseldine, 1983, 1985, 1987, 1990; Hjört *et al*., 1985; Häberle, 1991; Kugelman, 1990, 1991; Guðmundsson, 1997, 1998a; Stötter *et al*., 1999).

Aside from the terrestrial glacial geological record, contemporary accounts provide valuable information on the timing and magnitude of glacial fluctuations during the LIA (Table 2.1) because, in many cases, farmland or farms were overridden by ice masses or had to be abandoned due to the climate deterioration (e.g.; Henderson, 1819; Helland, 1882;; Thoroddsen, 1911, 1931 – 1935, 1958; Bárdarson, 1934; Thórarinsson, 1943; Pálsson, 1945, 2004; Magnússon, 1953; Ólafsson and Pálsson, 1975; Magnússon and Vídalín, 1980; Grove, 2004; Hannesdóttir *et al*., 2014). For instance, according to evidence given before the Þing on 1st June, 1702, Breiðármörk farm "has been quite deserted for the last 4 years and, like several other farms, it is still ravaged by water, gravel, and the passage of glaciers every year, until hardly any useful patch of grass is left except a small islet on which the houses were situated" (quoted Thórarinsson, 1943: 23). Similarly, according to Magnússon's *Chorographica Islandica* (1953, written 1702 – 1714) a grassy area of Hafrafell, situated between

Skaftafellsjökull and Svínafellsjökull, is described as “formerly accessible by paths, and with grazing for sheep in summertime; now this hill is so surrounded by glacier tongues that it can only be reached on foot and with great difficulty” (quoted Thórarinsson, 1943: 32).

Table 2.1: Summary of documented glacier advances and retreats in the 18th and 19th centuries. *Source:* After Grove (2004: 47).

Date	Source	Glacier	Observation
1704 – 5	Árni Magnússon	Sólheimajökull	Already blocked Jökulsá canyon
1772	Pálsson	Sólheimajökull	Advancing
1783	Thoroddsen	Sólheimajökull	Smaller than in 1705
1794	Pálsson	Sólheimajökull	Advance had blocked Jökulsá again
1820	Eyþórsson	Sólheimajökull	Jökulhöfud covered by ice
1883	Keilhack	Sólheimajökull	Jökulhöfud free of ice
1905	Thórarinsson	Sólheimajökull	Had retreated to its 1705 position
1201	Sveinn Pálsson	Skeiðarárjökull	Jökulhlaup from Núpslón
900 – 1400	Landnámebók, Diplomatarium Islandicum	Breiðamerkurjökull	Fjall and Breiðá farms still cultivated
1695	Land Register	Breiðamerkurjökull	Fjall farm abandoned by this date
1697	Land Register	Breiðamerkurjökull	Breiðá last cultivated
1712	Land Register	Breiðamerkurjökull	Fjall farm buildings covered by ice
1708 – 9	Land Register	Hafrafell	Surrounded by Skaftafellsjökull and Svínafellsjökull
1746	Sigurdur Stefánsson	Heinabergsjökull	Had dammed back Dalvatn lake
1756	Ólafsson	Heinabergsjökull	Reached the far Heinaberg
1756	Ólafsson and Pálsson	Breiðamerkurjökull	Still advancing
1756	Ólafsson and Pálsson	Stígárjökull	Had been advancing in recent decades
1756	Pálsson	Skeiðarárjökull	Was damming back Núpslón
1780s	Pálsson	Svínafellsjökull	Still enlarging
1782	Pálsson	Skeiðarárjökull	Bulging markedly
1784	Pálsson	Skeiðarárjökull	Last jökulhlaup from Núpslón
1787	Henderson	Skeiðarárjökull	Glacier advanced sharply
1794	Pálsson	Skeiðarárjökull	Retreating – Núpslón disappears
1794	Pálsson	Breiðamerkurjökull	Reached a maximum then retreated
1812 – 15	Henderson	Skeiðarárjökull	Recession interrupted by a stationary period
1820	Thienemann	Breiðamerkurjökull	Advance of *c*. 1000 m, still 2 km from sea
1830	P.M. Thorarensen	Breiðamerkurjökull	Advancing again
1836	Gaimard	Breiðamerkurjökull	Only 400 m from the sea
1836	Gaimard	Skaftafellsjökull	Close to Heinabergsjökull (and for *c*. 50 years)
1839	Gunnlaugsson	Breiðamerkurjökull	2200 m from the sea at Jökulsá
1869	Paijkull	Breiðamerkurjökull	Reached down to beach
1857 – 81	Helland	Breiðamerkurjökull	Retreat of about 600 m
1880	Thórarinsson	Heinabergsjökull	Advanced until recession began in 1887
1892	Thoroddsen	Breiðamerkurjökull	*c*. 250 – 1000 m from sea

2.1.2 Little Ice Age Type Events

Whilst most studies of Icelandic glacier fluctuations during the mid- to late Holocene have concentrated on the detail of the LIA period (e.g. Grove, 1988, 2001, 2004; Ogilvie and Jónsson, 2001), earlier glacier fluctuations have been subject to limited scientific attention, perhaps due to the paucity of evidence from earlier periods in the terrestrial glacial geological record (Kirkbride and Dugmore, 2006; Geirsdóttir *et al*., 2009). Based on inferences drawn primarily from moraine remnants, it has been suggested that the LIA represents the most recent in a series of *Neoglacial* cool periods (*cf*. Guðmundsson, 1997; Stötter *et al*., 1999; Kirkbride and Dugmore, 2006). Moraines on the forelands of small local glaciers in North, Central and South Iceland are ostensibly indicative of pre-LIA glacier fluctuations during the Holocene (Caseldine, 1987; Caseldine and Stötter, 1993; Stötter *et al*., 1999; Kirkbride and Dugmore, 2001, 2006, 2008; Schomacker *et al*., 2003; Principato, 2008). Glacial chronologies are, however, partial representations of a complex climate signal and the actual number of glacial advances is likely to be underestimated due to a loss of evidence with time, principally due to overriding of older moraine deposits or intense glaciofluvial erosion (Gibbons *et al*., 1984; Rose *et al*., 1997; Kirkbride and Brazier, 1998; Schomacker *et al*., 2003; Casely and Dugmore, 2004; Kirkbride and Dugmore, 2006; Kirkbride and Winkler, 2012; Barr and Lovell, 2014).

The earliest suggestions of pre-LIA glacier advances were put forward by Eyþórsson (1935) founded on investigations of Drangajökull, NW Iceland, together with observations of other Icelandic glaciers and their moraine systems. Subsequently, Thórarinsson (1949) argued that terminal moraines existed on the forelands of Vatnajökull outlets which were indicative of glacier advance during the *Subatlantic* period. Further scientific investigations by Thórarinsson (1955, 1958), which incorporated the use of tephrochronology, concluded that formation of the Stóralda moraine and Kvíámyrar-Kambsmyrarkambur moraine complex in the Öræfajökull region preceded the Öræfajökull eruption of 1362, assigning a Subatlantic age to these glacial advances on the basis of the prevailing model of glacial events at that time (*cf*. Einarsson, 1963). Later studies of Sólheimajökull (Dugmore, 1987, 1989; Dugmore and Sugden, 1991), Vatnajökull outlet glaciers (Sharp and Dugmore, 1985; Thompson, 1988; Black 1990) and corrie glaciers on the Tröllaskagi peninsula (Stötter, 1990, 1991, 1994; Häberle, 1991, 1994) provided further purported evidence for pre-LIA glacial advances during the Holocene. This emerging evidence was synthesised by Guðmundsson (1997) into the classic *Neoglacial* model of glaciation (Table 2.2).

Table 2.2: Tentative correlation of Holocene glacier advances in Iceland, as proposed by Guðmundsson (1997).

Time of glacier advance (BP)	Southern Iceland	Bracketing dates	Northern Iceland	Bracketing dates
	Ystagil	900 A.D.		
>1.2 ka < 1.5 ka		1.5 ka BP	Barkárdalur II	1.555 ± 90 ka BP
	Kvíárjökull	720 – 800±390 AD		
			Barkárdalur I	1.835 ka BP
Around 2 ka	Kvíárjökull	2.040±80 BP		2.24 ka BP
Around 3 ka	Hólsárgil	2.660±60 BP	Vatnsdalur II	2.8 ka BP
		3.480±60 BP		3.470 ka BP
>4 ka <7.000	Drangagil	7.210±60 BP	Baegisárdalur I	4.275 ka BP
		4.1 ka BP		4.700±205 ka BP
	Skálafellsjökull	5.710±90 BP	Vatnsdalur I	6 ka BP
		1362 AD		

More recently, Kirkbride and Dugmore (2006) synthesised a composite sequence of *Little Ice Age Type Events* (LIATEs) for southern and central Iceland on the basis of comparable moraine chronologies (Dugmore, 1989; Kirkbride and Dugmore, 2001b; Kirkbride and Dugmore, 2008), providing a stratigraphic nomenclature within which regional comparisons/correlations can be made at different temporal resolutions (Table 2.3). The term *Little Ice Age Type Event* was originally introduced by Wanner *et al*. (2000) in reference to quasi-regular glacier advances in the Swiss Alps with occurrence intervals of 200 – 400 years. Kirkbride and Dugmore (2006) applied a similar approach to Icelandic glacier events, defining a sequence of decadal-scale LIATEs nested within century-scale *Little Ice Age Type Periods* (LIATPs).

For comparative purposes, Kirkbride and Dugmore (2006) derived a set of *potential* LIATEs from negative anomalies in the bidecadal δ^{18}O record from the GISP2 ice core (Figure 2.1; Table 2.3). Whilst not all of the nominally defined 29 LIATEs may have resulted in glacier advance, owing to the complex synoptic climatology of the NW Atlantic (*cf*. Barlow, 2001), they do provide a complete record of cold decades in Greenland, a proportion of which should correlate with Icelandic glacier advances (Kirkbride and Dugmore, 2006). On the basis of moraine chronologies from Hrútfell and Eyjafjallajökull, only eight of the potential LIATEs in the Greenland δ^{18}O record were identified, which may reflect: (1) partial erosion of the moraine record; (2) deposition of multiple moraines within time periods bound by tephra isochrones; and (3) possible lack of correspondence between bidecadal-scale cold periods in Greenland and Iceland (Kirkbride and Dugmore, 2006).

Table 2.3: Little Ice Age Type Events (LIATEs) in Iceland and Greenland. Icelandic LIATEs are based on the moraine chronologies from Hrútfell (Kirkbride and Dugmore, 2006) and Eyjafjallajökull (Kirkbride and Dugmore, 2008). *Source:* Kirkbride and Dugmore (2006: 1704).

Icelandic LIATEs			Tephra isochrones	GISP2 LIATES	
Period	LIATE	Date		LIATE	Spike decades
	1	AD 1860 - 1920	Katla 1918	1	AD 1860 - 1880
			Hekla 1766	2	AD 1780 - 1800
“LIA”	2	AD 1680 - 1780	Katla 1721	**3**	**AD 1700 - 1740**
				4	AD 1660 - 1680
				5	AD 1580 - 1620
				6	AD 1520 - 1560
			Hekla 1300	**7**	**AD 1300 - 1360**
	3	AD 1180 - 1200		8	AD 1180 - 1200
			Hekla 1104	9	AD 1040 - 1080
“Dark Ages”	4	AD 700 - 900	Landnam *c.* AD 870	10	AD 760 - 820
				11	AD 720 - 740
				12	AD 640 - 700
	5	*c.* 1600 BP		13	AD 500 - 520
				14	AD 360 - 380
				15	**AD 180 - 220**
	6	*c.* 2000 - 2500 BP		16	BP 2150 - 2170
				17	BP 2270 - 2310
Subatlantic				18	BP 2450 - 2470
				19	BP 2630 - 2670
				20	BP 2770 - 2810
	7	*c.* 3000 BP	H3 *c.* 3300 cal. yr BP	**21**	**BP 2990 - 3030**
				22	BP 3370 - 3390
				23	BP 3570 - 3590
				24	**BP 3850 - 3910**
Early Neoglacial	8	*c.* 4500 - 5000 BP	H4 *c.* 4200 cal yr BP	25	BP 4350 - 4390
				26	BP 4430 - 4450
				27	BP 4610 - 4630
				28	**BP 4730 - 4810**
				29	BP 4990 - 5010
			↓ H5 *c.* 6200 cal. yr BP		

Shaded areas mark prolonged periods of reduced isotopic values in the GISP2 record (*Little Ice Age Type Periods*, LIATPs). Bold type denotes isotopically low spikes immediately following major declines into LIATPs.

Despite this, the composite sequence of LIATPs and nested LIATEs reveals considerable synchrony of century-scale periods of glacier expansion (LIATPs) between northern, central and southern Iceland. Moreover, decadal-scale advances (LIATEs) also appear to be recorded synchronously in moraine sequences from glacier forelands throughout Iceland (Kirkbride and Dugmore, 2006). This emerging pattern of correlative glacier advances conforms to the classic *Neoglacial* model of glaciation (*cf*. Guðmundsson, 1997).

2.2 Glacier fluctuations during the “observational” period

2.2.1 Variations of Icelandic glacier termini

Regular monitoring of variations of glacier termini in Iceland commenced in 1930, with observations being undertaken at 44 glaciers (Eyþórsson, 1931, 1935, 1963). Monitoring of

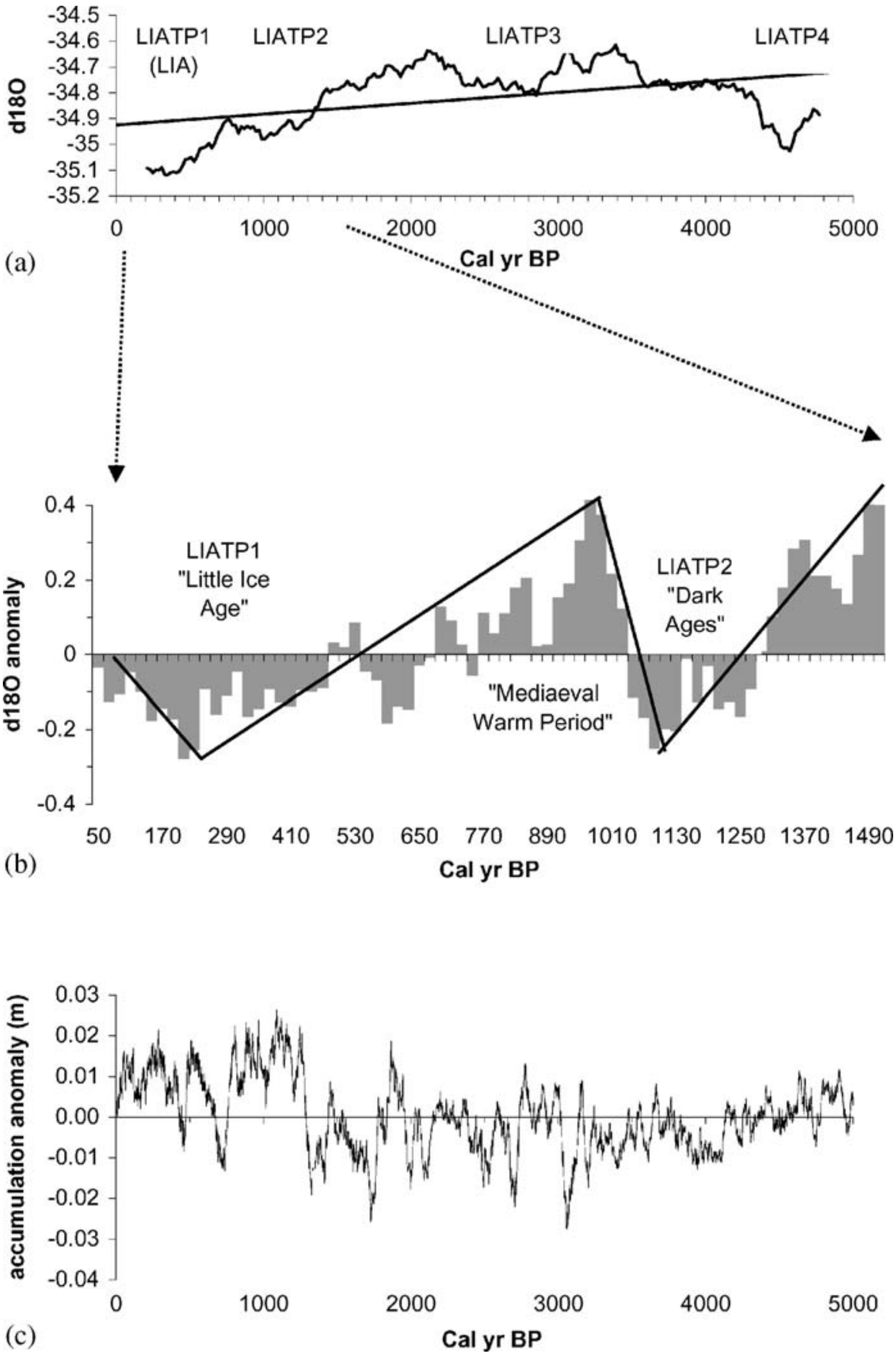

Figure 2.1: Climate proxies from the GISP2 ice core in central Greenland. (a) The last 5000 years of the δ^{18}O record smoothed with a 500-year filter. (b) Deviations from the mean value of the δ^{18}O record for the last 1500 years showing bidecadal changes within the period of the *Medieval Warm Period* and the *Little Ice Age*. (c) Fifty-year running mean of annual accumulation (Cuffey and Clow, 1997) expressed as deviations from the mean value for the last 5000 years. *Source:* Kirkbride and Dugmore (2006: 1703).

an additional 11 glacier termini began during the period 1948 – 1972 (Sigurðsson and Jónsson, 1995). Since 1951, the monitoring programme has been the responsibility of *Jöklarannsóknafélag Íslands* (the Icelandic Glaciological Society), with summaries of the measurements (*Jöklar breytingar*) being published annually in the periodical *Jökull* (e.g.

Eyþórsson, 1962 – 1966; Rist, 1967 – 1987; Sigurðsson, 1992, 1998, 2005b). Since 1964 a subset of the data has been sent to the World Glacier Monitoring Service (WGMS) and is published in *Fluctuations of glaciers* at 5-year intervals (Sigurðsson, 1998; Sigurðsson *et al*., 2007). The Icelandic Glaciological Society database now contains terminus-variation measurements for 60 different glaciers, with 41 outlet glaciers currently being actively monitored at 55 locations (Sigurðsson, 1998; Sigurðsson *et al*., 2007).

Glacier recession set in slowly in the 1890s following the LIA maximum of Iceland's glaciers, with retreat being notable but not rapid during the first quarter of the 20th Century (Thórarinsson, 1943; Björnsson, 1979, 1998; Sigurðsson, 2005a). The database of glacier-termini variations reveals that the period 1930 – 1960 was characterised by rapid retreat of all monitored ice-fronts, with retreat occasionally interrupted by surge activity at surge-type glaciers (Eyþórsson, 1931, 1963; Sigurðsson, 1998; Sigurðsson and Jónsson, 1995; Sigurðsson *et al*., 2007). By 1960, all monitored ice-margins had retreated from their 1930 position, though 10 – 20% of glacier termini were advancing in any given year (Sigurðsson and Jónsson, 1995; Jóhannesson and Sigurðsson, 1998; Sigurðsson *et al*., 2007). During the 1940s and 1960s the rate of ice-marginal retreat slowed, with many non-surge-type glaciers advancing to varying degrees in the decades following the 1960s (Figure 2.2; Sigurðsson and Jónsson, 1995; Sigurðsson *et al*., 2007). Small, non-surging valley glaciers with moderate elevation ranges typically displayed annual ice-margin retreat rates of ~10 m a^{-1} or less during the period 1930 to 1960, whereas several of the south-flowing Vatnajökull outlets exhibited retreat rates of 50 – 100 m a^{-1} during this period (Eyþórsson, 1963; Jóhannesson and Sigurðsson, 1998; Sigurðsson, 1998; Magnússon *et al*., 2005). During the 1990s many non-surge-type glaciers recommenced ice-marginal retreat, and by 2000 all monitored non-surge-type glaciers were retreating (Sigurðsson, 2005a; Sigurðsson *et al*., 2007). Over the past decade many of the monitored glaciers have shown increasingly rapid rates of ice-marginal retreat (e.g. Bradwell *et al*., 2013).

2.2.2 Variations in mass balance

Annual monitoring of glacier mass balance was initiated in 1988 at the Hofsjökull ice-cap; monitoring of glacier mass balance has since commenced at Vatnajökull (since 1991/1992), Langjökull (since 1996/97) and Drangajökull (since 2004/05) (Björnsson, 1971; Björnsson *et al*., 1998, 2002; Sigurðsson and Sigurðsson, 1998; Sigurðsson *et al*., 2004, 2007). The annual mass balance monitoring programme is managed by the Hydrological Service of the National Energy Authority of Iceland alongside the Institute of Earth Sciences, University of Iceland

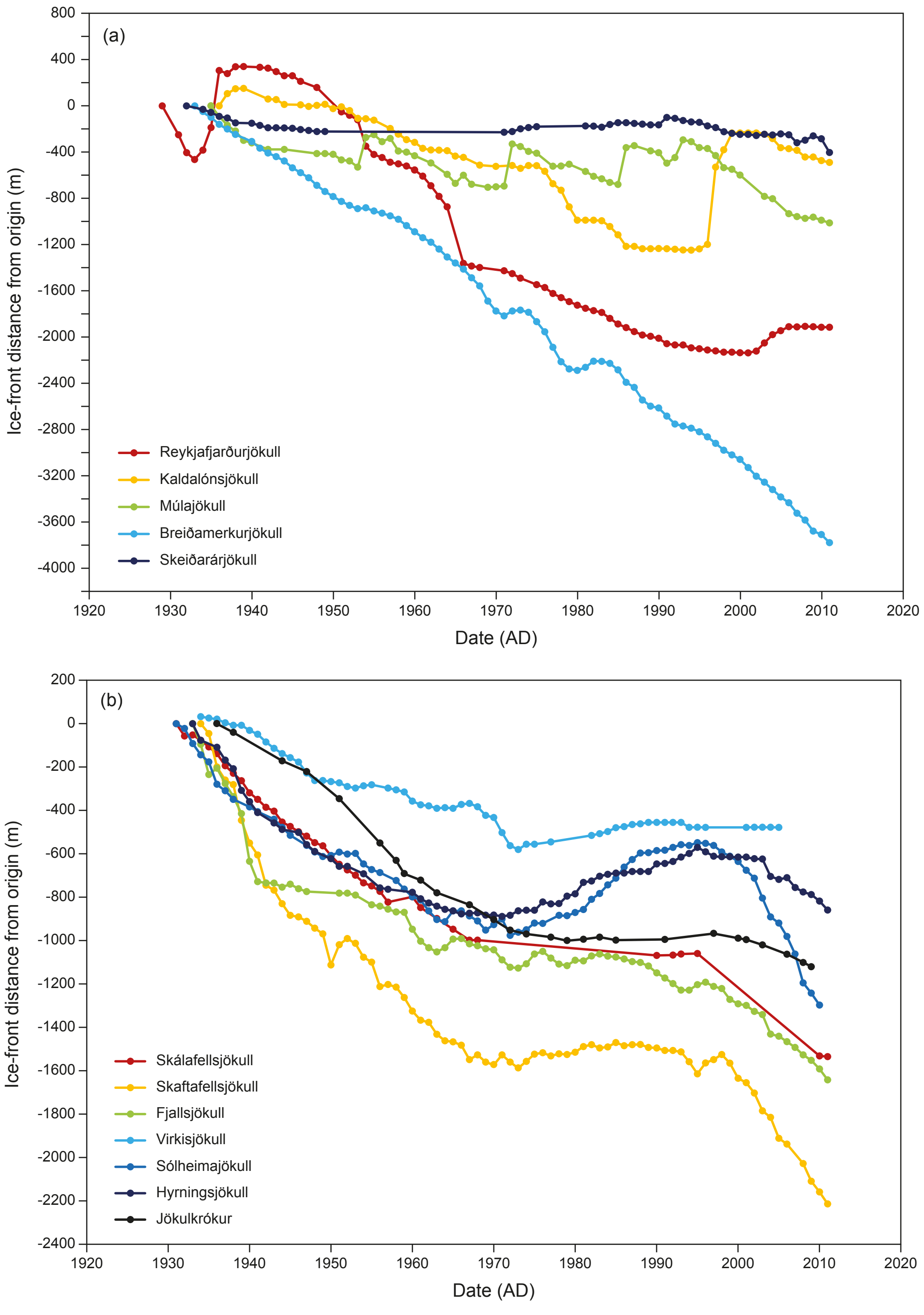

Figure 2.2: Glacier termini variations for a selection of Icelandic glaciers, taken from the database of the Icelandic Glaciological Society. The measurements for these glaciers illustrate both the spatial and temporal variability of glacier termini variations in Iceland throughout the observational period.

(Sigurðsson *et al*., 2007). Results of the mass-balance measurement programme are published by the WGMS in the *Glacier Mass Balance Bulletin* biannually (e.g. Haeberli *et al*., 2005, 2007, 2009; Zemp *et al*., 2011, 2013).

Mass balance measurements for the main ice-caps show alternating positive and negative mass balance during the period 1987 – 1995, but the mass balance has been predominantly negative since 1996 (Figure 2.3a; Sigurðsson *et al*., 2007). According to the database of measurements, variations in summer balance are much greater than those in winter balance. Mass balance measurements for Vatnajökull show that the winter balance was generally highest in the early 1990s, but decreased to a minimum between 1996 and 1997, before increasing to a maximum in 2003 (Björnsson and Pálsson, 2008; Björnsson *et al*., 2013). The annual net balance of the Vatnajökull ice-cap was positive from the commencement of measurements in 1991/92 until 1993/94, before approaching zero in 1994/95. Since then, Vatnajökull has exhibited negative mass balance (Figure 2.3b). For the period 1995 to 2010, the cumulative mass loss averaged over the Vatnajökull ice-cap was 13 m_{we} (metres of water equivalent; Björnsson *et al*., 2013). The net mass loss of Vatnajökull has, however, exhibited substantial annual variability during this period from 2 to 17 ± 1.5 Gt a^{-1} (–0.3 to –2.1 ± 0.15 m_{we} a^{-1} mean specific mass balance). As the subglacial topography of the main ice-caps in Iceland is well known, relative changes in ice volume can be estimated (Björnsson and Pálsson, 2008; Björnsson *et al*., 2013). Over the period 1995 to 2010, the Vatnajökull ice-cap lost 3.7% of its total ice mass. The mass balance records for the other ice-caps display similar characteristics, with mass losses of 22 m_{we} from Hofsjökull (11% of total ice mass) for the period 1995 – 2010 and 20 m_{we} from Langjökull (11% of total ice mass) for the period 1997 – 2010 (Sigurðsson *et al*., 2007; Björnsson and Pálsson, 2008; Björnsson *et al*., 2013). Extrapolating the mass changes to all Icelandic glaciers, using the mean specific balance for the measured glaciers, Björnsson *et al*. (2013) estimated total ice loss of 9.5 ± 1.5 Gt a^{-1} (~0.03 mm a^{-1} sea-level equivalent) since the mid-1990s, with mass loss for individual years ranging from 2.5 to 25 ± 1.5 Gt a^{-1} (Figure 2.3c). These estimates coincide with recent estimates of Icelandic ice mass loss (11 ± 2 Gt a^{-1}, 2003 – 2010) from the Gravity Recovery and Climate Experiment (GRACE) satellite gravity field measurements (Jacob *et al*., 2012).

Recently, a number of studies have employed differencing of digital elevation models (DEMs), derived from various satellite and airborne observations, to estimate changes in Icelandic glacier volume, providing a composite record of mass changes since the 1900s (Guðmundsson *et al*., 2011; Pálsson *et al*., 2012; Jóhannesson *et al*., 2011, 2013; Björnsson *et al*., 2013). The investigations indicate that average mass balance was only slightly negative over the first few decades of the 20th Century, though becoming increasingly negative in the 1930s (*c*. –1 m_{we} a^{-1}). The mass balance gradually increased again from the mid-1940s to the 1980s, though slowing to zero in the 1980s. Around 1990 some Icelandic glaciers gained mass but since the mid-1990s have displayed accelerating rates of mass loss, as demonstrated by the mass balance measurements (Björnsson *et al*., 2013).

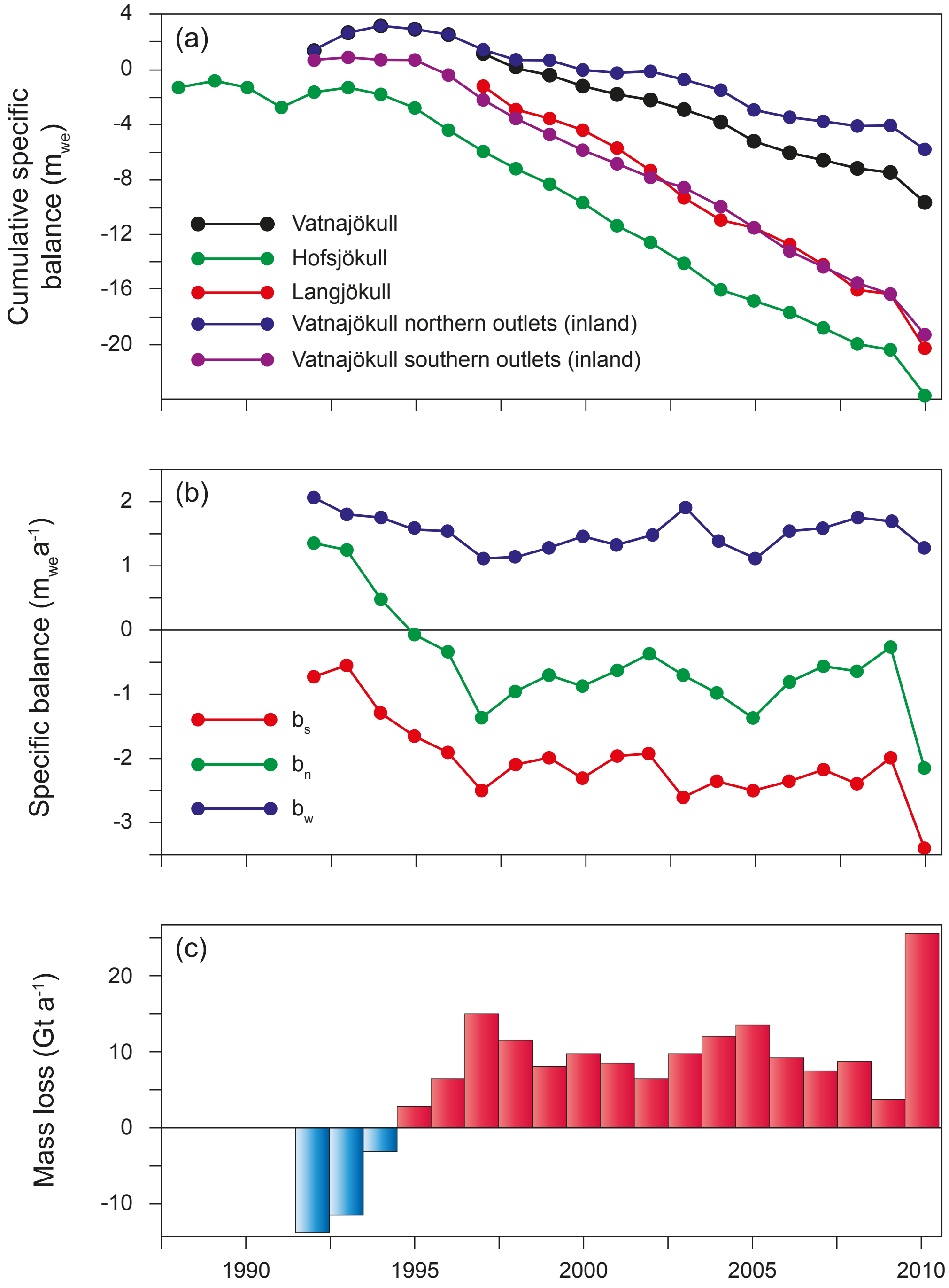

Figure 2.3: Cumulative specific balance, specific balance, and mass loss of Icelandic glaciers based on *in situ* measurements (Björnsson *et al*., 2013, and references therein). (a) Cumulative mass balance of Vatnajökull, Langjökull, and Hofsjökull, 1990–2010. Hofsjökull data have been bias corrected with geodetic measurements (Jóhannesson *et al*., 2013). (b) Specific mass balance of Vatnajökull, 1992–2010, given in metres of water equivalent (m_{we} a^{-1}) where b_w stands for winter balance, b_s summer balance, and b_n annual balance. (c) Estimated annual mass loss of all of Icelandic glaciers, 1992–2010.

2.2.3 Influence of climate on glacier fluctuations

Investigation of Icelandic meteorological data for the 20th Century reveals statistically significant positive trends in temperature, particularly in summer but also in annual temperature, consistent with warming trends observed elsewhere in Northwest Europe (*cf*. Hanna *et al*., 2004, and references therein). The greatest period of warming occurred between ~1919 and 1933, and is characterised by the largest increases of spring temperature (e.g. increase of 3.4°C at Reykjavík). Maximum temperatures over the entire meteorological record were reached in 1939 and 1941. Increases in summer temperature during the 1930s were followed by cooling between ~1940 and the early 1980s, concentrated in the period 1931 – 1960 (Sigurðsson and Jónsson, 1995; Jóhannesson and Sigurðsson, 1998; Hanna *et al*., 2004). Warming during the winter season persisted until the 1960s, before coming to an abrupt end in 1965 (Sigurðsson *et al*., 2007). Some of the coldest years and seasons of the period 1901 – 2000 were during the late 1970s and early 1980s, particularly 1979, 1983 and 1981 (Jóhannesson and Sigurðsson, 1998; Hanna *et al*., 2004). Since ~1985 temperatures have been warming, with a marked increase in both winter and summer temperatures occurring since the mid-1990s (Jóhannesson and Sigurðsson, 1998; Sigurðsson *et al*., 2007).

Annual and decadal variations in precipitation display greater local variability compared to the temperature data (Hanna *et al*., 2004; Sigurðsson *et al*., 2007). Meteorological records show a generally wet period during the 1930s, before a general decrease in precipitation from the 1930s to the 1960s. Precipitation values subsequently increased from the 1960s until around 1995 (Sigurðsson *et al*., 2007). Over the last ~40 years, inter-decadal variations have been prominent, with comparatively high precipitation occurring in the period 1970 – 1976 and around 1990 (Hanna *et al*., 2004; Sigurðsson *et al*., 2007).

General comparison of non-surge-type glacier termini variations since the 1930s with climate variations show ice-front fluctuations are in sympathy with air temperature variations, with the warming and cooling trends discussed above coinciding with periods of ice-marginal retreat and advance, respectively (Figure 2.4; Sigurðsson and Jónsson, 1995; Jóhannesson and Sigurðsson, 1998; Sigurðsson *et al*., 2007). Relatively high air temperatures during the period 1931 – 1960, particularly during 1931 and 1940, are associated with a period of rapid ice-front retreat (Figure 2.4). The reversal of this retreat trend to a period of advance after *c*. 1965 coincides with a period of climate cooling, and the number of non-surge-type advancing glaciers reached its maximum in 1975 – 1990 period following a summer air temperature minimum around 1980 (Jóhannesson and Sigurðsson, 1998; Sigurðsson *et al*., 2007). Icelandic glaciers returned to ice-marginal retreat during the 1990s, particularly after 1995, as temperatures began rising rapidly (Sigurðsson, 2005a; Sigurðsson *et al*., 2007). Thus, the instrumental record appears to demonstrate that summer air temperature variations exert a dominate control on Icelandic glacier variations (Sigurðsson and Jónsson, 1995; Jóhannesson and Sigurðsson, 1998; Sigurðsson *et al*., 2007).

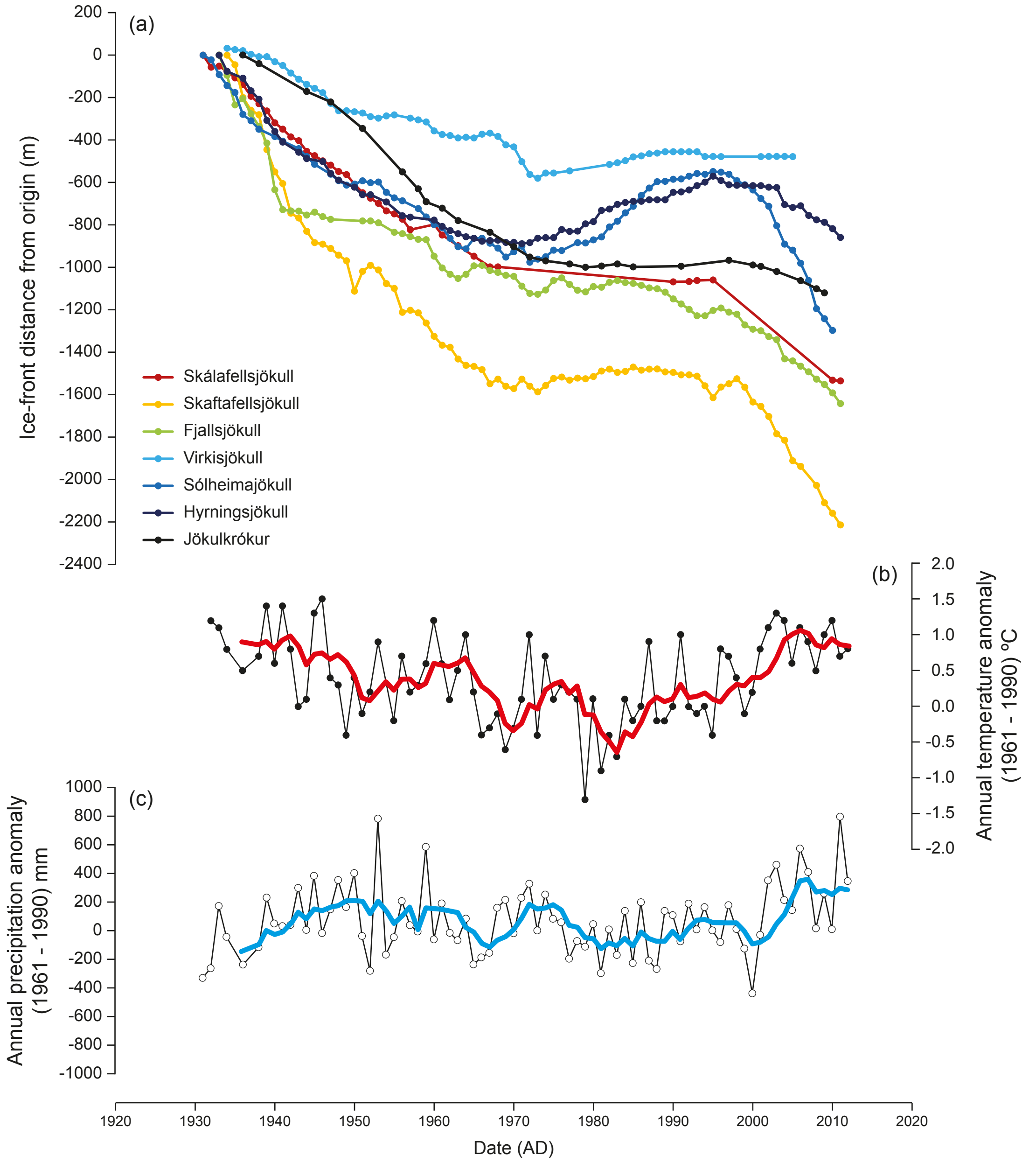

Figure 2.4: Comparison of temperature and precipitation variations since 1931 at Kirkjubæjarklaustur (South Iceland) with glacier termini variations at a selection of non-surge-type glaciers. Meteorological data has been supplied by *Veðurstofa Íslands* (Icelandic Meteorological Office), whilst glacier termini variations are taken from the Icelandic Glaciological Society database.

Whilst Icelandic glacier fluctuations have been compared to air temperature (e.g. Boulton, 1986; Sigurðsson and Jónsson, 1995; Jóhannesson and Sigurðsson, 1998; Bradwell, 2004a; Sigurðsson *et al*., 2007; Bradwell *et al*., 2013) and, to a limited extent, precipitation variability (Sigurðsson and Jónsson, 1995; Jóhannesson and Sigurðsson, 1998), there has been limited consideration of other climate variables (e.g. sea surface temperature and the North Atlantic Oscillation) and the complex interactions between them (e.g. Kirkbride, 2002; Mernild *et al*., 2014). Moreover, associations between summer air temperature and Icelandic termini variations are frequently based on comparison of time series plots, with limited statistical treatment (e.g. Sigurðsson and Jónsson, 1995; Jóhannesson and Sigurðsson, 1998; Sigurðsson *et al*., 2007; Bradwell *et al*., 2013). This restricts current understanding of contemporary Icelandic change and the wider significance of recent ice-frontal retreat in Iceland. Significantly, sea surface temperature (SST) variability and North Atlantic subpolar gyre dynamics have been implicated in recent Greenlandic glacier change (*cf*. Bjørk *et al*., 2012; Straneo and Heimbach, 2013). The current trend of ice-frontal retreat in Iceland could therefore be the result of a regional forcing mechanism. Thus, a consideration of a wider array of climate variables and their potential influence on Icelandic glaciers is of key importance for attaining greater understanding of recent ice-frontal retreat in Iceland and its wider significance.

2.3 The active temperate glacial landsystem

Icelandic lowland glaciers are typically *active temperate*, producing a sediment-landform archive that reflects a regional decadal to annual climatic signal (Boulton, 1986; Evans, 2003a). Consequently, the sediment-landform archives produced by Icelandic active temperate glaciers afford valuable climate archives. The Skálafellsjökull foreland is an exemplar of the active temperate piedmont lobe landsystem, and is an instructive modern analogue for the evolution of active temperate landsystems that have developed in mountain terrains with high glaciofluvial sediment yields (Evans and Orton, 2014).

Temperate glacier margins are mainly at pressure melting point (wet-based) for at least part of the year. Such glaciers are considered as *active* when they are capable of forward momentum even during overall recession (Evans, 2003a). This is manifest in the small winter re-advances that characterise receding Icelandic outlet glaciers (e.g. Sharp, 1984; Boulton, 1986; Krüger, 1995). During the winter, narrow frozen zones develop below the margins of many temperate glaciers owing to the penetration of a seasonal cold wave from the atmosphere through the thin ice (Krüger, 1994; Evans and Hiemstra, 2005; Evans, 2009a). The processes and major sediment-landform associations of active temperate glacier margins have been examined in detail (e.g. Sharp, 1982a, 1984; Krüger, 1985, 1993, 1994, 1997; Boulton, 1986; Boulton and Hindmarsh, 1987; Benn, 1995; Evans and Twigg, 2002; Evans and Hiemstra, 2005; Evans *et al*., submitted). Such studies inform models of sediment-landform produced at the margins of active temperate glaciers.

Below temperate glaciers, sequences of debris-rich basal ice are typically thin or absent (Hubbard and Sharp, 1989, 1993), with the exception of some localised concentrations of debris in basal ice facies related to glacio-hydraulic super-cooling (e.g. Alley *et al*., 1998, 1999; Lawson *et al*., 1998). Any debris-rich ice that does exist can also be elevated to the glacier surface by compressive flow (Evans, 2003a). Additionally, small quantities of subglacial debris may be elevated to englacial and supraglacial positions where marginal folding and thrusting take place (Evans and Twigg, 2002; Benn and Evans, 2010). However, the volume of debris transported through active temperature glaciers through these mechanisms is typically small. Consequently, supraglacial landforms and widespread ice stagnation topography are uncommon compared with temperate glaciers in high-relief settings (*cf*. Evans, 2003b, and references therein).

Previous studies of sediment-landform associations on the recently deglaciated forelands of active temperate glaciers have highlighted three dominant depositional domains: (1) the marginal morainic domain; (2) the subglacial domain; and (3) the glaciofluvial and glaciolacustrine domain (Figure 2.5; Evans and Twigg, 2002; Evans, 2003a). In addition to the three dominant depositional domains, isolated signatures of erratic/non-cyclic or site-specific processes may be evident in the sediment-landform record. Evidence of jökulhlaup activity (Maizels, 1997; Russell and Knudsen, 1999; Fay, 2002) and surging (Sharp, 1985a, b, 1988; Evans and Rea, 1999; Evans *et al*., 1999b) may be represented in the landform record of active temperate glaciers.

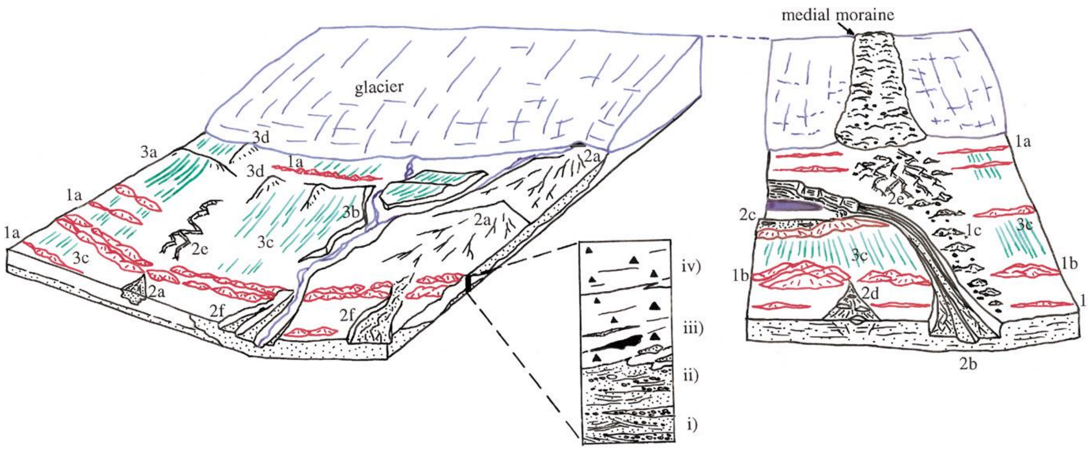

Figure 2.5: Annotated sketch of the active temperate glacial landsystem based on Breiðamerkurjökull and Fjallsjökull. Landforms are numbered according to their domain (1 = morainic domain; 2 = glaciofluvial domain; 3 = subglacial domain): (1a) small, often annual, push moraines; (1b) superimposed push moraines; (1c) hummocky moraine; (2a) ice-contact sandur fans; (2b) spillway-fed sandur fan; (2c) ice margin-parallel outwash tract/kame terrace; (2d) pitted sandur; (2e) eskers; (2f) entrenched ice-contact outwash fans; (3a) overridden (fluted) push moraines; (3b) overridden, pre-advance ice-contact outwash fan; (3c) flutes; and (3d) drumlins. The idealised stratigraphic section log shows a typical depositional sequence recording glacier advance over glaciofluvial sediments, comprising: (i) undeformed outwash; (ii) glaciotectonised outwash/glaciotectonite; (iii) massive, sheared till with basal inclusions of pre-advance peat and glaciofluvial sediment; and (iv) massive sheared till with basal erosional contact. *Source:* Reproduced from Evans and Twigg (2002: 2173).

2.3.1 The marginal morainic domain

The marginal morainic domain is characterised by areas of extensive, low-amplitude marginal dump, push and squeeze moraines (Price, 1970; Krüger, 1987; Evans *et al*., 1999a; Evans and Twigg, 2000, 2002) derived largely from material on the glacier foreland and often record annual recession of active ice (Sharp, 1984; Boulton, 1986; Krüger, 1995). The continuation of flutings over the proximal slopes and crests of many push moraines indicates that subglacial bedform and push moraine production is genetically linked (Evans and Twigg, 2002; Evans, 2003a). A subglacial deformation/ploughing origin of flutings (Boulton, 1976; Benn, 1994) thereby implies that push moraines are the product of the advection of subglacially deforming sediment to the ice margin (*cf*. Boulton and Hindmarsh, 1987; Boulton and Dobbie, 1998; Boulton *et al*., 2001) where squeezing and pushing then combine to create the moraine ridge. Short periods of re-advance or stability can produce larger push moraines (Krüger, 1993) through either: (1) the stacking of sub-marginally frozen sediment slabs (Alexander and Worsley, 1973; Humlum, 1985; Krüger, 1993, 1994, 1996; Matthews *et al*., 1995; Evans and Hiemstra, 2005); (2) dump, squeeze and push mechanisms operating at the same location over several years (Evans and Twigg, 2002); or (3) through the incremental thickening of ice-marginal wedges of deformation till (e.g. Johnson and Hansel, 1999). The marginal morainic domain is also characterised by wide and arcuate, low-amplitude ridges that are adorned with flutings and recessional push moraines, interpreted as glacially streamlined push moraines overridden by glaciers during major re-advances (Krüger, 1987; Evans *et al*., 1999b; Evans and Twigg, 2000, 2002; Evans and Orton, 2014).

2.3.2 The subglacial domain

The subglacial domain occurs on land surfaces between the ice-marginal morainic and glaciofluvial depo-centres, and is characterised by assemblages of flutings, drumlins and overridden push moraines (Krüger and Thomsen, 1984; Krüger, 1987; Benn, 1995; Hart, 1995; Evans *et al*., 1999a, b) owing to the thin and discontinuous covering of supraglacial sediment on the foreland of active temperate glaciers (Evans, 2003a, 2005). Additionally, the subglacial domain may be associated with areas of discontinuous, striated and polished bedrock often characterised by roches moutonnées, indicative of widespread abrasion and quarrying at the ice/bed interface (Evans, 2005; Benn and Evans, 2010; Evans and Orton, 2014). These sediment-landform assemblages have been linked to subglacial deforming layers in previous Icelandic research on active temperate glaciers (Boulton, 1987; Boulton and Hindmarsh, 1987; Benn, 1995; Hart, 1995; Benn and Evans, 1996). Experiments conducted at Breiðamerkurjökull demonstrated that the subglacial till was emplaced by deformation, and comprised a two-tier structure in response to ductile flow of an upper dilatant layer (A-horizon) and brittle shearing of a stiff lower layer (B-horizon; Boulton and Dent, 1974; Boulton, 1979; Boulton and Hindmarsh, 1987). Exposures through till sequences on Icelandic glacier forelands provide evidence for this vertical continuum, typically comprising glaciotectonised stratified proglacial outwash and localised glaciolacustrine sediments capped by subglacial traction till containing rafts of underlying material and the products of localised abrasion (Howarth, 1968; Dowdeswell and Sharp, 1986; Boulton, 1987; Benn and Evans, 1996, 2010; Evans, 2000; Evans and Twigg, 2002; Evans *et al*., 2006).

2.3.3 The glaciofluvial and glaciolacustrine domain

The glaciofluvial and glaciolacustrine domain is not unique to the active temperate glacial landsystem, as similar associations also occur in front of polythermal glaciers (*cf*. Evans, 2003b, and references therein). The glaciofluvial landforms typically represented at the margins of Iceland active temperate glaciers include ice-contact and spillway fed sandur fans (Price, 1969; Boulton, 1986), outwash tracts parallel to the ice-margin and kame terraces (Howarth, 1968; Evans and Orton, 2014), hochsandur fans (Krüger, 1997; Kjær *et al*., 2004), topographically channelized sandar, pitted sandar (Howarth, 1968; Price, 1969, 1971) and eskers of simple and complex, anabranched forms (Price, 1966, 1969; Howarth, 1971; Storrar, 2013; Storrar *et al*., submitted). Large areas of glaciofluvial forms such as recessional ice-contact fans (Boulton, 1986) and hochsandur fans (Krüger, 1997; Kjær *et al*., 2004) cut through, or are directed by, moraine ridges. Additionally, these outwash forms may be associated with small areas of pitted outwash (Price, 1969, 1971) and eskers are often linked to fan apices (Price, 1966, 1969).

Rigorous studies of eskers at Breiðamerkurjökull, augmented by surveying and mapping of the glacier terminus and proglacial area since 1945, have permitted the long-term morphological evolution of eskers to be assessed (Welch, 1967; Howarth, 1968, 1971; Price, 1969, 1973, 1982; Storrar, 2013; Storrar *et al*., submitted). Studies by Welch (1967), Howarth (1968, 1971) and Price (1969) report considerable esker surface lowering, indicative of englacial or supraglacial deposition. More recently, two types of esker complex, termed *topographically constrained* and *esker fan*, have been identified on the Breiðamerkurjökull foreland (Storrar, 2013; Storrar *et al*., submitted). The formation of these esker complexes is a function of a large sediment and meltwater supply combined with sufficiently small conduits, resulting in the choking of tunnels and the concomitant production of multiple distributaries. Simple esker systems predominate when sediment and meltwater supply is more limited (Storrar, 2013; Storrar *et al.*, submitted).

Ice-dammed and proglacial lakes are also common features around the receding margins of lowland temperate glaciers, particularly where the glacier has uncovered overdeepenings produced by long-term glacial erosion (Howarth and Price, 1969; Boulton *et al*., 1982; Björnsson, 1996; Bennett *et al*., 2000; Evans and Twigg, 2002; Schomacker, 2010; Evans and Orton, 2014). These lakes are significant sediment sinks on the forelands of temperate glaciers and give rise to the accumulation of thick sequences of glaciolacustrine sediments and shorelines and deltas (Shaw, 1977; Teller, 2003).

2.4 Annual moraines: important sediment-landform archives

Small-scale, annual ice-marginal fluctuations are manifest in the form of “annual” moraines in front of many active temperate glaciers in Iceland and elsewhere (Thórarinsson, 1967; Price, 1970; Worsley, 1974; Sharp, 1984; Boulton, 1986; Matthews *et al*., 1995; Evans and Twigg, 2002; Bradwell, 2004a; Bradwell *et al*., 2013; Reinardy *et al*., 2013), as outlined above. Such landforms have been subject to renewed interest over recent years, particularly with respect to extracting a climate signal through applying annual moraine spacing as a geomorphological proxy for patterns and rates of ice-marginal retreat (e.g. Bradwell, 2004a; Beedle *et al*., 2009; Lukas, 2012; Anderson *et al*., 2014).

According to previous studies, annual moraines are formed by short-lived seasonal re-advances during overall retreat (e.g. Andersen and Sollid, 1971; Boulton, 1986; Krüger, 1995). Despite an overall net negative mass balance over a number of consecutive years, much-reduced ablation in winter and early spring may result in a temporary switch to seasonally positive mass balance when the glacier snout advances (Lukas, 2012). Provided recession during the ablation season is greater than advance during the accumulation season over consecutive years, a long sequence of inset, consecutively younger annual moraines may be formed (Boulton, 1986; Bennett, 2001; Lukas, 2012). Consequently, annual moraines offer the opportunity to link ice-marginal moraines to specific climatic and glaciological conditions, and to increase understanding of the relationship between glacier dynamics and ice-marginal moraine formation (e.g. Boulton, 1986; Krüger, 1995; Lukas, 2012; Reinardy *et al*., 2013). In a Quaternary research context, the development of modern analogues underpinned by well-defined process-sediment-form relationships allow more informed genetic interpretations of ancient moraine assemblages and more realistic reconstructions of palaeoglacier dynamics and palaeoclimate (Evans, 2003b, 2009b; Lukas, 2012).

2.4.1 Geomorphological characteristics

Individual annual moraines display varying heights, ranging from < 0.5 m up to 8 m in some cases, and typically display asymmetric cross-profiles with gentler ice-proximal slopes and steeper distal slopes (Price, 1970; Worsley, 1974; Sharp, 1984; Krüger, 1995; Matthews *et al*., 1995; Bradwell, 2004a; Lukas, 2012; Reinardy *et al*., 2013). Annual moraines are often found in association with flutings, and may exhibit continuation of flutings over proximal slopes (e.g. Sharp, 1984; van der Meer, 1997; Evans and Twigg, 2002). In planform they display varying forms, ranging from arcuate features about the glacier margin (Figure 2.6a; Andersen and Sollid, 1971; Birnie, 1977; Krüger, 1995; Lukas, 2012; Reinardy *et al*., 2013) to striking saw-tooth or crenulate ridges (Figure 2.6b; Price, 1970; Sharp, 1984; Bradwell, 2004a). Annual moraines frequently take the form of continuous ridges that extend for several tens or hundreds of metres in length (e.g. Krüger, 1995; Bradwell, 2004a; Lukas, 2012) but in some cases may be fragmentary or diffuse (e.g. Reinardy *et al*., 2013). Where ridges are discontinuous, ridge fragments may be separated by small outwash fans, meltwater channels or silted-up depressions, indicative of postdepositional breaching of continuous moraines by meltwater streams and subsequent infilling of depressions (Lukas, 2012; Reinardy *et al*., 2013). Individual moraines also frequently display bifurcations and cross-cutting patterns, reflecting variable activity along an ice-front (Price, 1970; Sharp, 1984; Boulton, 1986; Krüger, 1994; Bennett, 2001). In addition to variations in activity along the length of the ice-margin, annual moraine morphology and planform geometry is also influenced by structural glaciology (e.g. Price, 1970; Sharp, 1984; Evans *et al*., submitted) and processes of formation (e.g. Birnie, 1977; Krüger, 1995; Matthews *et al*., 1995; Lukas, 2012).

2.4.2 Formation of annual moraines

Annual moraines typically contain a core of deformed sediment, with a re-worked surface and varying quantities of supraglacial debris (Sharp, 1984; Krüger, 1995; Bennett, 2001; Lukas, 2012; Reinardy *et al*., 2013). The significance of the supraglacial component is influenced by: (1) the availability of supraglacial debris sources, such as englacial conduit fills, emerging englacial debris septa and rock slope failures, to deliver material to the ice surface; (2) supraglacial drainage, which influences delivery and distribution of supraglacial debris; and (3) ice-margin geometry, which also controls delivery and distribution of material (*cf*. Lawson, 1982; Rogerson and Batterson, 1982; Krüger and Aber, 1999; Krzyszkowski, 2002; Krzyszkowski and Zielinski, 2002; Evans *et al*., 2010; Lukas, 2012; Kirkbride and Deline, 2013). The composition of the deformed sediment core varies according to the nature of the proglacial and/or subglacial sediment (depending on the process of formation), though commonly consists of subglacial diamicton and a surface veneer of supraglacial debris (Figure 2.7a; Price, 1970; Worsley, 1974; Sharp, 1984; Boulton, 1986; Krüger, 1995; Bradwell, 2004a; Bradwell *et al*., 2013; Reinardy *et al*., 2013). Although, in the only detailed sedimentological study of annual moraines formed by an alpine valley glacier, Lukas (2012) established that annual moraines at Gornergletscher, Switzerland are composed of proglacial outwash and debris flow units (e.g. Figure 2.7b), with subglacial traction till (*sensu* Evans *et al*., 2006) being entirely absent. Similarly, Johnson *et al*. (2010) have reported an absence of subglacial traction till in annual moraines at Múlajökull, Iceland. Investigations of clast fabric within the diamicton cores of annual moraines have revealed strong up-glacier dipping fabric on the ice-proximal side and a down-glacier dipping fabric on the distal side (Figure 2.7a; Sharp, 1984; see also Andrews and Smithson, 1966; Price, 1969, 1970).

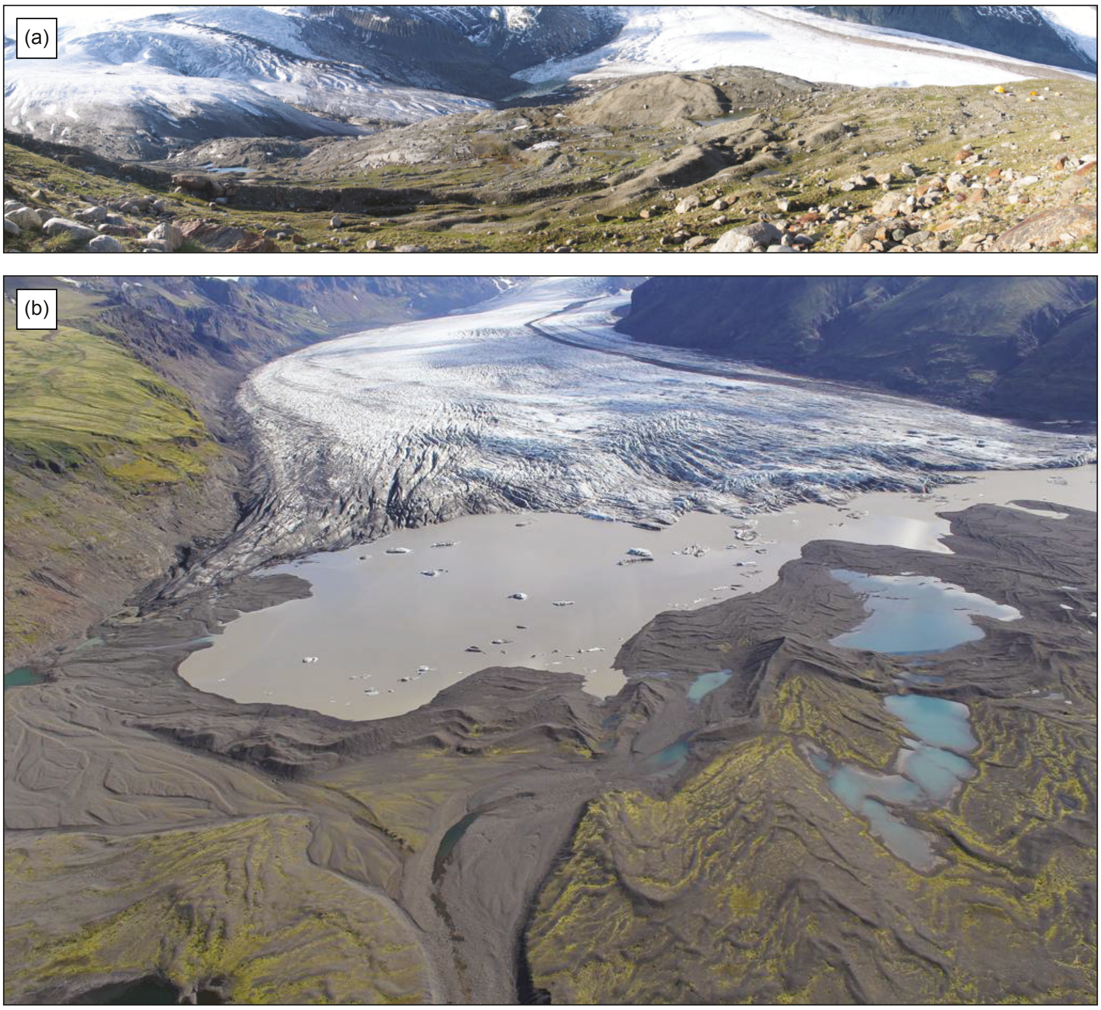

Figure 2.6: Photographs illustrating the typical planform geometry of annual moraines. (a) Field photograph of annual moraine ridges on the foreland of Gornergletscher (Swiss Alps) showing the typical arcuate planform and moraine asymmetry. Photograph: Sven Lukas (14.06.07). (b) Oblique aerial photograph of the Skaftafellsjökull foreland (SE Iceland) showing the striking saw-tooth planform of the annual moraines. Photograph: Andy Russell (13.07.14).

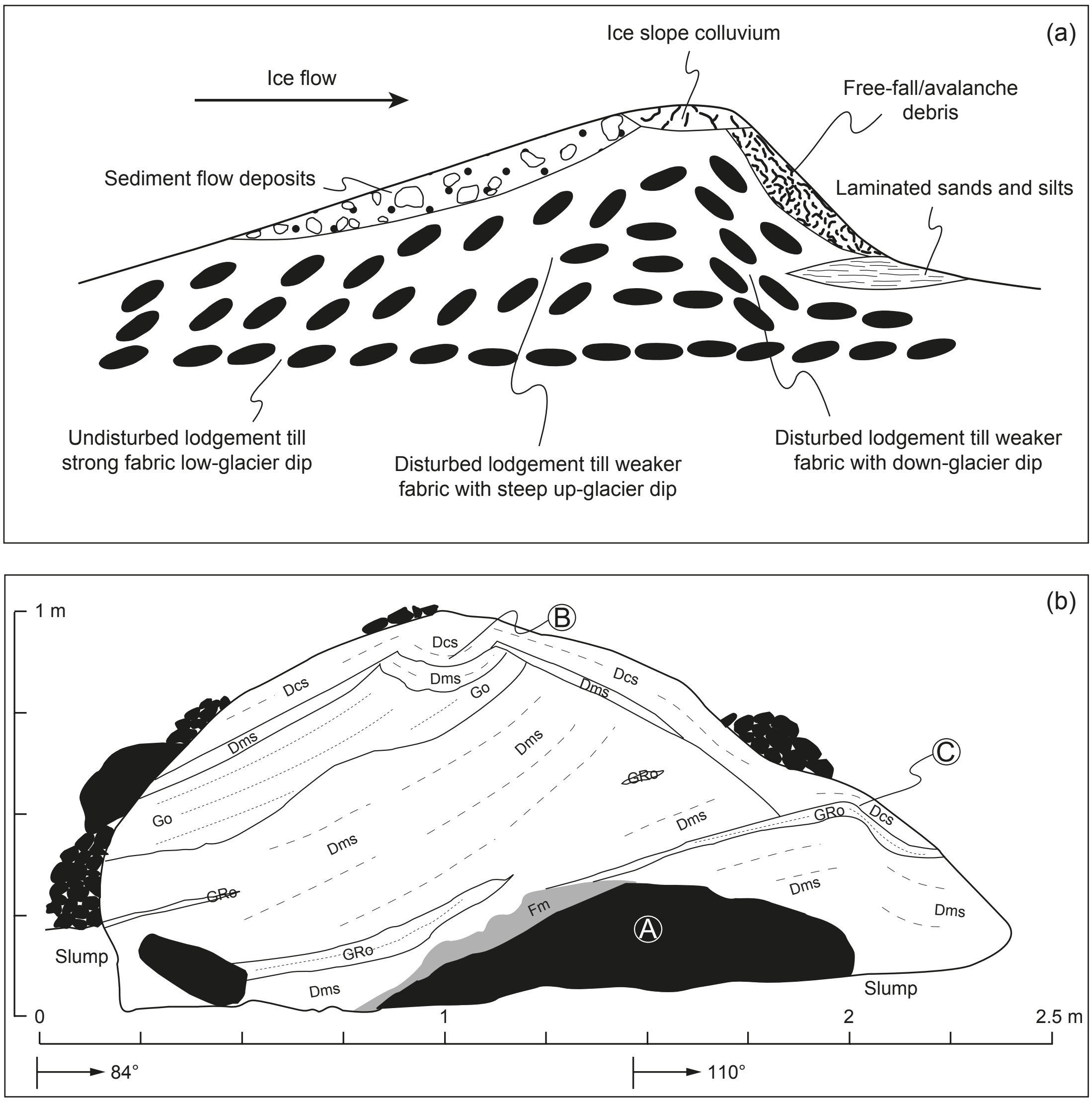

Figure 2.7: (a) Idealised internal composition and clast fabric of annual moraines according to Sharp (1984). Modified from Bennett (2001). (b) Sedimentological log showing the sedimentary composition of a deformed terrestrial ice-contact fan on the foreland of Gornergletscher, Switzerland (Lukas, 2012: 469). A. Prominent boulder. B. Channel-like structure. C. Unconformable drape of diamicton over openwork gravel units.

A range of genetic models have been posited for formation of the deformed sediment core in the literature, with no single hitherto proposed mechanism of formation able to account for the sedimentary composition and structure of all annual moraines. Thus, the term *annual moraines* encompasses a group of polygenetic glacial landforms. Price (1970) advocates a mechanism of squeezing of water-soaked till from beneath the glacier sole, as a result of static loading by ice, to produce proglacial moraine ridges which reflect ice-margin morphology (see also Hoppe, 1952; Andrews and Smithson, 1966; Price, 1973). Similarly, Sharp (1984) proposed a genetic model which couples annual moraine genesis to submarginal deformation of subglacial traction till (*sensu* Evans *et al*., 2006) and subsequent bulldozing of the extruded sediment. Depending on the efficacy of bulldozing capabilities, dead-ice may be incorporated into the moraine (inefficient bulldozing: *sensu* Lukas, 2012) as a consequence slumping of material onto the glacier surface and resulting differential ablation (Sharp, 1984; Lukas, 2012). Dead-ice incorporation within the moraine leads to significant post-depositional modification through sediment reworking, limiting the preservation potential of annual moraines formed through inefficient bulldozing (*cf*. Bennett, 2001; Kjær and Krüger, 2001; Lukas *et al*., 2005; Lukas, 2007a; Evans, 2009a; Lukas, 2012). Alternatively, annual moraine formation may occur through efficient or inefficient bulldozing of extant proglacial sediments (Boulton *et al*., 1974; Worsley, 1974; Birnie, 1977; Boulton, 1986; Lukas, 2012). A *snow-bank push* mechanism has also been invoked as a mode of annual moraine genesis, whereby deformation of sediment occurs along the suture between the advancing ice-margin and a frontal snow-bank (Birnie, 1977; Sharp, 1984). This genetic process results in the incorporation of winter snow within the moraine, resulting in significant post-depositional re-sedimentation and a rapid loss of the distinctive character of the moraine ridge (Birnie, 1977). Other models have advocated subglacial freeze-on (*sensu* Krüger, 1994, 1995) of basal, pre-existing proglacial and/or ice-marginal sediment and subsequent incremental melting out of the sediment during the ablation season (Andersen and Sollid, 1971; Krüger, 1995; Matthews *et al*., 1995; Krüger *et al*., 2010; Reinardy *et al*., 2013; see also Alexander and Worsley, 1973; Krüger, 1993, 1994, 1996; Evans and Hiemstra, 2005).

2.4.3 Application of annual moraines as climate proxies

Annual moraines potentially contain a seasonal signature of glacier response to climate fluctuations. Thus, annual moraine records identified in the geological record could represent valuable terrestrial climate archives (Bradwell, 2004a; Lukas, 2012; Bradwell *et al*., 2013). Since the spacing between successive annual moraines equates to the net ice-front recession in a single balance year (annual ice-margin retreat rate: IMRR), annual moraine sequences facilitate the examination of the relationship between IMRRs and climate variations (Lukas, 2012; Bradwell *et al*., 2013). The potential of annual moraines has long been realised, and several studies have examined this relationship (e.g. Sharp, 1984; Boulton, 1986; Krüger, 1995; Bradwell, 2004a; Beedle *et al*., 2009; Lukas, 2012; Bradwell *et al*., 2013). However, detailed statistical analysis of the relationship between IMRRs and different seasonal temperature signals is limited to a few studies (Bradwell, 2004a; Beedle *et al*., 2009; Lukas, 2012).

General comparison of IMRRs (annual moraine spacing) at maritime, lowland glaciers with climate variations have shown IMRRs are in tune with above-average ablation-season (summer) temperatures (Boulton, 1986; Krüger, 1995; Bradwell *et al*., 2013). More detailed statistical analysis conducted by Bradwell (2004a), the first study to explicitly report annual temperature series split into different seasonal signals, indicated a significant positive correlation between IMRRs and mean ablation-season (summer) temperatures ($r^2 = 0.56$, $p = 0.05$) at Lambatungnajökull, SE Iceland for the period 1931 – 1949 (Figure 2.8). This temporal coincidence between IMRRs and years of increased ablation-season temperature identified in previous studies (Sharp, 1984; Boulton, 1986; Krüger, 1995; Bradwell, 2004a; Bradwell *et al*., 2013) implies a rapid glacier *reaction time* (*sensu* Benn and Evans, 2010), with the ice-margin *reacting* almost instantaneously to climate variations at a sub-annual timescale (*cf*. Sigurðsson *et al*., 2007; Bradwell *et al*., 2013). This rapid short-term behaviour at the ice-margin should, however, be distinguished from the integrated longer-term behaviour of the whole glacier (glacier *response time*), which is usually of the order decades in maritime glaciers (*cf*. Jóhannesson *et al*., 1989; Haeberli, 1995; Bahr *et al*., 1998; Benn and Evans, 2010; Cuffey and Paterson, 2010; Bradwell *et al*., 2013). Indeed, whilst the time lag between climate variation and the detection of change at the glacier terminus is small, it does not necessarily indicate that the glacier terminus has fully responded to the climate variation (*cf*. Sigurðsson *et al*., 2007; Benn and Evans, 2010). In a more continental setting, Lukas (2012) established that IMRRs were somewhat weakly correlated with annual mean temperature ($r^2 = 0.1925$, $p = 0.0282$) and winter temperature ($r^2 = 0.2026$, $p = 0.0240$) anomalies. However, the extraction of a climate signal was complicated by other factors, particularly the presence of a reverse-bedrock slope from whence Gornergletscher is retreating (Lukas, 2012).

Although annual moraines represent a potentially valuable terrestrial climate archive, it should be recognised that the composite climate signal is complex, with multiple periodicities in climate reinforcing or modulating each other. As such, unravelling the relationship between moraine chronologies and climate variability (at a range of temporal scales) may not be straightforward (*cf*. Kirkbride and Brazier, 1998; Kirkbride and Winkler, 2012, and references therein). Indeed, it is widely recognised that glaciers filter the frequencies of climate variability to which glaciers respond (Kuhn, 1985; Jóhannesson, 1986; Oerlemans, 2007; Cuffey and Paterson, 2010; Winkler *et al*., 2010; Kirkbride and Winkler, 2012). Moreover, extracting a climate signal from annual moraine chronologies may be complicated by additional, non-climatic factors which are known to influence: (1) moraine formation (see Mercer, 1961; Funder, 1972, 1989; Punkari, 1980; Warren and Hulton, 1990; Warren, 1991; Kessler *et al*., 2006; Kaplan *et al*., 2009; Pratt-Sitaula *et al*., 2011; Anderson *et al*., 2012; Barr and Clark, 2012; Barr and Lovell, 2014); preservation (see Putkonen and O’Neal, 2006; Anderson *et al*., 2012; Kirkbride and Winkler, 2012; Barr and Lovell, 2014); and (3) ease of identification (see Barr and Clark, 2012; Barr and Lovell, 2014).

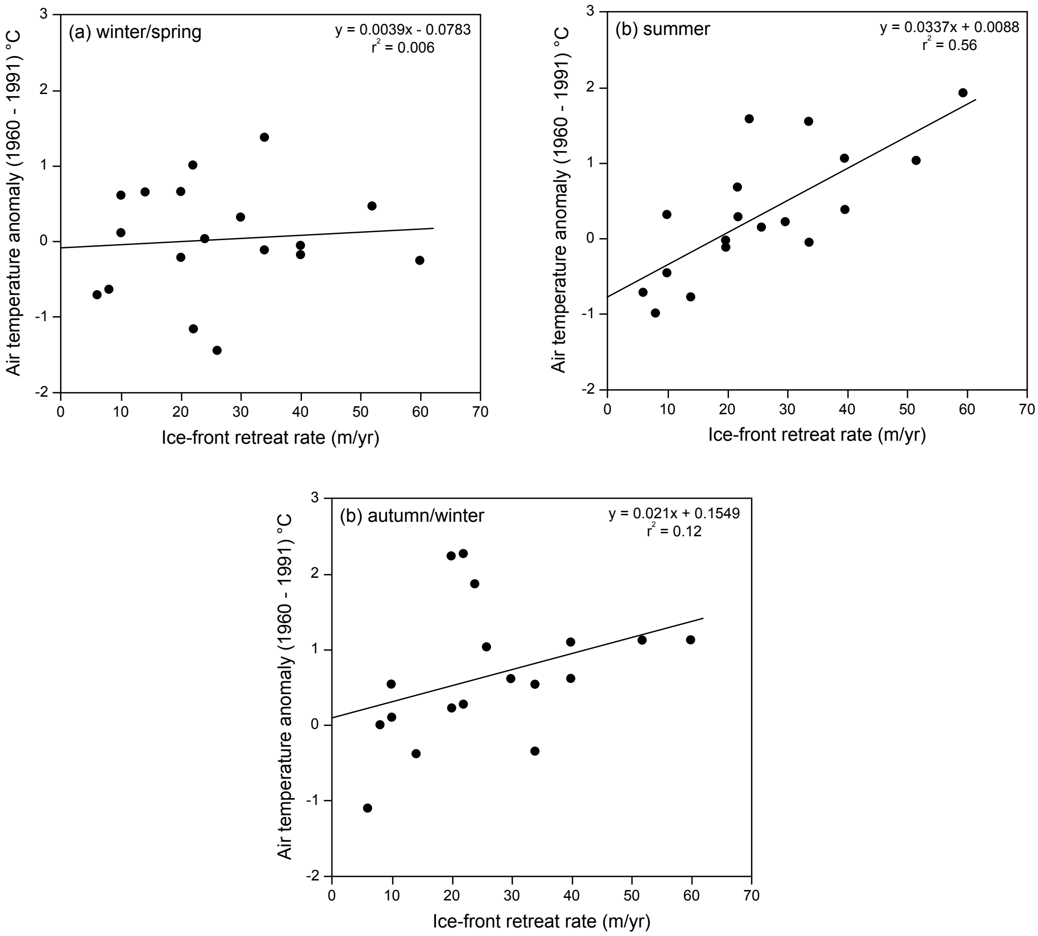

Figure 2.8: Comparison of seasonal temperature deviations from the 1961 – 1990 average at Hólar í Hornafirði and annual ice-margin retreat rates (IMRRs: m a^{-1}) at Lambatungnajökull. (a) winter/spring (1st February – 31st May); (b) summer (1st June – 30th September); and (c) autumn/winter (1st October – 31st January) for the period 1931 – 1949. Hólar í Hornafirði is located ~18 km South of Lambatungnajökull. Redrawn from Bradwell (2004a).

In terms of non-climatic controls on moraine formation, the propensity of moraines to form at topographic pinning points is particularly relevant to Icelandic outlet glaciers. Variations in valley width may regulate glacier mass balance and ice-margin stability, promoting moraine deposition in piedmont zones (*cf.* Dugmore, 1989; Barr and Clark, 2012; Barr and Lovell, 2014, and references therein). Many Icelandic outlet glaciers descend onto unconfined plains, spreading laterally to form piedmont lobes, thus topography could affect the integrity of moraine sequences (*sensu* Kirkbride and Winkler, 2012). However, the topographic independence of piedmont glaciers is likely to limit the importance of variations in valley width (Barr and Lovell, 2014).

Moraine chronologies evident in the modern landscape may represent only a sample of those that formerly existed, owing to erosional censoring of the moraine record (*cf.* Gibbons *et al.*, 1984; Kirkbride and Brazier, 1998; Kirkbride and Winkler, 2012; Barr and Lovell, 2014). Erosional censoring refers to the eradication of landforms and sediments from the geological record by syn- and post-depositional processes, reducing the climatic representativeness of the moraine record (Kirkbride and Winkler, 2012). Erosional censoring of the moraine record may occur through self-censoring, external censoring or a combination thereof (Table 2.4). Self-censoring may take two forms: (1) glacier advances may override, and remove, evidence through a process known as obliterative overlap (Gibbons *et al*., 1984; Kirkbride and Brazier, 1998; Kirkbride and Winkler, 2012); or (2) melting of debris-covered ice in ice-cored moraines (*cf*. Schomacker and Kjær, 2007, 2008; Schomacker, 2008; Lukas, 2011; Kirkbride and Winkler, 2012, and references therein). Self-censoring of Icelandic annual moraine records is particularly relevant as previous studies have identified local superimposition of moraines and ice-cored annual moraines on Icelandic forelands (e.g. Price, 1970; Sharp, 1984; Evans and Twigg, 2002; Evans and Orton, 2014). Following deposition, moraine ridges become vulnerable to a variety of external (i.e. non-glacial) processes which may result in erosion and censoring of the record (Table 2.4; Kirkbride and Winkler, 2012; Barr and Lovell, 2014). The Icelandic proglacial environment is one of the most inimical to moraine

Table 2.4: Processes resulting in the censoring of moraine sequences. *Source:* Kirkbride and Winkler (2012: 9) and Barr and Lovell (2014: 56).

Process	Effect	Timescale
Obliterative overlap	Re-advances of larger extent destroy landforms of earlier less extensive advances.	$10^1 – 10^5$ yr (Occasional)
Dead-ice melting	Moraine surfaces gradually lowered as ice cores melt (only applies to ice-cored moraines).	$10^2 – 10^3$ yr (Continuous)
Fluvial erosion	Lateral migration of river channels removes moraines by undercutting. Particularly effective on large proglacial fans with multiple avulsing channels and high peak discharges.	$10^1 – 10^3$ yr (Continuous)
Alluvial deposition	Effective at large coupled ice-margins where glacial-to-proglacial sediment transfer is efficient. Moraines on glacier foreland are buried by proglacial aggradation.	$10^2 – 10^4$ yr (Continuous)
Jökulhlaups	Wholesale destruction or burial of foreland landsystems by exceptional glaciovolcanic (subglacial) floods. Partial censoring by smaller floods may strip surface sediment from moraines and modify, but not destroy, pre-existing forms.	Hours to days. Episodic, rare at global scale, but regionally occasional.
Lake-drainage floods	Outburst floods from failed ice- and moraine-dammed lakes, or overwash events of displaced water by avalanching into lakes. Erosion of proximal deposits, possible burial in more distal locations.	Hours to days. Episodic, rare at global scale, but regionally occasional.
Rock avalanches	Incorporation of moraines into moving avalanche, and/or burial in avalanche run-out zones.	Minutes, rare, but regionally occasional.
Paraglacial slope processes	Erosion of unconsolidated, steep lateral moraine material, which may be stripped down to bedrock. Interaction with fluvial/glaciofluvial erosion possible. Downslope redeposition buries valley-floor moraines.	Repetitive over $10^1 – 10^3$ yr. Episodic, common.

preservation as a consequence of large braided outwash streams that characterise Icelandic outlet glaciers, some of which may provide conduits for jökulhlaups, and all of which feature influential channel avulsion in aggrading outwash plains (Kirkbride and Winkler, 2012).

An awareness of the abovementioned potential confounding factors is crucial when employing moraine chronologies to extract a climatic signal. The efficacy of these factors affects the integrity of the sequence, which is how faithfully the moraine sequence records climate variations rather than being a product of non-climatic factors, and thus the applicability of the moraine sequence as a climate proxy (*cf*. Kirkbride and Winkler, 2012; Barr and Lovell, 2014).

2.5 Summary

This chapter has reviewed the key literature pertinent to the research in this thesis, elaborating on concepts introduced in Chapter 1 and providing a conceptual framework for the findings that will be presented and synthesised in Chapters 5 – 7. Based on the current state of understanding, Icelandic glaciers are believed to have undergone their most extensive Holocene advances during the Little Ice Age (e.g. Thórarinsson, 1943; Guðmundsson, 1997; Hannesdóttir *et al*., 2014). This period of glacier advance is believed to be the most recent in a series of synchronous century-scale periods of glacier expansion (Little Ice Age Type Periods) and nested decadal-scale advances (Little Ice Age Type Events) that occurred throughout Iceland during the Neoglacial period (*cf*. Guðmundsson, 1997; Kirkbride and Dugmore, 2006). Measurements of annual-scale termini variations since the 1930s reveal non-surge-type Icelandic glaciers exhibited rapid retreat during the period 1930 – 1960 (Eyþorsson, 1931, 1963; Sigurðsson, 1998; Sigurðsson *et al*., 2007). In subsequent decades, many non-surge-type glaciers underwent re-advance before recommencing ice-frontal retreat during the 1990s. Since 2000, all monitored non-surge-type glaciers have been retreating (Sigurðsson, 2005a; Sigurðsson *et al*., 2007). These trends in termini variations have previously been associated with fluctuations of summer air temperature (e.g. Sigurðsson and Jónsson, 1995; Jóhannesson and Sigurðsson, 1998; Sigurðsson *et al*., 2007). However, consideration of other potential drivers of glacier change (e.g. sea surface temperature and the North Atlantic Oscillation) has been limited. This is currently limiting understanding of recent Icelandic glacier change and its wider significance, particularly regarding whether current ice-frontal retreat is being driven by a local or regional mechanism. Thus, analysis of a wider array of climate variables is necessary to further understanding of contemporary Icelandic glacier change.

The decadal-scale and annual-scale glacier fluctuations highlighted above are reflected in the sediment-landform assemblages that characterise the forelands of active temperate Icelandic glaciers (Evans and Twigg, 2002; Evans, 2003a; Evans and Orton, 2014; Evans *et al*., submitted). Active temperate glacial landsystems, of which the Skálafellsjökull foreland is an exemplar (*cf*. Evans and Orton, 2014), are characterised by three dominant depositional domains: (1) the marginal morainic domain; (2) the subglacial domain; and (3) the glaciofluvial and glaciolacustrine domain (Evans and Twigg, 2002; Evans, 2003a). Importantly, the small-scale recessional push/squeeze ("annual") moraines that characterise the marginal morainic domain provide a record of ice-frontal fluctuations at many active temperate glaciers in Iceland (e.g. Price, 1970; Sharp, 1984; Boulton, 1986; Evans and Twigg, 2002; Evans and Hiemstra, 2005; Bradwell *et al*., 2013). Long sequences of annual moraines potentially contain a seasonal signature of glacier response to climatic fluctuations and, therefore, represent a valuable terrestrial climate archive (e.g. Boulton, 1986; Bradwell, 2004a; Lukas, 2012; Bradwell *et al*., 2013). Thus, detailed examination of the characteristics of "annual" moraines on the Skálafellsjökull foreland could yield valuable insights into the recent pattern and rates of ice-marginal retreat. Nonetheless, it is important to recognise factors that could potentially affect the integrity of the "annual" moraine sequence(s), and hence their applicability (*cf*. Kirkbride and Winkler, 2012).

CHAPTER 3

Location and setting of Skálafellsjökull

This chapter aims to place the study area in context in terms of its geographic and geological setting (Section 3.1), climatic setting (Section 3.2) and glaciological setting (Section 3.3). The characteristics described in the first two sections have important roles in the glaciology and dynamics of Skálafellsjökull, as well as "annual" moraine formation and current glacier change. Given the importance of climate in glacier change, the climate of SE Iceland is analysed in further detail in Chapter 6, with Section 3.2 providing only a brief overview of the climatic setting of Skálafellsjökull. Section 3.3 describes the glaciological setting of the study area, considering the glaciological characteristics of the Vatnajökull ice-cap and the glacial history of Skálafellsjökull. This provides important context for the ice-frontal fluctuations explored in this thesis. In the fourth section of this chapter (Section 3.4), previous work at Skálafellsjökull is discussed, highlighting how the research in this thesis fits within the framework of research conducted at the outlet glacier. The contextual factors discussed in this chapter are subsequently referred to in Chapter 7, wherein the characteristics of the recessional ("annual") moraines on the Skálafellsjökull foreland are synthesised.

3.1 Geographic and geological setting

Skálafellsjökull is a non-surging piedmont outlet lobe draining the southeastern margin of the Vatnajökull ice-cap, situated in SE Iceland (Figures 3.1 and 3.2). Skálafellsjökull flows for *c.* 25 km from the Breiðabunga plateau in eastern Vatnajökull, descending steeply from the lava plateau onto a low elevation foreland and terminates at an altitude of *c*. 60 m a.s.l. on the Hornafjördur coastal plain (Sharp, 1984; Sigurðsson, 1998; McKinzey *et al*., 2004; Evans and Orton, 2014). At its northern margin, the piedmont lobe is topographically confined by the Hafrafellsháls mountain spur, which reaches a maximum elevation of *c*. 1008 m a.s.l. (Evans and Orton, 2014). The present-day glacier terminates in a snout zone *c*. 3 km wide, terminating on the sandur of Heinabergsvötn in the north and an area of heavily abraded, basalt bedrock outcrops on Hjallar in the southern part of the foreland (Sharp, 1982b; Evans and Orton, 2014). The contemporary Skálafellsjökull ice-margin is fronted by two proglacial lakes, the largest situated on Heinabergsvötn, and a smaller proglacial lake at the southern margin (Figure 3.2b). The development of ice-marginal lakes is a characteristic feature of the retreating southern Vatnajökull outlet glaciers (e.g. Björnsson *et al*., 2001; Nick *et al*., 2007; Schomacker, 2010).

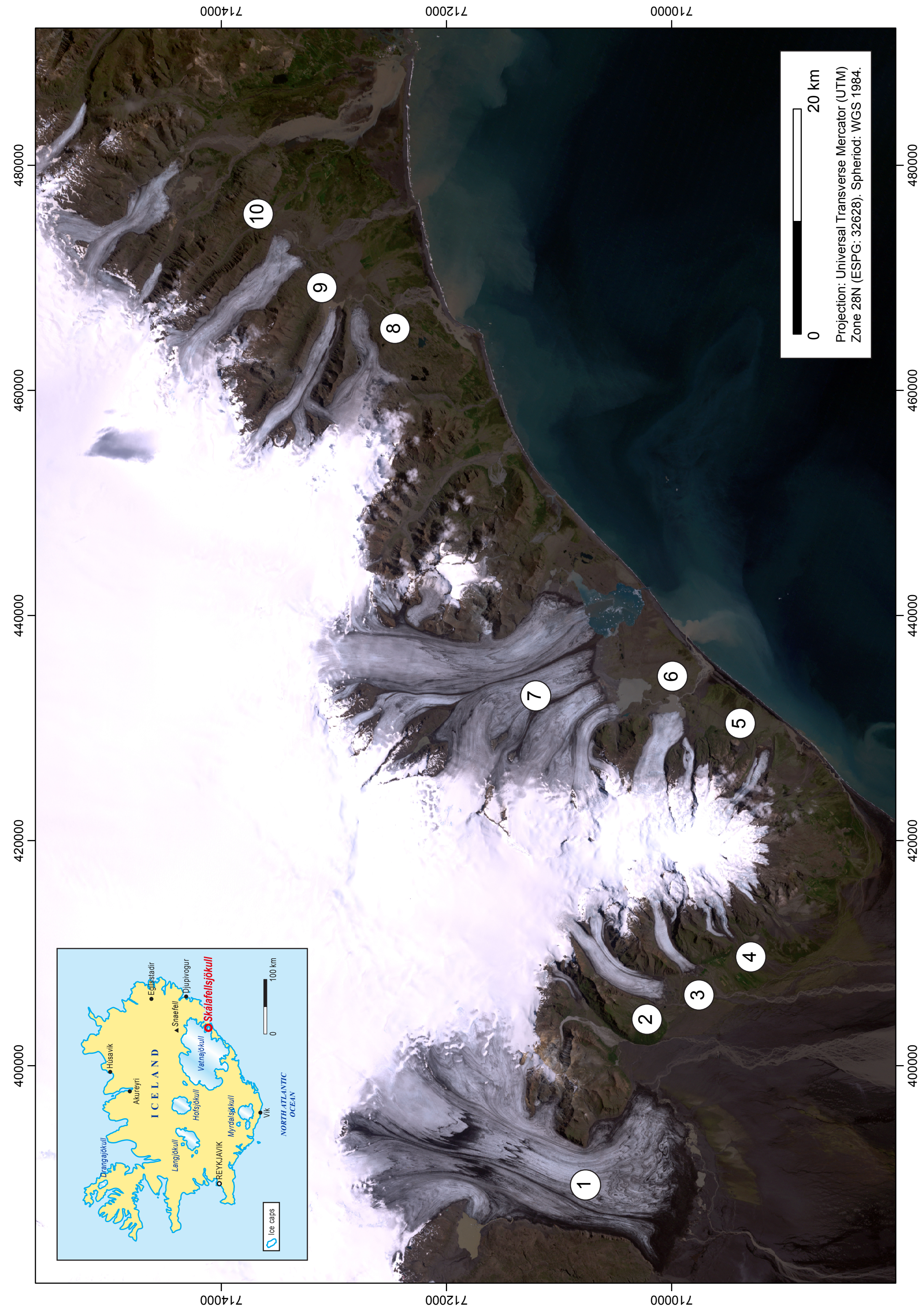

Figure 3.1: Satellite image and map of the Vatnajökull southern margin, showing the location of the study site and its relation to the other main outlet glaciers. Imagery is a Landsat 7 ETM+ scene (captured on 07.08.2006) displayed as a natural colour image (Bands 3, 2 and 1). Image L71217015_01520060807, downloaded from Global Land Cover Facility (GLFC; http://www.landcover.org). 1 = Skeiðarárjökull; 2 = Skaftafellsjökull; 3 = Svínafellsjökull; 4 = Virkisjökull-Falljökull; 5 = Kvíárjökull; 6 = Fjallsjökull; 7 = Breiðamerkurjökull; 8 = Skálafellsjökull; 9 = Heinabergsjökull; 10 = Fláajökull.

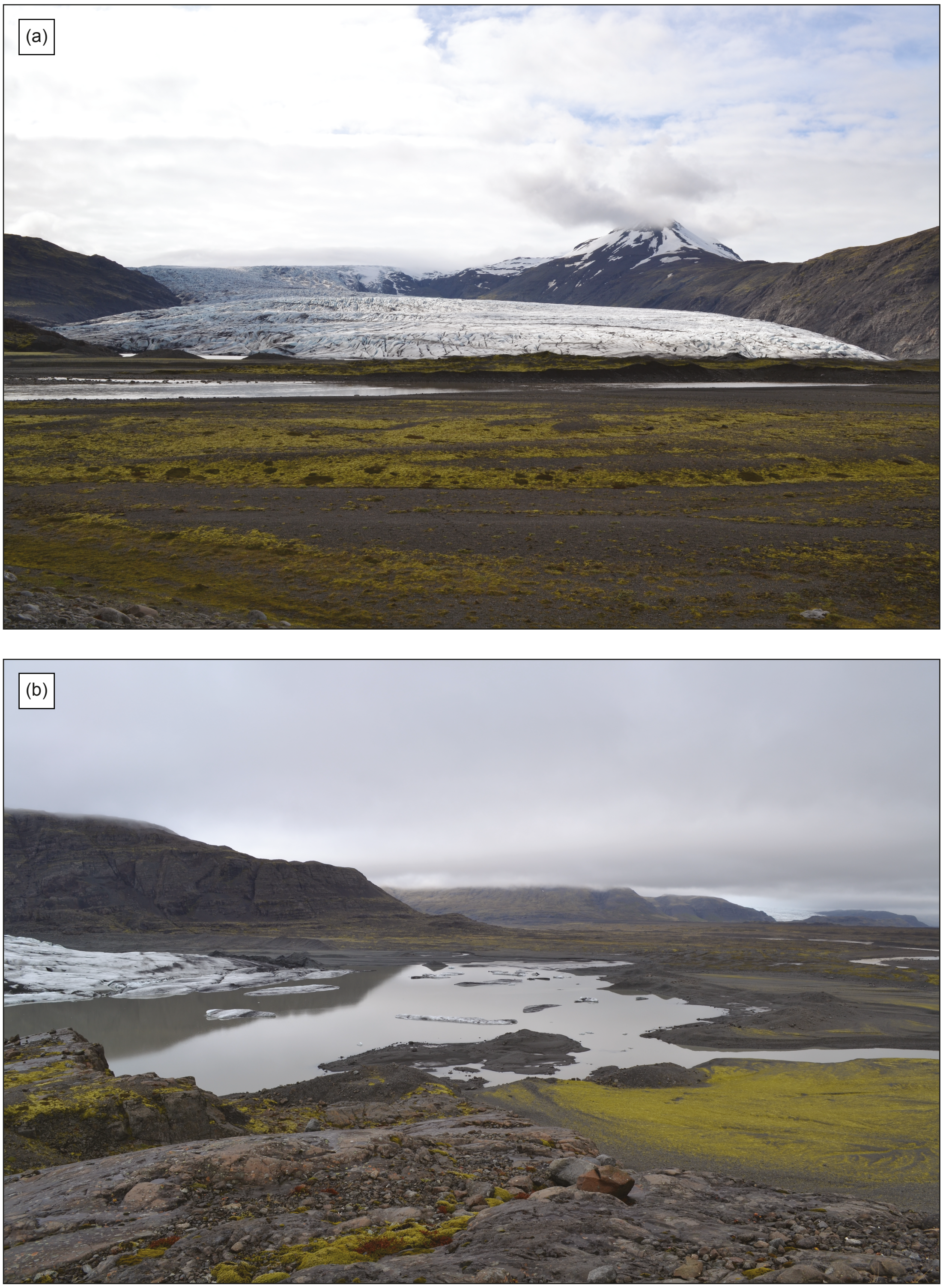

Figure 3.2: (a) Field photograph showing Skálafellsjökull flowing down onto Heinabergsvötn, with the mountain spur Hafrafellsháls confining the northern margin of Skálafellsjökull to the right of the photograph (27.05.14). (b) Photograph of the proglacial lake that has developed at the margin of Skálafellsjökull (21.05.14).

Skálafellsjökull is characterised by a high-elevation nevé and has an area of *c*. 137 km^2 (Randolph Glacier Inventory, 2014; Pfeffer *et al*., 2014). The glacier is predominantly nourished by the main Vatnajökull ice-cap but is also nourished by small accumulation basins along the northern side of the Kalfafellsfjöll ridge at its southern margin (Sharp, 1982b). The Kalfafellsfjöll ridge is breached by Sultartungujökull (also called Eyvindstungnajökull) a subsidiary outlet which diverges from the southern margin of Skálafellsjökull, draining into Stadardalur and presently terminates *c*. 400 m a.s.l. above the Jöklasel road (Sharp, 1982b; McKinzey *et al*., 2004; Sigurðsson and Williams, 2008).

The study area lies within the Tertiary Basalt Formation of Eastern Iceland, with the surrounding mountains comprised almost entirely of basalt flows. The basalt flows in this region constitute some of the youngest lavas of the Tertiary Basalt Formation, formed by repeated effusive eruptions *c*. 5 – 6 Ma BP (Thordarsson and Höskuldsson, 2002). These stacked flood basalts have been tilted and subsequently faulted by more recent tectonic activity (Saemundsson, 1979; Bradwell, 2001b). The bedrock geology of the Skálafellsjökull catchment is believed to consist largely of west-dipping basalt lavas which are interstratified with tuffs and tillites (Walker, 1964). Additionally, there is a gabbro intrusion situated beneath the southern margin of the glacier at Þormodarhnuta, and acid volcanic rocks and palagonite tuffs occur in the upper part of the catchment (Walker, 1964; Sharp, 1982b, 1984). According to Saemundsson (1979), the Breiðabunga plateau from whence Skálafellsjökull flows may be a subglacial central volcano complex.

The surficial geology of the Skálafellsjökull foreland is dominated by glacial and glaciofluvial deposits (Sharp, 1982b, 1984; Dowdeswell and Sharp, 1986; Evans, 2000; Evans and Orton, 2014). Extensive glacial outwash sands and gravels are prevalent across the foreland, similar to other southern Vatnajökull piedmont lobes (e.g. Evans and Twigg, 2002; Evans, 2003a, 2005). These glaciofluvial deposits are manifest either as coalescent proglacial outwash fans, with pitted and/or collapsed ice-contact surfaces (outwash heads), or as narrow strips of ribbon sandur deposited in channels incised through morainic and subglacial depo-centres (Evans and Orton, 2014). Till deposits on the Skálafellsjökull foreland are typically less than 3 m in thickness and exhibit the characteristics of subglacial traction till (*cf*. Sharp, 1982; Dowdeswell and Sharp, 1986; Evans, 2000; Evans *et al*., 2006; Evans and Orton, 2014). Thicker till deposits occur in low-relief areas of the foreland where pre-existing outwash deposits enabled widespread cannibalisation for the subglacial deformation process (Evans and Orton, 2014). Conversely, till deposits thicken only on the lee side of roches moutonnées in the southern part of the Skálafellsjökull foreland, an area where bedrock outcrops dominate (Sharp, 1982b, 1984; Evans and Orton, 2014).

3.2 Climatic setting

Located at the boundary between the relatively warm, saline Atlantic Ocean current and the colder, low-salinity current from the Arctic Ocean, Iceland is situated in a climatically sensitive position in the North Atlantic (Einarsson, 1984; Bradwell *et al*., 2006; Geirsdóttir *et al*., 2009; Ólafsdóttir *et al*., 2013). Situated between latitudes 63°23'N and 66°32'N and longitudes 13°30'W and 24°32'W, Iceland's climate is strongly influenced by the Icelandic Low, a semi-permanent low-pressure centre which forms one pole of the North Atlantic Oscillation (NAO; Hurrell, 1995; Hurrell *et al*., 2003). Due to the warm Irminger Current, which encircles the south, west and north coasts, the south coast of Iceland experiences a relatively mild and moist climate (Einarsson, 1984; Bradwell, 2001a; Geirsdóttir *et al*., 2009; Björnsson *et al*., 2013; Ólafsdóttir *et al*., 2013). Conversely, the North receives cold waters from a branch of the East Greenland and East Icelandic currents (Einarsson, 1984; Bradwell, 2001a). As a consequence of these surface currents, a steep climate gradient exists across Iceland (Stefánsson, 1969; Bradwell, 2001a; Geirsdóttir *et al*., 2009).

Weather conditions in Iceland are monitored by *Veðurstofa Íslands* (the Icelandic Meteorological Office) through a network of weather stations distributed throughout Iceland. The longest continuous record in SE Iceland is that of Teigarhorn (1873 – present) which is situated at 64°40.540'N, 14°20.663'W (20.7 m a.s.l.). Meanwhile, the nearest long-term weather station to the study site is located at Hólar í Hornafirði (64°17.995'N, 15°11.402'W; 16.0 m a.s.l.), situated approximately ~24 km East of Skálafellsjökull. Mean annual temperature values at Teigarhorn (1873 – present) and Hólar í Hornafirði (1921 – present) are in close agreement for the entire measurement period (Figure 3.3), with mean annual temperature at Teigarhorn generally being 0.6 – 0.9°C lower than those at Hólar í Hornafirði. Mean annual temperatures at Hólar í Hornafirði were 4.5°C for the period 1961 – 1990, whilst at Teigarhorn (~70 km N of Hólar í Hornafirði) mean annual temperatures were 3.7°C for the same period. Mean summer temperatures (1st June – 30th September; 1961 – 1990) at Hólar í Hornafirði are *c*. 9.0°C, although it is not uncommon for daily temperature maxima to exceed 20°C during the summer months. Temperatures during the autumn/winter (1st October – 31st January; 1961 – 1990) are typically –0.5°C to +4.5°C, averaging ~ 2.2°C. The meteorological data for Hólar í Hornafirði indicate that July is typically the warmest month during the year, with an average temperature of 10.2°C (1961 – 1990), whilst December is typically the coldest month with an average temperature of 0.0°C for the same period (Figure 3.4). Mean annual precipitation over the period 1961 – 1990 was *c*. 1500 mm at Hólar í Hornafirði. There is no definitive seasonal trend in precipitation in SE Iceland, though the wettest months are typically October, December and January (Figure 3.4).

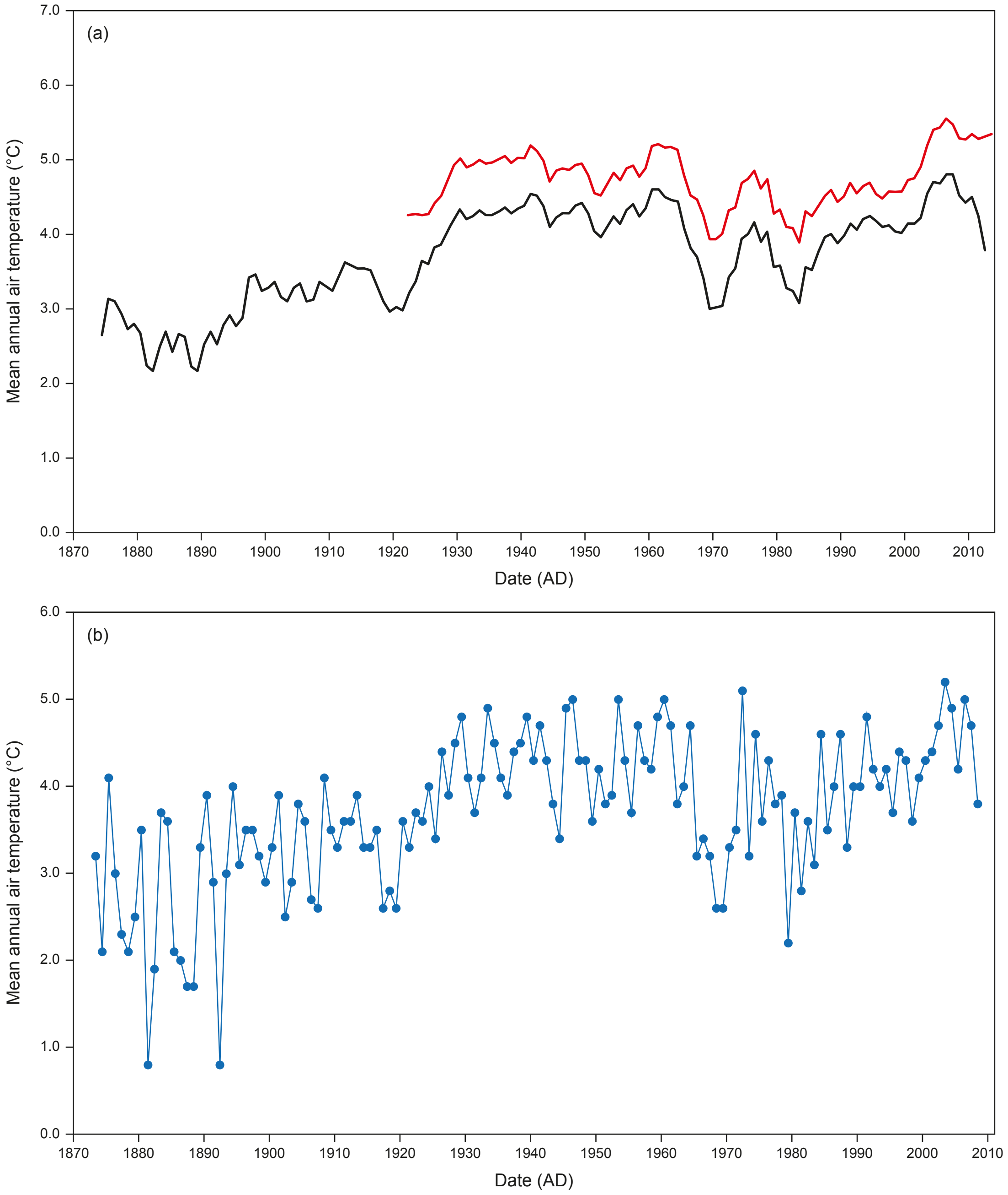

Figure 3.3: (a) Comparison between mean annual air temperatures at Teigarhorn (black line) and Hólar í Hornafirði (red line). Temperatures are plotted as five-year running means. (b) Mean annual temperature at Teigarhorn since 1873. This is longest temperature series from SE Iceland, and the second longest from Iceland. Meteorological data supplied by *Veðurstofa Íslands*. Graphs after Bradwell (2001a: 88).

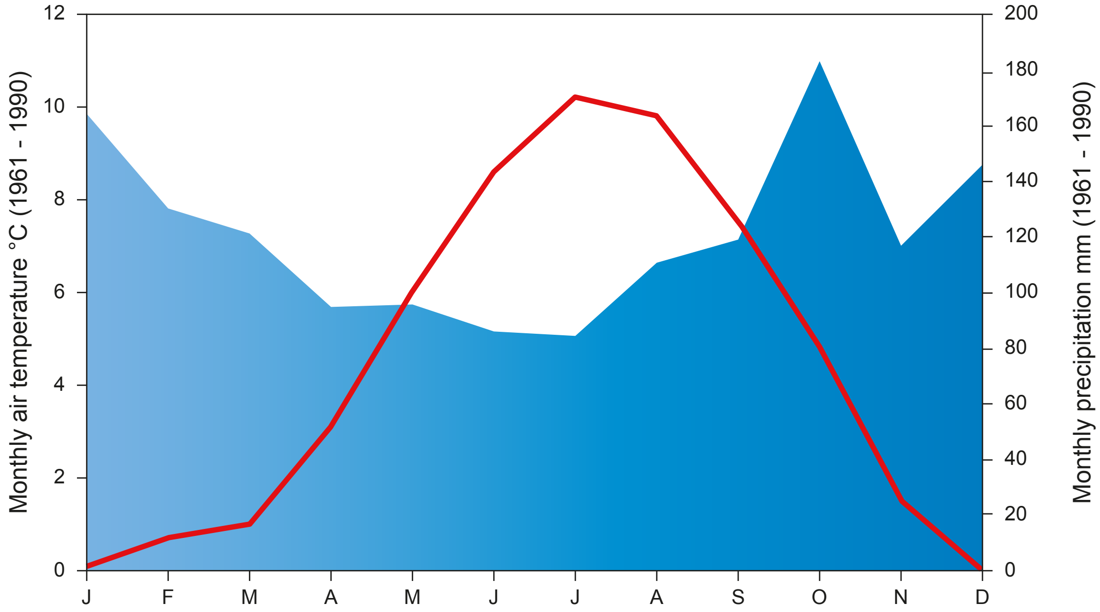

Figure 3.4: Mean monthly meteorological data from the Hólar í Hornafirði weather station (64°17.995'N, 15°11.402'W; 16.0 m a.s.l.). Mean monthly air temperatures for the period 1961 – 1990 are shown by the red line, whilst mean monthly precipitation is shown by the blue shading. Meteorological data supplied by *Veðurstofa Íslands*.

3.3 Glaciological setting

Vatnajökull covers an area of *c*. 8100 km^2 and is the largest non-polar ice-cap in Europe (Sigurðsson, 1998; Flowers *et al*., 2005; Björnsson and Pálsson, 2008). The ice-cap lies on a highland plateau, with six mountain ranges forming the main glaciation centres of the Vatnajökull ice-cap: Grímsfjall (1,700 m a.s.l.), Bárðarbunga (1,800 m a.s.l.), Kverkfjöll (1,930 m a.s.l.), Öræfajökull (2,000 m a.s.l.), Esjufjöll (1,600 m a.s.l.) and Breiðabunga (1,200 m a.s.l.). Moreover, the majority of the bed (88%) lies above 600 m a.s.l. (Björnsson and Pálsson, 2008). Vatnajökull has 46 officially named, discrete outlet glaciers, inclusive of the 13 Öræfajökull outlets (Sigurðsson and Williams, 2008). The outlets at the northern and western margins take the form of large, lobate surge-type glaciers, fluctuating independently of climate (e.g. Brúárjökull, Dyngjujökull, Tungnaárjökull; Thórarinsson, 1943; Björnsson, 1979, 1988; Sigurðsson, 1998). The southern and eastern margins are characterised by non-surge-type glaciers, with several of them terminating close to sea level (50 – 150 m a.s.l.). Some of the Vatnajökull outlets also exhibit both surge-type and climatically-sensitive behaviour (e.g. Breiðamerkurjökull; Jóhannesson and Sigurðsson, 1998). Öræfajökull, the southernmost portion of the Vatnajökull ice cap, is a glaciologically distinct ice centre covering the Öræfajökull stratovolcano (Sigurðsson, 1998; Bradwell *et al*., 2013).

The southern Vatnajökull outlet glaciers are classified as maritime (winter-type accumulation), temperate glaciers, with a strong preference towards mass loss during summer months (Björnsson, 1979; Björnsson *et al*., 1998). The ablation season typically extends between May and September. The annual net balance of Vatnajökull has been negative since 1995/1996, losing *c*. 0.8 m a^{-1} averaged over the entire ice cap (Björnsson and Pálsson, 2008). For the period 1995–2010, the cumulative mass loss averaged over the ice-cap was 13 m_{we} (8 m_{we} from the inland outlets and 20 m_{we} from the maritime outlets; Björnsson *et al*., 2013). During years of zero net balance, the Vatnajökull ice-cap typically discharges 501 $m^3 s^{-1}$ of water, relating specifically to summer balance (Björnsson *et al*., 1998; Björnsson and Pálsson, 2008). Thus, Vatnajökull is a dynamic conveyor in the hydrological cycle of SE Iceland (Flowers *et al*., 2005). In addition to surface melting, continuous geothermal activity at the bed of the Vatnajökull ice-cap and transitory volcanic eruptions during the 1990s resulted in *c*. 0.55 $km^3 a^{-1}$ of melting on average, equivalent to only 4% of total surface ablation during one average year of zero mass balance (Björnsson, 2002; Björnsson and Pálsson, 2008).

Skálafellsjökull, which flows from the southeastern margin of Vatnajökull, formerly coalesced with its neighbouring outlet Heinabergsjökull on the coastal plain of Hornafjördur (e.g. Figure 3.5; Danish General Staff, 1904; Wadell, 1920; Roberts *et al*., 1933; Thórarinsson, 1943; Pálsson, 1945; Hannesdóttir *et al*., 2014). Skálafellsjökull and Heinabergsjökull had begun retreating when Thoroddsen (1911) visited the area, though were still confluent during a survey of the area in 1929 (Eiriksson, 1931). By the time of the US Army Map Service aerial photograph survey in 1945, the glaciers had separated. Contemporary accounts from the 18th and 19th centuries provide valuable information on fluctuations of the combined Heinabergsjökull/Skálafellsjökull glacier (referred to as Heinabergsjökull) during this time period. For example, Ólafsson and Pálsson (1975, written 1772) state that “Heinabergsjökull has destroyed the central part of Hornafjördur, above which it is situated, one arm having reached right down on the plain to the farm Heinaberg, which nevertheless is still inhabited”. Based on the available documentary evidence, Thórarinsson (1943: 23) summarises the following history for the combined Heinabergsjökull/Skálafellsjökull glacier:

- 1700 – 1750: On the whole advance.
- *c*. 1750: Glacier larger than in 1938, probably larger than in 1898, and at maximum extension so far in historical times.
- 1750 – 1897: Glacier larger than in 1898.
- Years or decades immediately preceding 1839: Advance.
- 1857: Glacier in a very advanced position.
- 1860s: Probably stagnation or recession.
- 1870s – 1887: Mostly slight advance. Reached historical maximum extent.

- 1887 – 1903: 420 m retreat (–26 m a^{-1}).
- 1903 – 1930: 350 m retreat (–13 m a^{-1}).

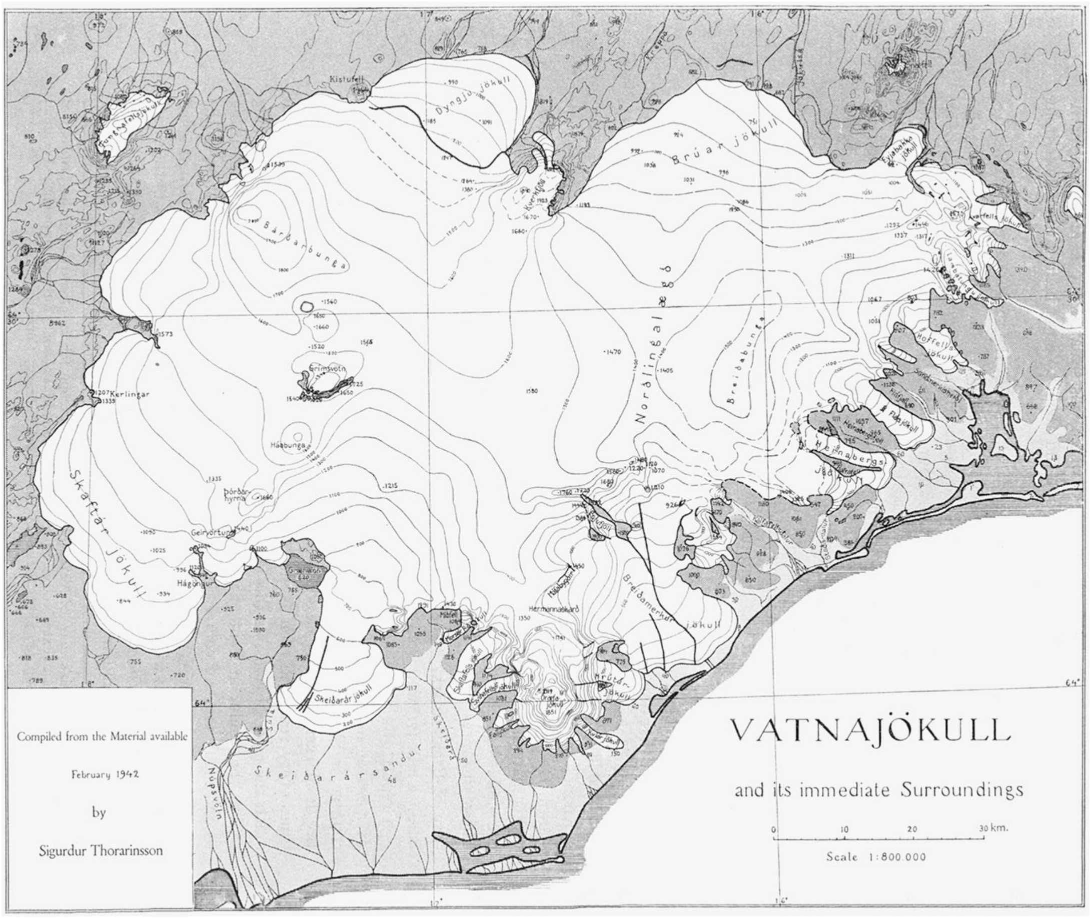

Figure 3.5: Map of the Vatnajökull ice-cap produced by Pálsson (1794), with minor alterations by Thórarinsson (1943).

Annual field measurements of ice-front fluctuations at Skálafellsjökull were conducted by the Icelandic Glaciological Society between the period 1930 and 1957, and intermittently during the 1960s (Sigurðsson, 1998). Sporadic measurements of glacier termini variations have been taken at Skálafellsjökull since the 1990s (Sigurðsson, 1998; 2005b), with the infrequency of the measurements reflecting the presence of the large proglacial lake at the ice margin which precludes direct tape measurements (O. Sigurðsson, pers. comm., 2013). The dataset of ice-measurements for Skálafellsjökull (Figure 3.6) reveals that the ice-front was retreating during the period 1932 – 1957, with particularly rapid ice-marginal retreat occurring between 1937 and 1942 (*c*. –41 m a^{-1}). However, the maximum amount of ice-marginal retreat in any given year occurred in 1932 (–57 m). Glacier advance occurred in 1960 (+25 m) and in the period 1992 – 1995 (+3 m a^{-1}). By 2011, the Skálafellsjökull had retreated 476 m relative to the 1995 ice-front position. Despite the sporadic nature of ice-front measurements for Skálafellsjökull, it is apparent that ice-front variations for this glacier exhibit the same general trends as similar sized glaciers in SE Iceland (Figure 3.6).

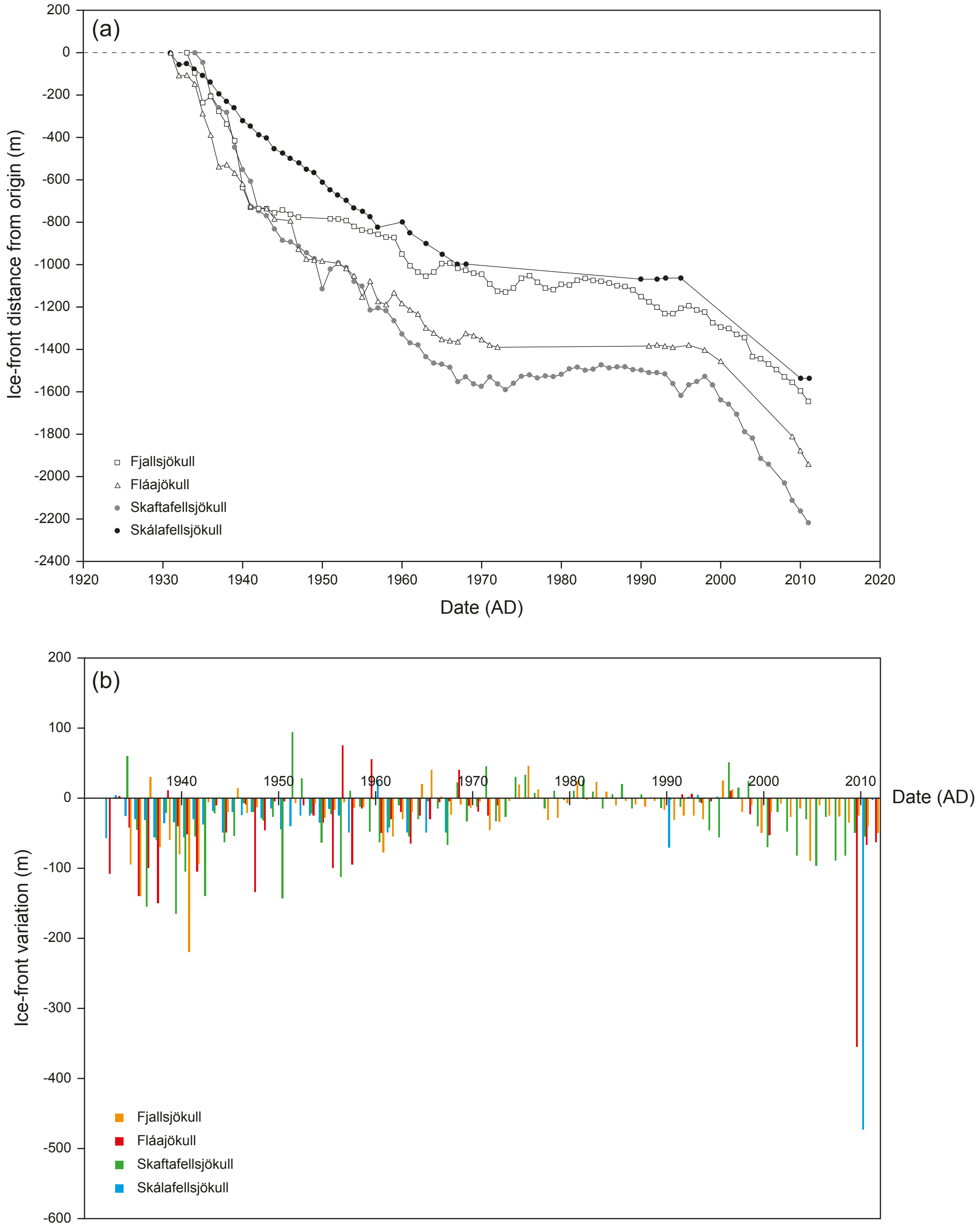

Figure 3.6: (a) Graph comparing the cumulative ice-front variations of Skálafellsjökull and those of similar-sized outlet glaciers. The data are plotted relative to terminus position in 1930, following the convention of the Icelandic Glaciological Society. (b) Yearly ice-front fluctuations of Skálafellsjökull and similar-size outlet glaciers. Note the large ice-marginal retreat evident for Fláajökull in 2009 and Skálafellsjökull in 2010 reflect gaps in the measurement record. Data is taken from the database of the Icelandic Glaciological Society.

3.4 Previous work

Skálafellsjökull has been the subject of a number of studies, investigating the glacial landsystem as whole (Evans and Orton, 2014), component sediment-landform assemblages (Sharp, 1982b, 1984; Dowdeswell and Sharp, 1986; Evans, 2000) and the timing of LIA maxima (Gordon and Sharp, 1983; Evans *et al*., 1999a; McKinzey *et al*., 2004, 2005; Orwin *et al*., 2008; Chenet *et al*., 2010, 2011; Dąbski, 2010). In a recent study, Evans and Orton (2014) mapped the surficial geology and glacial geomorphology of the Skálafellsjökull foreland, and neighbouring Heinabergsjökull foreland (Figure 3.7). Evans and Orton (2014) established that the Skálafellsjökull glacier foreland depicts a landsystem imprint of actively retreating temperate glaciers in a mountain environment with a high glaciofluvial sediment yield. Moreover, the landsystem is characterised by the three diagnostic depositional domains of the active temperate landsystem previously identified for Icelandic piedmont lobes: marginal morainic, subglacial and glaciofluvial/glaciolacustrine (see §2.3; Krüger, 1994; Evans and Twigg, 2002; Evans, 2003a, 2005, 2013; Benn and Evans, 2010, and references therein). The Skálafellsjökull glacier foreland also contains site-specific sediment-landform assemblages, notably overridden kame terraces on the southern part of the foreland. The survival of kame terraces is unusual and therefore the fluted kame terraces at Skálafellsjökull provide an important modern analogue for studies on palimpsest glacial landscapes, which are traditionally assumed to be produced by cold-based conditions in contrast to wet-based conditions at Skálafellsjökull (e.g. Forman *et al*., 1987; Hattestrand and Stroeven, 2002; Landvik *et al*., 2005; Davis *et al*., 2006). The combined landform record of Skálafellsjökull and Heinabergsjökull constitutes a modern glacial landsystem analogue for active temperate piedmont lobes associated with the construction of large outwash heads fed by high glaciofluvial sediment yields (Evans and Orton, 2014). In a palaeoglaciological sense this is one of the most common glacial depositional scenarios within the average style of glaciation during a typical cold stage (*cf.* Porter, 1989; McCarroll, 2006; Hubbard *et al*., 2009; Evans and Orton, 2014).

Research focused on the marginal morainic domain of the Skálafellsjökull foreland has previously been conducted by Sharp (1984). This study specifically examined a sequence of annual moraines within the southern part of the foreland, located in an area of roches moutonnées and a discontinuous sheet of fluted subglacial traction till (*sensu* Evans *et al*., 2006; Sharp, 1982b, 1984; Evans and Orton, 2014). Sharp (1984) identified four types of moraine ridges being formed at the southern margin of Skálafellsjökull (Figure 3.8). Firstly, Type A ridges consist of a till ridge with a fluted proximal slope recording glacier overriding

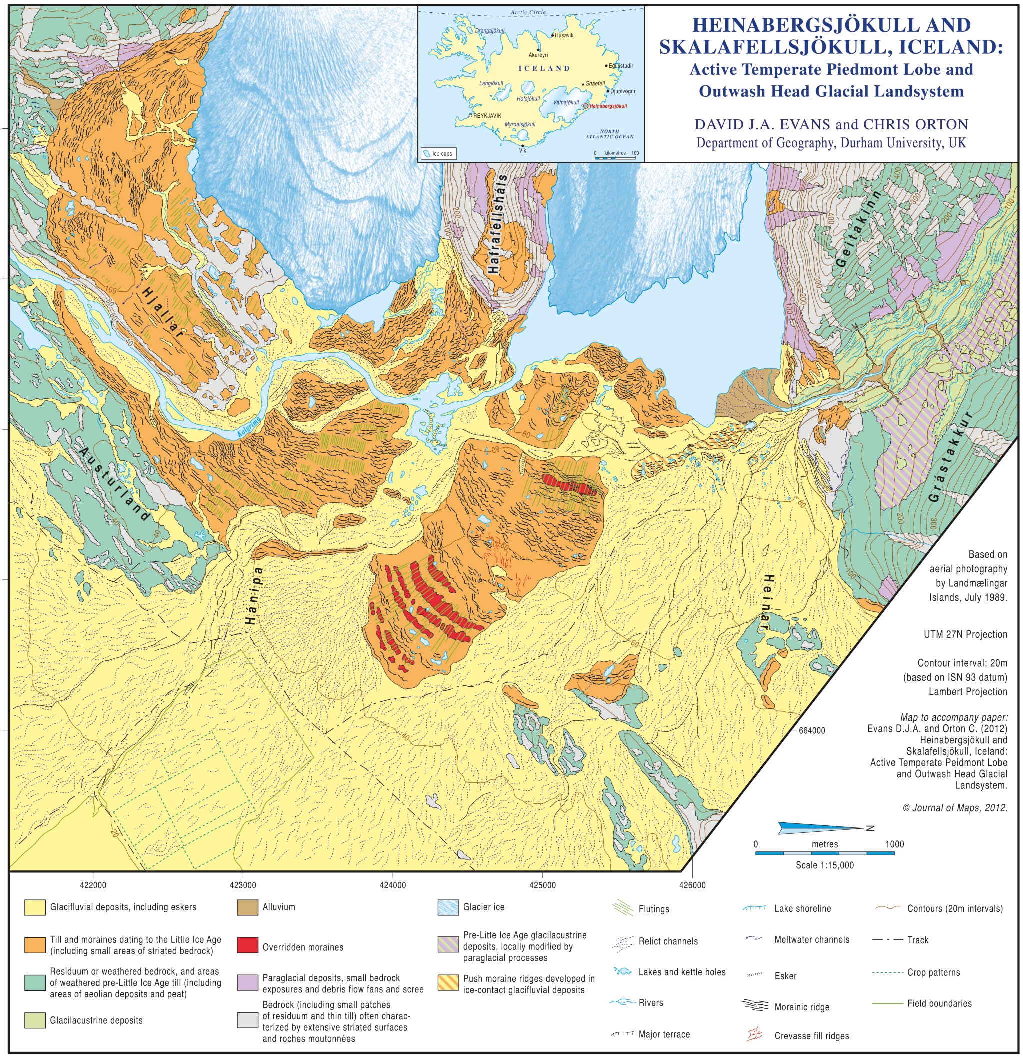

Figure 3.7: Map showing the surficial geology and glacial geomorphology of the Skálafellsjökull and Heinabergsjökull glacier forelands (Evans and Orton, 2014).

(Figure 3.8a). Type B moraines contain a Type A moraine core, but also have an ice core and a surface veneer of re-sedimented debris on the proximal slope (Figure 3.8b). The ice core results from burying of thin ice margins by sediment gravity flows. Type C moraines are superimposed on Type A cores and form wherever debris bands crop out on the surface (Figure 3.8c). As clean ice melts back, the debris bands insulate the underlying ice to produce an ice core on the proximal slope of the moraine. Debris flows are then common as the ice slowly melts out. Finally, Type D moraines are produced wherever marginal snowbanks are pushed forward and overridden by the glacier (Figure 3.8d; *cf*. Birnie, 1977). In contrast to the work of Sharp (1984), this study focuses predominantly on the annual moraine sequences in the central and northern parts of the Skálafellsjökull foreland. Nonetheless, this provides the opportunity to examine spatio-temporal variations in annual moraine properties and mechanisms of formation over the whole foreland.

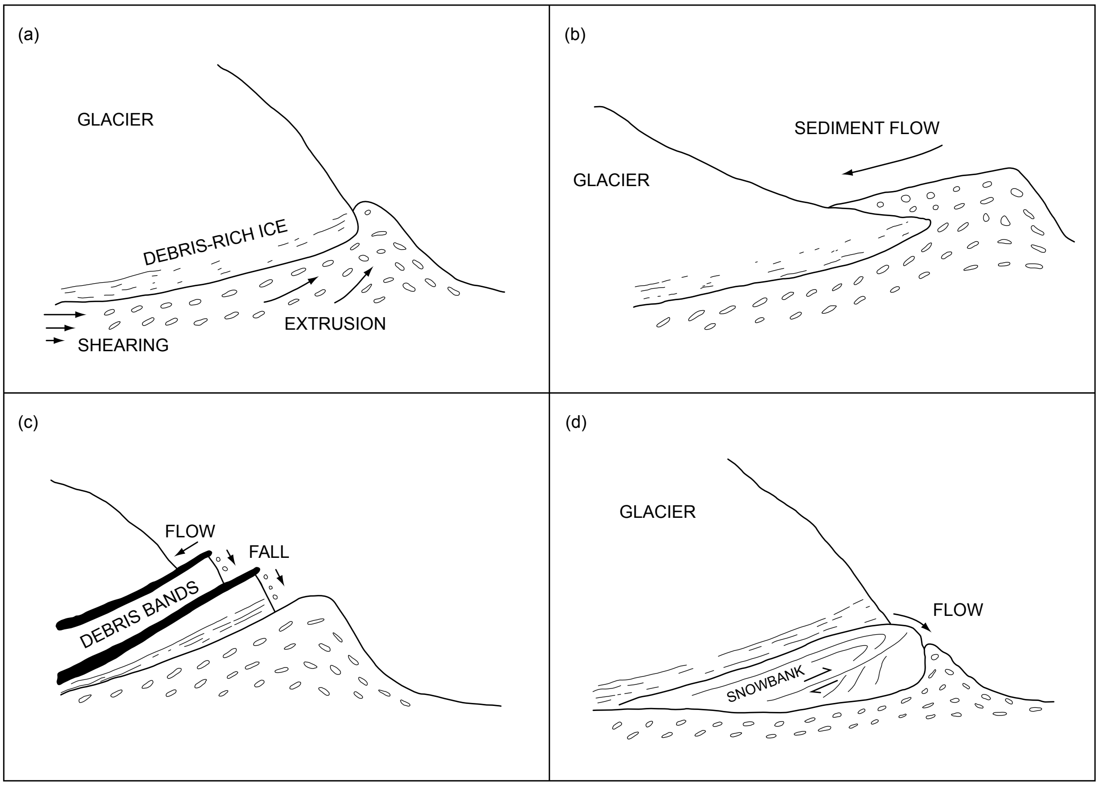

Figure 3.8: Diagram showing the four types of moraine ridges observed by Sharp (1984) at Skálafellsjökull. (a) Simple ridge formed of subglacial traction till (*sensu* Evans *et al*., 2006). (b) Ridge with an ice core incorporated by the flow of ridge sediments back over the glacier margin. (c) Ridge with an ice core isolated beneath thick englacial debris bands which have been exposed by backwasting of the overlying ice slopes. (d) Ridge formed at the distal edge a marginal snowbank which has been pushed forward by the glacier. Flow of debris derived from the basal ice has incorporated the snowbank into the ridge. *Source:* Redrawn from Sharp (1984: 85).

Previous investigations of the subglacial domain at Skálafellsjökull have principally focused on till sedimentology (Dowdeswell and Sharp, 1986; Evans, 2000). The general stratigraphic sequence of the Skálafellsjökull was reported by Sharp and Dugmore (1985) who highlighted an upward transition from minerogenic lacustrine silts through diatomite, peat and black sandy silt to massive matrix-supported diamicton. The juxtaposition of these sediments and their variable grain sizes are central to genetic interpretations of the massive diamictons (subglacial traction tills; *sensu* Evans *et al*., 2006) on the glacier foreland: the differing responses to stress imparted by overriding glacier ice has resulted in a vertical continuum comprising glaciotectonised gravel outwash overlain by two-tiered subglacial traction till typical of the region (Boulton and Dent, 1974; Boulton, 1979; Boulton and Hindmarsh, 1987; Benn, 1994, 1995; Benn and Evans, 1996; Evans, 2000). In a study of till fabrics, Dowdeswell and Sharp (1986) identified a two-tiered till stratigraphy at Skálafellsjökull, reflecting ductile deformation of upper till and brittle deformation of the lower till (Benn and Evans, 1996), similar to that previously observed at Breiðamerkurjökull (Boulton, 1979; Boulton and

Hindmarsh, 1987; Benn, 1995). Subsequent sedimentological analysis of a stratigraphic sequence exposed by river erosion in the Skálafellsjökull foreland (Evans, 2000) revealed a gradational vertical continuum from undeformed glaciofluvial outwash with diatomaceous mud pockets through an immature glaciotectonite to a massive diamicton, with the base of the diamicton displaying evidence of cannibalisation (*cf*. Hicock, 1992; Hicock and Dreimanis, 1989, 1992a, b; Hicock and Fuller, 1995; Evans *et al*., 1998).

Much debate remains regarding the veracity of the Skálafellsjökull LIA maximum and its subsequent retreat pattern, with the application of different lichenometric dating techniques having resulted in contrasting age assignments (*cf*. Evans *et al*., 1999a; McKinzey *et al*., 2004, 2005). The application of an age-size approach based on the average of the largest five lichens per surface (Evans *et al*., 1999a), together with the acceptance of historical documentation of an AD 1887 maximum age for the outermost LIA moraine (Thórarinsson, 1939), yields a recessional pattern post-dating AD 1887 (Figure 3.9). However, the application of a size-frequency approach (*cf*. Caseldine, 1991; Bradwell, 2001a, b, 2004b, and references therein), combined with tephrochronology, led McKinzey *et al*. (2004, 2005) to posit a revised chronology which implies an earlier LIA maximum of ~ AD 1820. Moreover, the revised chronology suggests long-term retreat interspersed with short-term re-advances or stillstands during the waning stages of the LIA (McKinzey *et al*., 2004, 2005). Recently, more complex,

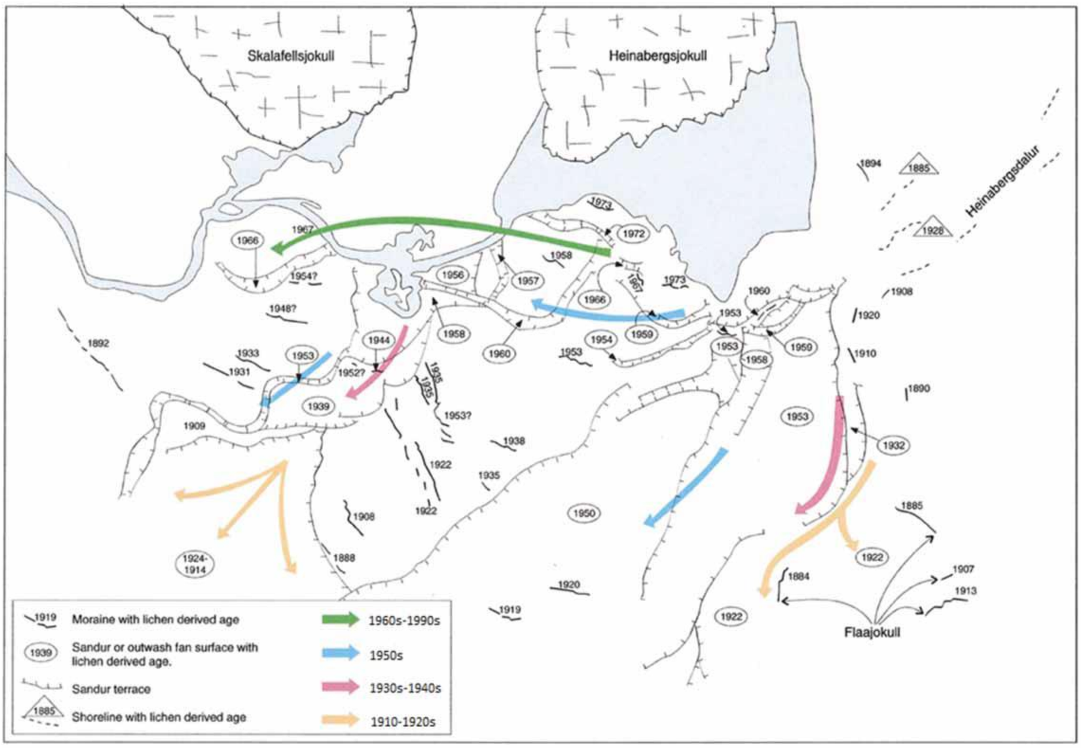

Figure 3.9: Reconstruction of the historical development of the Skálafellsjökull and Heinabergsjökull glacier forelands, based upon age-size lichenometric dating and combined with post-1945 aerial photography and historical documentation (from Evans *et al*. 1999a). The lichenometrically derived ages are based upon a growth rate of 0.80 mm a^{-1} and colonization lag time of 6.5 years. The coloured arrows depict the generalised ages and flow directions of the proglacial outwash system.

statistical approaches to lichenometry have been conducted, including using a Bayesian treatment of Generalised Extreme Value (GEV) distribution theory (Chenet *et al*., 2010; see also Naveau *et al*., 2005, 2007; Cooley *et al*., 2006; Jomelli *et al*., 2007, 2008) and the application of the U^2 statistic (Orwin *et al*., 2008; see also Watson, 1961). However, Bradwell (2009) has argued that the application of more complex statistical analyses, in the pursuit of greater reliability and/or improved accuracy, are unjustified, unsuitable to the user community and inappropriate for the subject matter.

3.5 Summary

This chapter has described the location and setting of Skálafellsjökull, placing the study site into context. Skálafellsjökull is a piedmont outlet lobe of the Vatnajökull ice-cap, SE Iceland, descending from a high elevation plateau onto an unconfined coastal plain (Sharp, 1984; Evans and Orton, 2014). The bedrock geology of the Skálafellsjökull catchment is believed to consist largely of west-dipping basalt lavas which are interstratified with tuffs and tillites (Walker, 1964). These glaciological, topographic and geological characteristics may have important implications on submarginal processes at Skálafellsjökull, as well as “annual” moraine formation and geomorphology. The maritime climatic setting of the glacier, and complex atmosphere-ocean interactions, will also have important implications for seasonal submarginal processes and the climate signal recorded by the “annual” moraines. Given the importance of climate variability in contemporary Icelandic glacier change, inter-annual variability in SE Iceland climate and the interplay between atmospheric and oceanic climate variables are explored in further detail in Chapter 6.

Documentary evidence and maps indicate that Skálafellsjökull formerly coalesced with the neighbouring Heinabergsjökull, and they remained confluent until sometime between 1929 and 1945 (Danish General Staff, 1904; Wadell, 1920; Roberts *et al*., 1933; Thórarinsson, 1943; Pálsson, 1945; Hannesdóttir *et al*., 2014). Ice-front measurements conducted at the glacier since the 1930s indicate Skálafellsjökull underwent similar fluctuations to other non-surge-type Vatnajökull outlet glaciers (e.g. Sigurðsson, 1998). Since the 1970s, however, measurements have been sporadic, limiting understanding of glacier change at Skálafellsjökull during this period. Thus, the sequences of recessional (“annual”) moraines previously identified on the Skálafellsjökull foreland (Sharp, 1984; Evans and Orton, 2014) offer the opportunity to gain important insights into ice-frontal fluctuations. Moreover, the previous study of “annual” moraine formation at Skálafellsjökull (Sharp, 1984) will allow spatio-temporal variations in “annual” moraine characteristics and mechanisms of formation over the whole foreland to be explored.

CHAPTER 4

Remote sensing and field-based techniques

This chapter describes the key remote sensing and field-based techniques used in this research to examine the characteristics of recessional ("annual") moraines on the Skálafellsjökull foreland. The principal methods employed were remote sensing observations, desk- and field-based geomorphological mapping, lichenometric dating and sedimentological analysis. Details of techniques employed for further analysis, such as statistical analysis of patterns, rates and drivers of ice-marginal retreat, are described in appropriate sections of the thesis. These additional methods utilise data obtained from the techniques outlined herein, and relate to the interpretation of moraine geomorphology, chronology and sedimentology. The following four sections provide detailed discussion of the approaches used in geomorphological mapping and map production (Sections 4.1 and 4.2), establishing a chronological framework for the recessional ("annual") moraines (Section 4.3) and examining processes of moraine formation (Section 4.4).

4.1 Remotely-sensed datasets and image preparation

For the purposes of glacial geomorphological mapping, four remotely-sensed datasets were acquired (Figure 4.1). High-resolution scans of 2006 colour aerial photographs with a resolution of 0.41 m GSD (Ground Sampled Distance) per pixel were obtained from the Icelandic survey company *Loftmyndir ehf*, whilst multispectral (8-band) and panchromatic satellite imagery captured by the WorldView-2 satellite sensor in June 2012 were acquired from *European Space Imaging*. The multispectral (8-band) satellite imagery and panchromatic images have resolutions of 2.0 m GSD and 0.5 m GSD, respectively. In addition, a further high-resolution remotely-sensed dataset has been used to aid mapping: a Digital Elevation Model (DEM) with a spatial resolution of 0.09 m, derived from imagery captured using an Unmanned Aerial Vehicle (UAV) during aerial surveys of the Skálafellsjökull foreland in the summer of 2013 (A. Clayton, pers. comm., 2014). The acquisition of imagery using UAVs represents a potentially effective and low-cost technique for producing high-resolution, 3D-geo-referenced data (e.g. d'Oleire-Oltmanns *et al.*, 2012; Hugenholtz *et al.*, 2012, 2013; Lucieer *et al.*, 2014) but its application in glaciology and glacial geomorphology has so far been limited (e.g. Whitehead *et al.*, 2013; Ryan *et al.*, 2014; Evans *et al.*, submitted). The spatial coverage of this dataset is, however, limited to selected areas and does not provide complete coverage of the Skálafellsjökull foreland. Thus, the 2006 aerial photographs and 2012 satellite imagery were largely used in the composition of the geomorphological maps (see below).

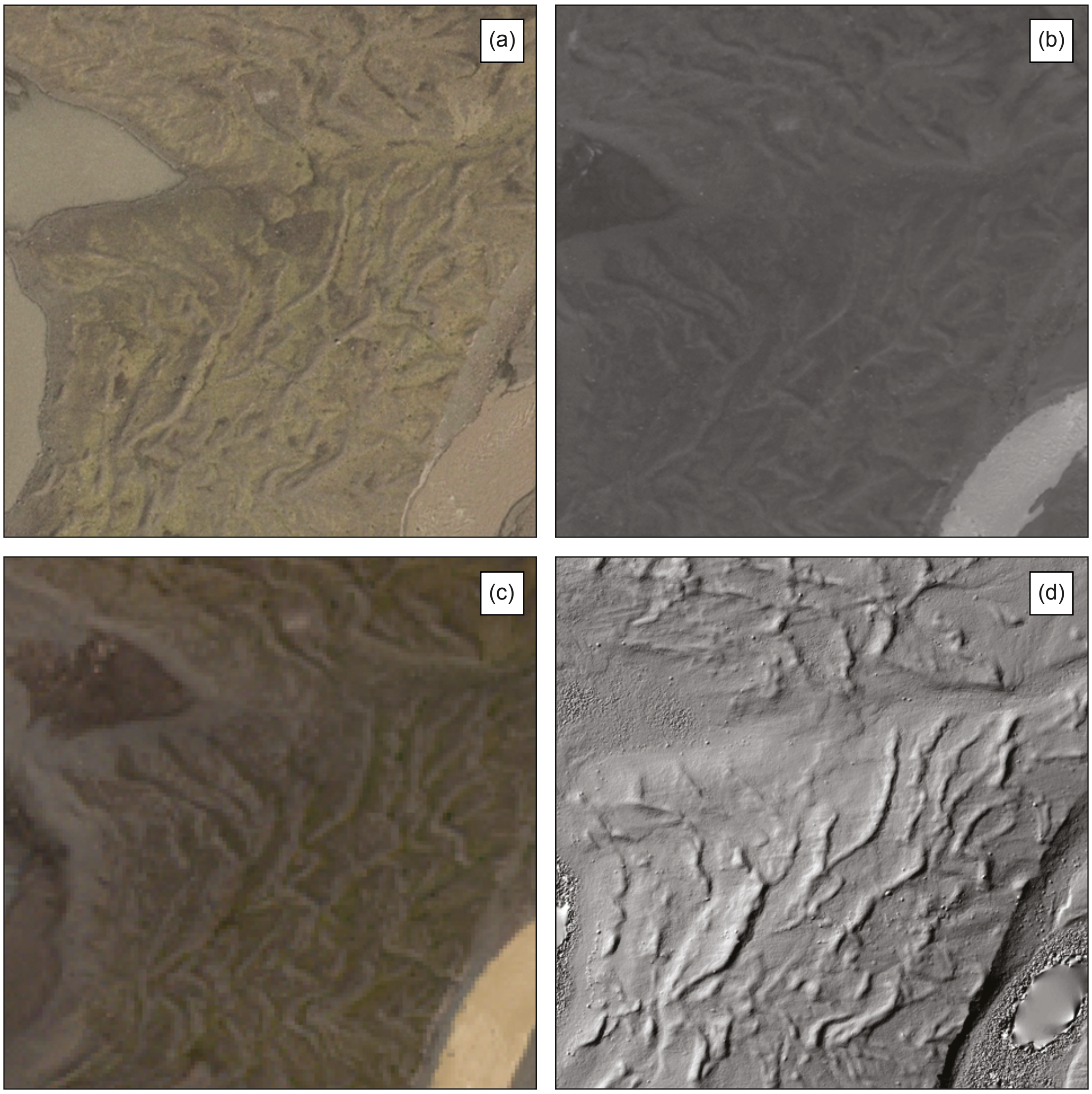

Figure 4.1: Extracts from the principal remotely-sensed datasets employed for glacial geomorphological mapping in this study. (a) Colour aerial photographs (0.41 m GSD) from 2006, *Loftmyndir ehf*. (b) Panchromatic satellite image (0.5 m GSD) from the WorldView-2 sensor, *European Space Imaging* (June 2012). (c) Multispectral satellite image (2.0 m GSD) from the WorldView-2 sensor, *European Space Imaging* (June 2012). (d) DEM data visualised as a hillshaded relief model, A. Clayton (pers. comm., 2014).

Aerial photographs contain varying degrees of geometric distortions, manifest mainly as relief displacement and variations in scale (Lillesand *et al.*, 2008; Campbell and Wynne, 2011). Digital photogrammetric processing was therefore conducted to generate an orthorectified aerial photograph and DEM based on the 2006 colour aerial photographs. For this purpose, the aerial photographs were processed in *Agisoft PhotoScan Professional Edition*, which utilises a *Structure-from-Motion* (SfM) approach. SfM operates under the same basic tenets as stereoscopic photogrammetry, namely that 3D structure can be resolved from a series of overlapping, offset images. However, it differs fundamentally from conventional photogrammetry in that the geometry of the scene, camera positions and orientation is solved automatically without the need to specify *a priori*, a network of targets with known 3D positions (Westoby *et al*., 2012). Instead, these are solved simultaneously using an iterative bundle adjustment procedure, based on a database of features automatically extracted from a set of multiple overlapping images (Snavely, 2008). Position information can then be introduced after model production in an arbitrary coordinate system, meaning that errors in ground control points (GCPs) will not propagate in the DEM (Clayton, 2011). The Universal Transverse Mercator (UTM) projection was utilised during photogrammetric processing, with the spheroid WGS84 for zone 28N (ESPG: 32628). This coordinate system is compatible with the system currently employed by *Landmælingar Íslands* (National Land Survey of Iceland) in the production of Icelandic maps.

Positional ground control for the aerial photographs was collected in the field using a Leica 1200 differential Global Positioning System (dGPS) between May and June 2014. The collected ground control points (GCPs) were processed using the Canadian Spatial Reference System Precise Point Positioning (CSRS-PPP: http://webapp.geod.nrcan.gc.ca/geod/tools-outils/ppp.php?locale=en) tool, with the corrections then applied in *Leica Geo Office 8.3*. The Coordinate Conversion and Datum Transformation in Iceland (cocodat^{i}: http://cocodati.lmi.is/cocodati/cocodat-i.jsp) tool was then employed to generate orthometric heights (height in m above sea level: H m a.s.l.) for the GCPs and to convert the coordinates to UTM projected coordinates for zone 28N. Orthometric heights generated using the cocodat^{i} tool are based on the ISN93 datum, ellipsoid GRS80 and applies the new Icelandic geoid model. For practical purposes GRS80 and WGS1984 can be considered approximately equal, since there is a difference of 0.1 mm in the semi-minor axis (*cf*. Rennen, 2004). The model generated in *Agisoft PhotoScan* was georeferenced to WGS 1984 / UTM Zone 28N using the processed positional ground control (n = 50). The generated DEM had a total reprojection error of 0.64 m (x = 0.33 m, y = 0.29 m and z = 0.47 m). An orthophoto mosaic with a cell size of 0.41 m was then produced using the DEM for the purposes of landform mapping.

The satellite imagery obtained from *European Space Imaging* was purchased as 'Ortho Ready Standard' and had been projected to UTM Zone 28N, spheroid WGS1984. The imagery had been resampled in *ERDAS Imagine* using the 4x4 cubic convolution method. The supplied imagery was orthorectified in *ArcMap 10.2* using the DEM generated from the 2006 aerial photographs in *Agisoft PhotoScan*. Following orthorectification, a pan-sharpened, natural colour multispectral image (3-band: Blue, Red Green) with a resolution of 0.5 m GSD per pixel was generated using the IHS method in *ArcMap* (Figure 4.2). The IHS method uses Intensity, Hue and Saturation Colour to merge the high-resolution panchromatic data (0.5 m GSD) with medium-resolution multispectral data (2.0 m GSD) in order to produce a multispectral image with higher-resolution properties.

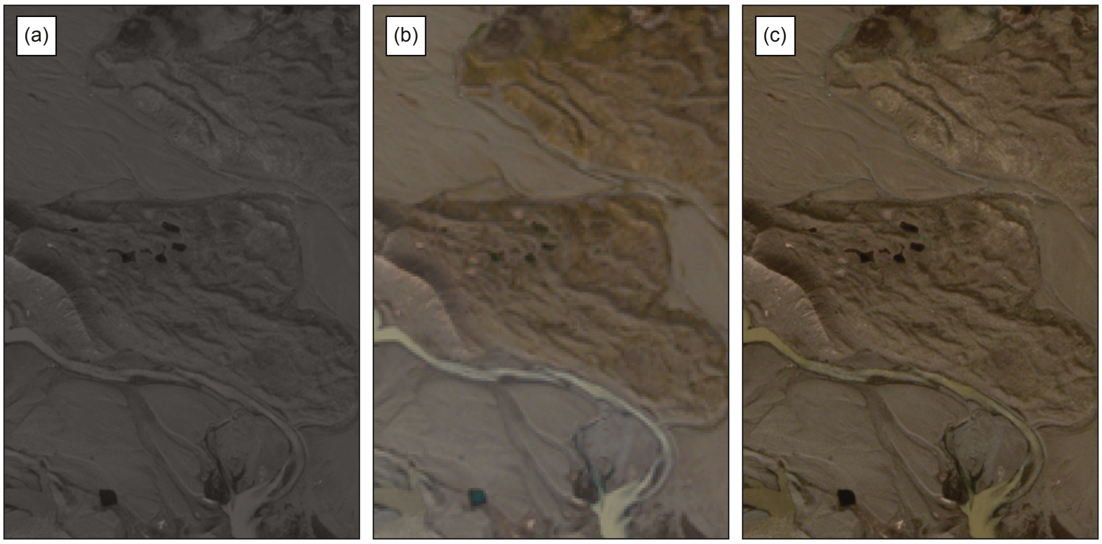

Figure 4.2: Comparison of the processed satellite imagery used in this research. (a) Panchromatic satellite image (0.5 m GSD). (b) Multispectral satellite image (2.0 m GSD). (c) Pansharpened 3-band natural colour image (0.5 m GSD).

For meaningful graphical and analytical purposes, the DEM data were converted into hillshaded relief models using *Spatial Analyst* in *ArcMap*. Hillshaded relief models were produced using an illumination angle of 30° and azimuths set at orthogonal positions of 45° and 315° (Figure 4.3). These properties have been extensively used in generating hillshaded relief models for the purposes of glacial geomorphological mapping and have been suggested as optimal settings for visualisation (e.g. Smith and Clark, 2005; Chen and Rose, 2008; Hughes *et al*., 2010; Boston, 2012a, b; Pearce *et al*., 2014). Displaying the DEM data as hillshaded relief models with differing azimuths avoids azimuth bias and permits geomorphological features to be viewed under different lighting conditions, which can increase the visibility of subtle landforms (Smith and Clark, 2005; Pearce *et al*., 2014).

4.2 Mapping techniques

Detailed glacial geomorphological mapping was conducted from the above-identified imagery, combined with field investigations conducted in May and June 2014 to ground truth the desk-based mapping. This approach of applying multiple remotely-sensed datasets,

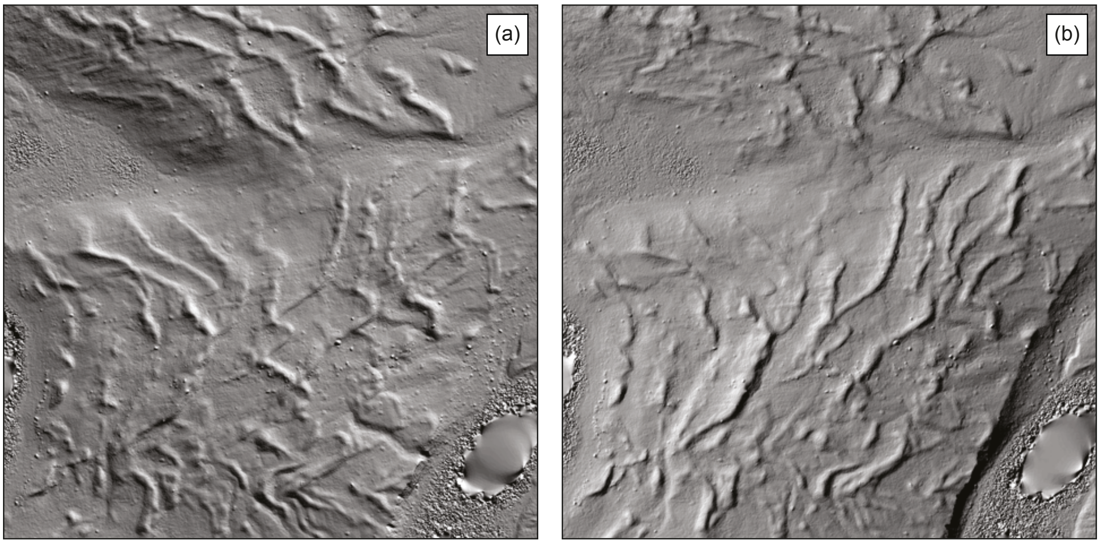

Figure 4.3: Extracts from hillshaded relief models showing annual moraines on the foreland of Skálafellsjökull. The models are derived from the DEM provided by A. Clayton, pers. comm., 2014. (a) Hillshaded relief model generated using an illumination angle of 30° and an azimuth of 45°. (b) Hillshaded relief model generated using an illumination angle of 30° and an azimuth of 315°. The difference in appearance of the annual moraines between the two models is apparent, demonstrating the value of visualising the data with different azimuths.

augmented by field-based geomorphological investigations, has been extensively applied in the context of both glacierized and glaciated landscapes, encompassing a variety of geographical locations (e.g. Bennett *et al*., 2010; Boston, 2012; Bradwell *et al*., 2013; Reinardy *et al*., 2013; Brynjólfsson *et al*., 2014; Darvill *et al*., 2014; Evans *et al*., 2014; Jónsson *et al*., 2014; Pearce *et al*., 2014). The application of both the interpretation of remotely-sensed data and field surveys permits a holistic approach to mapping, wherein the advantages of each method can be combined to produce an accurate map with robust genetic interpretations (*cf*. Brown *et al*., 2011; Boston, 2012a, b).

The principal focus of the glacial geomorphological mapping was to produce detailed mapping of annual moraines on the foreland of Skálafellsjökull, providing a framework to examine patterns and rates of ice-marginal retreat at Skálafellsjökull. The mapping aimed to build on the previous small-scale landsystem mapping produced by Evans and Orton (2014). Individual maps have been produced based on the 2006 aerial photographs and 2012 satellite imagery, providing a visual demonstration of recent ice-marginal retreat and the evolution of the glacier foreland. In addition to these two larger-scale maps, detailed sample mapping of annual moraines has been conducted based on hillshaded relief models generated from the high-resolution DEM provided by A. Clayton (pers. comm., 2014), allowing the complexity of annual moraine distribution and geomorphology to be explored.

Overlays of geomorphological features were digitally drawn in *ArcMap 10.2* using the remotely-sensed data, with individual vector layers created for each geomorphological feature. The initial interpretation of the remotely-sensed data and on-screen digitisation were then checked in the field. In order to enhance the accuracy of mapping and reduce errors which may arise from misinterpretation of features, examination of the remotely-sensed data was conducted both prior to and after the field investigations (*cf*. Lukas and Lukas, 2006; Boston, 2012a, b; Pearce *et al*., 2014). The final digitised features were then exported to *Adobe Illustrator CC* for final editing and map production, along with a contour layer calculated at 20 m intervals using *Spatial Analyst* in *ArcMap* and the 2006 DEM to derive the elevation data.

4.3 Chronological techniques

A chronological framework for ice-marginal fluctuations of Skálafellsjökull was established using a combination of two approaches. Firstly, examination and cross-correlation of an imagery archive spanning the period 1945 to 2012 was employed (Figure 4.4). In addition to the remotely-sensed data identified in §4.1, a dataset of panchromatic photographs covering 1945 to 1989 has been compiled from *Landmælingar Íslands*. The examination of this imagery archive allows ages to be assigned to recessional ("annual") moraines formed during the period 1945 – 2012. As imagery for the archive is not complete (i.e. images are not available for every year), ages were assigned to "annual" moraines on the basis of counting the number of ridges between moraines of known age. In areas of the foreland with continuous sequences of moraines, it is assumed that the moraines formed on an annual basis if the number of ridges between two moraines of known age is equal to the time elapsed between the formation of those reference moraines (e.g. Sharp, 1984; Krüger, 1995; Bradwell, 2004a; Krüger *et al*., 2010). In order to determine the age of moraines formed prior to the period covered by the imagery record, lichenometric surveys were conducted on a sub-sample of moraines (*n* = 14), following the methodology used previously in SE Iceland (Bradwell, 2001a, b, 2004a, b; McKinzey *et al*., 2004, 2005; Bradwell *et al*., 2006, 2013).

For landforms formed over the last three or four centuries in glacial environments, lichenometric dating is often the only dating technique available, avoiding the difficulties associated with other surface-dating tools such as dendrochronology, radiocarbon dating and weathering-based techniques (e.g. Matthews, 1980; Heikinnen, 1994; McCarroll, 1991). Lichenometric dating involves using measurements of lichen size or another index, such as lichen size-frequency distributions, as an indicator of surface age (e.g. Beschel, 1950; Benedict, 1967, 1985; Denton and Karlén, 1973; Matthews, 1975; Innes, 1983; Bull and

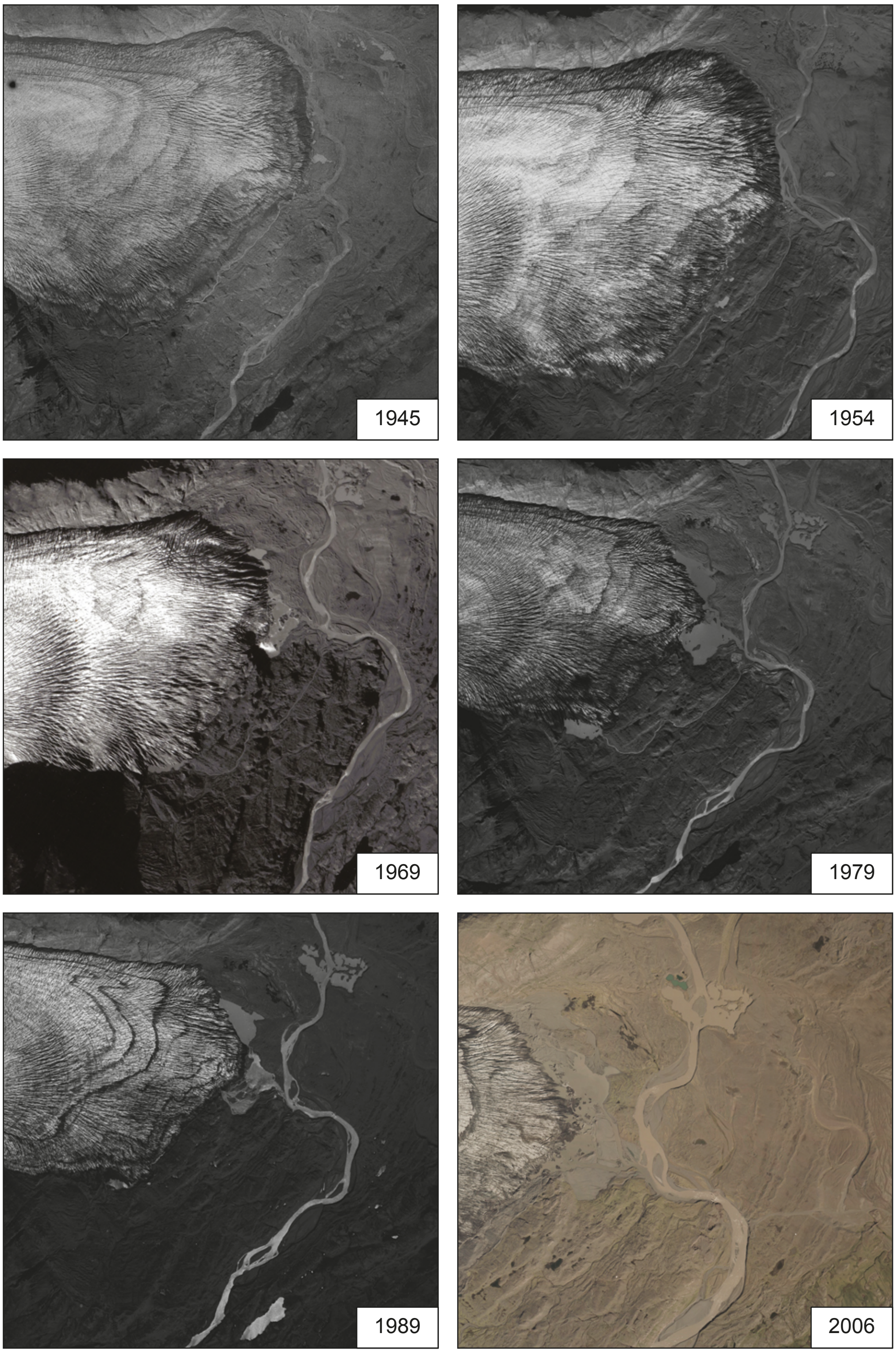

Figure 4.4: Aerial photograph extracts taken from the imagery archive compiled for this study showing the extent of glacier ice in each year and the sequential development of the foreland.

Brandon, 1998; Bradwell, 2001a, b, 2004b). In Iceland, several workers have employed lichenometry in order to estimate the age of various glacial features (e.g. Jaksch, 1970; Gordon and Sharp, 1983; Caseldine, 1983, 1991; Maizels and Dugmore, 1985; Thompson and Jones, 1986; Kugelmann, 1991; Guðmundsson, 1998a, b; Evans *et al*., 1999a; Kirkbride and

Dugmore, 2001a; Bradwell, 2001a, b, 2004a, b). A number of locally calibrated lichen growth curves, based on various measurement approaches (*cf.* Bradwell, 2001a, b; McKinzey *et al.*, 2004), now exist for glacier forelands in Southeast Iceland (e.g. Gordon and Sharp, 1983; Evans *et al.*, 1999a; Bradwell, 2001b, 2004b).

In this study, the longest axis of >200 thalli of the crustose, yellow-green lichen *Rhizocarpon* Section *Rhizocarpon* (Figure 4.5) were measured to the nearest millimetre in fixed areas of *c.* 50 m^2 on the proximal slopes of moraines. Investigations by Bradwell (2001b) found this sample size to be satisfactory for dating studies in Iceland. Thalli were identified to the section level as advocated by Innes (1982, 1985), using the criteria of Poelt (1988). Care was taken to restrict measurements to thalli of *Rhizocarpon* Section *Rhizocarpon* (formerly known as the *Geographicum* group: Runemark, 1956) as classified by Cernohorský (1977) and to exclude lichens of Section *Alpicola*, which are known to have different growth rates (Innes, 1982, 1983). Thalli less than 5 mm in diameter were omitted from the surveys. Elongate and irregular thalli were measured regardless of their shape, whilst coalescent thalli were disregarded (Bradwell, 2001a; 2004a, b). Measurements were restricted to non-vesicular, basaltic rocks. Lichenometric dating was restricted to moraines that are believed to be more than 30 years old based on the imagery archive, as lichenometry is deemed inapplicable on surfaces less than 30 years old due to the uncertain nature of lichen colonisation and the initial growth phase (Beschel, 1950, 1961; Armstrong, 1983; Innes, 1988).

Figure 4.5: Photograph of a *Rhizocarpon* Section *Rhizocarpon*, with Recta compass-clinometer for scale.

In order to examine the lichen population distribution, graphs were plotted for each of the fourteen lichen populations, constructed using the logarithm of the frequency (%) as the dependent variable and lichen thallus diameter (mm) as the independent variable (e.g. Bradwell, 2001b, 2004b). A class interval of 3 mm was chosen for lichen diameter, as advocated in previous studies (e.g. Innes, 1986; Caseldine and Baker, 1998; Bradwell, 2001a). Lichens falling below the modal class in each lichen population were omitted from the analysis. Linear regression analyses were then conducted using the least-squares regression method, enabling size-frequency distributions to be described in the form $y = mx + c$ (e.g. Bradwell, 2001a, 2004b; McKinzey *et al*., 2004). This size-frequency method also enables the prediction of the '1 in 1000' thallus (Andersen and Sollid, 1971; Locke *et al*., 1979), namely the x-intercept (lichen diameter, mm) at a $\log_{10}$ frequency of -1 (Bradwell, 2001a). Both the regression gradient and '1 in 1000' thallus have been successfully employed to describe lichen population distributions (e.g. Benedict, 1967, 1985; Locke *et al*., 1979; Caseldine, 1991; Bradwell, 2001b). An advantage of undertaking size-frequency analysis is that problems regarding the incorporation of reworked ('older') debris are eradicated: anomalously large lichen thalli that pre-date the time of surface exposure can be easily detected and disregarded (Bradwell, 2001a, b).

For comparison, three different lichenometric dating curves previously constructed for SE Iceland were employed to derive possible moraine surface ages (Table 4.1; Figure 4.6). These include the linear (long axis) *age-size* curve calibrated by Gordon and Sharp (1983), the curvilinear *age-size* curve of Bradwell (2001a, b) and the *age-gradient* dating curve developed by Bradwell (2004b). The Gordon and Sharp (1983) age-size dating curve was developed specifically for the Skálafellsjökull foreland, and was calibrated using long-axis measurements of the largest lichen on moraine surfaces of known age. However, Gordon and Sharp (1983) employed a different sampling strategy to that used in this study, with measurements restricted to the largest lichen of the aggregate species *Rhizocarpon geographicum* in an area covering 150 m^2 on the proximal moraine surface slope. This difference in sampling strategy could potentially introduce error into ages derived using the Gordon and Sharp (1983) dating curve. More recently, Bradwell (2001a, b) developed a curvilinear age-size dating curve for SE Iceland using *Rhizocarpon* Section *Rhizocarpon* and is calibrated using the largest lichen in a single lichen population on independently dated substrates. This lichenometric dating curve suggests the relationship between largest lichen diameter and date of abandonment is best described by a third-order polynomial function (Figure 4.6; Bradwell, 2001a, b; McKinzey *et al*., 2004). However, the Bradwell (2001a, b) curve uses control sites from a range of precipitation zones, which could introduce error into

Table 4.1: Summary of lichenometric methods used to calibrate lichen dating curves employed in this study. *Source:* After Bradwell (2001a: 139) and McKinzey *et al*. (2004: 323).

Reference	Survey date	Location	Lichen species	Lichen parameter measured	Number of lichens measured[a]	Survey area (m^2)	Calibration surfaces	Calibration method	Oldest surface (Date AD)	Ecesis (years)[b]	Growth rate (mm/yr)
Gordon and Sharp (1983)	1980	Skálafells-jökull	R. geog.	Long axis	1	150	Moraines	Largest lichen	1887	15	0.987
Bradwell (2001a, b)	1999	SE Iceland	R. Section R. (includes R. geog.)	Long axis	*c*. 300	30	Glacial bedrock Moraines Rockfall Lava flow Jökulhlaup deposit	Largest lichen	1727	-	-
Bradwell (2004)	1999	SE Iceland	R. Section R. (includes R. geog.)	Long axis	*c*. 300	30	Glacial bedrock Moraines Rockfall Lava flow Jökulhlaup deposit	Largest lichen Size-frequency population gradient	1727	-	-

[a] Number of lichens used to derive surface age e.g. 1 = the largest lichen was employed to determine surface age

[b] Time lag for a lichen spore to arrive on and successfully colonise a surface

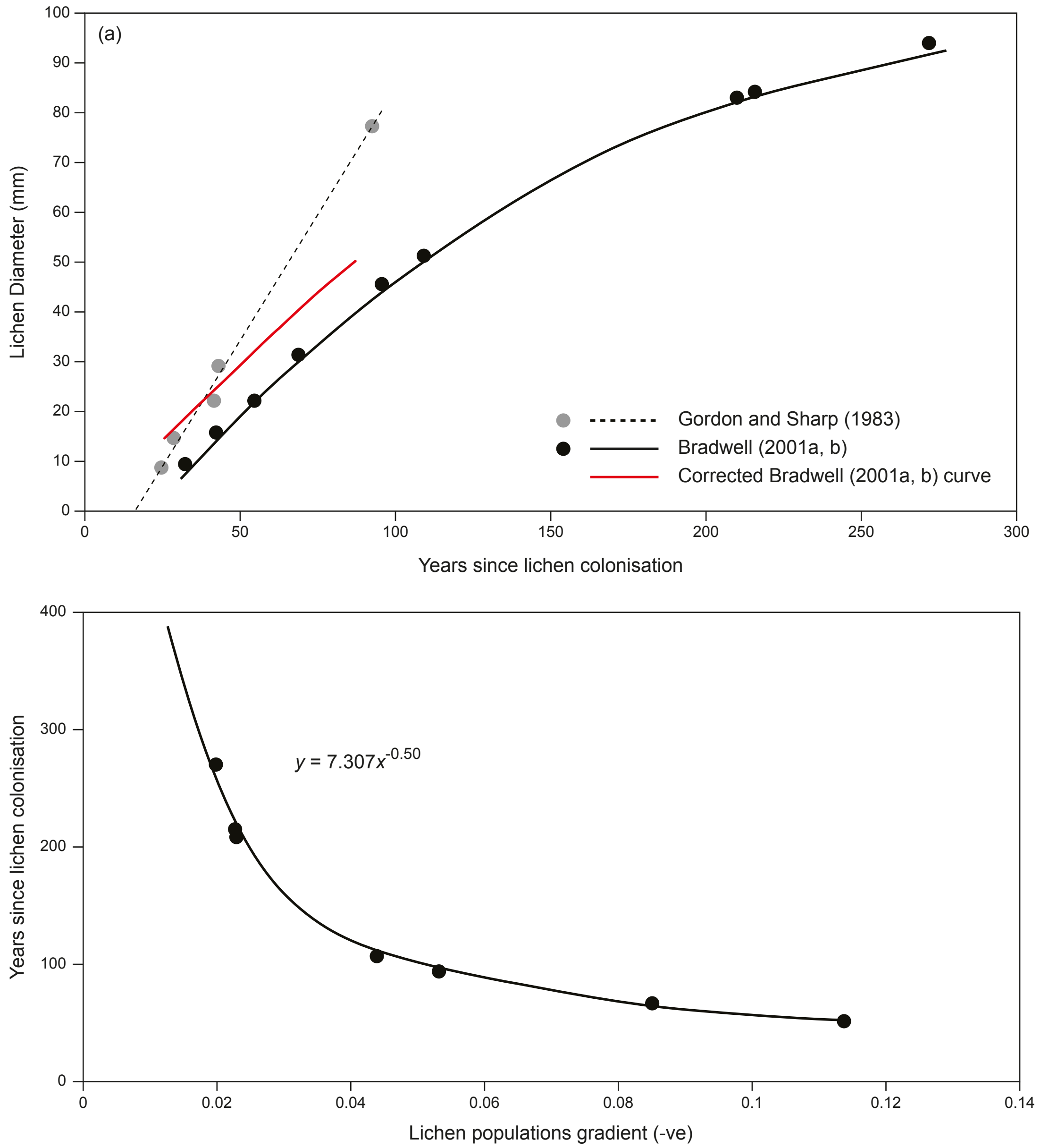

Figure 4.6: Lichenometric dating curves for southeast Iceland. (a) Age-size curve from Gordon and Sharp (1983) and Bradwell (2001a, b). The curvilinear age-size curve of Bradwell (2001a, b) corrected for 2014 survey is also shown. (b) Curvilinear age-gradient curve of Bradwell (2004b).

age estimates derived using this curve as lichen growth rates are believed to vary with precipitation (*cf.* Evans *et al.*, 1999a; Armstrong, 2015). Using the gradient of the size-frequency distributions collected from the aforementioned control sites, Bradwell (2004b) constructed a curvilinear *age-gradient* curve, which plots the age of reliably dated surfaces (*cf.* Bradwell, 2001a, b) against the gradient of lichen population size–frequency distributions (McKinzey *et al.*, 2004). Estimates of the date of surface abandonment calculated using the Bradwell (2001a, b) age-size curve have been recalibrated to 2014 using the growth rates derived by Bradwell and Armstrong (2007). On the basis of a mean diametral growth rate of 0.64 mm yr^{-1} (Bradwell and Armstrong, 2007) and a time difference of 15 years between the original curve construction and this study, a correction factor of 9.6 mm was applied.

Corrections were only applied to lichen thalli between 15 and 50 mm where growth rates are broadly constant (*cf*. Bradwell *et al*., 2013). The linear age-size curve developed by Evans *et al*. (1999a) for south coast Icelandic glacier forelands has not been employed due to incompatibility with the sampling strategy utilised in this study. The methodology employed by Evans *et al*. (1999a) uses *Rhizocarpon geographicum sensu lato* (*cf*. Innes, 1982, 1983, 1985) and involves measuring the long axis of the five largest lichens across the whole moraine surface, with the average of these five measurements subsequently used to derive a date of abandonment.

4.4 Sedimentological techniques

Sedimentological investigations of manually-created exposures were undertaken to examine moraine-forming processes, following standard sedimentological procedures previously applied to ice-marginal moraines in both former and contemporary glacial environments (e.g. Lukas, 2005a, b, 2007b, 2012; Benn and Lukas, 2006; Reinardy *et al*., 2013). Exposures through moraines were created manually using a foldable shovel, with marker cairns then placed along the base of the section at regular intervals and a tape measure hung from the top of the exposure (e.g. Lukas, 2012). A measured sedimentological log of each clean section was drawn on squared-millimetre paper in the field: the moraine profile, prominent boulders and contacts were drawn on the field log first, with increasing detail added progressively. In order to increase planimetric accuracy of the section logs, a photomosaic of each section was produced. The field log was overlain on the photomosaic in *Adobe Illustrator CC* and then digitised to produce the final section logs. Individual sedimentary units were identified on the basis of their visual physical properties following guidelines detailed by Evans and Benn (2004), and logged using the lithofacies code of Benn and Evans (1998) (Figure 4.7). The nature of contacts between individual units was also recorded. The dip and strike of moraine surface slopes were measured using a Recta DS50 compass-clinometer, with an accuracy of ± 5° (*cf*. Hubbard and Glasser, 2005).

Clast shape analysis was conducted to provide valuable information on the source of glacial debris in the “annual” moraines (*cf*. Benn and Lukas, 2006; Lukas, 2007; Lukas *et al*., 2013). Clast shape was determined using well-established methods introduced by Benn and Ballantyne (1993, 1994). From each logged section, 50 clasts from the same lithology (basalt) were sampled at random, their three orthogonal axes measured and roundness determined visually. Although the influence of clast size on shape has not satisfactorily been tested before, sampling was restricted to clasts with maximum *a*-axes of 25 cm (*cf*. Lukas *et al*., 2013). An assessment of differential transport paths was undertaken using the RA-C_{40} and RWR-C_{40}

indices (Figure 4.8): the RA-C_{40} index is useful in differentiating between active (subglacial, fluvial) and passive (supraglacial) transport, whilst the RWR-C_{40} index is valuable in distinguishing between different active transport pathways (*cf.* Brook and Lukas, 2012; Lukas *et al.*, 2013, in press). Control samples from Fláajökull, SE Iceland (Lukas *et al.*, 2013; D. Evans, pers. comm., 2014) were employed as reference since no control samples were collected for Skálafellsjökull in this study.

Diamicton	
Dm	Diamicton, matrix-supported
Dmm	Diamicton, massive, matrix-supported
Dms	Stratified matrix-supported diamicton
Dcm	Clast-supported diamicton
Dmg	Matrix-supported, graded
Dml	Matrix supported, laminated
--- (p)	Includes clast pavement
--- (g)	Graded diamicton
--- (b/s)	Banded / sheared

Silts and Clays (<0.063 mm)	
Fm	Fines, massive
Fl	Fines, laminated.
Flv	Fine lamination with rhythmites or varves.
Frg	Graded or climbing-ripple cross-lamination
Fcpl	Cycopels
Fp	Intraclast or lens
---(d)	with dropstones
--- (w)	with dewatering

Sands (0.063 to 2 mm)	
Sm	Massive sand
St (A)	Ripple cross laminated (Type A)
St (B)	Ripple cross laminated (Type B)
St (S)	Ripple cross laminated (Type S)
Scr	Climbing ripples
Ssr	Starved ripples
Sr	Sand, ripple-cross laminated
Sh	Very fine to very coarse and horizontally / planar bedded or low angle cross lamination
Sd	Deformed bedding
St	Medium to very coarse trough cross-bedded
Sp	Medium to very coarse planar cross-bedded
Sl	horizontal or draped lamination
Sh	Sheared sand
Sfo	Deltaic foresets
Sfl	Flasar bedded
Se	Erosional scours with intraclasts and crudely cross-bedded
Su	Fine to coarse with broad shallow scours and cross-stratification
Sc	Steeply dipping planar cross bedding
Suc	Upward coarsening
Suf	Upward fining
Srg	Graded cross-lamination
SB	Bouma sequence
Scps	Cycoplasms
--- (d)	with dropstones
--- (w)	with dewatering

Fine Gravel (2-8 mm)	
GRcl	Massive with clay laminae
GRch	Massive and infilling channels
GRh	Horizontally bedded
GRm	Massive and homogenous
GRmb	Massive and pseudo-bedded
GRmc	Massive with isolated outsize clasts
GRmi	Massive with isolated, imbricated clasts
GRmp	Massive with clast stringers
GRo	Openwork structure
GRruc	Repeated upward-coarsening cycles
GRruf	repeated upward-fining cycles
GRt	Trough cross-bedded gravel
GRcu	Upward coarsening (inverse grading)
GRfu	Upward fining (normal)
GRp	Cross-bedded
GRfo	Deltaic foresets

Coarse Gravel (8-256 mm)	
Gms	Matrix supported, massive gravel
Gm	Clast supported, massive
Gsi	Matrix supported, imbricated
Gmi	Clast supported, massive, imbricated
Gfo	Deltaic foresets
Gh	Horizontally-stratified gravel
Gt	Trough cross-bedded gravel
Gp	Gravel, planar-cross bedded
Gfu	Upward fining (normal grading)
Gcu	Upward coarsening (inverse grading)
Go	Open framework gravels
Gd	Deformed bedding
Glg	Palimpsest (marine) or bedload lag

Boulders (>256 mm)	
B	Boulders
Bh	Horizontally-bedded boulders
Bms	Matrix supported, massive
Bcg	Clast supported, graded
BL	Boulder lag or pavement
Bfo	Deltaic foresets
Bmg	Matrix supported, graded

Figure 4.7: Lithofacies code employed during the logging of sediment exposures in this study. *Source:* Benn and Evans (1998).

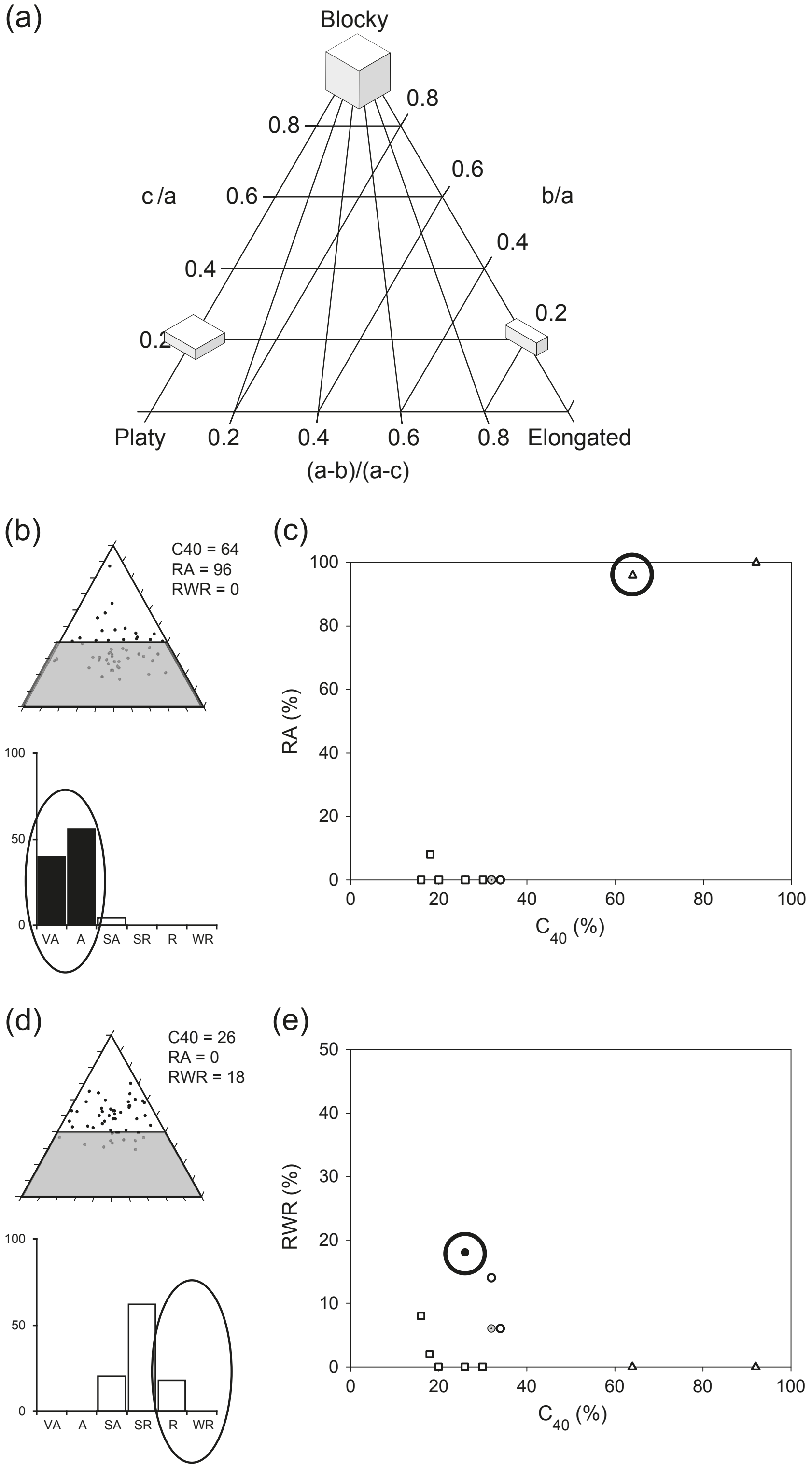

Figure 4.8: Example of how the different elements of clast shape analysis, as devised by Benn and Ballantyne (1993, 1994), are used. (a) Schematic ternary diagram, showing axial scales and end member clast forms. (b) Example ternary diagram and frequency distribution of clast roundness data of a supraglacial sample to illustrate how the C_{40}- and RA-indices are calculated (shown by grey area and black ellipse, respectively). (c) RA-C_{40}-covariance diagram illustrating how the different indices are used to discriminate between different samples. (d) Ternary diagram and frequency distribution of a distal fluvial sample to illustrate how the RWR-index is calculated. (e) RWR-C_{40}-covariance diagram illustrating how the different indices are used to discriminate between different samples. All data used are from eclogite sampled at Findelengletscher (Lukas *et al.*, 2012, in press). *Source:* Lukas *et al.* (2013: 98).

4.5 Summary

This chapter has reviewed the key remote sensing and field-based methods used in this research to examine the characteristics of recessional ("annual") moraines on the foreland of Skálafellsjökull. Geomorphological mapping, through both desk- and field-based approaches, underpins the research in this thesis, providing a framework for exploring the characteristics of the "annual" moraines. Desk-based mapping employed four remotely-sensed datasets, encompassing a range of spatial scales and temporal intervals. The remotely-sensed data included high-resolution scans of 2006 colour aerial photographs (0.41 m GSD), multispectral (8-band) WorldView-2 satellite imagery captured in June 2012 (2.0 m GSD) and associated panchromatic images (0.5 m GSD), along with a DEM generated from UAV imagery captured during surveys in the summer of 2013 (spatial resolution: 0.09 m). The application of these different approaches permits a holistic approach to mapping, wherein the advantages of the respective methods can be combined for accurate map production with robust genetic interpretations (Boston, 2012a, b). Moreover, the range of remotely-sensed data employed allowed geomorphological maps to be produced at different spatial scales and timesteps.

A chronological framework for the recessional ("annual") moraines on the Skálafellsjökull was established using two approaches: (1) examination and cross-correlation of an imagery archive spanning the period 1945 – 2012; and (2) lichenometric surveys of a sub-sample of moraines. This study employed the sampling strategy outlined by Bradwell (2001a, b), and subsequently utilised elsewhere in SE Iceland (Bradwell, 2004a, b; McKinzey *et al*., 2004, 2005; Bradwell *et al*., 2006; Bradwell *et al*., 2013). This sampling approach involves measuring the longest axis of >200 thalli of lichen *Rhizocarpon* Section *Rhizocarpon* in fixed area quadrats on the proximal slopes of moraines. Size-frequency analysis was subsequently undertaken to examine lichen population distribution for each of the moraines (e.g. Bradwell, 2001b, 2004b; McKinzey *et al*., 2004). For comparison, a range of lichenometric dating curves were employed to derive estimates of the data of moraine abandonment, including: (1) the linear (long axis) age-size curve developed for the Skálafellsjökull foreland by Gordon and Sharp (1983); (2) the curvilinear age-size curve calibrated by Bradwell (2001a, b) for SE Iceland glacier forelands; and (3) the age-gradient curve developed by Bradwell (2004b) for SE Iceland glacier forelands.

Sedimentological analysis of manually-created exposures through "annual" moraines was undertaken to provide information on landform genesis. Sedimentological investigations followed established procedures, including section logging and description, lithofacies analysis and clast shape analysis (*cf*. Benn and Ballantyne, 1993, 1994; Evans and Benn, 2004;

Lukas *et al*., 2013). These procedures have been widely employed in investigations of ice-marginal moraine genesis, both in glaciated and glacierized environments, and have provided valuable insights into glacier dynamics (e.g. Lukas, 2005a, b, 2007b, 2012; Benn and Lukas, 2006; Reinardy *et al*., 2013).

CHAPTER 5

Moraine geomorphology, sedimentology and chronology

This chapter presents the results of geomorphological, sedimentological and chronological investigations of recessional (“annual”) on the Skálafellsjökull foreland. The distribution and geomorphological characteristics of the moraines, along with associated glacial geomorphological features, are described in Section 5.1. Further detailed analyses of moraine morphometry are also presented in this section. Section 5.2 examines the chronology of moraines on the glacier foreland through a combination of remote sensing observations and lichenometric analyses. These data are then employed to derive a chronology for moraine formation and allows the frequency of moraine formation to be assessed. The sedimentary composition and structure of the moraines are subsequently examined in Section 5.3, enabling the genetic processes of moraine formation to be evaluated. Section logs and clast shape data are presented and interpreted for four moraines, which are considered representative of the facies associations evident in the Skálafellsjökull foreland. The wider significance of the results will be discussed in Chapter 7, with the data providing a framework for exploring patterns, rates and drivers of recent ice-marginal retreat at Skálafellsjökull.

5.1 Moraine distribution and geomorphology

Glacial geomorphological mapping reveals a series of *minor moraines* distributed across the Skálafellsjökull foreland, with long, largely uninterrupted sequences of moraines occurring on the northern and central parts of the glacier foreland. Additionally, numerous minor moraines are evident in close proximity to the southeastern margin of Skálafellsjökull. Excerpts from the geomorphological maps show the pattern and distribution of minor moraines on the central and northern parts of the foreland (Figure 5.1) and minor moraines at the southeastern Skálafellsjökull margin (Figure 5.2). Fully interpreted geomorphological maps showing the pattern and distribution of moraines in the entire mapped area are found in Appendix I and II, based on 2006 aerial photographs (Appendix I) and 2012 satellite imagery (Appendix II). An indication of the distribution and coverage of glaciofluvial sediments is also presented on the geomorphological maps, though this mapped unit has been simplified in places so as not to detract from the detail of the mapped morainic features. Mapping of the Skálafellsjökull foreland surficial geology has been presented by Evans and Orton (2014).

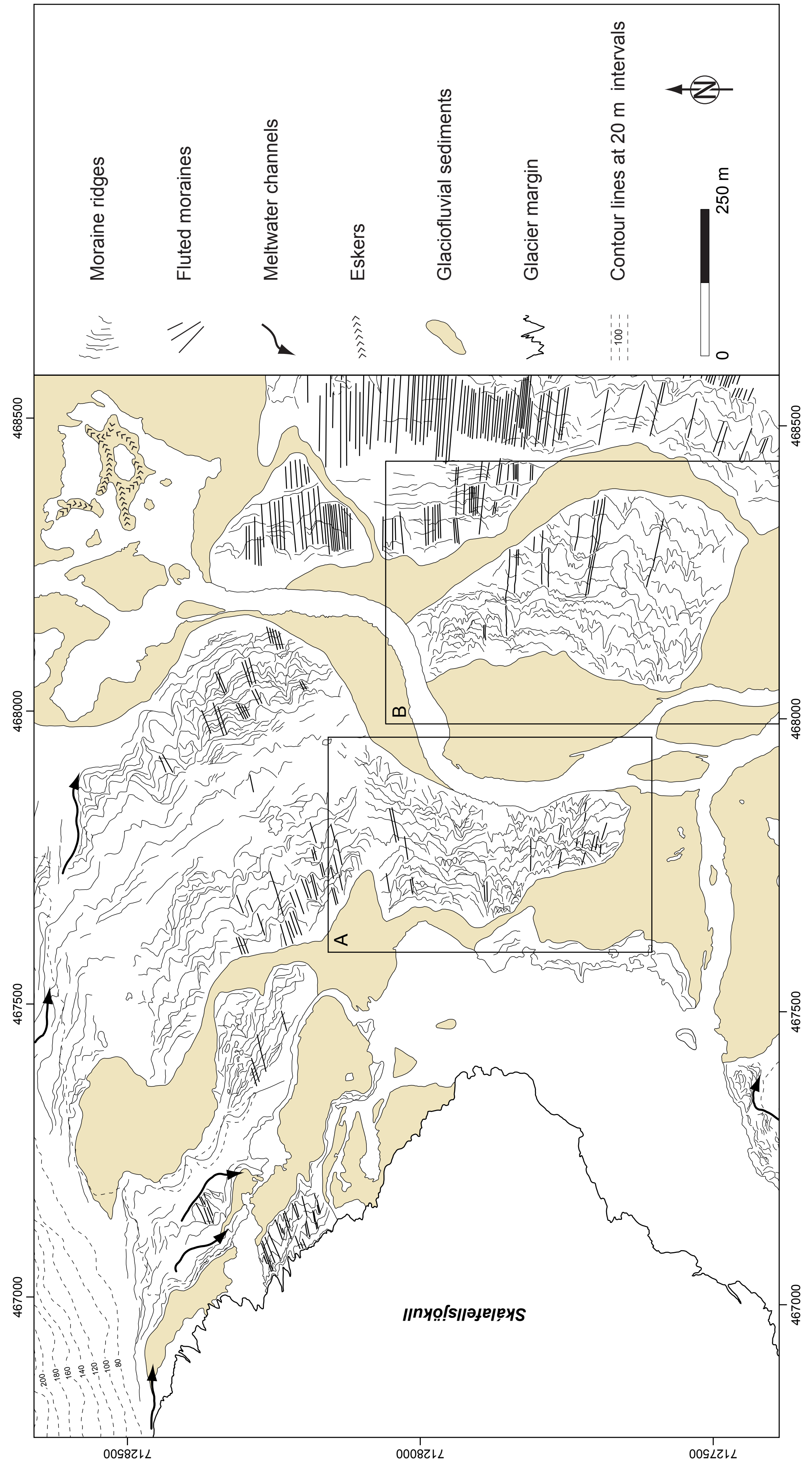
Moraine ridges
Fluted moraines
Meltwater channels
Eskers
Glaciofluvial sediments
Glacier margin
Contour lines at 20 m intervals
100
0
250 m
N
A
B
Skálafellsjökull
467000
467500
468000
468500
7128500
7128000
7127500
200
180
160
140
120
100
80

Figure 5.1: Extract glacial geomorphological map of the northern and central parts of the Skálafellsjökull foreland, illustrating the distribution of minor moraines. Boxes marked A and B show areas that have been subject to more detailed, large-scale mapping using the UAV-generated DEM (Figures 5.6 and 5.7). Mapping is based on 2012 imagery captured by the WorldView-2 satellite and supplied by *European Spacing Imaging* (ID: 103001001A462900). Map projection is WGS 1984 / UTM Zone 28N (ESPG: 32628).

The moraines on the northern and central parts of the foreland take the form of mostly continuous ridges that may extend up to *c.* 530 m in length. However, these ridges may locally consist of a number of moraine fragments, ranging in length from ~ 3 – 20 m, which form part of longer morainic chains (Figure 5.1). By contrast, the minor moraines at the southeastern margin of Skálafellsjökull are predominantly discontinuous and fragmentary in nature, with longer, continuous moraine ridges being limited in number (Figure 5.2). In total, 3201 moraine fragments were mapped on the Skálafellsjökull foreland (based on 2012 imagery). Lateral spacing between moraine fragments across the glacier foreland ranges from *c.* 3 m to 35 m. In places fragments are occasionally separated by relict stream channels, indicative of postdepositional breaching of longer, continuous ridges by meltwater streams. Crest-to-crest spacing (or longitudinal) spacing between individual chains of minor moraines ranges from ~5 m to 60 m on the Skálafellsjökull foreland.

In planform, moraine ridges on the Skálafellsjökull foreland exhibit a distinctive *sawtooth* or crenulate pattern, with *teeth* pointing in a down-ice direction and *notches* pointing upglacier (Figure 5.3; *cf.* Matthews *et al*., 1979; Burki *et al*., 2009). Teeth exhibit maximum wavelengths and amplitudes of *c.* 50 m and c. 39 m, respectively, whilst notches exhibit maximum wavelengths and amplitudes of *c.* 47 m and *c.* 41 m (Figure 5.4). Complexities in the general planview geometry occur locally, with individual moraine ridges exhibiting bifurcations and cross-cutting patterns (Figure 5.5). Ponding occurs occasionally on the distal side of teeth, particularly in the central parts of the glacier foreland. Minor moraines on the Skálafellsjökull foreland are typically asymmetrical in cross-sectional geometry, with cross-profiles displaying shorter, steeper distal slopes and longer, gently-sloping ice-proximal surface slopes: distal slope angles typically range between 20 – 30°, whilst ice-proximal slopes are generally between 15 – 20°. Individual minor moraines have heights ranging from *c.* 0.2 m to 1.5 m, with moraine width being between *c.* 2 m and 18 m. Visually there appears to be no noticeable difference in the cross-sectional geometry of teeth and notches, though notches perhaps tend to be slightly taller and wider. Moraine crestlines are strewn with cobbles and occasional boulders, with moraine surfaces largely covered by gravel to cobble sized material. Occasional large, angular boulders (*a*-axis > 2 m) occur on the moraine surfaces or strewn between

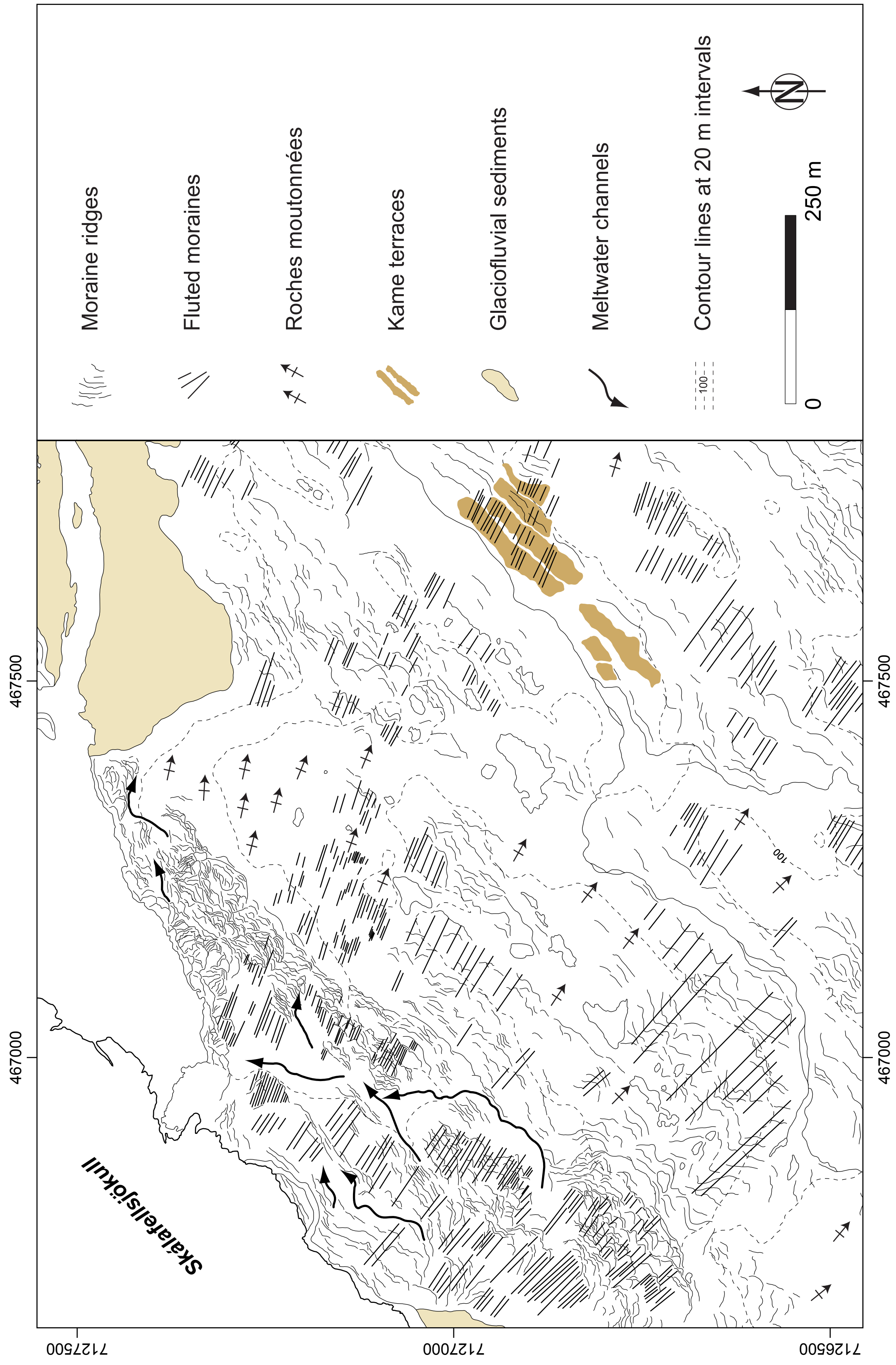
Moraine ridges
Fluted moraines
Roches moutonnées
Kame terraces
Glaciofluvial sediments
Meltwater channels
Contour lines at 20 m intervals
100
0
250 m
N
Skalafellsjökull
467000
467500
7127500
7127000
7126500
100

Figure 5.2: Extract glacial geomorphological map of the southern Skálafellsjökull foreland, illustrating the distribution of minor moraines. Mapping is based on 2012 imagery captured by the WorldView-2 satellite and supplied by *European Spacing Imaging* (ID: 103001001A462900). Map projection is WGS 1984 / UTM Zone 28N (ESPG: 32628).

individual moraine fragments. Lithologies of the cobbles and boulders reflect the local bedrock geology, with non-vesicular basalts dominant.

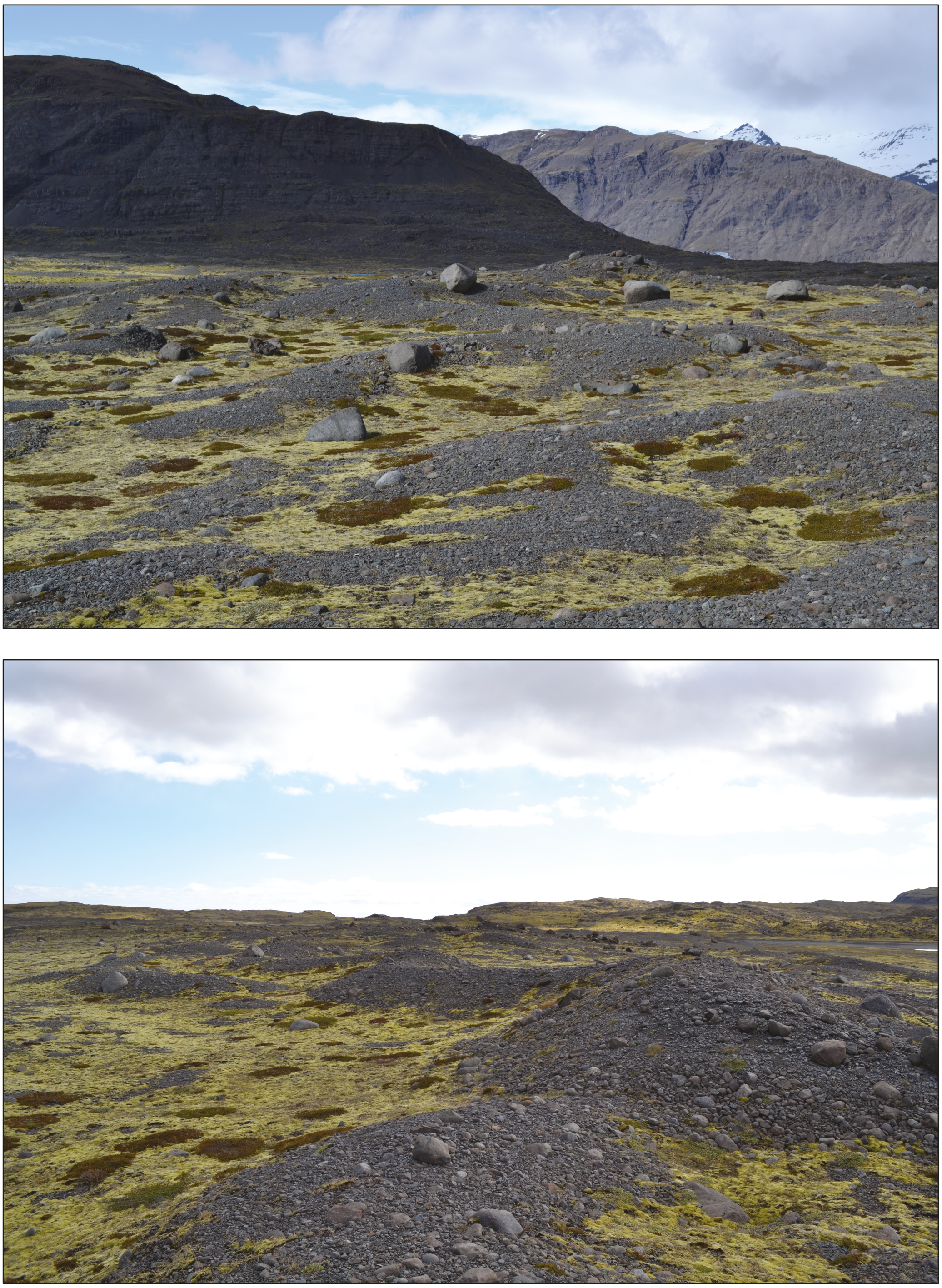

Figure 5.3: Field photographs illustrating the characteristic *sawtooth* planform of moraines on the foreland of Skálafellsjökull.

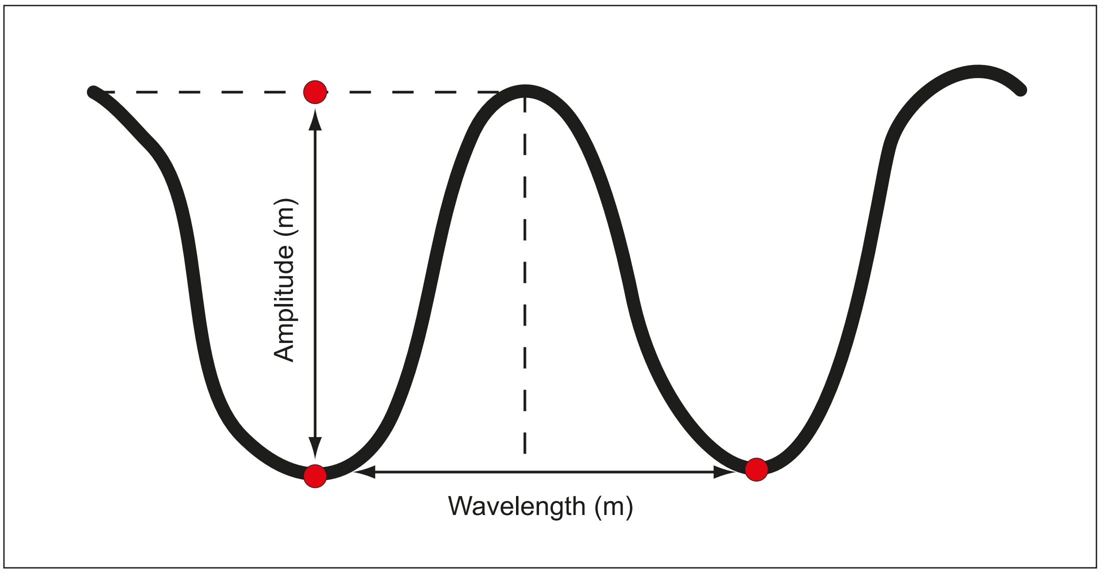

Figure 5.4: Planform of an idealised *sawtooth* moraine showing the method for calculating the wavelength and amplitude of *teeth* and *notches*. After Burki *et al*. (2009).

Figure 5.5: UAV image illustrating the complex patterns of moraines on the glacier foreland, with evidence of bifurcations and localised superimposition of moraines. Photograph: Alex Clayton.

The availability of a high-resolution DEM produced from photographs acquired using a UAV (§4.1; A. Clayton, pers. comm., 2014) has also enabled high-resolution, large-scale sample mapping of moraines on the Skálafellsjökull foreland to be undertaken. The DEM does not provide complete coverage of the glacier foreland but mapping of the bounding break of slope for individual moraines in two selected areas (areas A and B; see Figure 5.1) provides a clear visualisation of the planform geometry that characterises minor moraines on the Skálafellsjökull foreland and the local complexities in the planview pattern (Figures 5.7 and 5.8). Both areas exhibit the striking sawtooth or crenulate pattern, with area A exhibiting frequent bifurcations (Figure 5.6). Meanwhile, area B exhibits a highly complex pattern of moraines, with numerous incidences of ridge cross-cutting and superimposition (Figure 5.7).

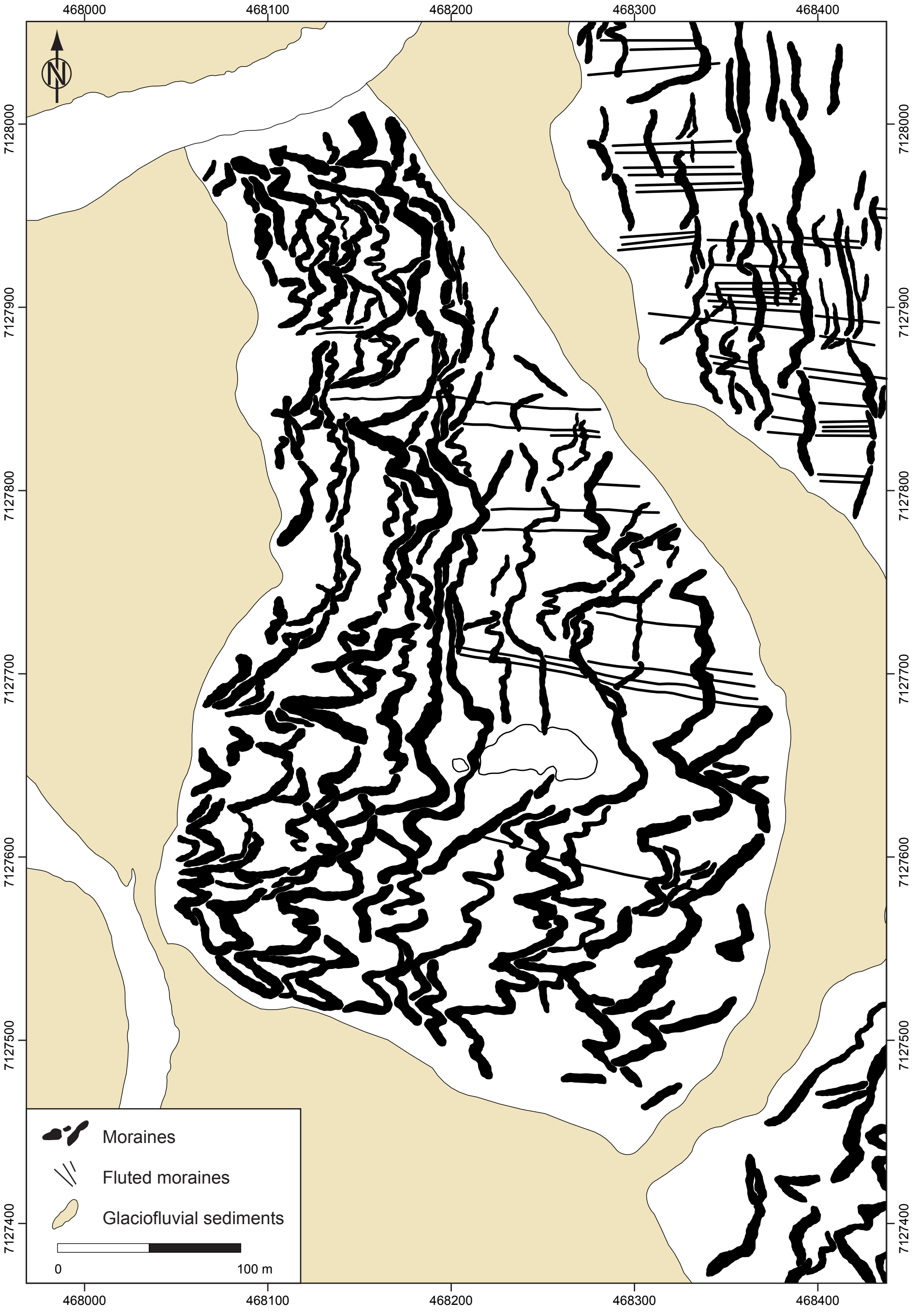

Figure 5.6: Detailed, large-scale glacial geomorphological map illustrating the distribution and planform geometry of minor moraines in area A (see Figure 5.1). Mapping is based on the UAV-generated DEM. Map projection is WGS 1984 / UTM Zone 28N (ESPG: 32628).

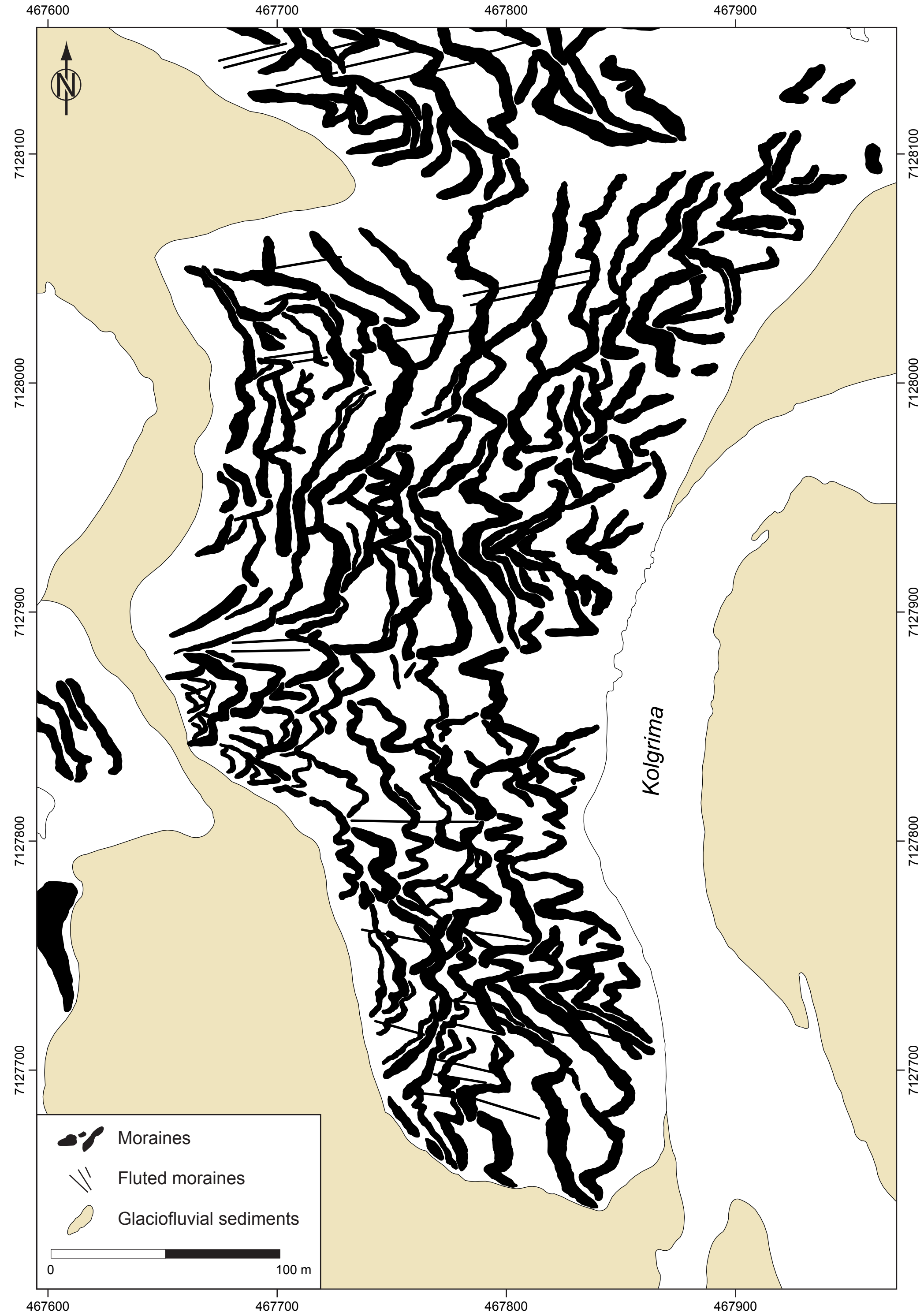

Figure 5.7: Detailed, large-scale glacial geomorphological map illustrating the distribution and planform geometry of minor moraines in area B (see Figure 5.1). Note the complex cross-cutting patterns and bifurcations in this area of the foreland. Mapping is based on the UAV-generated DEM. Map projection is WGS 1984 / UTM Zone 28N (ESPG: 32628).

5.1.1 Morphometric analyses

The available dataset of mapped minor moraines (n = 3201), combined with the additional dataset of mapped moraine polygons and availability of a high-resolution DEM (spatial resolution: 0.09 m) allows the morphometry of the moraines to be explored. Moraine morphometry has been given limited treatment in the literature, with investigations restricted to a few studies (Matthews *et al.*, 1979; Burki *et al.*, 2009; Bradwell *et al.*, 2013). However, examining moraine morphometry using similar approaches to those applied to other glacial landforms (e.g. Clark *et al.*, 2009; Spagnolo *et al.*, 2010, 2014; Stokes *et al.*, 2013b; Storrar *et al.*, 2014) may provide useful insights into glacier dynamics and debris transport (debris availability).

Length – The length of the minor moraines was extracted from the mapped polyline features in *ArcMap* (*n* = 3201). Moraines in the study area exhibit a unimodal distribution and are highly positively skewed (4.54). Distributions are also leptokurtic, displaying an excess kurtosis of 36.14 (Figure 5.8). The extracted values indicate that the majority of minor moraine fragments are less than 40 m in length (74.85%), with the mean and median lengths being 35.24 m (σ = 34.94 m) and 25 m, respectively. Only 5.40% of the mapped moraines exceed 100 m in length. Examination of length values for areas A and B shows that they conform to the aforementioned general trends, exhibiting unimodal distributions with positive skewness. Areas A and B do exhibit slightly larger mean values by comparison to the entire dataset, with mean lengths of 51.03 m (Area A; σ = 48.82 m) and 40.9 m (Area B; σ = 40.08 m). Thus, the analysis indicates that minor moraines on the Skálafellsjökull foreland are largely fragmentary in nature.

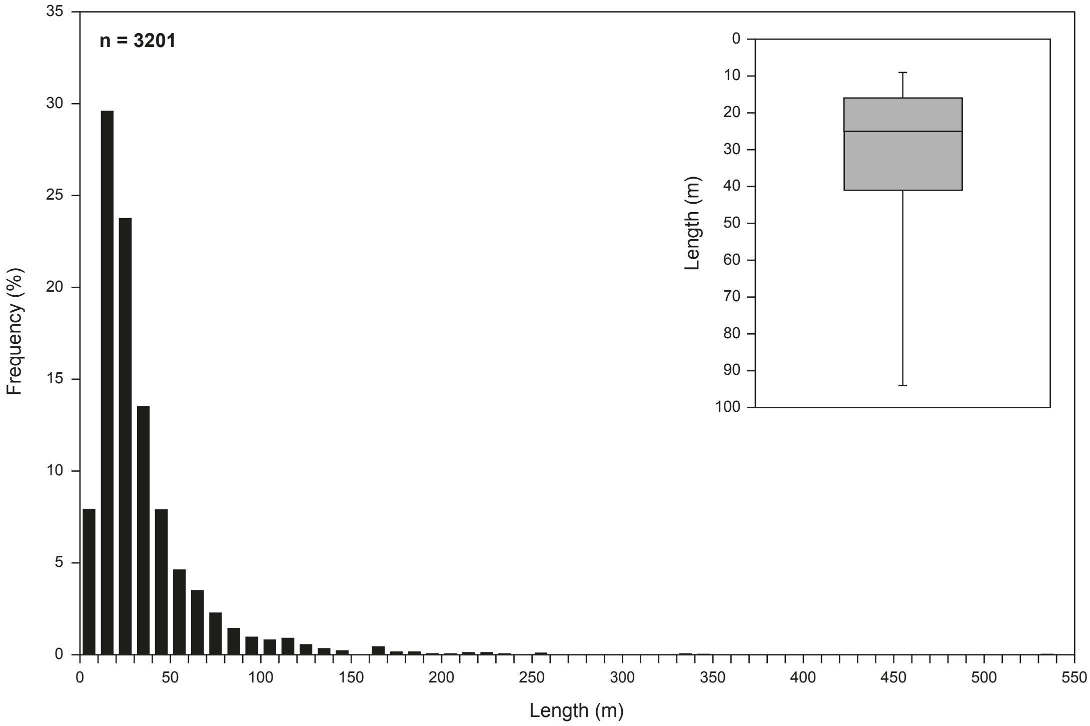

Figure 5.8: Histograms and summary statistics of mapped moraine lengths for the entire dataset. Box-and-whisker plots show the 25th and 75th percentiles (grey box), and the 5th and 95th percentiles (whisker ends). The mean (horizontal line) is also shown.

Width – Moraine widths have been extracted from the mapped polygons in *ArcMap*. Widths were obtained along 30 transects, 15 in area A and 15 in area B, allowing variations in width along individual moraine ridges to be captured in the dataset. Similar to moraine length, moraine widths exhibit a unimodal, leptokurtic distribution, with an excess kurtosis of 2.89 and a positive skewness value (1.39; Figure 5.9). Moraine widths in the two areas range between 1.42 m and 18.35 m, with a mean value of 5.74 m (σ = 2.78 m) and a median of 5.24 m (*n* = 345). Moraines predominantly display widths of 3 – 8 m, with 75.00% of moraines displaying lengths within this range.

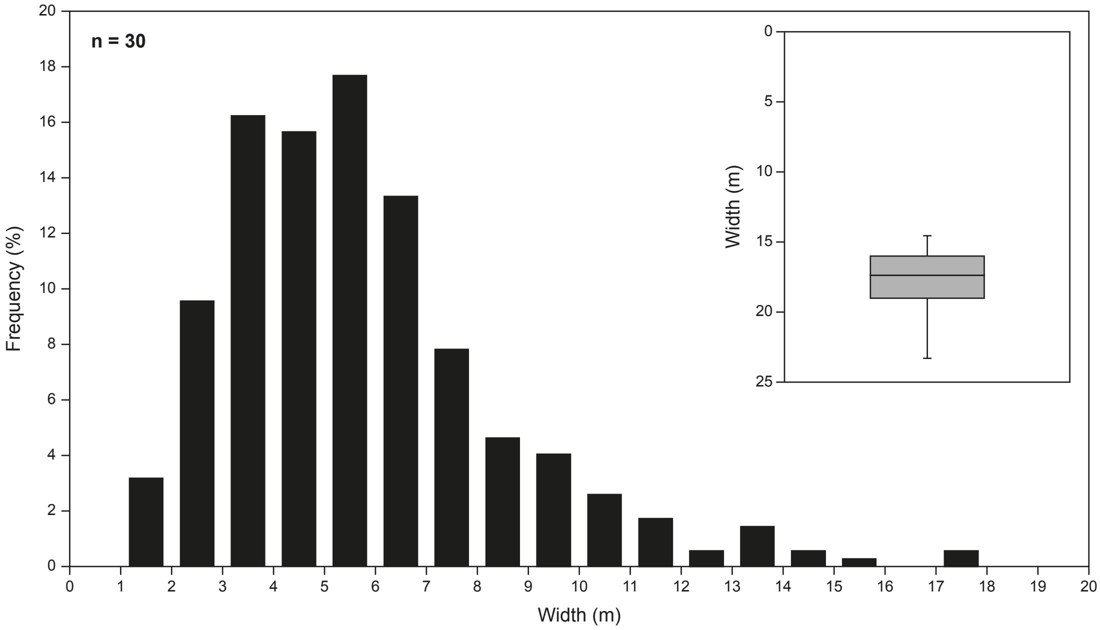

Figure 5.9: Histograms and summary statistics of extracted moraine widths for the entire dataset. Box-and-whisker plots show the 25th and 75th percentiles (grey box), and the 5th and 95th percentiles (whisker ends). The mean (horizontal line) is also shown.

Surface area – Moraine surface area was extracted from the database of mapped moraine polygons using *ArcMap* (*n* = 375). As with moraine length and width, moraine surface area exhibits a unimodal, leptokurtic distribution with high positive skewness (3.02), and an excess kurtosis of 12.58 (Figure 5.10). Moraine surface area values range between 6 m^2 and 1739 m^2, with the majority of moraines (68.53%) having surface areas of between 1 and 200 m^2. The mean surface area value for the dataset is 194.88 m^2 (σ = 219.42 m), whilst the median is 120 m^2.

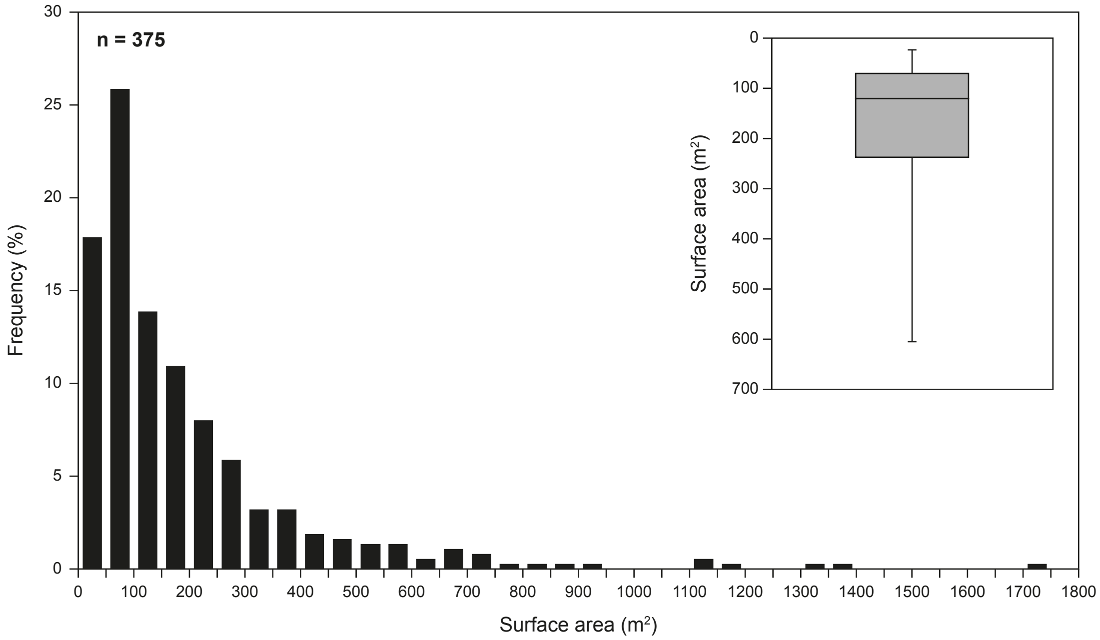

Figure 5.10: Histograms and summary statistics of extracted moraine surface area data. Box-and-whisker plots show the 25th and 75th percentiles (grey box), and the 5th and 95th percentiles (whisker ends). The mean (horizontal line) is also shown.

Variations between teeth and notches – In a previous study of moraines displaying distinctive sawtooth planform geometry, Matthews *et al.* (1979) demonstrated that statistically significant differences existed between morphometric characteristics of moraine teeth and notches at Bødalsbreen, southern Norway: notches had greater heights ($p < 0.01$) and steeper ice-proximal slopes ($p < 0.001$) than teeth. In order to examine whether teeth and notches exhibit different morphological characteristics on the Skálafellsjökull foreland, a sample of 50 moraine cross-sectional profiles, in areas A and B, have been extracted from the high-resolution DEM in *ArcMap* (Figure 5.11). Using the extracted moraine profiles, the width and height of each tooth and notch have been calculated.

Moraine notches have a mean height of 0.67 m ($\sigma = 0.29$ m), with values ranging between 0.19 m and 1.48 m. By comparison, teeth have a slightly lower mean value of 0.60 m ($\sigma = 0.33$ m), with the range of heights being 0.15 – 1.48 m. The width of teeth ranges between 3.71 m and 15.44 m, with a mean value of 8.56 m ($\sigma = 3.10$ m) and a median of 8.19 m. Conversely, notches exhibit greater mean and median values of 9.73 m ($\sigma = 1.87$ m) and 9.50 m, respectively. Notch width ranges between 6.03 m and 13.72 m. In order to establish whether the observed differences in morphometric characteristics are statistically significant, an *unpaired*, non-parametric test was applied (the Wilcoxon rank-sum or Mann Whitney U test; *cf.* Mann and Whitney, 1947; Siegel, 1956; Blair and Higgins, 1980; Fay and Proschan, 2010). The results of the statistical analyses (Table 5.1) indicate that there is no statistically significant difference between the two independent sample distributions ($p > 0.05$).

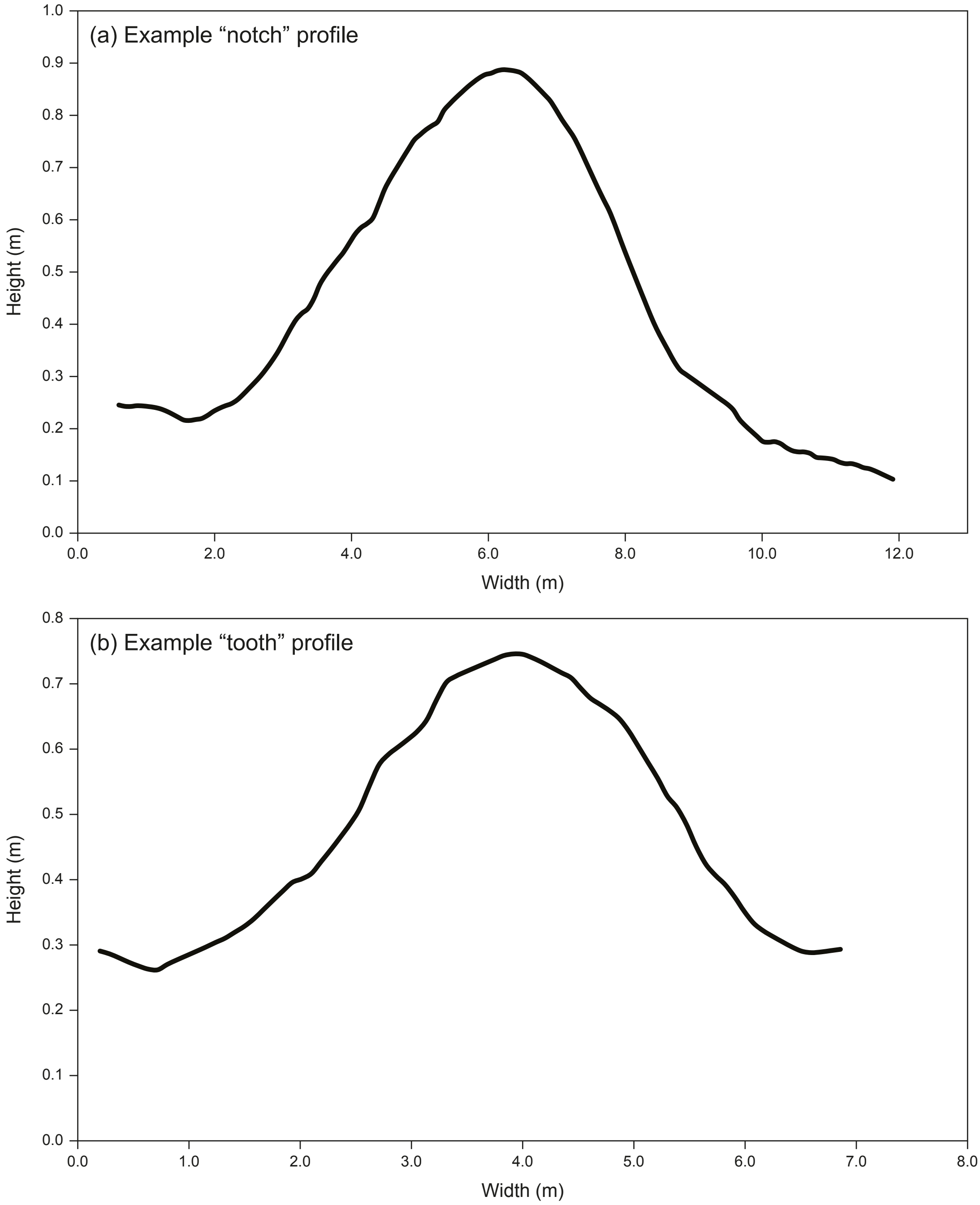

Figure 5.11: Example moraine cross-profiles extracted from *ArcMap*, illustrating the typical morphology of *teeth* (a) and *notches* (b) on the Skálafellsjökull foreland.

Table 5.1: Wilcoxon rank-sum test to examine the statistical significance of differences between the morphological characteristics of teeth and notches.

Moraine	Sample size		Mean		Standard Deviation		Significance of differences
	Teeth	*Notches*	*Teeth*	*Notches*	*Teeth*	*Notches*	
Height (m)	26	24	0.60	0.67	0.33	0.29	Not significant
Width (m)	26	24	8.56	9.73	3.10	1.87	Not significant

Relationship between width and spacing – Previously it has been shown that larger annual moraines are frequently more closely spaced, with smaller annual moraines associated with wider crest-to-crest spacing (e.g. Bradwell *et al.*, 2013). Larger, closely-spaced moraines are suggested to reflect a period of negative mass balance and strong forward motion, whereas smaller, wider-spaced moraines result from greater ablation and less forward movement at the ice-front. In order to examine the relationship between moraine size and crest-to-crest spacing at Skálafellsjökull, moraine width and crest-to-crest spacing were extracted from *ArcMap* along 30 transects (as mentioned above). Bivariate analysis of moraine width and crest-to-crest spacing using least squares regression (Figure 5.12) demonstrates a weak, but statistically significant, positive correlation between moraine width and spacing for the entire dataset ($r^2 = 0.0595$, $p < 0.0001$). Thus, moraine width appears to vary largely independently of moraine spacing at Skálafellsjökull.

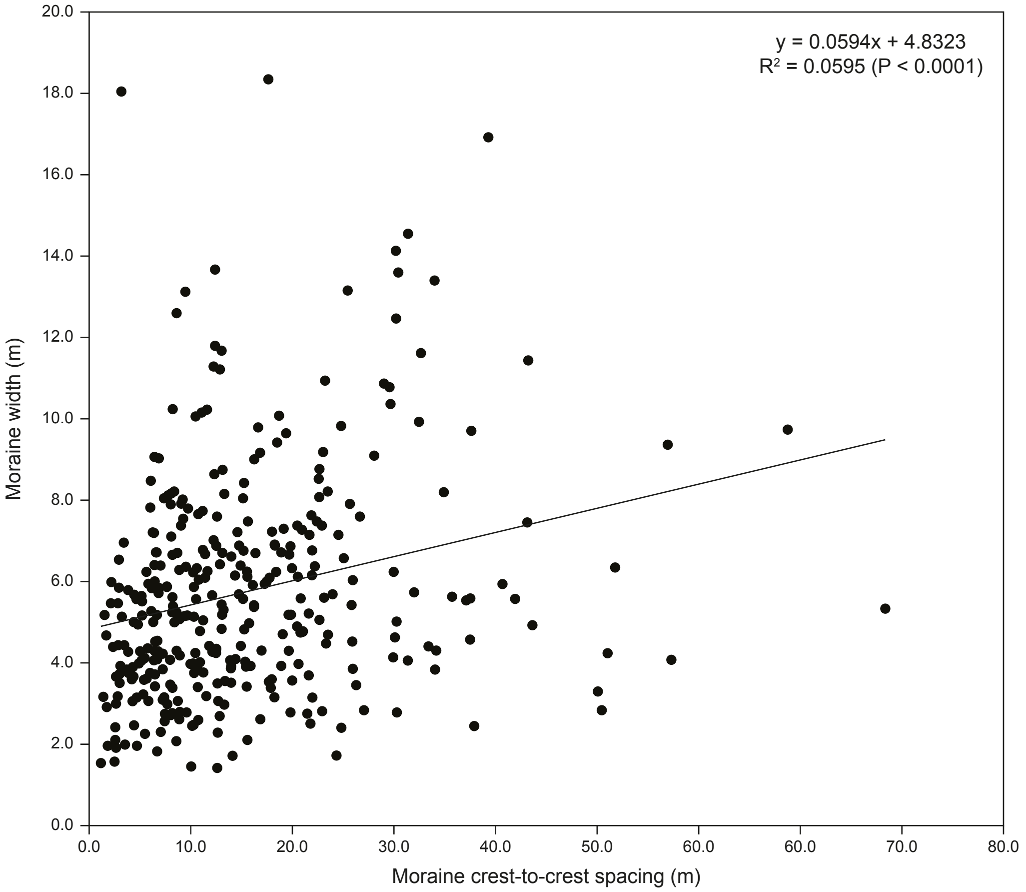

Figure 5.12: Bivariate plots of moraine spacing against moraine width for the entire dataset.

5.1.2 Associated glacial geomorphological features

Minor moraines on the Skálafellsjökull foreland are frequently found in close association with flutings, which may extend on to the ice-proximal slopes of moraines in places (Figure 5.13).

Mapped flutings range in length from 7 m to 201 m, with a mean value of 42.8 m (n = 951; 2012 imagery). On the reverse basalt bedrock slope near the southern/southeastern margin of Skálafellsjökull, minor moraines and flutings are also found in association with an abundance

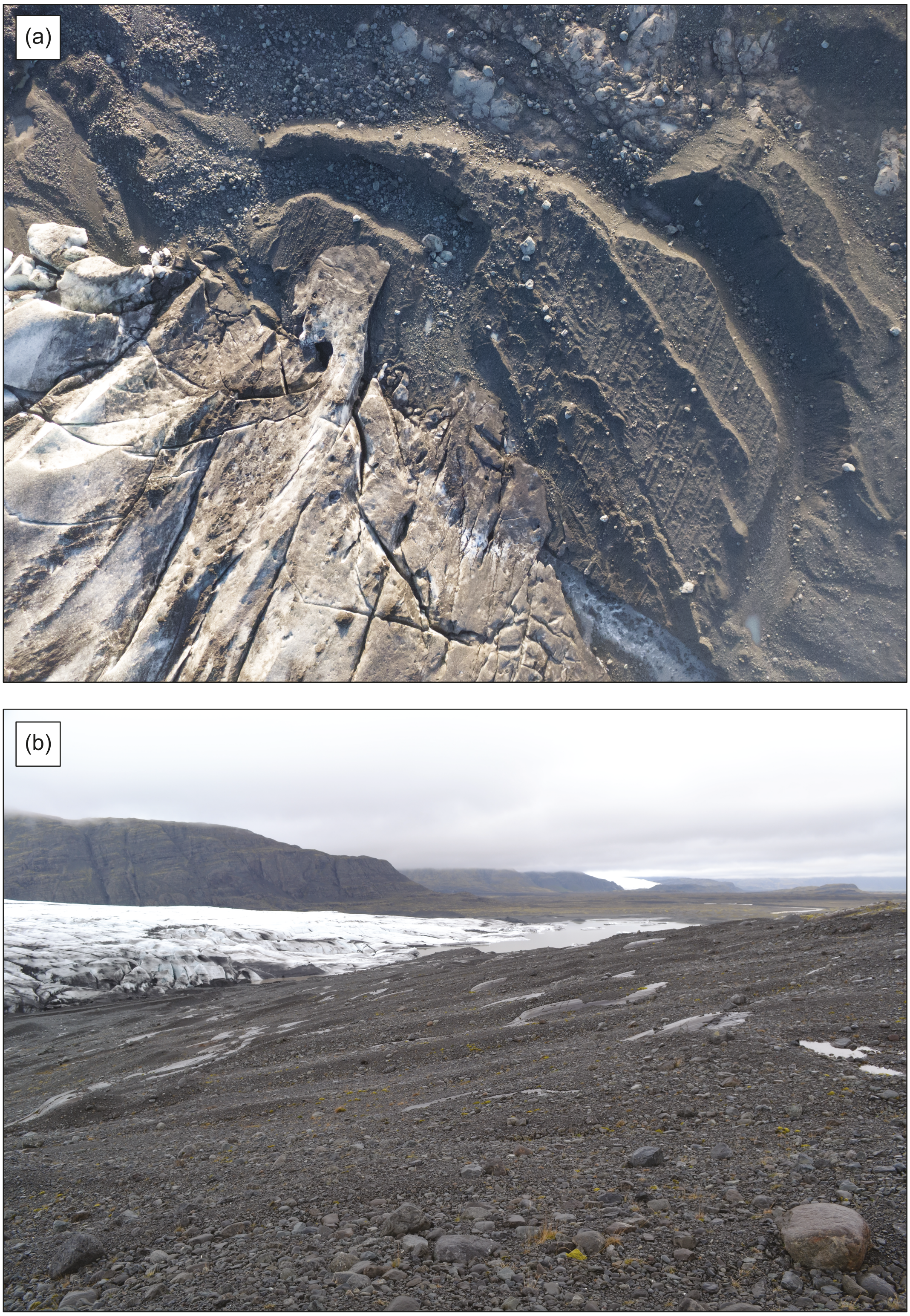

Figure 5.13: Photographs of flutings on the foreland of Skálafellsjökull. (a) UAV image of minor moraines and flutings at the 2013 ice-margin. Note the slight displacement of flutings either side of moraine ridges. Photograph: Alex Clayton. (b) Field photograph across the southern part of the Skálafellsjökull foreland showing the close association of flutings and minor moraines (21.05.14).

of roches moutonnées: flutings often extend from the lee-side faces of roches moutonnées. This area of the glacier foreland is also characterised by a number of recessional meltwater channels and a contemporary meltwater stream running along the ice-margin (Figure 5.14). Locally, meltwater accumulates along parts of the southern margin to form a small ice-marginal lake. At the time of the field investigations (May – June 2014), minor moraines in close proximity to the contemporary ice-margin could be found partially submerged by ponded and slow-moving meltwater (Figure 5.14b). In addition to the aforementioned glacial geomorphological features, a number of incidences of buried ice were identified in the southern part of the foreland during field investigations (Figure 5.15). The close association of flutings and minor moraines on the Skálafellsjökull foreland suggests the formation of these geomorphological features may be intimately linked, as has previously been suggested at Icelandic glaciers (*cf.* Boulton, 1976; Boulton and Hindmarsh, 1987; Benn, 1994; Evans and Twigg, 2002; Evans, 2003a). Meanwhile, the large quantities of meltwater and the reverse bedrock slope evident in the southern part of the glacier foreland may have important implications for submarginal processes and/or moraine formation. These concepts are considered further in Chapter 7, wherein the moraine sedimentology data and processes of moraine formation are synthesised.

5.2 Moraine chronology

5.2.1 Remote sensing and field observations

A first order assessment of the age of the minor moraines and the frequency of their formation is provided by examination and cross-correlation of the archive of imagery for Skálafellsjökull, which spans 1945 – 2012. Examination of the remotely-sensed datasets indicates that minor moraines have formed during the following periods: 1945 to 1964; 1969 to 1974; and from 2006 to 2012. Minor moraines mapped in area A (see Figure 5.6) are evident on the oldest vertical aerial photograph, captured by the US Army Mapping Service in 1945, indicating minor moraines were also formed prior to 1945. The 1945 Skálafellsjökull margin is situated in close proximity to a minor moraine which appears to reflect the intricate ice-front morphology, though the quality and resolution of the imagery is relatively poor. Based on the available aerial photographs, it is also evident that the entire suite of minor moraines in area A were formed prior to September 1954, as the ice-margin had retreated from the area by this time (Figure 5.16). Furthermore, the good quality, higher-resolution (*c.* 0.64 m GSD) 1954 photograph reveals that the minor moraines are prominent, *fresh-looking* features. The moraines display a more subdued appearance in later aerial photographs (e.g. 1969, 1979, 1982), implying that these features were formed not long prior to 1954. Examination of the available aerial photographs and satellite imagery also indicates that this area of the glacier foreland was not subsequently overridden by ice. However, owing to a lack of remotely-sensed

Figure 5.14: (a) Field photograph of a meltwater channel in the southern part of the glacier foreland. Person for scale. (b) Field photograph of the meltwater stream flowing along the southeastern Skálafellsjökull margin (29.05.14). Ponding of meltwater occurs along this part of the ice-margin, partly submerging deposited moraines.

data for the time period 1947 – 1954, combined with the fact that moraines in this sequence formed prior to the earliest aerial photograph, formation dates (and frequency) cannot be confidently ascribed to this sequence of moraines without additional chronological evidence.

Figure 5.15: Field photograph of an exposure of buried glacier ice in the southern Skálafellsjökull foreland (13.06.14). Foldable shovel for scale.

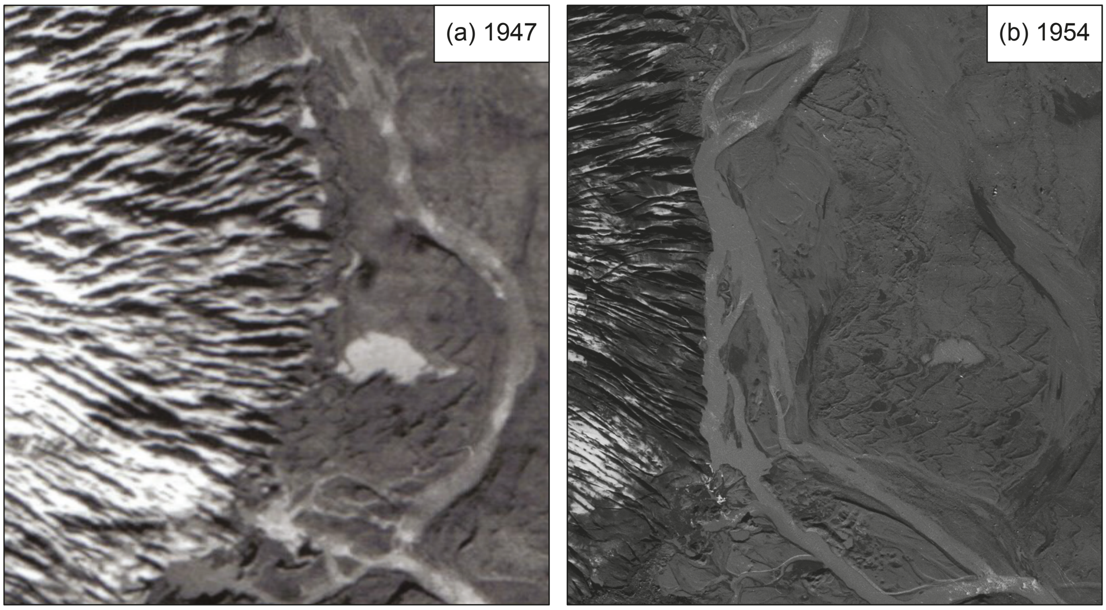

Figure 5.16: Aerial photograph extracts of the Skálafellsjökull foreland showing moraines in area A (north-orientated). Photographs were captured by Landmælingar Íslands in (a) 1947 and (b) 1954.

The sequence of minor moraines on the northern part of the Skálafellsjökull foreland, located to the north of area B (see Figures 5.1 and 5.2), formed some time during the period 1945 – 1964 on the basis of aerial photograph evidence (Figure 5.17). The outermost moraine in this sequence is ascribed a formation date of 1945 based on the available photographs, with another 12 moraines subsequently formed prior to 1957. The 1957 ice-margin is situated in close proximity to a minor moraine in this sequence, suggesting formation during a small 1956/1957 winter re-advance. The four aerial photographs captured during the period 1945 – 1957 show Skálafellsjökull was in overall retreat throughout this period, with no evidence of re-advance. This is supported by ice-front measurements by the Icelandic Glaciological Society which demonstrate Skálafellsjökull underwent ice-marginal retreat each year between 1945 and 1957, averaging ~28.5 m a^{-1}. Based on this evidence, combined with fact that the number of minor moraines formed during the period 1945 – 1957 is equivalent to the time elapsed between the bracketing ages, these minor moraines are interpreted as annual recessional moraines (*cf.* Krüger, 1995; Bradwell, 2004a; Krüger *et al*., 2010; Bradwell *et al*., 2013). The minor moraines deposited inside the 1957 annual moraine cannot be conclusively interpreted as annual moraines due to a paucity of aerial photographs and ice-front measurement data between 1957 and 1964. Moreover, examination of the 1969 aerial photograph reveals the glacier re-advanced onto this part of the foreland, introducing complexity to this part of the mapped moraine sequence and precluding confident formation date estimation.

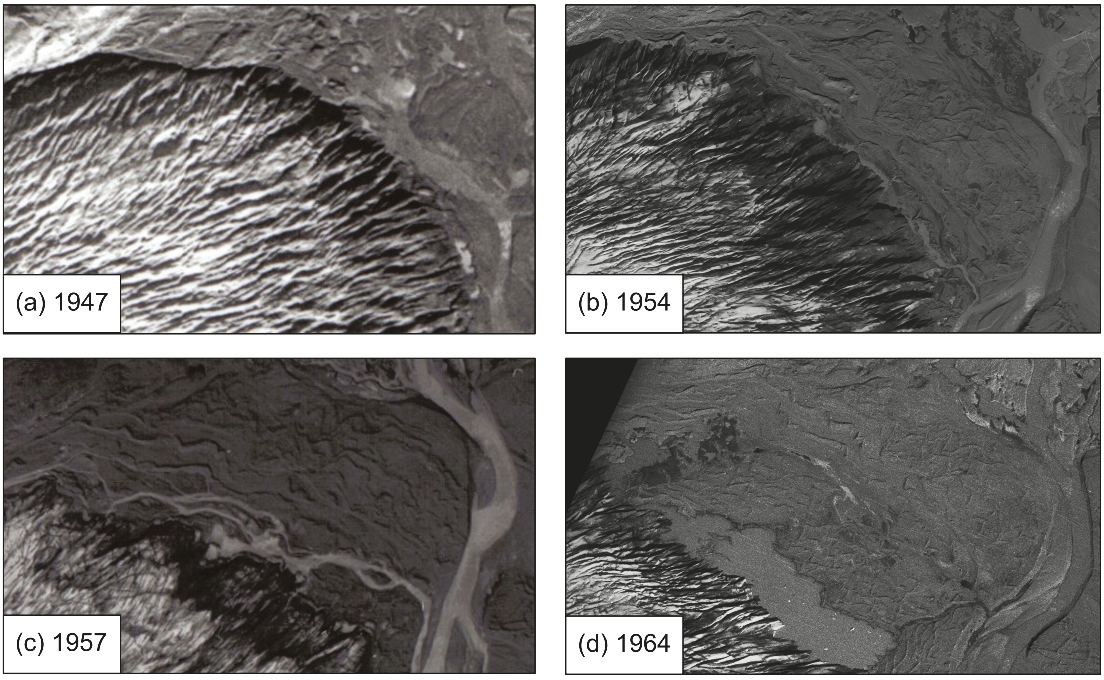

Figure 5.17: Aerial photograph extracts showing the retreat of the Skálafellsjökull and formation of minor moraines on the northern part of the glacier foreland (north-orientated).

The suite of minor moraines mapped in area B (see Figure 5.7) was formed between 1954 and 1969 based on the aerial photographs obtained from *Landmælingar Íslands* (Figure 5.18). The northeastern and eastern parts of the sequence have been partially affected by meltwater activity, as well as the evolution and migration of the Kolgrima River: minor moraines evident close to the 1954 ice-margin have been subject to postdepositional modification or have been obliterated altogether (Figure 5.18). Furthermore, the innermost (western) part of the moraine sequence has been affected by glacier re-advance, when Skálafellsjökull re-advanced sometime between 1964 and 1969. Unfortunately there is a paucity of ice-front measurement data during the 1960s and 1970s to verify the timing of this re-advance. Moreover, it is unknown how extensive this re-advance was or how long this period of re-advance may have persisted after 1969. The ice-margin had, however, retreated from this area of the foreland by 1975, with the ice-marginal lake substantially increasing in size between 1969 and 1975. Bracketing ages for this moraine suite can only be confidently ascribed to minor moraines situated in close proximity to the 1957 and 1964 ice-margins. Within these bracketing minor moraines six further minor moraines are identifiable, equivalent to the time elapsed between the bracketing moraines. As such, these minor moraines are believed to be annual moraines formed between 1957 and 1964.

A further sequence of minor moraine ridges is evident on the northern part of the Skálafellsjökull foreland, situated to the northwest of area B and to the west of the moraine sequence discussed above. Based on the available photographic evidence, this suite was formed between 1969 and 1975 (Figure 5.19). As with the above sequences, these minor moraines are believed to represent annual moraines. Following 1975, Skálafellsjökull was relatively stable in this area of the foreland, appearing to occupy roughly the same position between 1979 and 1989 (Figure 5.19). No further minor moraines were formed during this period. Minor moraines were subsequently formed at the northeastern margin between 1989 and 2006, situated inside a substantially larger moraine (height: *c*. 9 – 10 m), but their ages are unknown owing to a lack of remotely-sensed data between 1989 and 2006. Furthermore, it is unknown whether additional (annual) moraines formed during this period and were then subsequently obliterated, either by glacier re-advance or glaciofluvial activity. Comparison of mapping from the 2006 aerial photographs and 2012 satellite imagery shows that seven minor moraine ridges, displaying distinctive sawtooth planform geometries, have been formed at this part of the Skálafellsjökull margin between 2005/2006 and 2011/2012 (Figure 5.20). As the number of moraine ridges formed during this period is equal to the time elapsed, these moraines are interpreted as annual moraines.

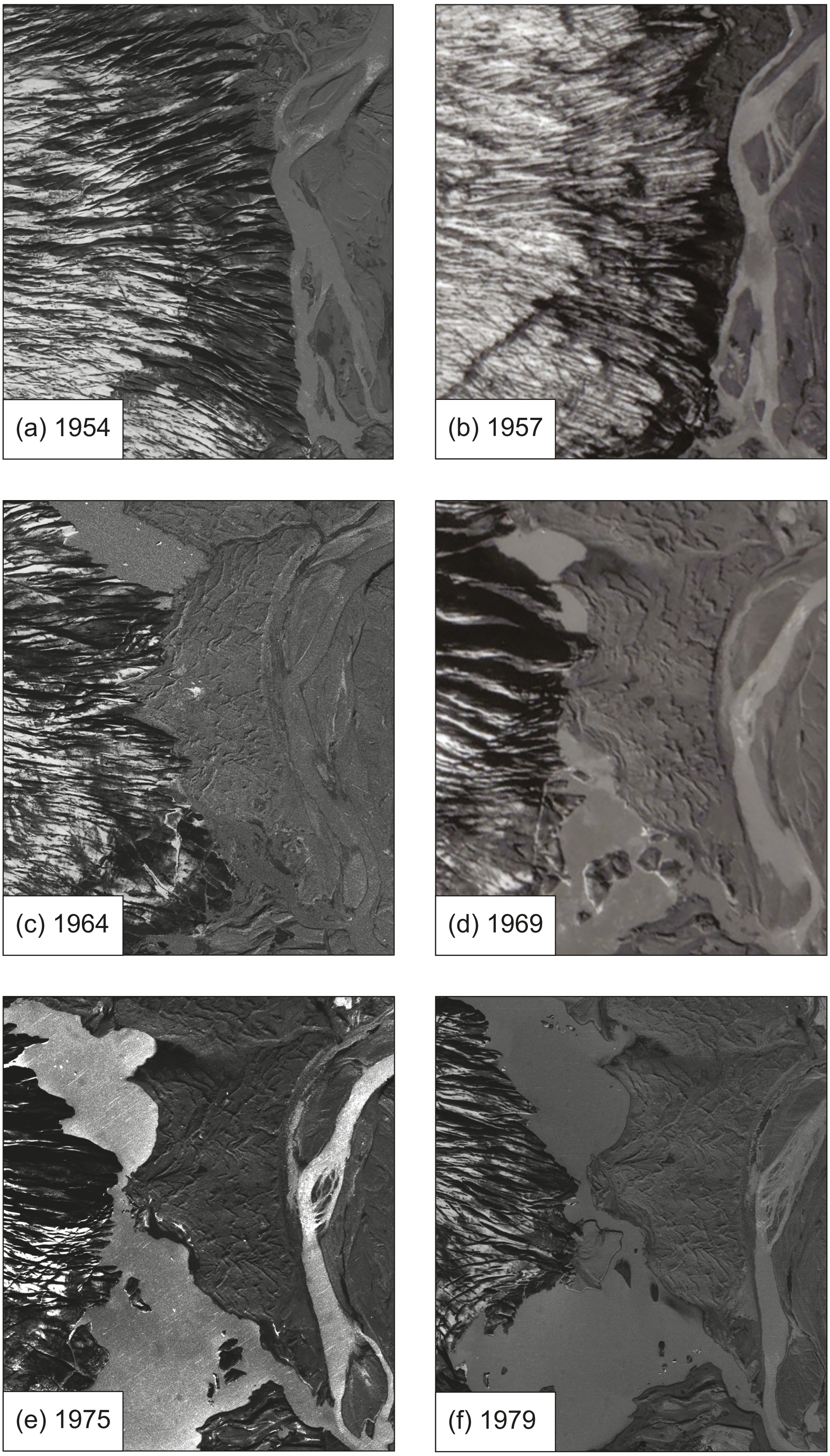

Figure 5.18: Aerial photograph extracts showing the retreat of Skálafellsjökull and formation of minor moraines in area B during the period 1954 – 1969 (north-orientated). Extracts from 1969 and 1975 illustrate the rapid retreat of the ice-margin and expansion of the ice-marginal lake.

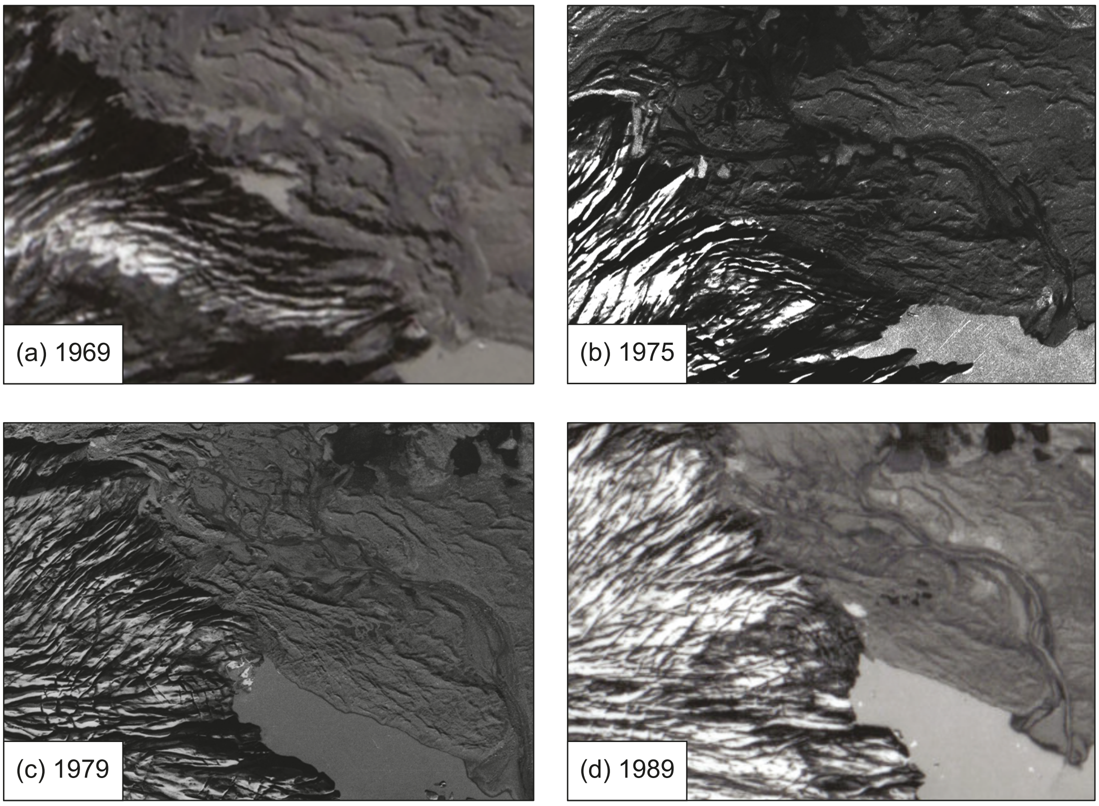

Figure 5.19: Aerial photograph extracts showing the evolution of the glacier foreland and deposition of moraines at the northeastern margin of Skálafellsjökull (north-orientated). Note the relatively stable ice-margin between 1975 and 1989.

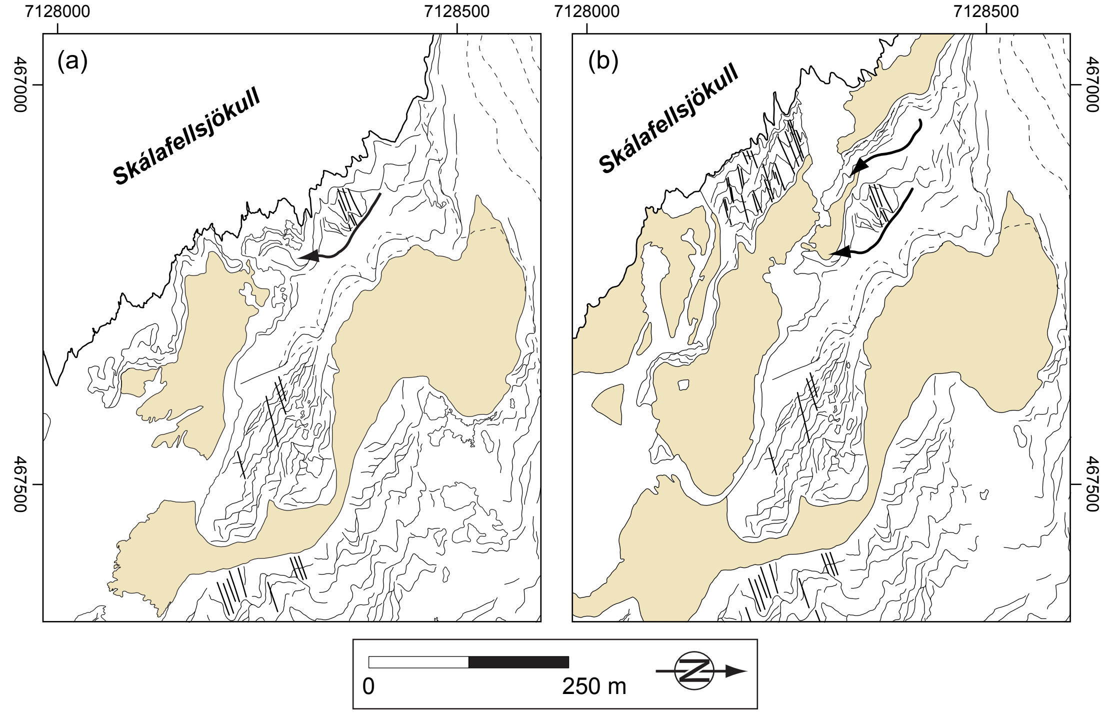

Figure 5.20: Geomorphological map extracts illustrating the retreat of the Skálafellsjökull northeastern margin and deposition of moraines between 2006 and 2012. (a) Extract of geomorphological mapping based on 2006 aerial photographs captured by *Loftmyndir ehf*. (b) Mapping based on 2012 satellite imagery captured by the WorldView-2 satellite and supplied by *European Space Imaging*.

At the southeastern margin of Skálafellsjökull, relatively few (<24) minor moraines were formed during the period 1945 – 1969. Between 1979 and 1989 the southeastern margin was relatively stable and limited moraine formation occurred in this area based on the photographic evidence (Figure 5.21). A number of minor moraines have been formed in this area since 1989 but due to a lack of data (remote sensing and ice-front measurements) relating to ice-marginal variations of Skálafellsjökull during the 1990s, age estimates cannot be confidently assigned to these moraines. Geomorphological mapping based on the 2006 and 2012 imagery indicates that numerous minor moraines have been formed in this part of the glacier foreland during 2006 – 2012 (Figure 5.22). Field investigations conducted between May and June 2014 identified a number of minor moraines that have formed since 2012, and there is evidence of ongoing moraine formation at the ice-margin (Figure 5.23). In the area of the foreland deglaciated since 2006 more than nine minor moraines have formed, implying moraines have

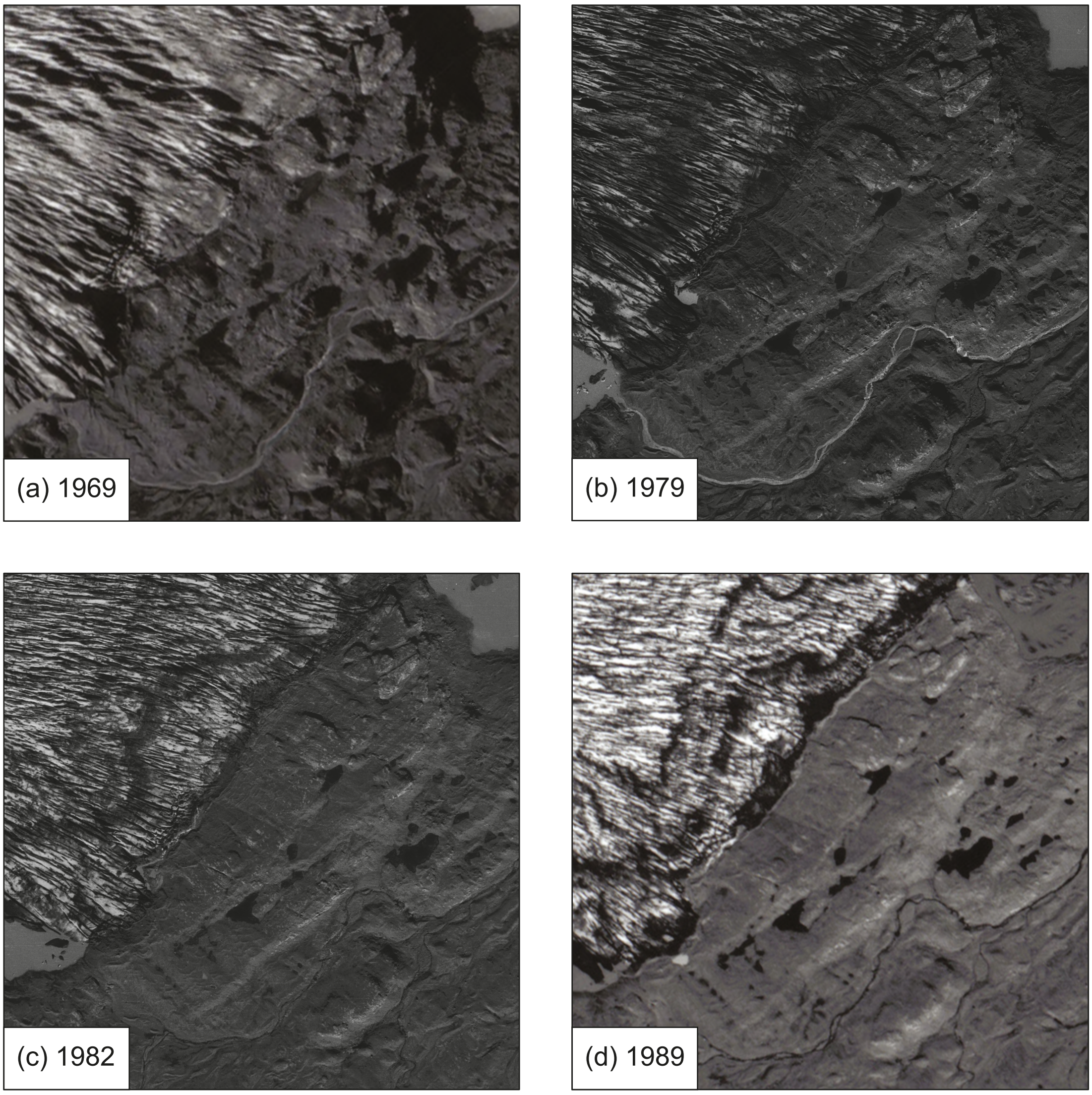

Figure 5.21: Aerial photograph extracts showing the stability of the southeastern ice-margin during the period 1979 and 1989 (north-orientated).

formed on a sub-annual basis. Sub-annual formation is indicated by the geomorphology of these minor moraines, with small moraines identifiable in the field with heights of <20 cm. Owing to these complicating factors, and without aerial photographs for every year between 1945 and 2012, minor moraines in this part of the glacier foreland cannot be confidently ascribed age estimates.

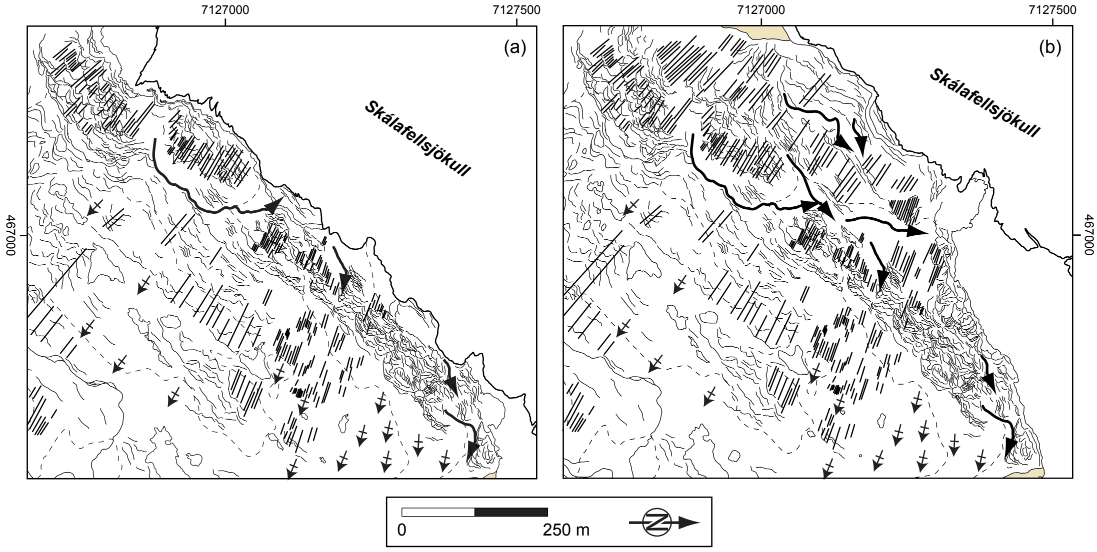

Figure 5.22: Geomorphological map extracts illustrating the retreat of the Skálafellsjökull southeastern margin and deposition of moraines between 2006 and 2012. (a) Extract of geomorphological mapping based on 2006 aerial photographs. (b) Mapping based on 2012 satellite imagery.

5.2.2 Lichenometric analysis

In order to establish the age of the minor moraines in area A formed prior to the oldest aerial photograph (prior to 1945), and to verify whether these moraines were formed annually, lichenometric surveys were conducted on the ice-proximal slope of each moraine, where possible, following established procedures (see §4.3; Bradwell, 2004a, b, 2004b). The lichen populations measured on the moraines have been plotted as log-normal plots of frequency against class size (Figure 5.24) following the method outlined elsewhere (see §4.3; Benedict, 1967, 1985; Bradwell, 2001a, b). The lichen populations have been described, using least-squares regression analysis, in the form $y = mx + c$. Assuming that the measured lichens constitute a single lichen population rather than a composite one, the plotted points should lie along a linear regression line, with the largest lichen in each lichen population falling below the theoretical ‘1 in 1000’ diameter threshold (*cf.* Andersen and Sollid, 1971; Locke *et al.*, 1979; Caseldine, 1991; Cook-Talbot, 1991; Bradwell, 2001a, b, 2004b). All lichen populations follow a straight line approximately and show a strong negative correlation between lichen diameter and $\log_{10}$ frequency, with r^2 values ranging from 0.8580 to 0.9763 (Figure 5.25). Furthermore, the lichen populations fall below the predicted ‘1 in 1000’

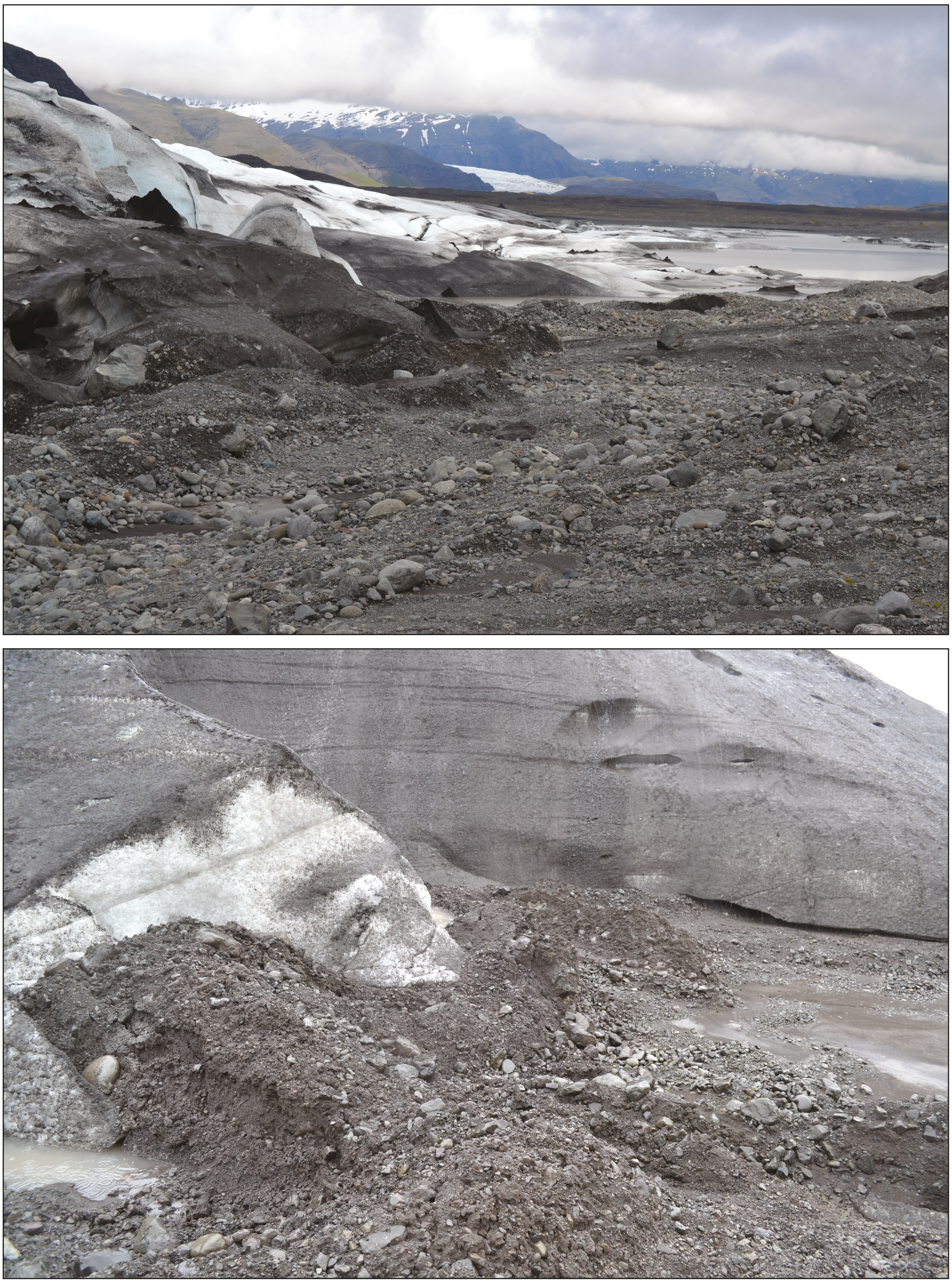

Figure 5.23: Field photographs showing examples of ongoing moraine production at the margin of Skálafellsjökull. Photographs were taken during fieldwork between May and June 2014.

diameter in all cases. Thus, the lichens comprise single, rather than composite, size-frequency populations and the largest lichen in each population can therefore be applied to derive dates for the moraines using the *age-size* dating curve of Bradwell (2001a, b).

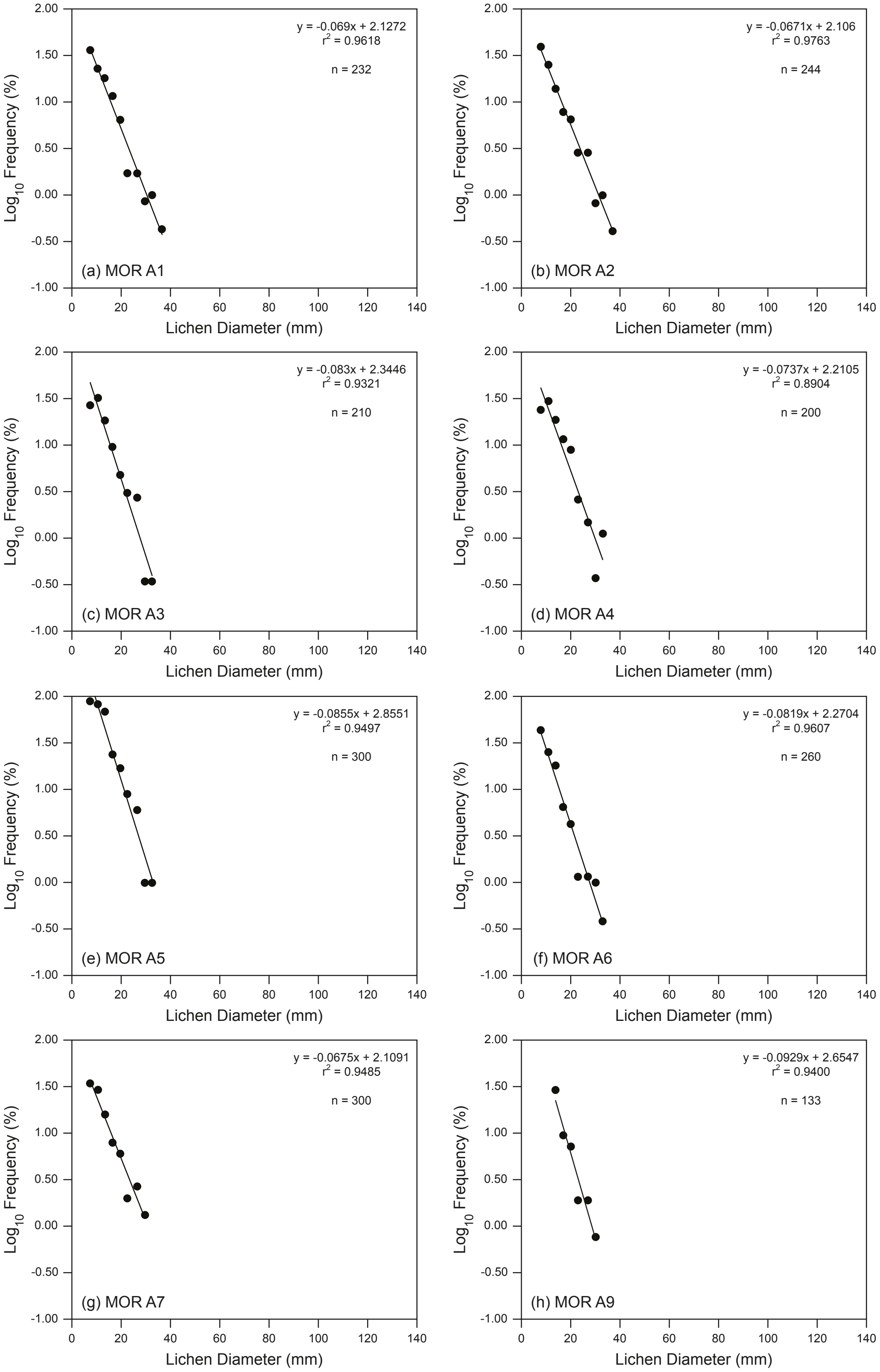

Figure 5.24: Lichen size-frequency plots for moraines in area A of the Skálafellsjökull foreland.

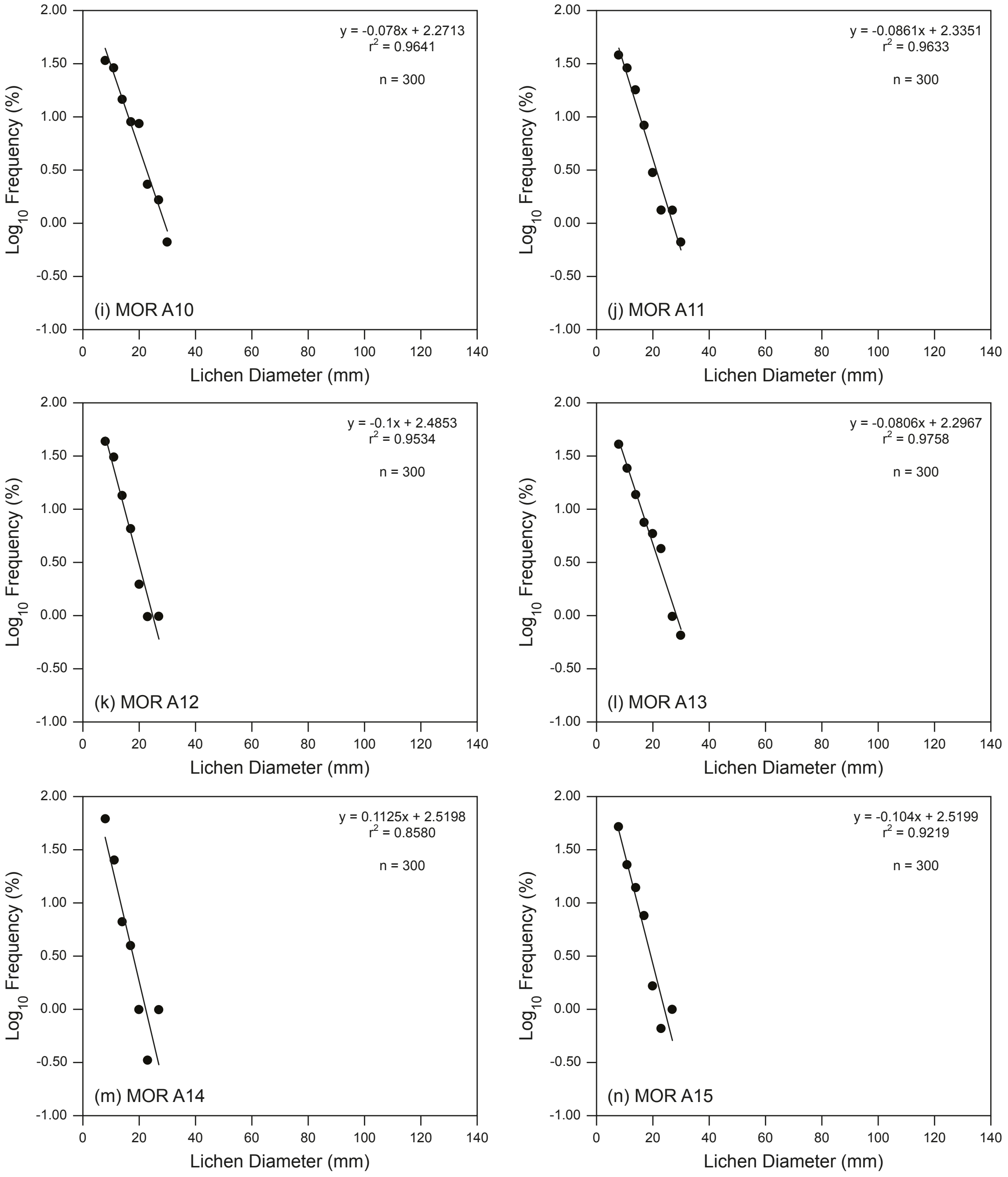

Figure 5.24 continued.

Estimates of the timing of moraine abandonment for each ridge in area A have been derived using a variety of dating curves (see §4.3; Gordon and Sharp, 1983; Bradwell, 2001a, b, 2004b) for the purposes of comparison (Table 5.2). The lichenometric survey on the ice-proximal slope of the outermost moraine ridge (A1) recorded a largest lichen (LL) of 36 mm and a single population ($r^2 = 0.9618$, $p < 0.0001$). Using this LL value and the *age-size* dating curve of Bradwell (2001a, b), abandonment of the moraine surface is dated to AD 1940 ± 7. By comparison, the Gordon and Sharp (1983) age-size dating curve, based on long axis measurements on surfaces of known age at Skálafellsjökull, yields an older date of AD 1929 ± 9. Finally, the *age-gradient* curve of Bradwell (2004b) produces an estimate of AD 1933 ±

8. Based on the archive of remotely-sensed data available for Skálafellsjökull (see above), it is known that the ice-margin had retreated from moraine A1 prior to 1945 and that the glacier has not subsequently re-advanced into this part of the foreland. The lichenometric dating curves therefore indicate that moraine ridge A1 formed in the date range 1920 – 1947 AD.

Table 5.2: Estimates of the date of moraine abandonment in area A (see Figure 5.6) derived from a variety of dating curves developed for SE Iceland.

Moraine	Largest-lichen diameter (mm)	Date of surface (AD) based on Bradwell (2001)[c]	Date of surface (AD) based on Gordon and Sharp (1983)[c, d]	Gradient (-ve)	Date of surface (AD) based on Bradwell (2004)[c]
MOR A1	36	1940 ± 7	1929 ± 9	0.0690	1933 ± 8
MOR A2	34	1943 ± 7	1931 ± 8	0.0671	1931 ± 8
MOR A3	31	1948 ± 7	1934 ± 8	0.0910	1951 ± 6
MOR A4	32	1946 ± 7	1933 ± 8	0.0814	1944 ± 7
MOR A5	31	1948 ± 7	1934 ± 8	0.0855	1947 ± 7
MOR A6	31	1948 ± 7	1934 ± 8	0.0819	1946 ± 7
MOR A7	30	1949 ± 6	1935 ± 8	0.0675	1931 ± 7
MOR A8[a]	-	-	-	-	-
MOR A9[b]	30	1949 ± 6	1935 ± 8	0.0929	-
MOR A10	30	1949 ± 6	1935 ± 8	0.0780	1941 ± 7
MOR A11	29	1951 ± 6	1936 ± 8	0.0861	1948 ± 7
MOR A12	27	1954 ± 6	1938 ± 8	0.1000	1956 ± 7
MOR A13	28	1953 ± 6	1937 ± 8	0.0806	1944 ± 7
MOR A14	26	1957 ± 6	1939 ± 8	0.1125	1962 ± 5
MOR A15	24	1959 ± 6	1941 ± 7	0.1040	1958 ± 6

[a] Unable to identify sufficient lichen in fixed area quadrat; [b] Less than 200 lichen above modal class therefore not used to generate 'age-gradient' date; [c] All dates reported with 10% error (Innes 1988; Noller and Locke 2001); [d] Age estimates incorporate ecesis.

In the 1945 aerial photograph, moraine A10 is situated in close proximity to the ice-margin and is hypothesised to have been formed during a small winter re-advance during 1944/1945. The lichenometric survey on moraine A10 recorded a LL value of 30 mm and revealed a single lichen population ($r^2 = 0.9641$, $p < 0.0001$). As such, the largest lichen is not considered to be anomalous (*cf*. Bradwell, 2001a, b). Estimates of the date of moraine A10 abandonment derived from the Bradwell (2001a, b) age-size curve and Bradwell (2004b) age-gradient curve are entirely consistent with the hypothesis of formation during a 1944/1945 winter re-advance, with even the most well-calibrated lichenometric dating having an optimum precision of only 5 – 10% (Innes, 1988; Noller and Locke, 2000). Comparison of the dates derived from the Gordon and Sharp (1983) dating curve with the available aerial photographs implies the age-size curve of Gordon and Sharp (1983) consistently overestimates the timing of moraine abandonment in this suite. On this basis, moraine A10 is confidently ascribed a formation date of winter 1944/1945.

Lichenometry investigations conducted on the ice-proximal slope of the innermost moraine ridge (A15) yielded a LL of 24 mm, with the lichens comprising a single population (r^2 = 0.9219, p = 0.0005). The Bradwell (2001a, b) age-size dating curve produces an estimate of AD 1959 ± 6 for the timing of abandonment for moraine A15. As with moraines A1 and A10, the Gordon and Sharp (1983) dating curve yields an older estimate (AD 1941 ± 7) for moraine A15. An estimate of AD 1958 ± 6 is derived from the age-gradient curve of Bradwell (2004b). It is known from the aerial photograph inventory that Skálafellsjökull had retreated from this part of the foreland by 1954 and there is no evidence for re-advance into this suite of moraine ridges. Thus, the moraine ridge dates to the lower range of values derived from the Bradwell (2001a, b) age-size dating curve and Bradwell (2004b) age-gradient curve. Based on the available aerial photograph evidence, moraine A15 was abandoned after AD 1947 and therefore formed at the higher range of values obtained using the Gordon and Sharp (1983) curve. Using these strands of evidence, it is deduced that moraine A15 formed sometime between 1947 and 1954.

Notwithstanding the veracity of the timing of moraine formation, the dates derived using the Bradwell (2001a, b) and Gordon and Sharp (1983) age-size dating curves appear to be broadly consistent with annual moraine formation in area A. Conversely, the Bradwell (2004b) age-gradient curve yields inconsistent dates, implying the moraine suite is interspersed with apparently *younger* moraine ridges. It has previously been acknowledged by Bradwell (2004b) that it is unlikely that the age-gradient curve can be accurately used to date surfaces formed within the last *c*. 70 years due to the exponential nature of the dating curve. Given that the suite of minor moraines in area A is believed to have formed between the ~1930s and early 1950s, this appears to explain the apparently erroneous estimates derived using the age-gradient curve. Whilst the dates of moraine abandonment yielded from the Bradwell (2001a, b) age-size dating curve are broadly consistent with annual formation, the location of control sites used in calibrating this curve may introduce errors into the precise dates obtained. As highlighted in Chapter 4, the Bradwell (2001a, b) age-size curve is based on measurements of independently dated surfaces which encompass a range of precipitation zones (*cf*. Evans *et al*., 1999a). Lichen growth rates are known to be influenced by local environmental factors such as precipitation (see Innes, 1985; Benedict, 1990; Evans *et al*., 1999a; Bradwell, 2001a, Bradwell and Armstrong, 2007; Armstrong, 2015, and references therein). Thus, the dating curve may yield erroneous estimates for the timing of abandonment, particularly as Skálafellsjökull is situated in a zone of high precipitation (*cf*. Evans *et al*., 1999a). Meanwhile, Gordon and Sharp (1983) employed a different sampling strategy to that utilised in this study, with long axis measurements of the aggregated species *Rhizocarpon geographicum* undertaken in areas of 150 m^2 on the proximal side of moraines. As such, estimates of the timing of moraine abandonment derived from the Gordon and Sharp (1983) dating curve may have errors associated with them.

Despite the issues highlighted above, and excluding the dates derived from the Bradwell (2004b) dating curve, the lichenometric analysis and supporting evidence (remotely-sensed data and field observations) appear to strongly support the hypothesis that the moraines formed annually. Furthermore, the geomorphological characteristics of the moraines are similar to other features interpreted as annual moraines in SE Iceland and elsewhere (e.g. Boulton, 1986; Krüger, 1995; Bradwell, 2004a; Lukas, 2012; Bradwell *et al*., 2013; Reinardy *et al*., 2013), strongly suggesting annual formation relating to minor re-advances of the Skálafellsjökull ice-margin during overall glacier recession. Accepting that (1) moraine A10 formed during a small winter re-advance in 1944/1945 based on the aerial photographic evidence and (2) moraines in this suite formed on an annual basis, the suite of minor moraines in area A are believed to have formed between winter 1935/1936 and 1949/1950 (Table 5.3).

Table 5.3: Formation dates for moraines in area A of the Skálafellsjökull foreland (see Figure 5.6) as deduced from remote sensing observations and lichenometric analysis.

Moraine	Date of surface (AD)
MOR A1	1935/1936
MOR A2	1936/1937
MOR A3	1937/1938
MOR A4	1938/1939
MOR A5	1939/1940
MOR A6	1940/1941
MOR A7	1941/1942
MOR A8	1942/1943
MOR A9	1943/1944
MOR A10	1944/1945
MOR A11	1945/1946
MOR A12	1946/1947
MOR A13	1947/1948
MOR A14	1948/1949
MOR A15	1949/1950

5.3 Moraine sedimentology

5.3.1 Section descriptions

Sections were created through the width of four representative moraines in order to assess the genetic processes of annual moraine formation at Skálafellsjökull through detailed sedimentological analysis. The locations of these moraine exposures were carefully selected after test pits (n = 15) had been created through moraines spread across the glacier foreland. This sampling strategy follows that outlined in previous studies of annual moraines (Lukas, 2012; Reinardy *et al.*, 2013). Due to accessibility issues, it was not possible to sample moraines formed at the northern margin of Skálafellsjökull. Therefore, moraines formed at the southeastern margin were sampled, despite the difficulties in ascribing age estimates to these features (see §5.2.1), in order to capture the range of contemporary genetic processes. The example moraine sections presented and described below are considered a representative subsample of the facies associations evident within the annual moraines on the Skálafellsjökull foreland.

Moraine SKA-04 – This moraine is located within the suite of moraines in area A (64.27662°N; 015.65767°W), with a natural exposure having been created through the northern part of the moraine through fluvial erosion by the Kolgrima River. Moraine SKA-04 has a rounded top and is a low-amplitude, symmetrical ridge: moraine surface slopes dip at angles of 18°. The moraine extends to 130 m in length, reaches 6 m in width and is *c*. 0.8 m in height. The surface of this ridge is strewn with a number of large boulders which have *a*-axis measurements exceeding 1.5 m. Based on remote sensing observations and lichenometric analysis this moraine ridge is believed to have formed during a winter re-advance in 1945/1946. Moraine SKA-04 is largely comprised of dark-grey/brown matrix-supported diamicton (Dmm), which is massive in appearance and displays no sedimentary structures (Figure 5.25). On the distal side of the moraine, a zone of compact, matrix-supported diamicton (Dmm(s)), exhibiting a fissile appearance, is evident. This zone of fissile diamicton extends up to ~0.98 m in width at the base of the section, and reaches a maximum height of ~0.65 m. Fissility is imparted on this unit by the presence of sub-horizontal and anastomosing partings (Figure 5.26). In places, these sub-horizontal partings exhibit a cross-cutting pattern. A prominent, faceted and bullet-shaped boulder at the base of this section displays numerous striations on its surface.

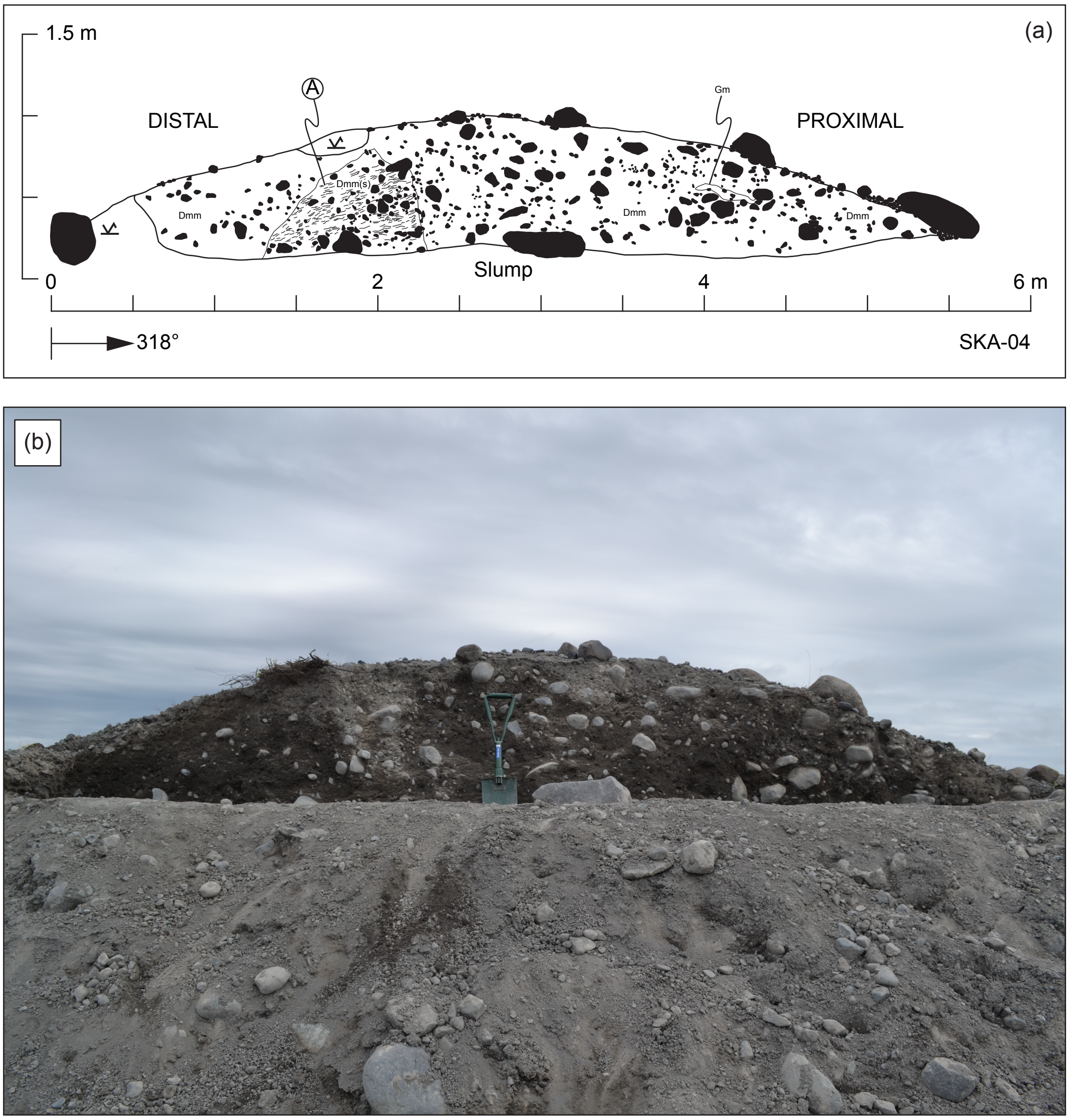

Figure 5.25: (a) Log of the exposure created through moraine SKA-04. A. Zone of fissile diamicton (Dmm(s)). (b) Photograph of the exposure through moraine SKA-04.

Moraine SKA-07 – This section is through the northern face of a crenulate moraine in the southwestern part of the Skálafellsjökull foreland (64.268111°N; 015.68353°W). The moraine is 32 m in length, has a width of ~2.3 m and reaches a maximum height of 0.45 m. Moraine SKA-07 has no clearly developed crestline, displaying a rounded top. In cross-section the moraine is asymmetrical, with a shorter, steeper distal slope (196/24 W) and longer, gentler ice-proximal slope (196/20 E). Based on the available aerial photographs and satellite imagery, moraine SKA-07 was most likely formed during the winter of 2006/2007 as it is situated just inside the 2006 ice-margin position. In section this moraine is largely comprised of a dark-grey/brown clast-supported diamicton (Dcm), which is structurally massive (Figure 5.27). The matrix of the diamicton is dominated by silt and clay and contains clasts with maximum *a*-axis lengths of 15 cm. Within this clast-supported diamicton are occasional pods

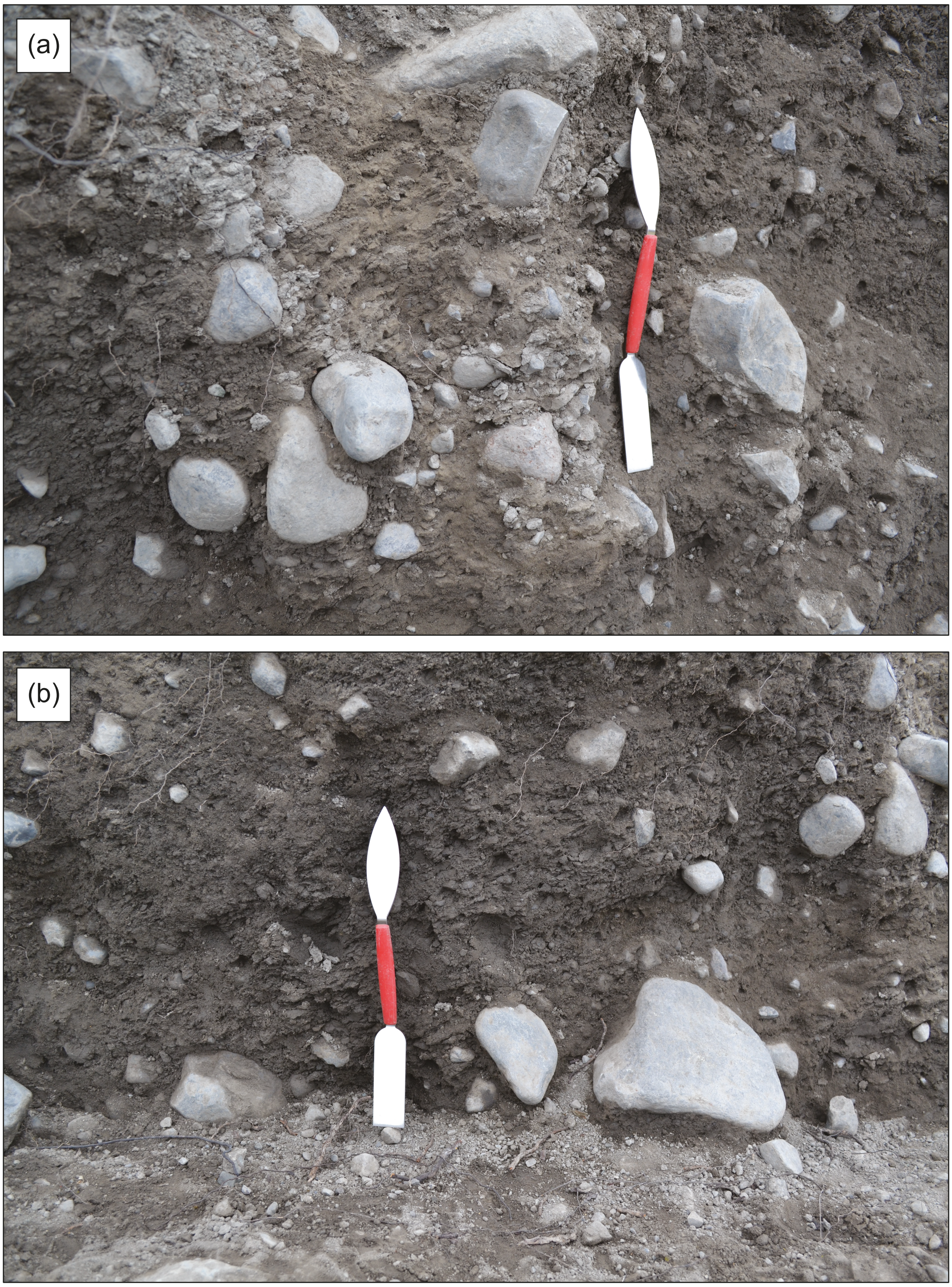

Figure 5.26: Close-up photographs of the anastomosing partings that give a fissile appearance to the diamicton marked A in the section log (Figure 5.25).

of massive gravels (Gm) and inclusions of fines (Fl). The gravel units are poorly- to moderately-sorted, fine-medium gravel, reaching maximum thicknesses of 5 cm. A prominent feature of SKA-07 is the deformed unit of fines (Fl) which includes occasional outsized clasts (Figure 5.28). The sedimentary composition and structure evident within moraine SKA-07 is dominant throughout the foreland, with the majority of test pits exhibiting similar characteristics.

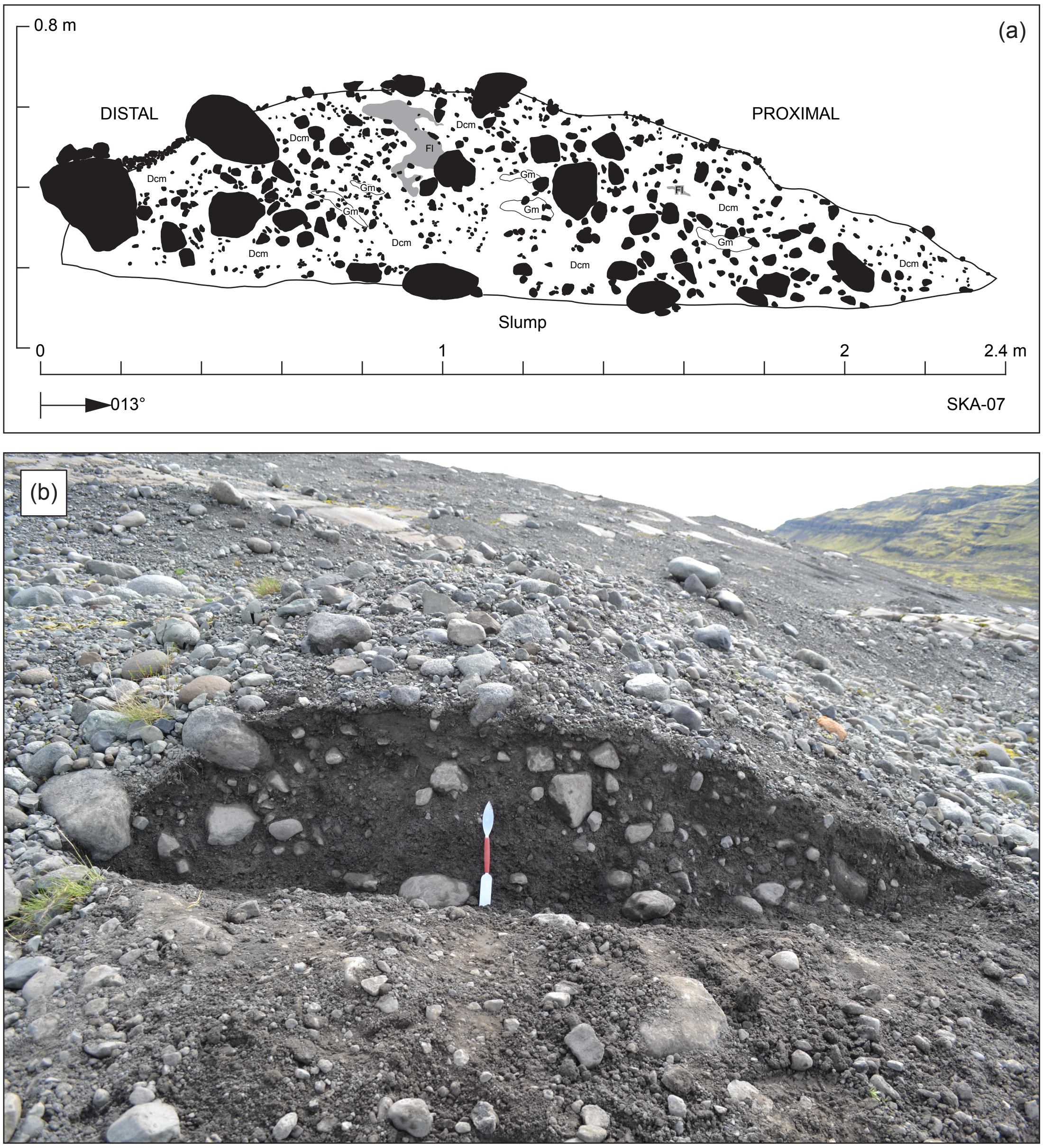

Figure 5.27: (a) Section log for moraine SKA-07 and (b) photograph of the exposure through the cross-section of the moraine.

Moraine SKA-11 – This is the most complex of the sections examined on the Skálafellsjökull foreland. Moraine SKA-11 is a broadly linear feature, which is also situated near the present ice-margin, to the east of the meltwater stream that flows along the ice-front (64.264721°N; 015.69118°W). Based on remote sensing observations and field investigations, it is believed that this moraine formed some time during 2011/2012. The ridge has a well-defined crestline, and exhibits a slightly steeper distal slope (094/31 SE) than ice-proximal slope (102/29 NW) in cross-section. Moraine SKA-11 is *c*. 21 m in length, has a width of ~2.8 m and reaches a

Figure 5.28: Close-up of the distal side of moraine SKA-07 showing the folded fine sediments.

maximum height of 0.79 m. An exposure created through the southwestern face of this moraine ridge (Figure 5.29) reveals two lithofacies associations (LFA). LFA1 comprises stacked sequences of matrix-supported, stratified diamictons (Dms) and (crudely) horizontally-bedded granule and gravel units (GRh, G(h), Gh), with occasional interbeds of sorted sediments (Sm). This lithofacies association occurs on the ice-proximal side of moraine SKA-13 and dips at an angle of *c*. 29°, following the surface of the ice-proximal slope (Figures 5.29 and 5.30). The diamictic facies in LFA1 display a grey/brown colour and a loose, friable character, with layers of matrix-supported, stratified diamicton reaching a maximum thickness of *c*. 19 cm. Individual layers of the (pseudo-) horizontally bedded gravels reach maximum thicknesses of *c*. 13 cm, whilst the horizontally bedded granule to fine gravel unit reaches a maximum thickness of *c*. 12 cm. The lower, crudely horizontally bedded gravel (G(h)) is medium to coarse grade, whereas the uppermost horizontally bedded gravel (Gh) is fine to medium grade gravel. Interbedded between the stratified diamicton and lower gravel lithofacies, is a unit of massive, medium to coarse sand which reaches a maximum thickness of 4 cm. The remainder of moraine SKA-11 is formed of LFA2, which comprises a very loose, silty-sandy, massive, matrix-supported diamicton (Dmm), together with massive sand (Sm) and pods/lenses of massive and openwork gravels (Gm, Go). A large, prominent pod of medium to coarse, poorly sorted, massive gravel (Gm) occurs on the distal side, and reaches a maximum thickness of 28 cm. Layers/lenses of medium to coarse, massive sand (Sm) occur within this gravel unit, locally reaching thicknesses of 3 cm, but tapering out to the left and right. The lowermost unit of massive sand includes out-sized clasts. A further lens of sorted sediment (Sm) occurs within the massive, matrix-supported diamicton, locally extending up to 9 cm before tapering out to the right. Lenses of massive and openwork gravel in LFA2 reach thicknesses of 6 cm. On the lower right-hand (distal) side of the section, lenses of massive granules and gravels dip approximately parallel to the surface slope at angles of 30 – 31°. In the upper-right of the moraine, the gravel units appear to have undergone deformation. Moraine SKA-11 was prone to collapse throughout excavation, reflecting the very loose, friable character of the diamictic sediments in LFA2.

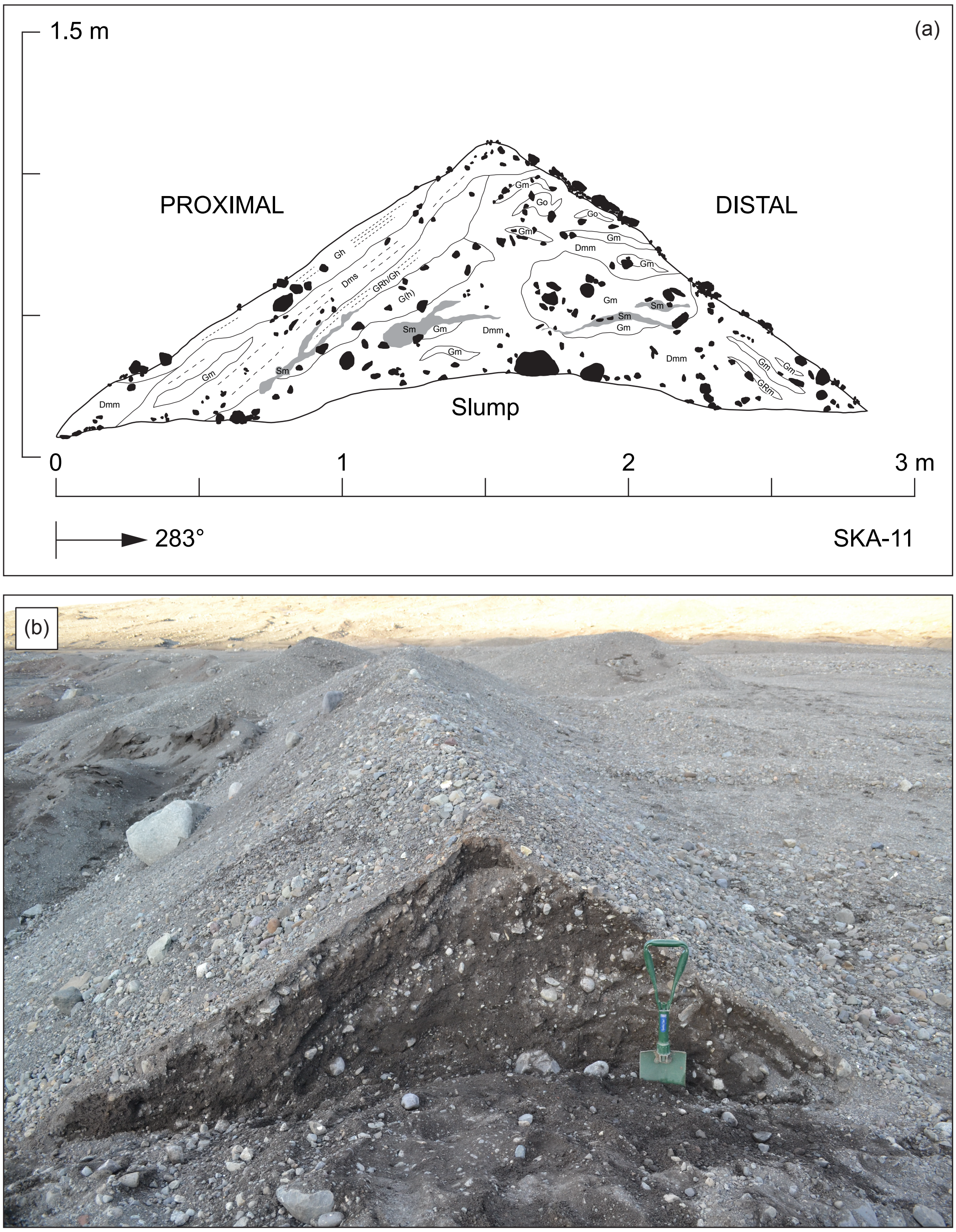

Figure 5.29: (a) Log of the exposure through moraine SKA-13. (b) Photograph of the exposed section.

Figure 5.30: Photograph of the stacked sequences of stratified diamicton (Dms) and (crudely) horizontally bedded granules and gravels (Gh, GRh) that comprise LFA1.

Moraine SKA-13 – Moraine SKA-13 has a distinctive morphology and appearance, which contrasts with that of the majority of moraines within the glacier foreland: only one other moraine ridge was found to have similar characteristics. This moraine is situated close to the contemporary southeastern margin of Skálafellsjökull (64.26753°N; 015.68968°W) and is likely to have formed during a winter re-advance in 2012/2013 on the basis of remote sensing and field observations. This moraine fragment is arcuate in planform geometry and exhibits a sharp crestline, reaching *c*. 31 m in length. In cross-section this ridge reaches a maximum height of ~1 m and a maximum width of ~2.1 m, and displays an asymmetric cross-profile: the ice-proximal slope is gentler (022/29 SW) than the distal slope (021/24 NE). The surface of this ridge is strewn with numerous cobbles and boulders, with boulders reaching maximum *a*-axis lengths of ~0.75 m. A manual exposure was created through the southern face of moraine SKA-13, perpendicular to the moraine crestline (Figure 5.29). In section the moraine is comprised largely of a massive, matrix-supported diamicton (Dmm). The matrix of the diamicton unit has a red/brown colour and has a high clay content. This section is visually dominated by the edge-rounded, boulder-sized clasts sitting within the diamicton matrix, which reach maximum *a*-axis lengths of 0.35 m. Aside from the diamicton unit, a core of massive, poorly-sorted gravel (Gm) is evident at base of the section on the ice-proximal side of the moraine. The gravel core is fine to medium, with maximum *a*-axis lengths of 7 cm. No other lithofacies or sedimentary structures were evident within this exposure.

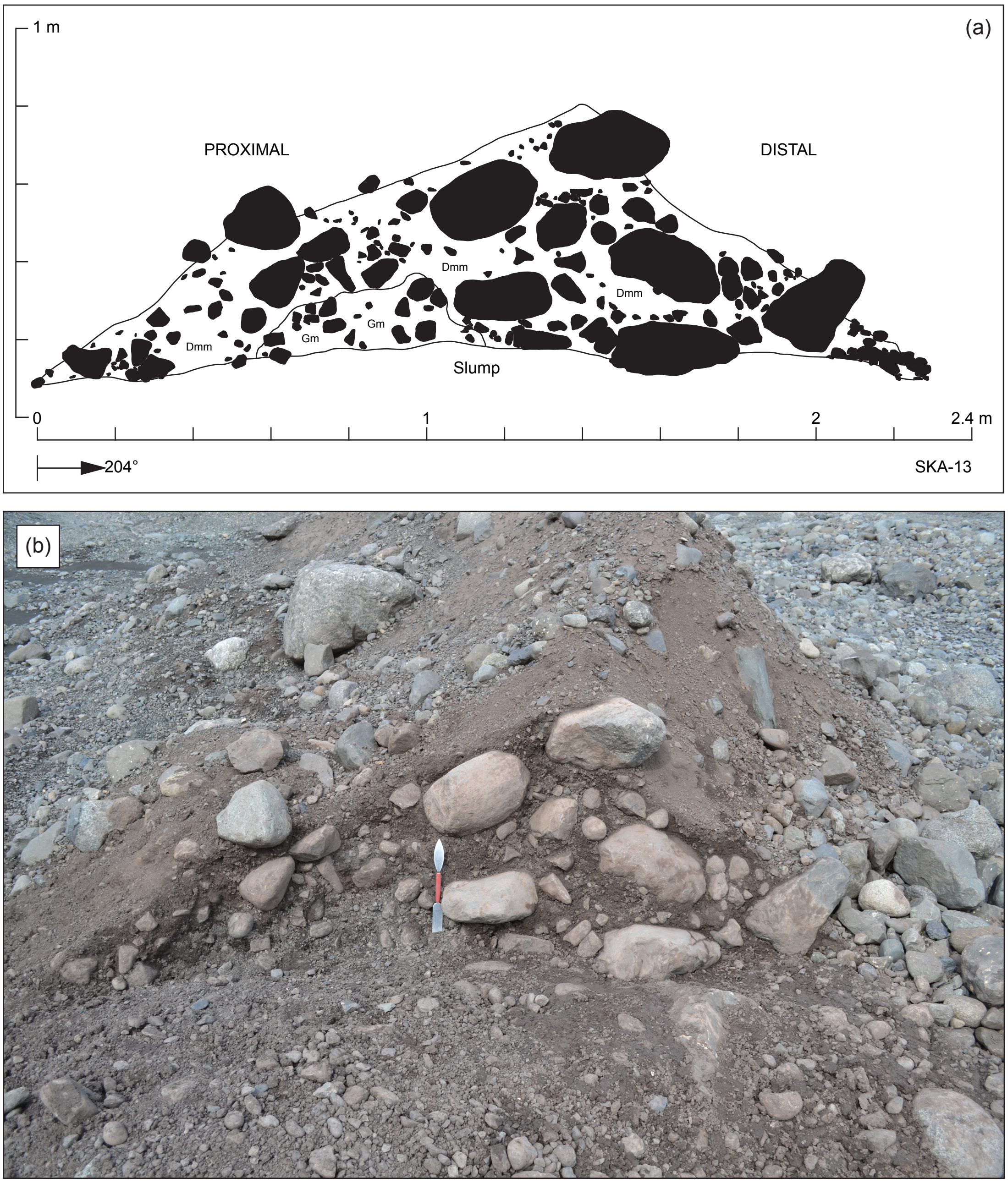

Figure 5.31: (a) Log of the exposure through moraine SKA-13. (b) Photograph of the manual exposure created through the southern face of the moraine.

5.3.2 Clast shape analysis

Clast shape measurements were undertaken to determine the sources and transport pathways of glaciogenic sediments within the moraines, using standard procedures (see §4.4; Benn and Ballantyne, 1993, 1994; Benn, 2004; Brook and Lukas, 2012; Lukas *et al*., 2013). As no control samples were collected from Skálafellsjökull in this study, control samples from Fláajökull, an active temperate outlet of the southern margin of Vatnajökull, were employed as reference (Lukas *et al*., 2013; D. Evans, pers. comm., 2014). Fláajökull exhibits dominant subglacial and fluvial erosion and transport, with multiple and complex transfers of material between the subglacial and glaciofluvial realms (Figure 5.32; Lukas *et al*., 2013). This corresponds well with findings from Skálafellsjökull where Evans (2000) has found convincing stratigraphical evidence for these processes working at the base of the glacier.

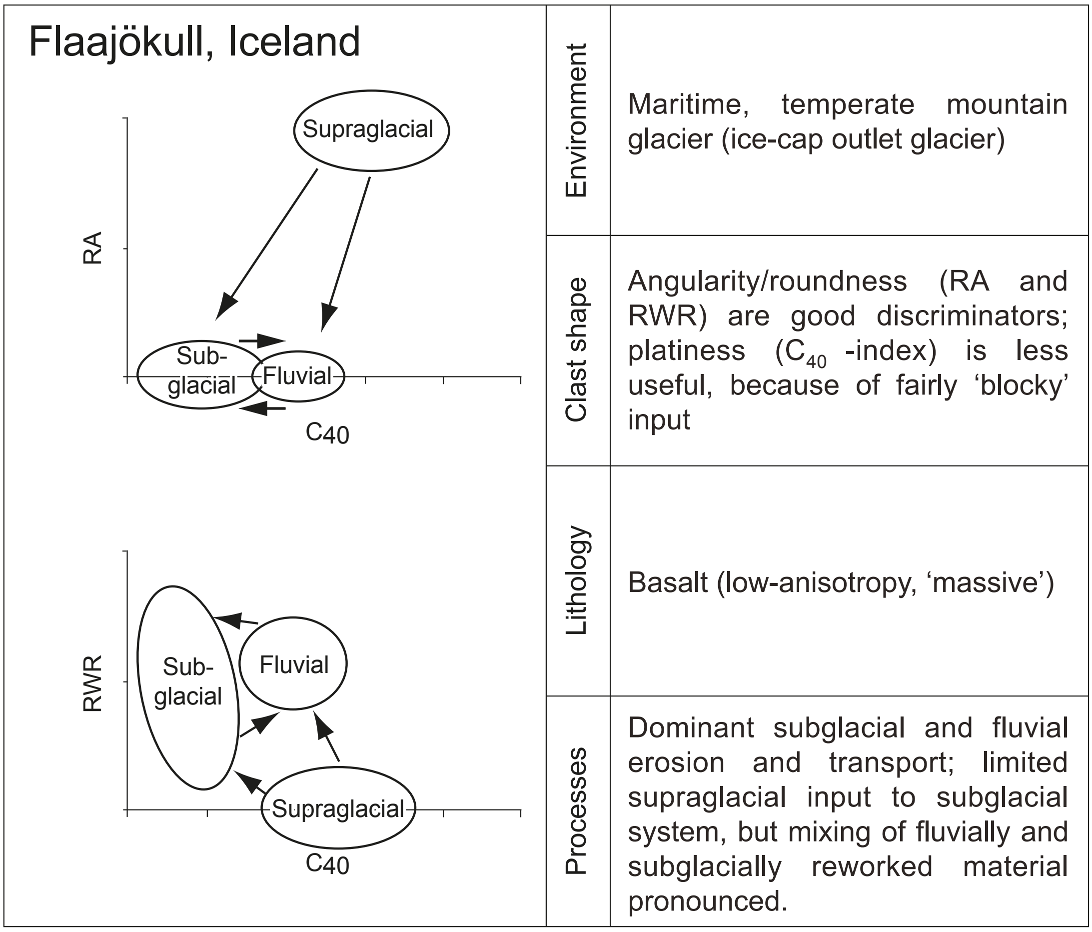

Environment	Maritime, temperate mountain glacier (ice-cap outlet glacier)
Clast shape	Angularity/roundness (RA and RWR) are good discriminators; platiness (C_{40} -index) is less useful, because of fairly 'blocky' input
Lithology	Basalt (low-anisotropy, 'massive')
Processes	Dominant subglacial and fluvial erosion and transport; limited supraglacial input to subglacial system, but mixing of fluvially and subglacially reworked material pronounced.

Figure 5.32: Schematic summary of the covariance plots for Fláajökull, SE Iceland. Adapted from Lukas *et al*. (2013).

Clast shape analysis was conducted on samples of basaltic clasts taken from exposed diamicton units within each of the four moraine sections described above. The samples are predominantly blocky, with the low C_{40} values (ranging from 14 to 24) for each of the samples indicating a low percentage of oblate and proclate clasts (Figure 5.33). Examination of the edge roundness data indicates that the samples are dominated by subangular to subrounded clasts, with moraine SKA-04 exhibiting a somewhat greater percentage of rounded clasts (26%) compared to the other moraines. In all cases, the moraines contain a low percentage (2%) of well-rounded clasts. Comparison of the four samples with the control samples obtained from Fláajökull, using covariance plots of both RA-C_{40} and RWR-C_{40}, suggests the diamicton units were derived from subglacial material (Figure 5.34). Three of the samples lie

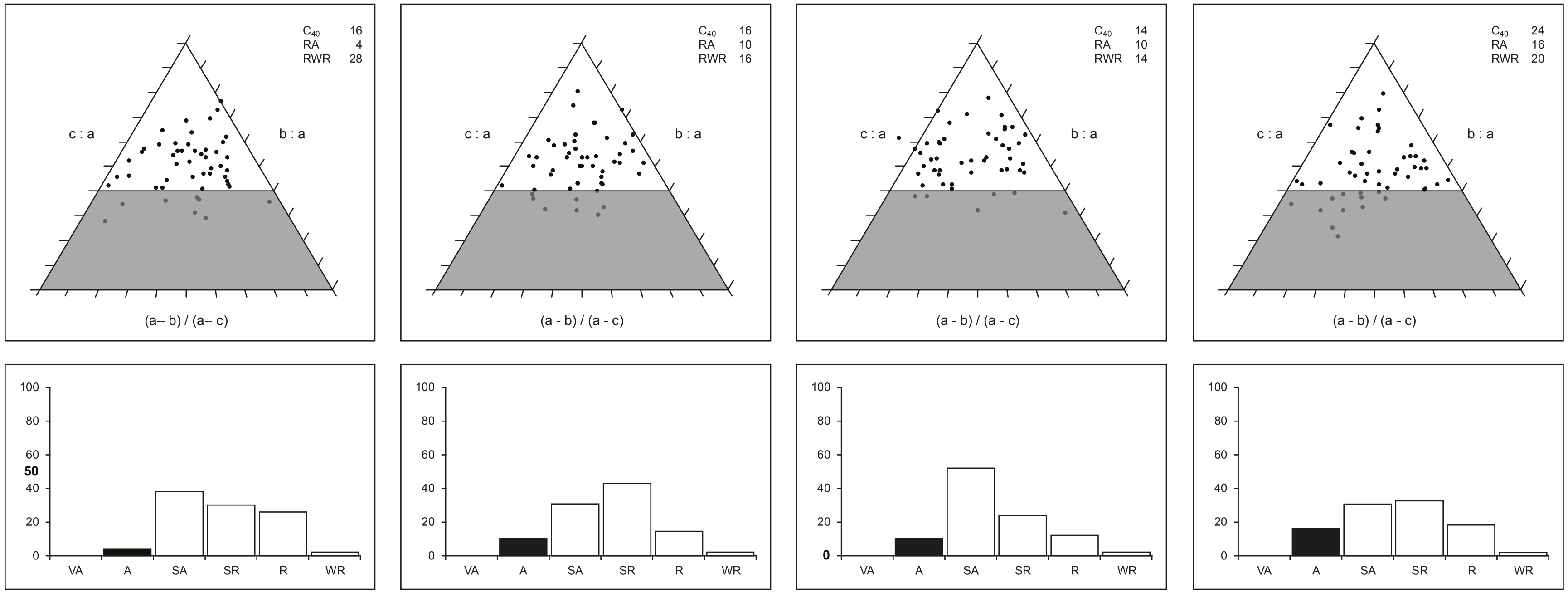

(a) SKA-04 (Dmm) (b) SKA-07 (Dcm) (c) SKA-11 (Dmm) (d) SKA-13 (Dmm)

Figure 5.33: Results of the clast shape analyses conducted on samples obtained from the moraines described in the above section. Ternary diagrams and indices were derived using a modified version of TriPlot (Graham and Midgley, 2000) provided by S. Lukas (pers. comm., 2014). Roundness classes for the frequency distribution plots follow the scheme of Benn and Ballantyne (1994).

slightly above the subglacial control envelope on the RA-C_{40} covariance plot, but each sample lies within the subglacial control envelope on the RWR-C_{40} covariance plot. Supporting evidence for a subglacial origin is provided by the presence of numerous striated and faceted clasts within the moraine sections. Thus, the clast-shape data indicates the dominance of subglacial processes, and strongly suggests the sediments exposed in section reflect transport in the subglacial traction zone (*cf.* Boulton, 1978; Benn, 1992; Benn and Ballantyne, 1994; Lukas, 2005a, b, 2007b).

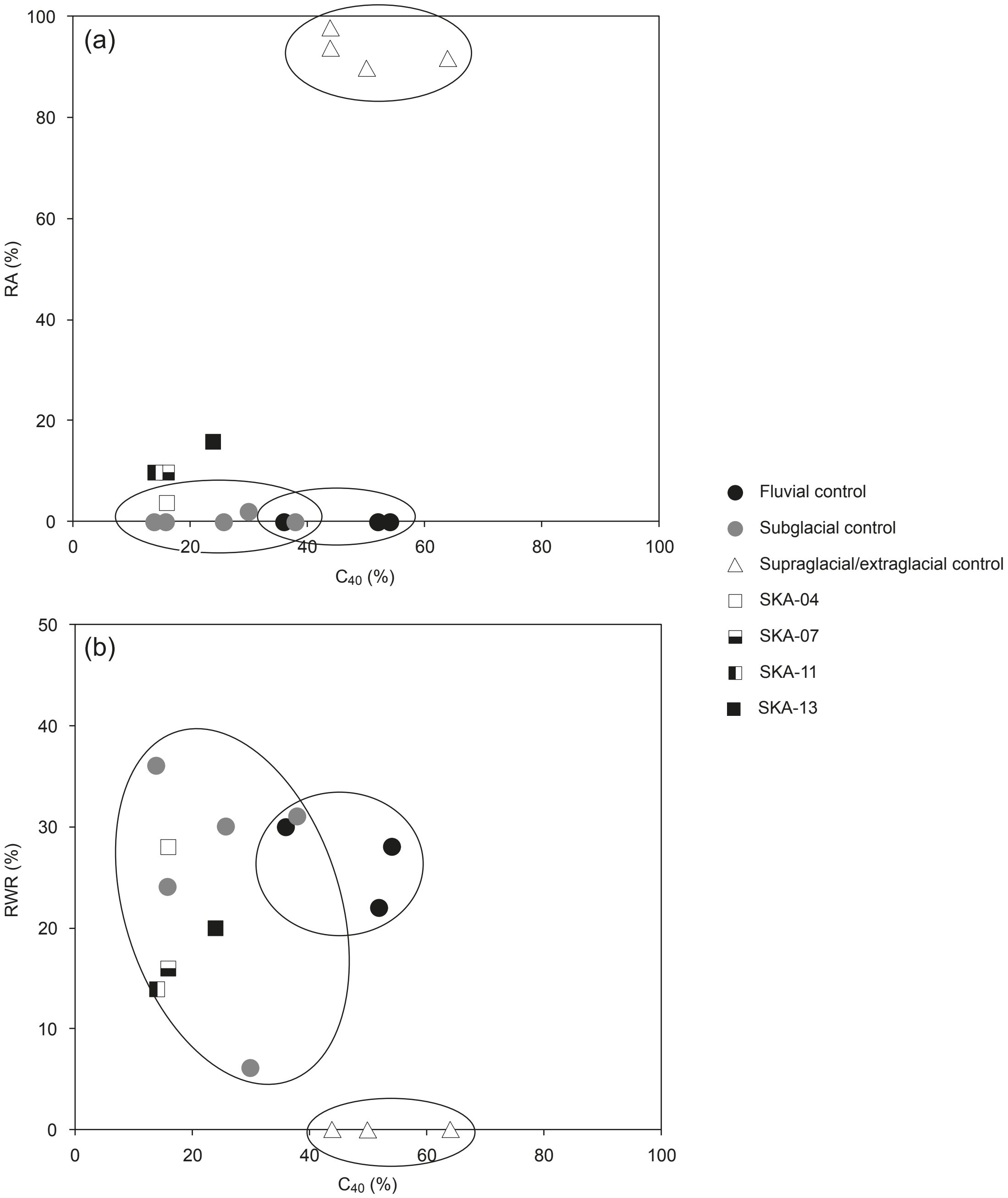

Figure 5.34: Covariance plots displaying the RA-index plotted against the C_{40}-index (a) and the RWR-index plotted against the C_{40}-index (b) for the various control samples and moraine sections. Samples from the moraines suggest they contain subglacially-sourced material.

5.3.3 Interpretation of sections

Moraine SKA-04 – The massive, homogenous, matrix-supported diamicton (Dmm) that comprises the majority of moraine SKA-04 has the appearance of a subglacial traction till (*sensu* Evans *et al*., 2006). Indeed, the diamicton unit is similar in appearance to the upper A horizons in the two-tiered till sequences reported from Skálafellsjökull and sites elsewhere in Iceland (Boulton *et al*., 1974; Boulton, 1979; Dowdeswell and Sharp, 1986; Boulton and Hindmarsh, 1987; Benn, 1995; Evans, 2000a; Evans and Twigg, 2002). These A horizons have been interpreted as dilatant tills which have undergone pervasive (ductile) deformation (e.g. Boulton and Hindmarsh, 1987; Benn, 1994, 1995; Benn and Evans, 1996). Meanwhile, the zone of fissile, matrix-supported diamicton (Dmm(s)) on the distal side of moraine SKA-04 is similar in appearance to the B horizon in the abovementioned two-tiered structure. These till layers have been interpreted as slowly deforming till undergoing brittle or brittle-ductile shear (e.g. Boulton and Hindmarsh, 1987; Benn, 1994, 1995; Benn and Evans, 1996; Evans, 2000). The fissile partings evident within moraine SKA-04 are interpreted as brittle shear structures, consistent with emplacement of the material as a subglacial traction till (*cf*. Evans *et al*., 2006; Benediktsson *et al*., 2009; Ó Cofaigh *et al*., 2011). Clast shape analysis conducted for moraine SKA-04 supports a subglacial origin for the constituent material, with material having undergone transport in the subglacial traction zone. Based on the available sedimentological evidence, combined with field observations at the contemporary ice-margin, it is suggested that the diamictic sediments within moraine SKA-04 are deformed subglacial sediments that have been extruded from the base of the glacier (*cf*. Price, 1970; Sharp, 1984; Evans and Hiemstra, 2005). This extruded subglacial traction till (*sensu* Evans *et al*., 2006) was subsequently bulldozed by the ice-front (*cf*. Sharp, 1984; Evans and Hiemstra, 2005). The sawtooth planform geometry of moraine SKA-04 is therefore interpreted as reflecting the formation of pecten (with associated radial crevasses) at the ice-margin, where teeth and notch forms are explained by the radial pattern of crevasses (*cf*. Price, 1970; Matthews *et al*., 1979; Sharp, 1984). In summary, moraine SKA-04 is interpreted as a squeeze/push moraine comprising extruded subglacial traction till.

Moraine SKA-07 – As with the diamicton units in moraine SKA-04, the massive, clast-supported diamicton which comprises the majority of moraine SKA-07 is interpreted as a subglacial traction till (*sensu* Evans *et al*., 2006) The macroscopically massive diamicton, with a high clast content, is similar to that found within “annual” moraines on other Icelandic glacier forelands and interpreted as subglacial sediments that have been extruded or squeezed from beneath the glacier (*cf*. Price, 1970; Evans and Hiemstra, 2005). The folded unit of fine sediments (Fl) on the distal side of the moraine indicates that the sediments have undergone deformation, most likely through pushing (or bulldozing) of extruded material. The lenses of sorted sediments within moraine SKA-07 are interpreted as glaciofluvial sediments resulting from fluvial processes acting in the subglacial realm that were subsequently incorporated into the deforming sediments and extruded at the ice-margin. Based on the available evidence, moraine SKA-07 is therefore interpreted as being formed through submarginal deformation and extrusion of water-soaked tills through marginal crevasses and into crenulations or pecten of the ice-margin (*cf*. Hoppe, 1954; Price, 1970; Sharp, 1984; Evans and Hiemstra, 2005). The process of submarginal deformation and extrusion of semi-liquid subglacial traction till is believed to be coupled with the process of bulldozing, leading to the production of a *saw-tooth* or crenulate moraine ridge which reflects the intricacies of the ice-front (*cf*. Sharp, 1984). Observations at the contemporary ice-margin provide evidence of bulldozing of subglacially-sourced sediments, whilst the clast shape data (see §5.3.2) also suggests the diamicton was sourced and transported in the subglacial environment. As with moraine SKA-04 above, moraine SKA-07 is therefore interpreted as a squeeze/push moraine and would be referred to as a ‘Type A’ ridge under the classification of Sharp (1984).

Moraine SKA-11 – The stacked layers of stratified diamicton and (crudely) bedded gravels that constitute LFA1 on the ice-proximal side of moraine SKA-11 are interpreted as slabs emplaced in the moraine through subglacial freeze-on (*cf*. Harris and Bothamley, 1984; Krüger, 1993, 1994, 1995, 1996; Matthews *et al*., 1995; Evans and Hiemstra, 2005; Reinardy *et al*., 2013). The (pseudo-) horizontally-bedded gravels and sorted sediments (Sm) within this lithofacies association are interpreted as fluvial sediments deposited either at the ice-margin or beneath the ice-margin in the glaciofluvial subglacial environment (*cf*. Matthews *et al*., 1995; Reinardy *et al*., 2013). These fluvial deposits would have become frozen to the glacier toe during the winter season and then melted out incrementally during the ablation season to form a moraine ridge (*cf*. Evans and Hiemstra, 2005; Reinardy *et al*., 2013). The loose, sandy, massive diamicton (Dmm), massive sand (Sm) and gravels (Gm, Go) that comprise LFA2 may relate to pushing of unfrozen glaciofluvial sediment in front of the advancing frozen slabs (*cf*. Matthews *et al*., 1995; Evans and Hiemstra, 2005; Reinardy *et al*., 2013) and then subsequent collapse due to the effects of gravity. The deformed lenses of gravel in the upper-right (distal side) of the moraine seem to support the interpretation of material being pushed in front of the frozen-on sediment slabs. In the southern part of the Skálafellsjökull foreland, where moraine SKA-11 is located, a meltwater stream runs along the ice-margin and ponding of meltwater occurs at the ice-front during the ablation season, therefore allowing glaciofluvial sediment deposition to occur. Up-arching of the ice-margin could occur where the glacier advanced onto an obstacle such as a previously deposited ridge (embryonic moraine) or a snow-bank (Matthews *et al*., 1995). Alternatively, build-up of subglacial and fluvial sediments on the distal side of a moraine ridge during glacier re-advance may have eventually led to limited up-arching of the glacier, particularly where sediment is frozen (Krüger, 1993; Reinardy *et al*., 2013). It is possible that this may be the case with moraine SKA-11: LFA2 appears to have been pushed up in front of the dipping layers of horizontally bedded gravels and stratified diamicton on the ice-proximal side of the moraine (*cf*. Reinardy *et al*., 2013). To summarise, moraine SKA-11 formed through a process of subglacial freeze-on of sediment slabs and subsequent melt-out during the ablation season. This genetic model is similar to that observed elsewhere in Iceland and at the margins of Norwegian outlet glaciers (e.g. Krüger, 1995; Matthews *et al*., 1995; Evans and Hiemstra, 2005; Reinardy *et al*., 2013).

Moraine SKA-13 – Although containing no sedimentary (deformation) structures indicative of pushing/bulldozing of sediment, this moraine is interpreted as a push moraine. This interpretation is largely based on the morphological similarity of this moraine with that of ridges interpreted as push moraines elsewhere. In particular, the asymmetrical cross-profile with the steeper distal slope and gentler ice-proximal slope is a common feature of push moraines (*cf*. Worsley, 1974; Birnie, 1977; Matthews *et al*., 1979; Bennett, 2001; Benn and Evans, 2010; Lukas, 2012). The presence of a massive, medium to coarse gravel (Gm) core at the base of the section is interpreted as evidence of re-working and incorporation of sediments deposited by a proglacial stream. This combined with the sharp, well-defined nature of the moraine crestline and the numerous large cobbles and boulder-sized clasts within the moraine perhaps points towards bulldozing of extant proglacial material by the ice-margin, rather than bulldozing of extruded material. The lack of deformation structures recorded within moraine SKA-13 is thought to reflect the clast/boulder rich content of the constituent material. However, without clast fabric data it is not possible to establish convincingly how material was emplaced in this moraine. Clast shape data for moraine SKA-13 suggests that the constituent diamicton was subglacially sourced and transported (see §5.3.2). To summarise, moraine SKA-13 is interpreted as a push moraine, formed by bulldozing of pre-existing proglacial materials of subglacial origin, with inclusion of fluvial deposits.

5.4 Summary

Glacial geomorphological mapping through a combination of desk- and field-based mapping has identified a series of minor moraine ridges on the Skálafellsjökull foreland. These moraines display distinctive *sawtooth* or crenulate planform geometries (*cf*. Price, 1970; Matthews *et al*., 1979; Bradwell, 2004a) and largely comprise moraine fragments less than 40 m in length. Minor moraines are frequently found in association with flutings, whilst in the southern part of the foreland moraine ridges and flutings are located in close proximity to an abundance of roches moutonnées and a series of recessional meltwater channels. On the basis of remote sensing observations and lichenometric analysis, minor moraines on the northern and central parts of the glacier foreland are interpreted as *annual moraines*. Annual moraine production occurred during the periods 1936 – 1964, 1969 – 1974, and from 2006 onwards. Age estimates cannot be ascribed confidently to moraines on southern part of the glacier foreland due to a paucity of remotely-sensed data and ice-front measurements. Detailed sedimentological investigations of annual moraines on the Skálafellsjökull foreland indicate moraines form by the following genetic process combinations: (1) submarginal deformation of subglacial traction till (*sensu* Evans *et al*., 2006) and subsequent bulldozing of the extruded material (*cf*. Price, 1970; Sharp, 1984); (2) efficient bulldozing of proglacial materials (*cf*. Lukas, 2012); and (3) subglacial freeze-on of sediment slabs and subsequent melt-out during the ablation season (*cf*. Krüger, 1993, 1994, 1995, 1996; Matthews *et al*., 1995; Evans and Hiemstra, 2005; Reinardy *et al*., 2013). Thus, annual moraines on the Skálafellsjökull foreland are formed by a combination of ice-marginal processes and can therefore be considered representative of previous ice-fronts positions. As such, these moraines can be employed as a geomorphological proxy for patterns and rates of ice-marginal retreat.

CHAPTER 6

Inter-annual variability in SE Iceland climate

The aim of this chapter is to introduce the potential climatic drivers of recent ice-marginal retreat at Skálafellsjökull, namely air temperature, sea surface temperature, precipitation and the North Atlantic Oscillation, and to explore the inter-annual variability of these potential forcing mechanisms. Statistical analysis is conducted to examine the interplay between the climate variables (e.g. the relationship between air temperature and sea surface temperature) through the application of covariance plots and least squares regression analysis. The common convention in testing the *statistical significance* of the relationships is followed here, whereby $p < 0.05$ indicates a *statistically significant fit* between the regression line and the data, $p < 0.01$ indicates a *highly statistically significant fit* and $p < 0.001$ indicates a *very highly statistically significant fit*. Seasonal signals have been extracted for each of the variables for comparison, with seasons following the convention of *Veðurstofa Íslands* (the Icelandic Meteorological Office): the short Icelandic spring is defined as April and May; the long summer is defined as June to September; autumn is defined as October and November; and winter is defined as December to March (*cf*. Hanna *et al*., 2004). The examination of inter-annual variability in SE Iceland climate will provide context for investigating the drivers of recent ice-marginal retreat in Chapter 7.

6.1 Climate variability at an inter-annual timescale

6.1.1 Inter-annual variability in air temperature

For the purposes of analysing inter-annual variability in SE Iceland, ambient air temperature (AAT) values have been used from Hólar í Hornafirði (64°17.995'N, 15°11.402'W; 16.0 m a.s.l.), the nearest long-term weather station to Skálafellsjökull. During the period 1930 – 2012, the mean AAT value at Hólar í Hornafirði was 4.77 °C ($\sigma = 0.59$ °C), with a median value of 4.78 °C. The maximum negative deviation of AAT from the 1961 – 1990 annual AAT average (4.44 °C) during this period was –1.46 °C (in 1979), whilst the maximum positive deviation was 1.44 °C (in 2003). The trends in deviations of annual AAT from the 1961 – 1990 average are illustrated in Figure 6.1. Between 1996 and 2012 annual AAT exhibited a positive deviation from the 1961 – 1990 average, with six of the last ten years during that period exhibiting an anomaly greater than 1 °C. Moreover, the period 2002 – 2006 exhibits the greatest positive annual AAT anomaly for any five-year period on record, with an average of 1.07 °C. Conversely, the period 1965 – 1971 is characterised by negative annual AAT anomalies, with an average of –0.71 °C. This is the only period in the meteorological record from Hólar í Hornafirði that displays consecutive years with negative annual AAT anomalies.

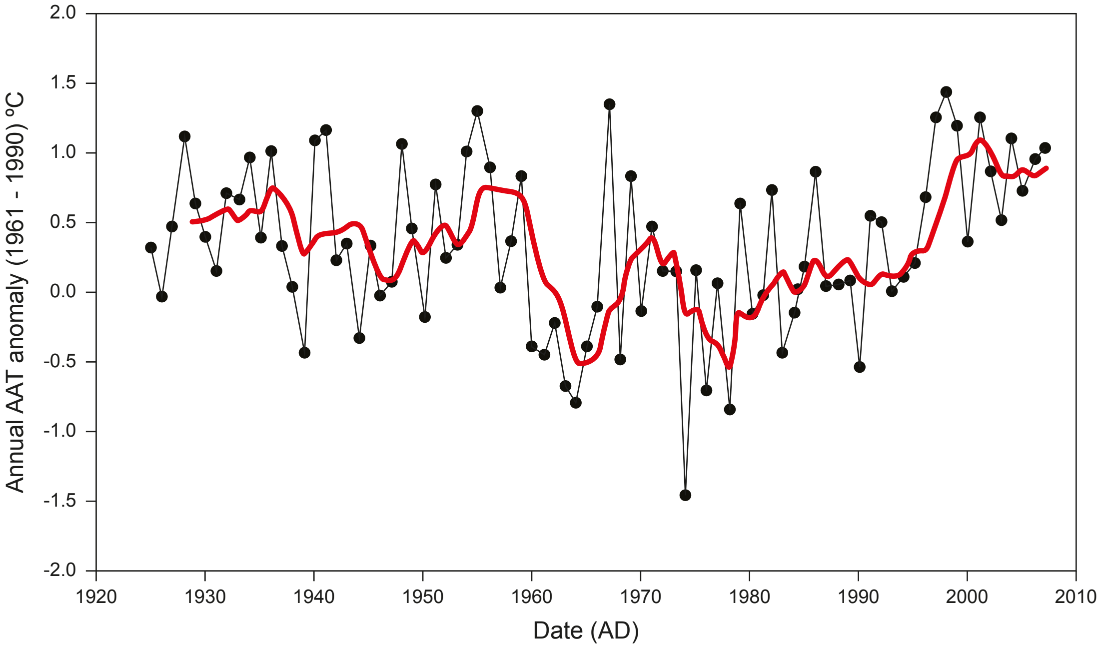

Figure 6.1: Time series plot illustrating the deviations of annual ambient air temperature (AAT) from the 1961 – 1990 average at Hólar í Hornafirði. Red line shows a five-year moving average.

Previous studies examining IMRRs of Icelandic outlet glaciers, equivalent to annual moraine spacing, have found periods of greater glacier recession are largely associated with above-average ablation season (summer) temperatures (Boulton, 1986; Krüger, 1995; Bradwell, 2004a; Bradwell *et al*., 2013). Thus, it appears appropriate to examine inter-annual variability in summer AAT values in SE Iceland. During the period 1930 – 2012, mean and median summer AAT values were 9.44 °C (σ = 0.65 °C) and 9.33 °C, respectively. As with annual AAT, the maximum negative deviation (–1.09 °C) from the 1961 – 1990 average (9.03 °C) occurs in 1979. Meanwhile, the maximum positive deviation in summer AAT during the period 1930 – 2012 was 1.87 °C, occurring in 1933. The period 2002 – 2006 exhibits the greatest positive AAT anomaly for any five-year period on record, with an average of 1.21 °C. Furthermore, during the period 2003 – 2012, five years exhibit temperature anomalies greater than 1.5 °C. The longest period of consecutive years with negative AAT anomalies occurs between 1968 and 1971, with an average of –0.25 °C. Other periods with consecutive negative summer AAT anomalies occur between 1963 and 1965 (average: –0.34 °C), and between 1981 and 1983 (average: –0.55 °C). These general trends in summer AAT anomalies are illustrated in Figure 6.2.

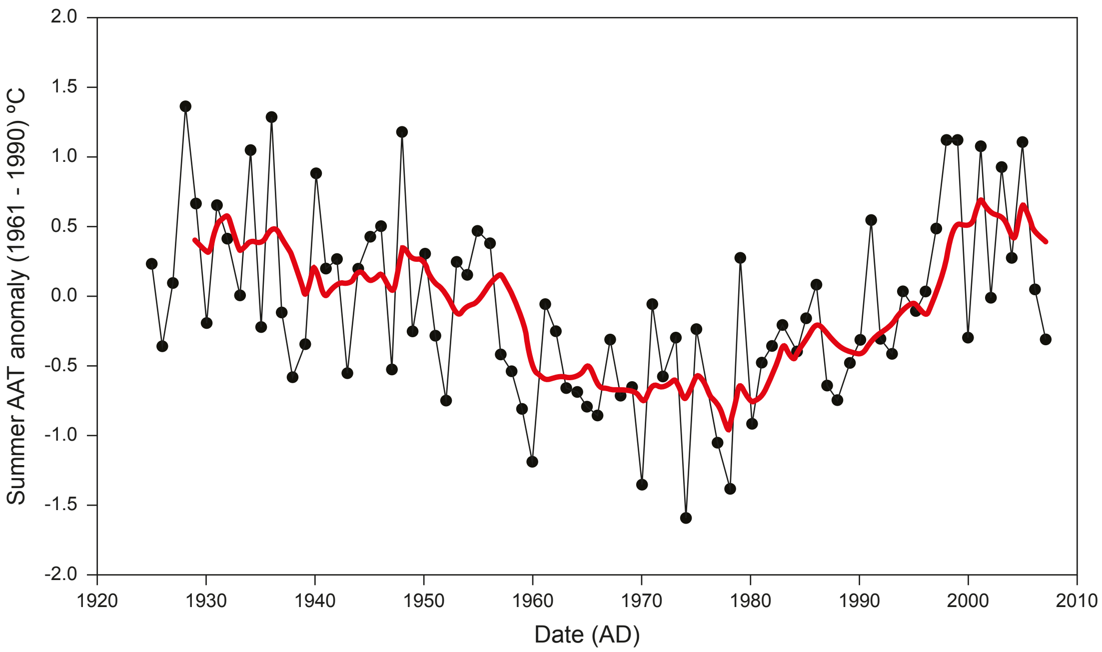

Figure 6.2: Time series plot illustrating the deviations of summer ambient air temperature (AAT) from the 1961 – 1990 average at Hólar í Hornafirði. Red line shows a five-year moving average.

6.1.2 Inter-annual variability in precipitation

In order to examine inter-annual precipitation variations in SE Iceland, precipitation data from Hólar í Hornafirði has been employed, where monitoring began in 1931 and continued until 2011 when the station was closed. During the period 1932 – 2011, the mean total precipitation value for this weather station was 1570 mm a^{-1} (σ = 307 mm), with a median value of 1510 mm. The maximum positive deviation (1224 mm) from the 1961 – 1990 average (1426 mm) at Hólar í Hornafirði occurs in 2002. Conversely, the maximum negative deviation in total annual precipitation during the period 1932 – 2011 was –476 mm, which occurred in 1965. The longest period of consecutive years with negative precipitation anomalies occurred between 1964 and 1967 (average: –258 mm). This period of negative precipitation anomalies coincides with a period of negative annual AAT anomalies, which persisted from 1965 – 1971 (see §6.1.1). Meanwhile, the period 1941 – 1948 displayed sustained positive precipitation anomalies (average: 310 mm), representing the longest period of positive precipitation anomalies at Hólar í Hornafirði. During this 8-year period, seven of the eight years exhibited positive AAT anomalies (average: 0.47 °C), with three of those years displaying deviations >1 °C. The general trends in total annual precipitation are illustrated in Figure 6.3.

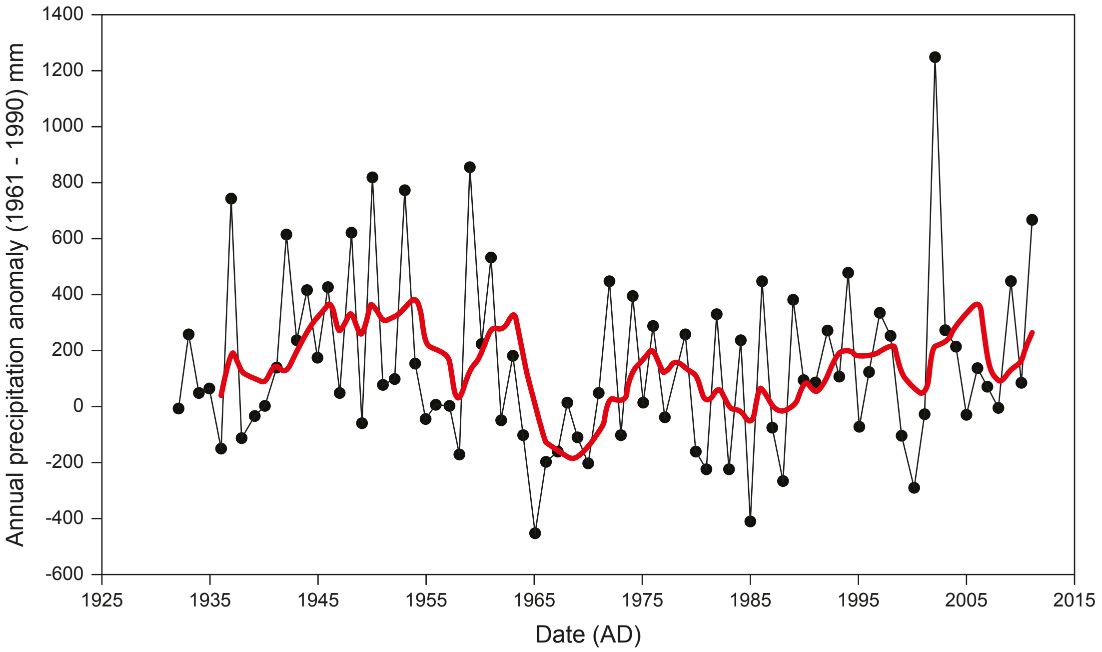

Figure 6.3: Time series plot illustrating the deviations of total annual precipitation (mm) from the 1961 – 1990 average at Hólar í Hornafirði. Red line represents a five-year moving average.

Previous investigations of glacier termini variations have demonstrated that changes in accumulation season precipitation can exert an important control on annual ice-frontal variations, though terminus response may lag by up to five years (Salinger *et al.*, 1983; Sigurðsson and Jónsson, 1995; Sigurðsson *et al.*, 2007; Beedle *et al.*, 2009; Laumann and Nesje, 2009; Winkler *et al.*, 2009). Furthermore, annual moraines both at Skálafellsjökull (see §5.2) and elsewhere in SE Iceland (e.g. Price, 1970; Boulton, 1986; Bradwell, 2004a; Evans and Hiemstra, 2005; Bradwell *et al.*, 2013) are believed to form during the course of a winter re-advance. Thus, it would appear fruitful to examine inter-annual variability in winter and spring precipitation. During the period 1932 – 2011, mean precipitation values (based on monthly average) for spring and summer were 94 mm per month (σ = 47 mm) and 150 mm per month (σ = 45 mm), respectively. The maximum negative deviation in average monthly spring precipitation (–78 mm per month) occurs in 1935, whereas the maximum negative deviation in winter precipitation (–79 mm per month) occurs in 1965. The longest period of sustained negative spring precipitation anomalies occurs between 1997 and 2001, averaging –40 mm per month. Conversely, the period 1968 – 1971 represents the longest period of negative winter precipitation anomalies (average: –14 mm per month). Maximum positive deviations in average monthly precipitation occur in 1942 and 1948 for spring (163 mm per month) and winter (134 mm per month), respectively. The longest period of consecutive positive spring precipitation anomalies lasts only three years, occurring between 1970 and 1972 (average: 28.6 mm per month). By contrast, the longest period of positive winter precipitation anomalies occurs between 1942 and 1946 (average: 61.3 mm per month). These general trends in spring and winter precipitation anomalies are illustrated in Figure 6.4.

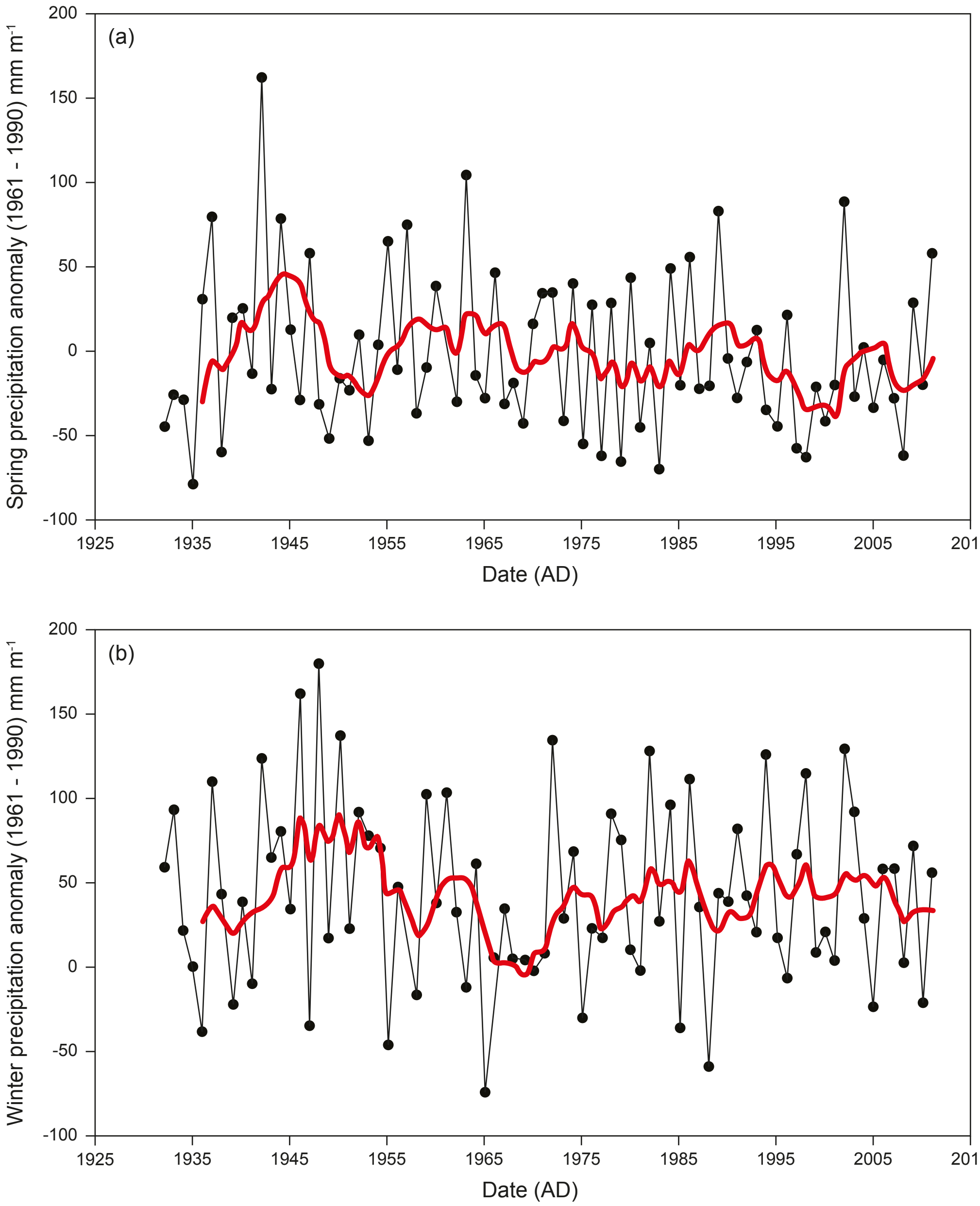

Figure 6.4: Time series plots illustrating the deviations of spring (a) and winter (b) precipitation from the 1961 – 1990 average at Hólar í Hornafirði. Red lines represent a five-year moving averages. Note that precipitation anomalies are based on monthly averages rather than total precipitation.

6.1.3 Inter-annual variability in the North Atlantic Oscillation

A key mode of inter-annual climatic variability in the North Atlantic region results from fluctuations in sea-level pressure that occur between *c*. 30 and 70°N, termed the *North Atlantic Oscillation* (NAO; e.g. Walker and Bliss, 1932; Rogers, 1984; Hurrell, 1995, 1996; Hurrell and van Loon, 1997; Nesje *et al*., 2000; Hurrell *et al*., 2003). This large-scale, regional North

Atlantic variability in sea-level pressure is expressed using the NAO index, which is the mean sea-level pressure difference between the Azores High and Icelandic Low (Hurrell and van Loon, 1997). For the purposes of the analysis herein, the station-based Hurrell NAO index (Hurrell and NCAR Staff, 2014) is employed. This index is based on the difference of normalised sea level pressure between Lisbon, Portugal and Stykkisholmur/Reykjavík, Iceland.

During the period 1930 – 2012, the annual NAO index ranged from –5.96 (occurring in 2010) to 3.88 (occurring in 1990), with a mean value of 0.08 (σ = 1.91). The 1960s displayed pronounced negative NAO index values, with nine out of eleven years exhibiting a negative NAO index between 1960 and 1970 (average: –1.36). This period of pronounced negative NAO index values coincides with periods of negative AAT and precipitation anomalies (see §6.1.1 and §6.1.2). The only other period on record with 5 or more years of negative annual NAO index values occurs between 1977 and 1981 (average: –0.97). Conversely, the period 1989 – 1994 displays pronounced positive NAO index values (average: 2.42). An earlier phase of positive NAO occurred between 1972 and 1976 (average: 1.02). Aside from these phases of pronounced negative and positive NAO, the annual NAO index exhibits large year-to-year variability (Figure 6.5).

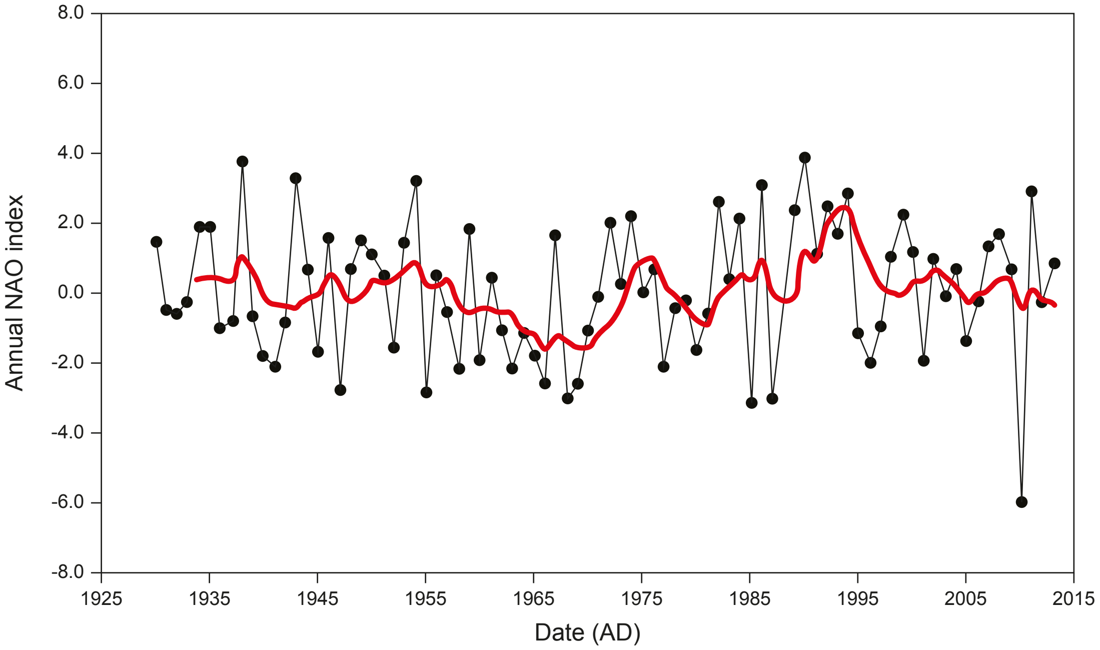

Figure 6.5: Time series plot illustrating the fluctuations of the annual NAO index. Red line represents a five-year moving average. NAO index values were obtained from the station-based Hurrell NAO database (Hurrell and NCAR Staff, 2014).

The NAO index is most pronounced both in amplitude and areal extent during the winter months, when it accounts for over a third of the total variance in sea-level pressure (*cf.* Cayan, 1992a; Hurrell, 1995; Hurrell and van Loon, 1997). The winter (December – March) Hurrell NAO index had a mean value of 0.14 (σ = 2.07) during the period 1930 – 2012, with a range between –4.89 (occurring in 1969) and 5.08 (occurring in 1989). Phases of negative NAO index values for four or more consecutive years occur only twice, in 1962 – 1966 (average: –2.68) and 1968 – 1971 (average: –2.20). These periods of pronounced negative NAO coincide with a phase of negative winter AAT anomalies, which occurred between 1965 and 1971 (average: –1.30 °C). Conversely, the most pronounced phase of positive winter NAO index values was evident during 1989 – 1995 (average: 3.29). Interestingly, this prominent period of positive NAO also coincides with a phase negative winter AAT anomalies, with five of the seven years exhibiting negative winter AAT anomalies (average: –0.59 °C). The general trends in winter NAO index are illustrated in Figure 6.6, demonstrating the high inter-annual variability.

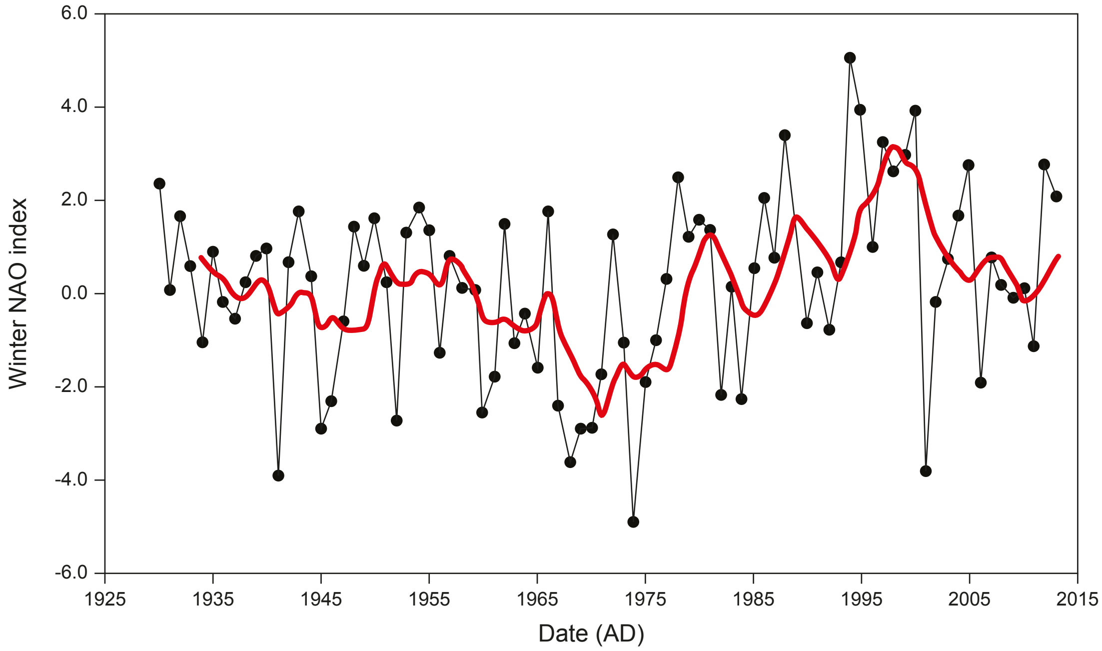

Figure 6.6: Time series plot illustrating the fluctuations of the winter (December – March) NAO index. Red line represents a five-year moving average. NAO index values were obtained from the station-based Hurrell NAO database (Hurrell and NCAR Staff, 2014).

6.1.4 Inter-annual variability in sea surface temperature

Owing to its location in a climatically sensitive position in the North Atlantic, Iceland's climate is strongly influenced by variability in atmosphere and ocean circulation (*cf.* Einarsson, 1984; Bradwell *et al.*, 2006; Geirsdóttir *et al.*, 2009; Ólafsdóttir *et al.*, 2013). In particular, SE Iceland is strongly influenced by the warm Irminger Current, which results in relatively mild and moist climate in this region of Iceland (Einarsson, 1984; Bradwell, 2001b; Geirsdóttir *et al*., 2009; Björnsson *et al*., 2013; Ólafsdóttir *et al*., 2013). Sea surface temperature (SST) anomalies have been extracted from the Second Hadley Centre SST dataset (HadSST2) in order to explore inter-annual variability in ocean surface conditions. The HadSST2 dataset takes the form of a monthly 5 x 5° grid array (Rayner *et al*., 2006). SST anomalies for the purposes of this study have been extracted from four grid cells covering latitudes 57.5 – 67.5°N and longitudes 7.5 – 17.5°W, with the values from the grid cells averaged to provide an indication of SST variations in proximity to SE Iceland. It should be noted that restricting the SST anomaly domain does not imply SE Iceland climate is only influenced by variability in this region of the North Atlantic. Indeed, Icelandic climate may be influenced by variability in far-travelled ocean currents (*cf*. Walter and Graf, 2002; Phillips and Thorpe, 2006). However, such atmosphere-ocean interactions are highly complex and exploring such variability is beyond the scope of this study.

The period 1930 – 2012 exhibited a mean annual SST anomaly of 0.20 °C (σ = 0.32 °C), with SST values ranging from –0.56 °C to 0.93 °C. Prominent phases of positive SST anomalies occurred during the periods 1933 – 1940 (average: 0.36 °C), 1953 – 1962 (average: 0.38 °C) and 1997 – 2012 (average: 0.54 °C). This latter period of elevated SST values coincides with a period of positive annual AAT anomalies (see §6.1.1), with AAT anomalies >1 °C displayed on six occasions during 2003 – 2012. Conversely, periods of negative annual SST anomalies for five or more years occur only twice, in 1985 – 1989 (average: –0.09 °C) and 1992 – 1996 (average: –0.18 °C). These phases of negative SST anomalies occur alongside a period of pronounced negative NAO index values (see §6.1.3). The general trends in annual SST anomalies are illustrated in Figure 6.7.

6.2 Interplay between atmospheric and oceanic climate variables

6.2.1 Influences on air temperature

As outlined above, the climate of SE Iceland is strongly influenced by variability in ocean surface currents (*cf*. Einarsson, 1984; Bradwell, 2001b; Geirsdóttir *et al*., 2009; Björnsson *et al*., 2013; Ólafsdóttir *et al*., 2013). Covariance analysis is employed here to examine the degree to which variability in SST has influenced air temperature at an inter-annual timescale since the *c*. 1930s. Covariance plots of SST anomalies and AAT anomalies show positive correlations between the variables both in the annual and seasonal signatures (Figure 6.8).

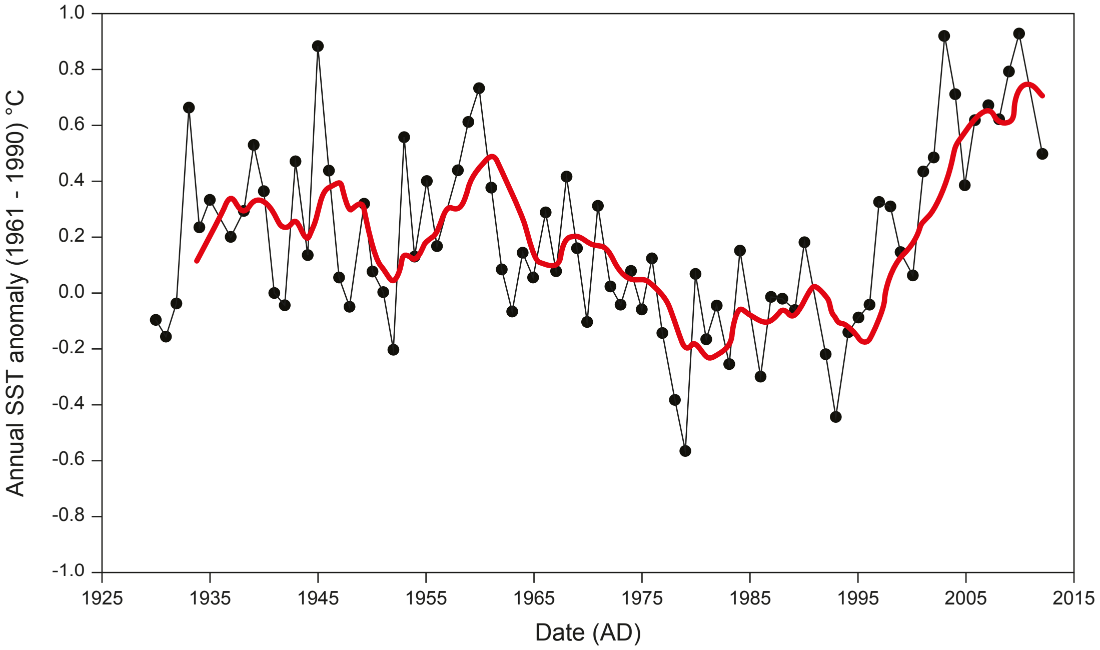

Figure 6.7: Time series plot illustrating the deviations of sea surface temperature (SST) from the 1961 – 1990 average. SST values are based on the average of values in a grid array covering latitudes 57.5 – 67.5°N and longitudes 7.5 – 17.5°W. Red line represents a five-year moving average.

Least squares regression analysis indicates that the regression lines are a very highly significant fit to the data in all cases ($p < 0.0001$), with coefficients of determination (r^2) ranging from 0.2075 – 0.5477. Furthermore, the regression analysis indicates that the regression line for the summer signature (Figure 6.8c) is the most effective, with ~55% of the variance in the data explained by the regression line. Conversely, the regression line for winter temperature (Figure 6.8e) is the least effective at explaining the variance in the data ($r^2 = 0.2075$). Nonetheless, the analysis of AAT anomalies at Hólar í Hornafirði and SST anomalies implies AAT in SE Iceland is strongly influenced by concurrent variability in SST, particularly with respect to the summer (Figure 6.3c) and autumn (Figure 6.8d) months.

A large degree of the inter-annual climatic variability in the North Atlantic region is thought to result from fluctuations in the NAO (see §6.1.3; Rogers, 1984; Hurrell, 1995, 1996; Hurrell and van Loon, 1997; Nesje *et al*., 2000; Bradwell, 2001b; Hanna and Cappelen, 2003; Hurrell *et al*., 2003; Hanna *et al*., 2004, 2008; Bradwell *et al*., 2006). As a consequence of its proximal location to one pole of the NAO, the climate of Iceland is strongly influenced by the NAO (Einarsson, 1984; Bradwell, 2001b; Hanna *et al*., 2004; Bradwell *et al*., 2006; Geirsdóttir *et al*., 2009; Ólafsdóttir *et al*., 2013). Following 1980, particularly around 1990, the NAO tended to remain in an extreme phase and explains statistically a substantial part of the observed temperature variability in western Norway (Hurrell, 1995; Hurrell and van Loon, 1997; Nesje *et al*., 2000). Furthermore, Hanna *et al*. (2004) demonstrated somewhat weak but statistically significant correlations between air temperature from selected Icelandic weather stations and the NAO. On this basis, it seems pertinent to explore the relationship between inter-annual variability in AAT at Hólar í Hornafirði and the NAO Index.

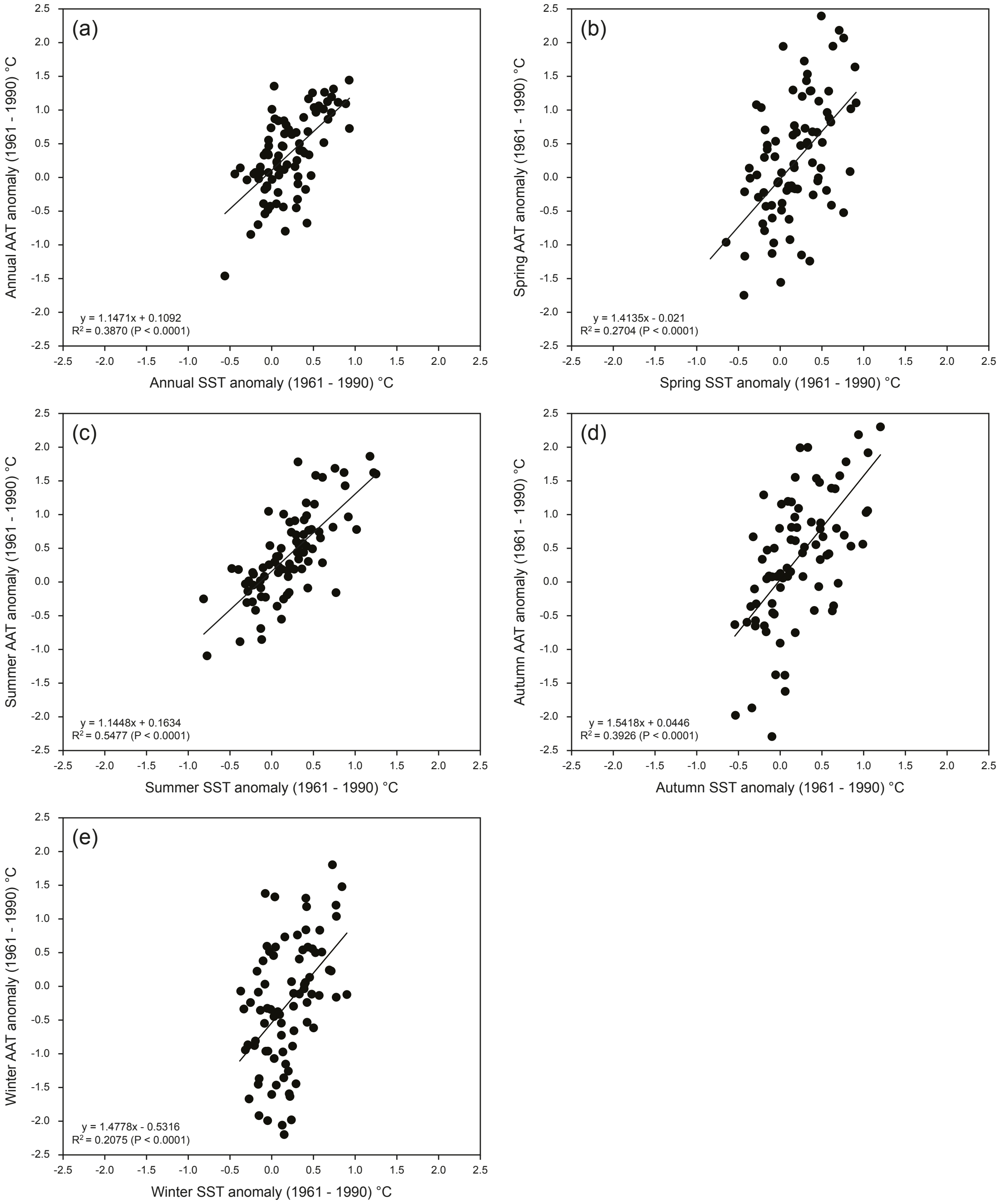

Figure 6.8: Covariance plots of seasonal variations in ambient air temperature (AAT) at Hólar í Hornafirði and sea surface temperature (SST) between latitudes 57.5 – 67.5°N and longitudes 7.5 – 17.5°W. Temperature values are expressed as deviations from the respective 1961 – 1990 averages. Values from 1945 are excluded from the data analysis owing to a lack of SST data. SST data has been extracted from the HadSST2 dataset (Rayner *et al.*, 2006).

For comparative purposes, seasonal averages of the monthly NAO index have been calculated. The seasonal Hurrell station-based NAO indices (Hurrell, 1995; Hurrell and NCAR Staff, 2014) have not been employed as the seasons do not follow the convention of *Veðurstofa Íslands* (the Icelandic Meteorological Office). Covariance plots of seasonal variations in the Hurrell station-based NAO index (Hurrell and NCAR Staff, 2014) and AAT show no apparent visual correlations (Figure 6.9). Moreover, least squares regression analysis indicates no statistically significant relationships between the NAO index and AAT anomalies (p > 0.05) except for the summer signal (Figure 6.9c). Nonetheless, the coefficient of determination (r^2) for the summer signature only explains ~8% of the variance in the data (p = 0.0121). This statistical analysis therefore implies that the NAO has a limited influence on inter-annual variability in AAT.

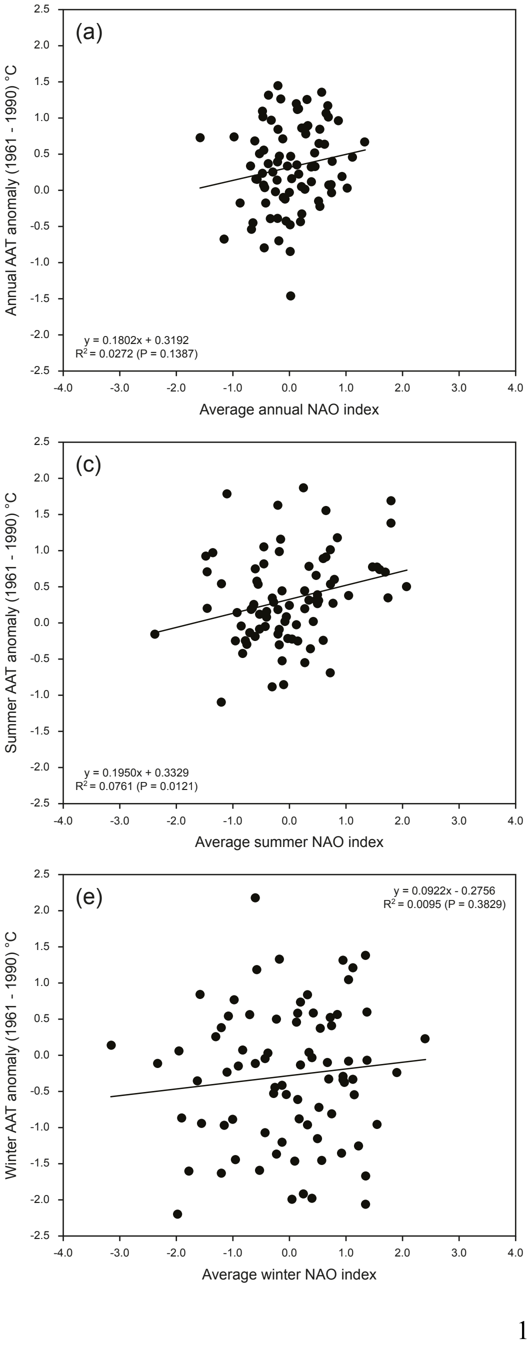

Figure 6.9: Covariance plots of seasonal variations in ambient air temperature (AAT) at Hólar í Hornafirði and the North Atlantic Oscillation (NAO) index. AAT values are expressed as deviations from the respective 1961 – 1990 averages. NAO index values are based on averages of monthly values.

6.2.2 Influences on precipitation

Precipitation variability in the North Atlantic region has previously been linked to North Atlantic SST patterns (e.g. Colman, 1997; Colman and Davey, 1999; Benestad and Melson, 2002; Phillips and McGregor, 2002), with Phillips and Thorpe (2006) attempting to use North Atlantic SST anomalies as predictors of Icelandic precipitation. Examination of this relationship for SE Iceland through covariance analysis (Figure 6.10) indicates weak, but statistically significant correlations between SST and precipitation anomalies for summer ($r^2 = 0.1225$, $p = 0.0016$) and autumn ($r^2 = 0.1081$, $p = 0.0029$). However, no statistically significant relationships are found for the other seasonal signatures. This relatively simple statistical analysis implies that SST anomalies and precipitation do not vary concomitantly at an inter-annual timescale, and that SST therefore has a limited influence at this timescale. However, precipitation patterns could potentially lag behind SST variations (*cf*. Phillips and Thorpe, 2006, and references therein). Additionally, North Atlantic SST variability may influence precipitation patterns through longer-term decadal to multi-decadal (referred to as the *Atlantic Multidecadal Oscillation* (AMO); *cf*. Kerr, 2000; Knight *et* al., 2005; Alexander *et al*., 2014; Drinkwater *et al*., 2014) signals. Nonetheless, such analysis is beyond the scope of this study.

Given the abovementioned coincidence of periods of negative precipitation anomalies and periods of negative AAT anomalies (see §6.1.2), it seems appropriate to examine the relationship between precipitation and AAT further. Covariance plots of AAT and precipitation anomalies show visual positive correlations (Figure 6.11). Furthermore, least squares regression analysis indicates that the regression lines are a very highly statistically significant fit to the data in all cases ($p < 0.0001$), with r^2 values ranging from 0.1819 – 0.2383. This statistical analysis therefore implies precipitation in SE Iceland is partly influenced by concurrent variations in ambient air temperature at an inter-annual timescale, perhaps reflecting greater moisture availability at warmer temperatures.

As highlighted above the NAO is a key mode of climate variability in the North Atlantic region (see §6.1.3). Variations in precipitation in this region have previously been attributed to

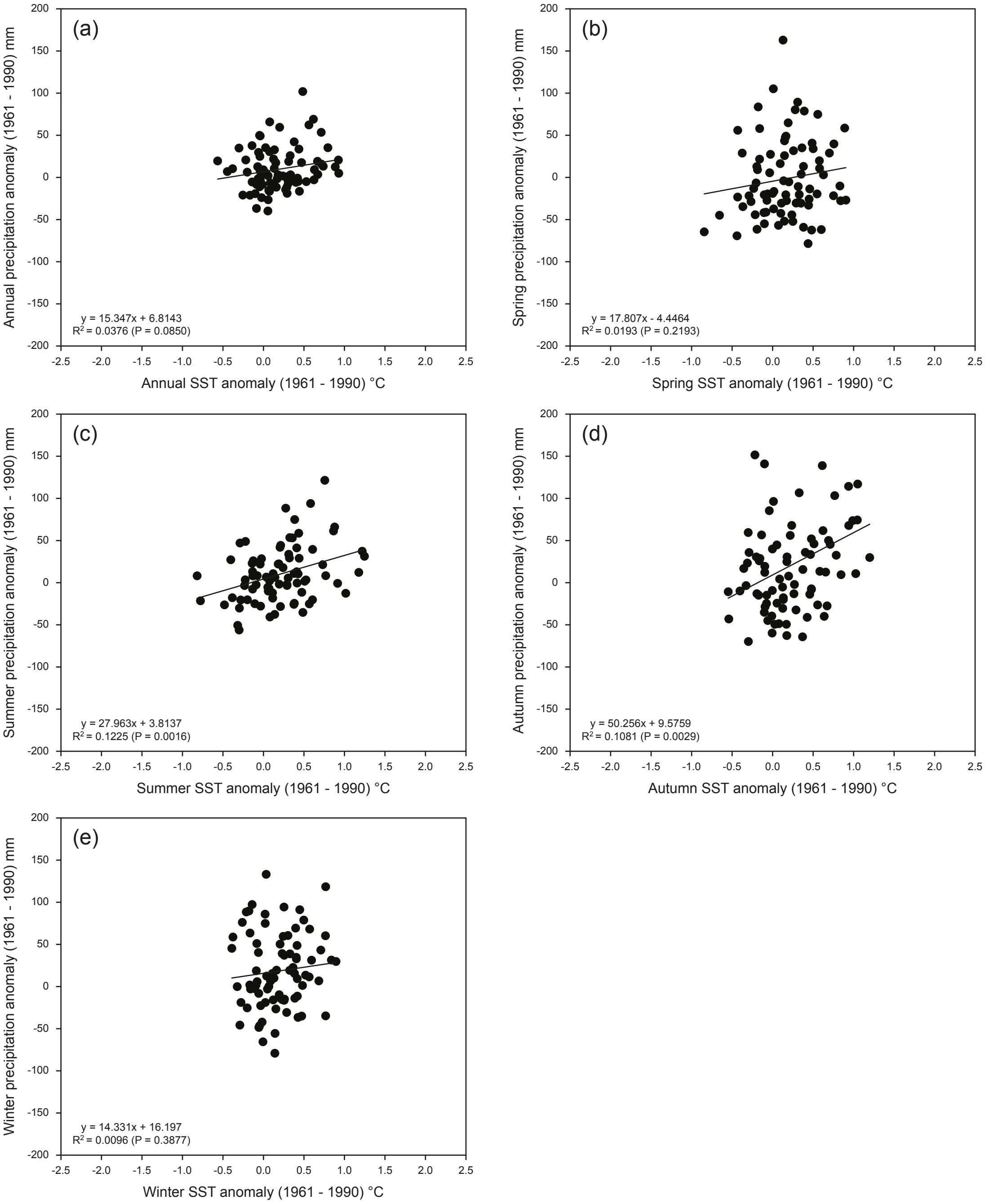

Figure 6.10: Covariance plots of seasonal variations in precipitation at Hólar í Hornafirði and sea surface temperature (SST) between latitudes 57.5 – 67.5°N and longitudes 7.5 – 17.5°W. Temperature values are expressed as deviations from the respective 1961 – 1990 averages. Note that precipitation anomalies are based on monthly averages rather total precipitation. Values from 1945 are excluded from the data analysis owing to a lack of SST data.

fluctuations in the NAO (e.g. Hurrell, 1995; Sodemann et al., 2008; Trouet et al., 2009, 2012; Olsen et al., 2012). For example, in Bergen, western Norway 59% of the total variance in winter (December – March) precipitation is explained by fluctuations in the NAO index (Nesje et al., 2000). Covariance analysis of seasonal precipitation anomalies at Hólar í Hornafirði and the Hurrell NAO index (Figure 6.12) indicates visual positive correlations between the two variables in all seasons except autumn (October and November). Inter-annual fluctuations in the NAO are most successful at accounting for the variability in spring ($r^2 = 0.1820$, $p < 0.0001$) and winter ($r^2 = 0.1804$, $p < 0.0001$) precipitation anomalies. Conversely, there is no statistically significant relationship between the NAO index and precipitation anomalies for the autumn signature ($r^2 = 0.0137$, $p < 0.3006$). Nevertheless, this statistical analysis implies that the NAO has some effect on inter-annual variations in precipitation values.

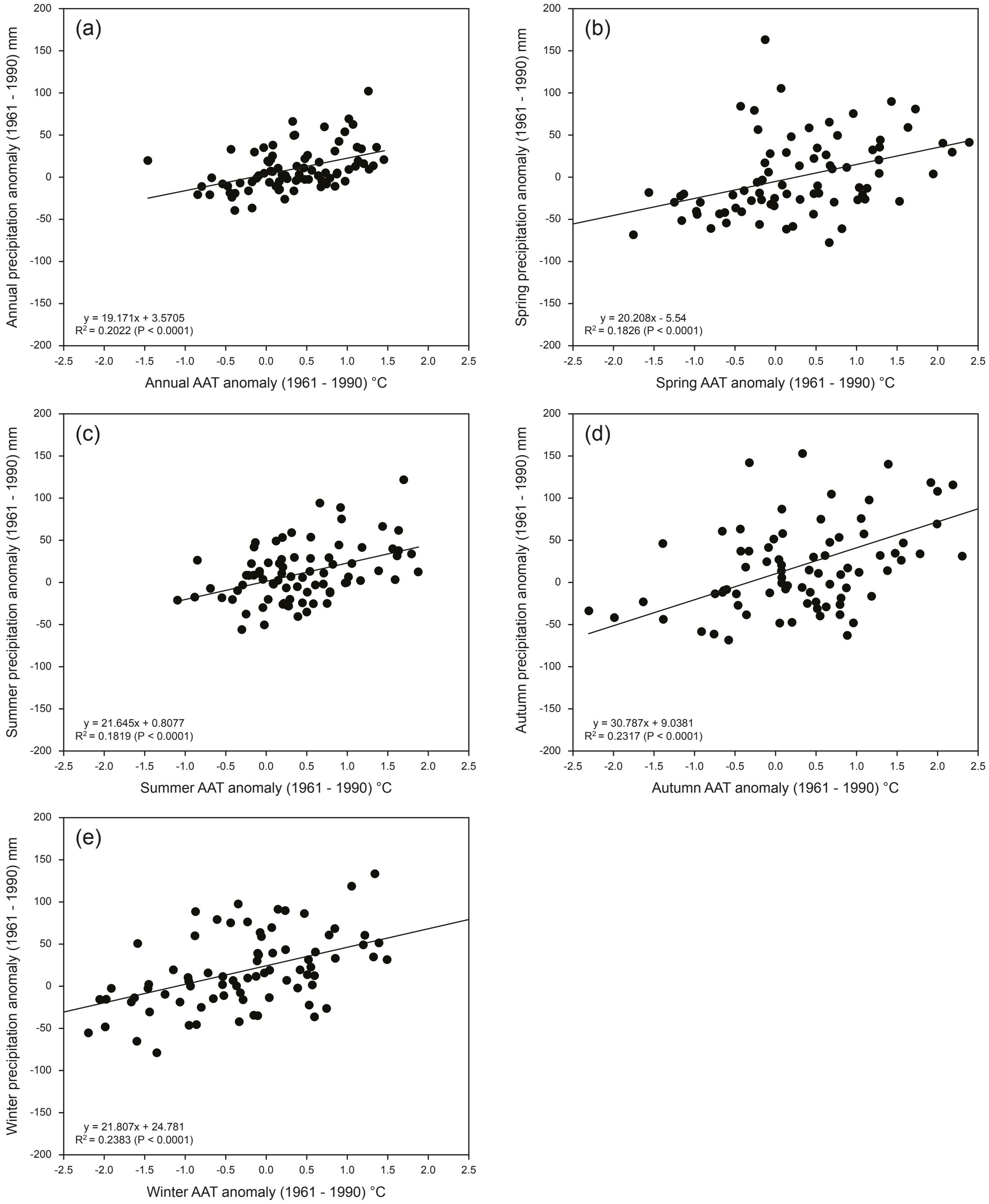

Figure 6.11: Covariance plots of seasonal variations in precipitation and ambient air temperature (AAT) at Hólar í Hornafirði. Values are expressed as deviations from the respective 1961 – 1990 averages. Note that precipitation anomalies are based on monthly averages rather total precipitation.

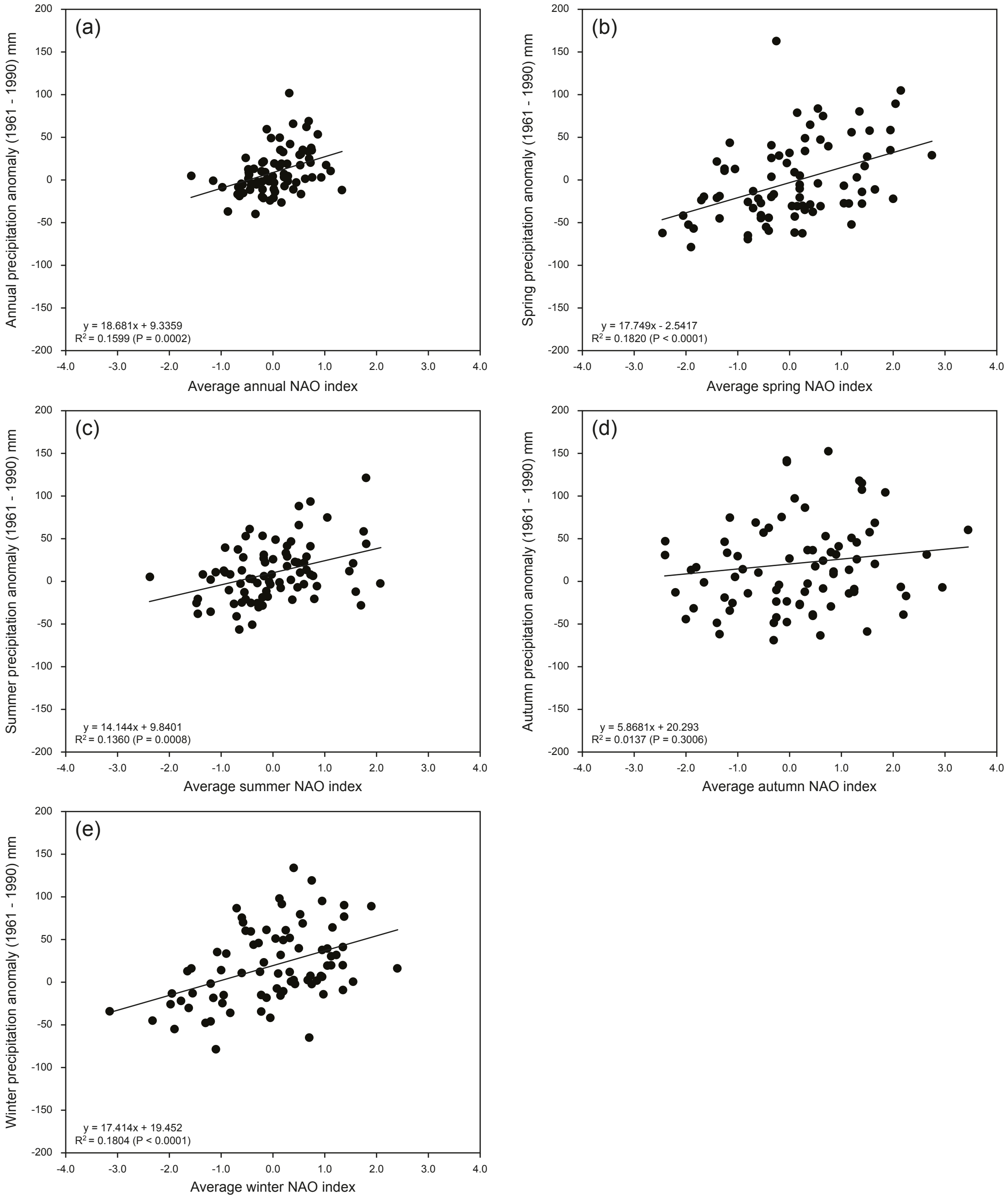

Figure 6.12: Covariance plots of seasonal variations in precipitation at Hólar í Hornafirði and the Hurrell NAO index. Precipitation values are expressed as deviations from the respective 1961 – 1990 averages. Precipitation anomalies and NAO index values are based on averages of monthly values.

6.2.3 North Atlantic atmosphere-ocean interactions

It has long been recognised that SST fluctuations are intimately linked to the dynamics and variability of the NAO, with Bjerknes (1964) hypothesising that fluctuations in the NAO index strongly influence SST anomalies at inter-annual timescales (see also Cayan, 1992a, b; Battisti *et al.*, 1995; Delworth, 1996; Deser and Timlin, 1997; Marshall *et al.*, 2001; Visbeck *et al.*, 2003; Hurrell and Deser, 2009). Conversely, decadal variability in ocean dynamics is in turn believed to strongly influence the NAO, with studies identifying significant correlations between SST anomalies and the NAO (*cf.* Bjerknes, 1964; Rowntree, 1976; Mehta *et al.*, 2000; Robertson *et al.*, 2000; Sutton *et al.*, 2000; Rodwell and Folland, 2002; Hurrell *et al.*, 2003; Park and Latif, 2005). The relationship between inter-annual variability in the NAO and SST is explored here through relatively simple statistical analysis. Covariance plots of seasonal variations in the two variables show no visual correlations (Figure 6.13). Furthermore, least squares regression analysis indicates no statistically significant relationships exist between

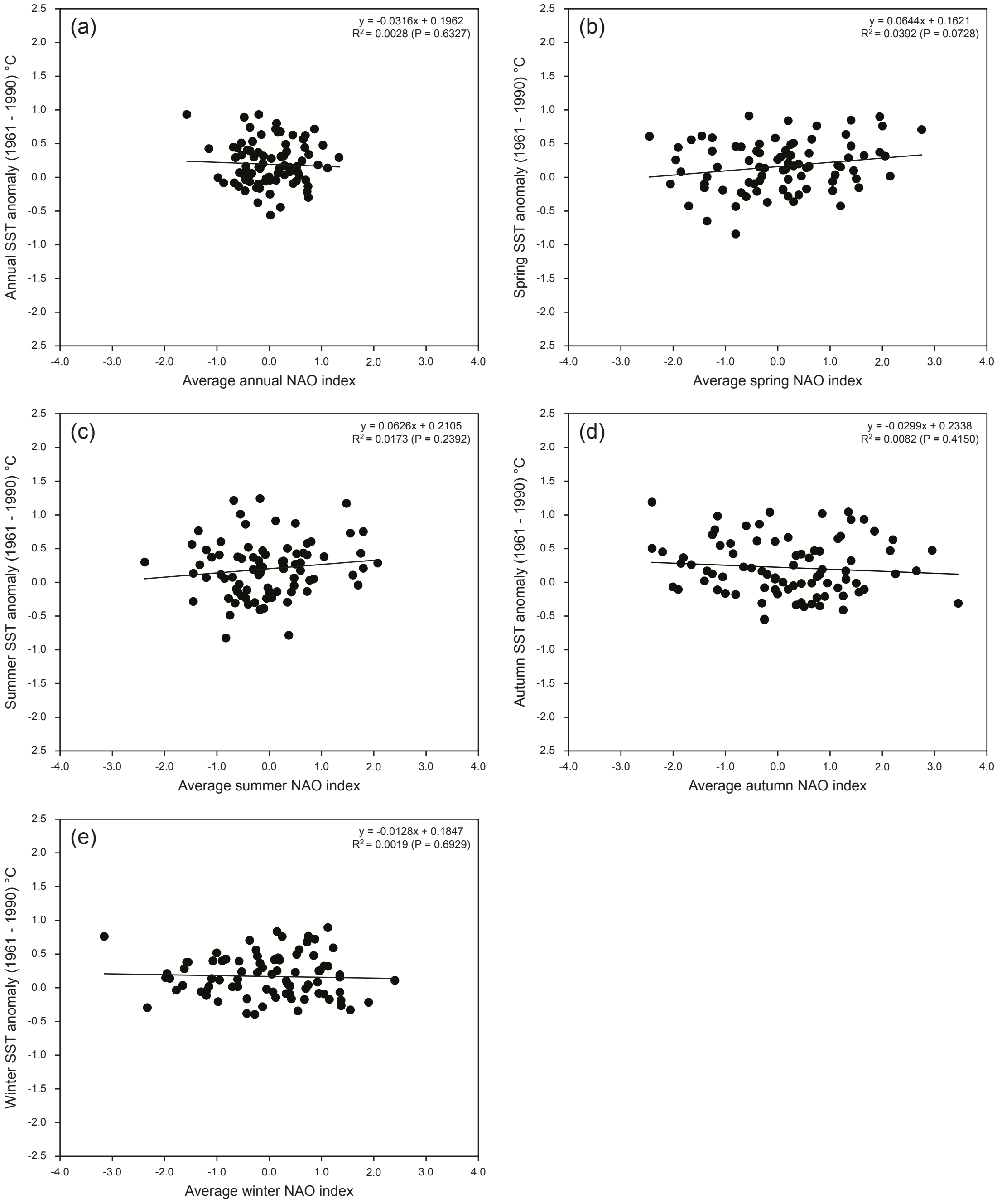

Figure 6.13: Covariance plots of seasonal variations in the Hurrell NAO index and sea surface temperature (SST). SST values are expressed as deviations from the respective 1961 – 1990 averages, and represent average values between latitudes 57.5 – 67.5°N and longitudes 7.5 – 17.5°W. NAO index values are based on averages of monthly values.

seasonal averages of NAO and SST anomalies ($p > 0.05$). However, this absence of correlation may reflect the somewhat rudimentary nature of the statistical analysis employed herein, rather than indicating no relationship exists between the NAO and SST.

6.3 Summary

This chapter has examined inter-annual variability in SE Iceland climate since *c*. 1930, considering the following key variables: ambient air temperature (AAT); precipitation; the North Atlantic Oscillation (NAO); and sea surface temperature (SST). Examination of meteorological data from Hólar í Hornafirði shows that prominent phases of negative annual AAT anomalies occurred during the *c*. 1960s – 1970s, coinciding with pronounced negative precipitation anomalies. Moreover, the 1960s and 1970s are characterised by a prominent phase of negative NAO. However, the most pronounced negative phase of the NAO occurred between 1989 and 1995. Since 1996 annual AAT anomalies have remained positive, with six out of ten years during the period 2003 – 2012 exhibiting AAT anomalies >1 °C. Furthermore, 2002 – 2006 represented the warmest five-year period during the record, with an average AAT anomaly of 1.07 °C. These positive AAT anomalies coincide with a period of positive SST anomalies, which has been ongoing since 1997. Covariance analysis to explore the interplay between these atmospheric and oceanic climate variables indicates AAT is strongly influenced by SST variability, with least squares regression analysis identifying *very highly statistically significant* ($p < 0.001$) relationships for each seasonal signal. Meanwhile, AAT appears to exert a key control on precipitation in SE Iceland, with *very highly statistically significant* relationships again recognised for each seasonal signal. The NAO also appears to have an important influence on precipitation, but to a slightly lesser degree. However, statistical analysis to examine the interplay between SST values and the NAO showed no statistical significant relationships. The analysis conducted herein demonstrates that inter-annual variability in SE Iceland climate reflects complex atmosphere-ocean interactions. Recognising this complexity in the climate signal will be of key importance when examining the potential drivers of recent ice-marginal retreat at Skálafellsjökull in the next chapter.

CHAPTER 7

Significance of annual moraines at Skálafellsjökull

This chapter synthesises the geomorphological, chronological and sedimentological evidence presented in Chapter 5, along with the climate data discussed in Chapter 6. Firstly, Section 7.1 synthesises the moraine sedimentology data and initial interpretations of the moraine sections, with genetic models presented and described for the moraine-forming processes identified at Skálafellsjökull. The wider significance of these processes of annual moraine formation is considered through comparison with hitherto-proposed genetic processes, both from Iceland and elsewhere. Having examined annual moraine sedimentology and processes of formation, the significance of the form (or morphology) of the annual moraines on the Skálafellsjökull foreland is considered in Section 7.2. The interplay between topography and structural glaciology and its influence on annual moraine geomorphology is the principal focus, with the effect of climate on the annual moraines considered in the following section. The annual moraines are applied as geomorphological proxies for patterns and rates of ice-marginal retreat at Skálafellsjökull in Section 7.3, with annual ice-margin retreat rates (IMRRs) calculated from annual moraine spacing. The climatic implications of these patterns and rates of ice-marginal retreat are subsequently discussed, with potential drivers of ice-marginal retreat examined using covariance analysis. The wider significance of the patterns, rates and drivers of ice-marginal retreat at Skálafellsjökull is also considered through comparison with findings from other outlet glaciers in the North Atlantic region. Finally, Section 7.4 assesses the applicability of annual moraines as climate indicators, wherein potential geomorphological and chronological issues associated with using annual moraine sequences are highlighted.

7.1 Synthesis of annual moraine genetic processes

The sedimentological data presented and described in §5.3 strongly suggest that the majority of annual moraines at Skálafellsjökull are formed through a combination of squeezing and bulldozing (or pushing) of subglacial sediments, though pre-existing proglacial sediments, in the form of immature subglacial traction tills (*sensu* Evans *et al.*, 2006) and glaciofluvial deposits, may be locally bulldozed into a moraine ridge. In limited instances submarginal sediment slabs may be emplaced in the annual moraines through subglacial freeze-on (*sensu* Krüger, 1994, 1995). Moraines at Skálafellsjökull are predominantly composed of subglacial traction tills (*sensu* Evans *et al.*, 2006), with no apparent evidence for the incorporation of supraglacial debris flow deposits: the clast shape analysis is a particularly strong indicator of the dominance of subglacial transport pathways (see §5.3.2; Boulton, 1978; Benn, 1992; Benn and Ballantyne, 1994; Lukas, 2005, 2007). The absence of supraglacial debris within the annual moraines is attributed to the lack of appreciable debris cover on the glacier surface. Supraglacial debris point sources are limited to isolated debris cones at the southeastern Skálafellsjökull margin. Reworking of material on the distal side of annual moraines was evident in some sections, as reported in previous studies of Icelandic annual moraines (Sharp, 1984; Krüger, 1994, 1995), though it was not ubiquitous.

Sedimentological evidence for the incorporation of submarginal sediments through subglacial freeze-on (*sensu* Krüger, 1994, 1995) was restricted to two moraine exposures, both situated at the southeastern margin of Skálafellsjökull. In this area of the foreland the glacier is retreating from a reverse bedrock slope and exhibits a relatively thin and gently-sloping ice-front. Additionally, meltwater accumulates and flows along the southeastern margin, appearing to undercut the ice-front in places (Figure 7.1). It is suggested that these topographic and glaciological characteristics provide propitious conditions for subglacial freeze-on of sediments in this part of the foreland. The relatively thin ice-margin and undercutting by meltwater allows the penetration of a winter freezing front, leading to freeze-on of submarginal sediments (*cf*. Krüger, 1993, 1994, 1995, 1996; Matthews *et al*., 1995; Evans and Hiemstra, 2005; Reinardy *et al*., 2013). The maximum thickness of ice through which the freezing front can penetrate is believed to be *c*. 15 m (Harris and Bothamley, 1984; Cuffey and Paterson, 2010). Interestingly, negative AAT anomalies occurred at Hólar í Hornafirði in the winter of 2011 (–0.12 °C) and the spring of 2012 (–0.41 °C), the period in which moraine SKA-11 is believed to have formed. Thus, climatic factors may exert some control over the localised occurrence of subglacial freeze-on of sediments at Skálafellsjökull, with relatively cold winter conditions combined with a thin ice-margin providing favourable conditions for this mode of formation. The restricted incidence of subglacial freeze-on at Skálafellsjökull compared to outlets of the Mýrdalsjökull ice-cap (Krüger, 1993, 1994, 1995, 1996; Krüger *et al*., 2010) is thought to be a function of: (1) the relatively steep, temperate ice-margin making it more difficult for deep penetration of the freezing front (*cf*. Krüger, 1995; Lukas, 2012); and (2) a difference in climatic regime. In contrast to the coastal outlets of southern Vatnajökull (e.g. Skálafellsjökull), Mýrdalsjökull is controlled by a more continental climate with severe winters and colder, more prolonged springs (*cf*. Krüger, 1995).

The topography and bedrock geology of the southern part of the Skálafellsjökull foreland also has an important role in other genetic processes identified. As highlighted above, the ice-margin is retreating from a reverse bedrock slope in this area. Furthermore, the bedrock slope is of basaltic lithology, preventing permeation of surface waters (meltwater) and generating an aquiclude. Consequently, surface waters flow back down the slope towards the ice-margin, accumulating in channels and ponds at the ice-front. This combination of topographic and geological factors results in highly saturated subglacial/submarginal sediments and high pore-water pressure. The presence of this viscous slurry and high pore-water pressure at the base of the glacier leads to submarginal deformation and ice-marginal squeezing (Price, 1970; Boulton and Dent, 1974; Boulton *et al*., 1974, 2001; Sharp, 1984; Boulton, 1987; Boulton and Hindmarsh, 1987; Benn, 1995; Hart, 1995; Evans and Twigg, 2002; Evans and Hiemstra, 2005; Roberts and Hart, 2005). This extruded sediment is subsequently bulldozed into a moraine ridge by the ice-front (*cf*. Sharp, 1984). Poorly drained submarginal conditions have also been observed to play an important role in the development of recessional push/squeeze moraines exhibiting sawtooth planforms at Fláajökull (*cf*. Evans and Hiemstra, 2005; Evans *et al*., submitted). Deformable sediments are also manifest in the form of widespread flutings at Skálafellsjökull (*cf*. Boulton, 1976; Benn, 1994), which are found in close association with annual moraines in the southern part of the Skálafellsjökull foreland (Evans and Orton, 2014). The close association of annual moraines and flutings in this part of the foreland suggests that these features are genetically linked (*cf*. Evans and Twigg, 2002; Evans, 2003a). Formation of these moraines through push/squeeze mechanisms is consistent with a subglacial deformation/ploughing origin for the flutings (*cf*. Boulton, 1976; Boulton and Hindmarsh, 1987; Benn, 1994; Boulton and Dobbie, 1998; Boulton *et al*., 2001).

Figure 7.1: Field photograph showing the gently-sloping, relatively thin southeastern Skálafellsjökull ice-margin (06.06.14). Meltwater flowing along the ice-margin has resulted in undercutting.

The range of genetic processes identified at Skálafellsjökull is similar to hitherto-proposed genetic models of moraine formation at Icelandic glaciers. In particular, push/squeeze moraines have been identified at a number of Icelandic outlet glaciers (*cf.* Price, 1970; Sharp, 1984; Evans and Twigg, 2002; Evans and Hiemstra, 2005). Moreover, the emplacement of frozen-on sediment slabs has previously been proposed (*cf.* Krüger, 1993, 1994, 1995, 1996; Evans and Hiemstra, 2005). Similar models invoking subglacial freeze-on have also been posited for Norwegian outlet glaciers (Matthews *et al.*, 1995; Reinardy *et al.*, 2013). However, the incidence of subglacial freeze-on is not widespread at Skálafellsjökull. Important differences between the range of processes identified herein and previous models of annual moraine formation are as follows: (1) no evidence was found for snow-cover having a significant role in moraine genesis or postdepositional modification (Price, 1970; Birnie, 1977; Sharp, 1984); (2) dead-ice incorporation as a result of inefficient bulldozing was not apparent, with no ice-cored moraines identified (Sharp, 1984; Lukas, 2012); (3) there was no evidence for dead-ice incorporation as a result of isolation of an ice core beneath englacial debris bands (Sharp, 1984); and (4) terrestrial ice-contact fans were not evident at Skálafellsjökull (Lukas, 2012). Of the moraine types previously identified at Skálafellsjökull by Sharp (1984), only Type A ridges have been identified (Figure 7.2). This difference may partly reflect changes in glacier dynamics, ice-margin structure/morphology and/or climatic conditions. Examination of ambient air temperature (AAT) and sea surface temperature (SST) data in the previous chapter demonstrated that positive AAT and SST anomalies have occurred since *c*. 1996, with pronounced anomalies (> 1 °C) occurring in the last *c*. 10 years. As such, climate may have an important control on the incorporation of dead-ice and snowbanks in the moraines. However, the occurrence of dead-ice incorporation (Types B and C) and the influence of snowbanks (Type D) cannot be entirely ruled out as: (1) sedimentological investigations were undertaken part way through the ablation season (June); and (2) moraine forming processes were not investigated at the northeastern Skálafellsjökull margin. The absence of terrestrial ice-contact fans (Lukas, 2012) reflects the lack of appreciable supraglacial debris cover and limited availability of supraglacial point sources (*cf.* hochsandur fans; Krüger, 1997; Kjær *et al.*, 2004).

Based on the sediment composition and structure of the annual moraines (see §5.3), the following three categories of moraine-forming processes can be distinguished at Skálafellsjökull: (1) submarginal deformation and subsequent bulldozing of the extruded sediments (SKA-07; Figure 7.3); (2) efficient bulldozing of pre-existing proglacial material (SKA-13; Figure 7.4); and (3) emplacement of frozen-on submarginal sediment slabs (SKA-11; Figure 7.5).

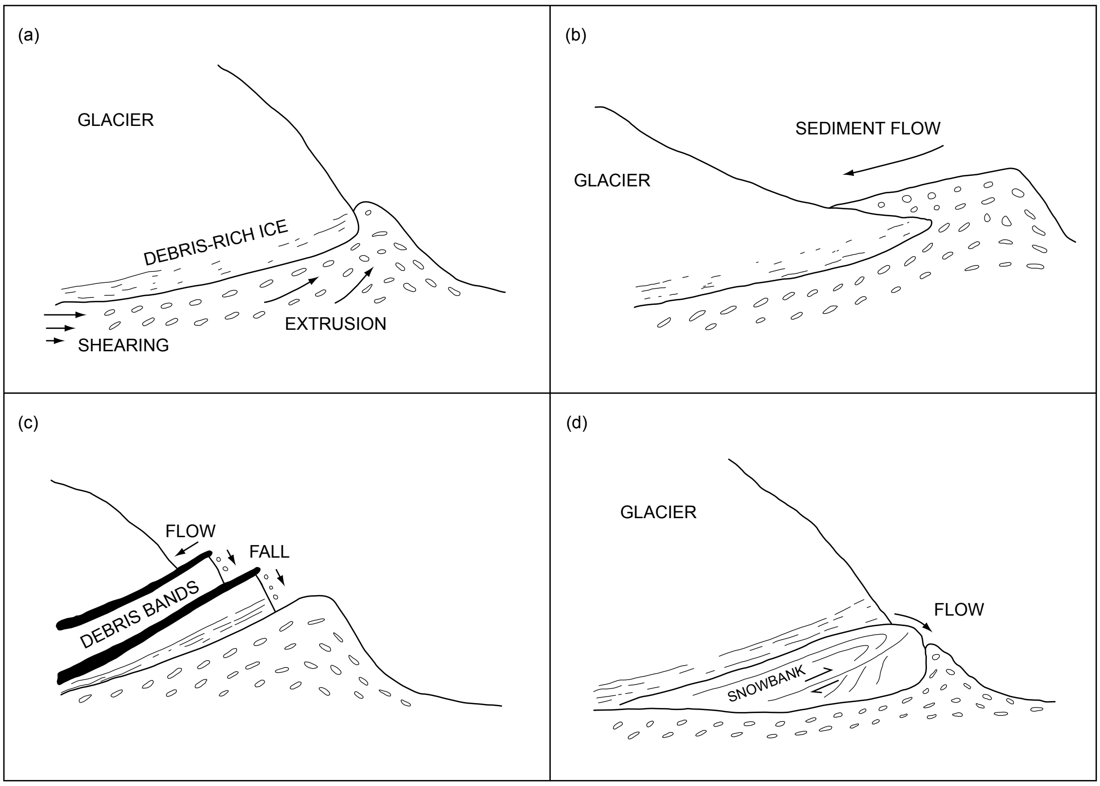

Figure 7.2: Diagram showing the four types of moraine ridges observed by Sharp (1984) at Skálafellsjökull. (a) Simple ridge formed of subglacial traction till (*sensu* Evans *et al*., 2006). (b) Ridge with an ice core incorporated by the flow of ridge sediments back over the glacier margin. (c) Ridge with an ice core isolated beneath thick englacial debris bands which have been exposed by backwasting of the overlying ice slopes. (d) Ridge formed at the distal edge a marginal snowbank which has been pushed forward by the glacier. Flow of debris derived from the basal ice has incorporated the snowbank into the ridge. *Source:* Redrawn from Sharp (1984: 85).

7.1.1 Efficient bulldozing of extruded submarginal sediments

Sedimentological investigations of SKA-07, combined with field observations at the contemporary ice-margin, allow the following sequence of events to be reconstructed (Figure 7.3). This process is dominant throughout the foreland, occurring both on the portions of the foreland with a lower surface gradient and on the reverse bedrock slope in the south. Moreover, this sequence of events appears to apply best where the ice-front is relatively steep and where pecten is well-developed at the terminus. During the melt season, an increase in meltwater descending to base of the glacier saturates the underlying subglacial materials and elevates porewater pressures (Andrews and Smithson, 1966; Price, 1970; Evans and Hiemstra, 2005). Where the glacier is situated on a reverse bedrock slope, runoff of surface water back down the slope also contributes to this process. The elevation of porewater pressures and saturation of the subglacial sediments leads to submarginal deformation and ice-marginal squeezing (1) (Price, 1970; Sharp, 1984; Evans and Twigg, 2002; Evans and Hiemstra, 2005). During the winter re-advance (2), the extruded sediments are bulldozed by the advancing ice-front, leading to ductile deformation and folding of sorted sediments incorporated within the moraine. As retreat commences in the spring (3), localised reworking of the moraine surface slopes may occur due to gravitational and glaciofluvial activity. The relative steepness of the ice-front ensures that efficient bulldozing occurs (*sensu* Lukas, 2012) and, therefore, no material slumps onto the glacier surface. Consequently no dead-ice is incorporated within the moraine (3 – 4).

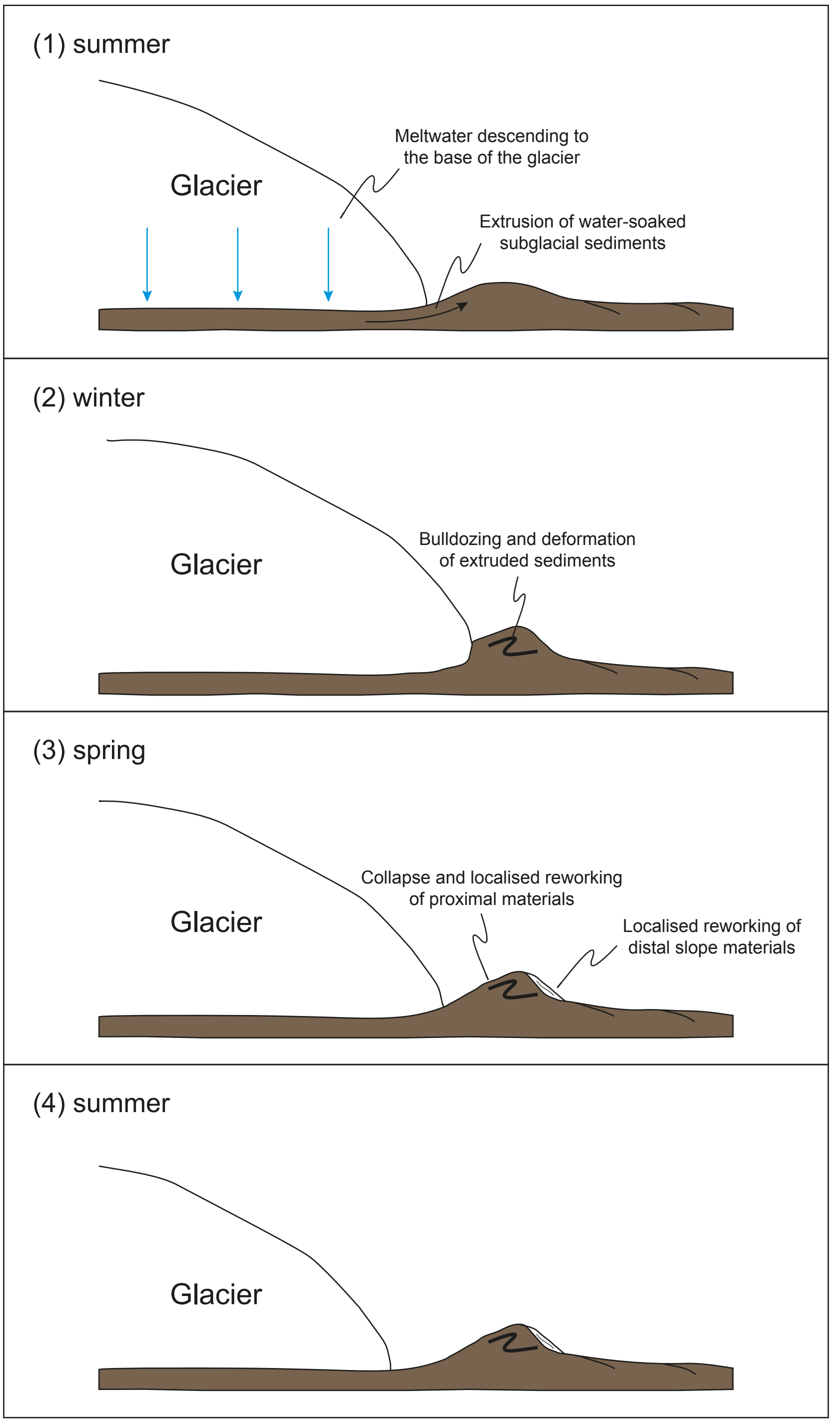

Figure 7.3: Schematic model of annual moraine genesis through efficient bulldozing of extruded submarginal sediments at Skálafellsjökull, as reconstructed from representative sections (SKA-04 and SKA-07) on the glacier foreland. For a detailed explanation of the processes, see §7.1.1.

7.1.2 Efficient bulldozing of pre-existing proglacial sediments

This sequence of events (Figure 7.4) applies where Skálafellsjökull is retreating from the reverse bedrock slope in the southern part of the foreland, and where the ice-margin is relatively steep (1). Accumulation of meltwater along the southeastern ice-margin allows glaciofluvial deposition, whilst thin spreads of (immature) subglacial traction tills (*sensu* Evans *et al*., 2006) are also evident on the foreland. During the course of the winter re-advance (2), the proglacial material is bulldozed by the advancing glacier to form a ridge. Where the material is cobble/boulder-rich, as in SKA-13, the sediments record limited evidence of having undergone proglacial deformation. Following initiation of ice-marginal retreat during the spring (3), the ice-proximal slope collapses due to loss of support and may undergo localised reworking. In the case of SKA-13, the cobble/boulder-rich composition of the moraine results in relatively steep surface slopes and limited action by gravitational processes. The steepness and bulldozing capabilities of the ice-margin ensure that no material is transferred onto the glacier surface (*cf*. Lukas, 2012). As a result, no glacier ice is cut-off from the active margin and buried within the moraine (3 – 4).

7.1.3 Emplacement of sediment slabs through freeze-on

The sequence of events reconstructed for SKA-11 (Figure 7.5) occurs where the ice-margin is relatively thin and retreating from a reverse bedrock slope in the southern part of the foreland (1). Due to penetration of the winter freezing front (2), slabs of subglacial and glaciofluvial sediments become frozen to the underside of the glacier snout during winter re-advance (*cf*. Krüger, 1993, 1994, 1995, 1996; Matthews *et al*., 1995; Evans and Hiemstra, 2005; Reinardy *et al*., 2013). As the ice-margin re-advances, the frozen-on sediment is moved as an integral part of the glacier sole and overrides the foreland (Krüger, 1995). Proglacial materials may also begin to build up and be pushed as the ice-front continues to re-advance (Reinardy *et al*., 2013). During the spring (3), this frozen-on sediment begins to melt out incrementally, forming a ridge containing diamicton, gravel and sand units dipping upglacier (*cf*. Krüger, 1993, 1995, 1996; Evans and Hiemstra, 2005; Reinardy *et al*., 2013). As the glacier continues to retreat during the summer (4), a moraine ridge comprising upglacier dipping sediment units is revealed. Localised reworking of the distal slope may occur through mass movement activity, as in the case of SKA-11. The genetic model outlined for SKA-11 is similar to that previously proposed for annual moraine formation elsewhere (Krüger, 1995; Reinardy *et al*., 2013).

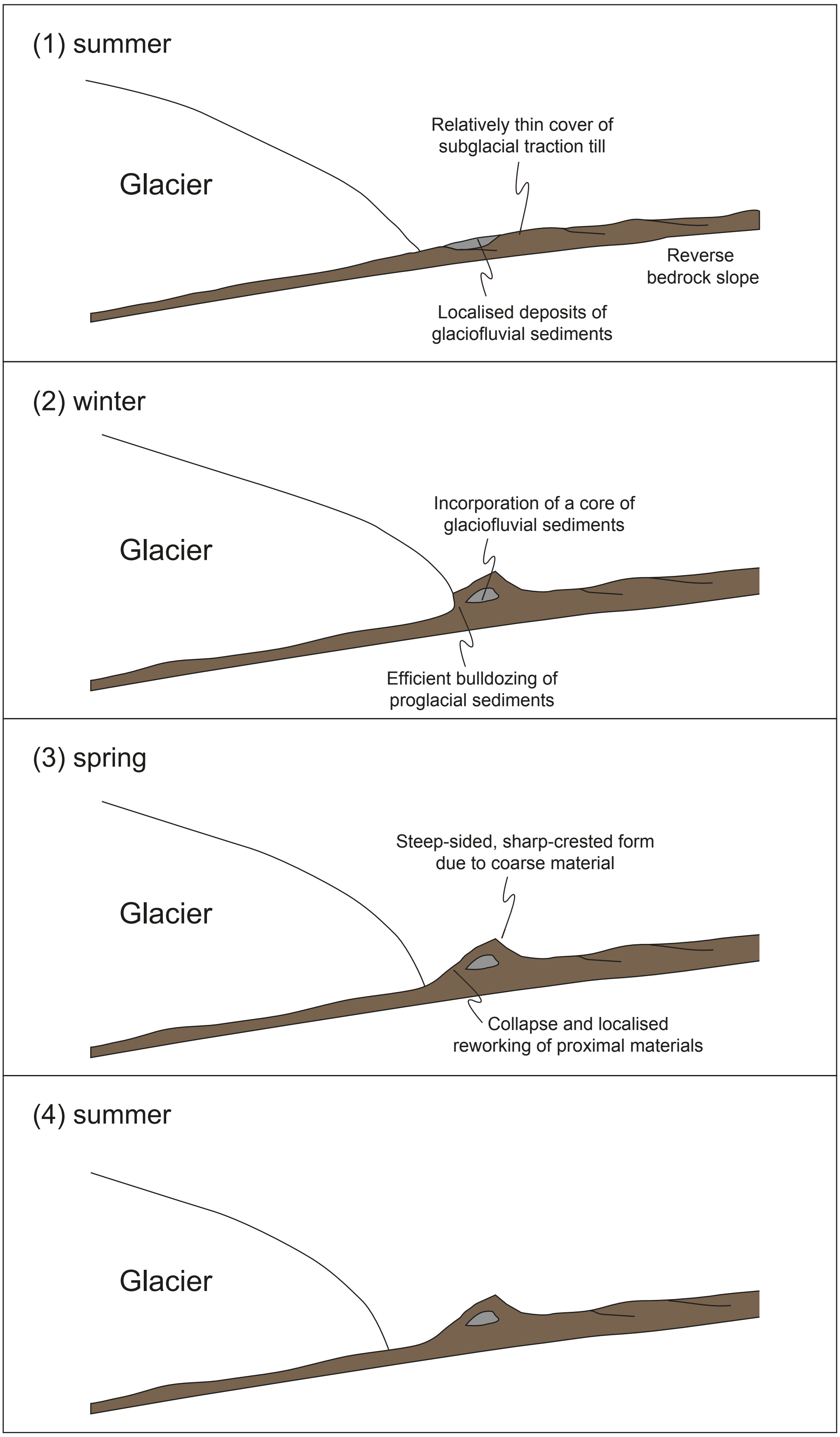

Figure 7.4: Schematic model of annual moraine genesis through efficient bulldozing of pre-existing proglacial sediments at Skálafellsjökull, as reconstructed from a representative section (SKA-13) on the glacier foreland. For a detailed explanation see §7.1.2.

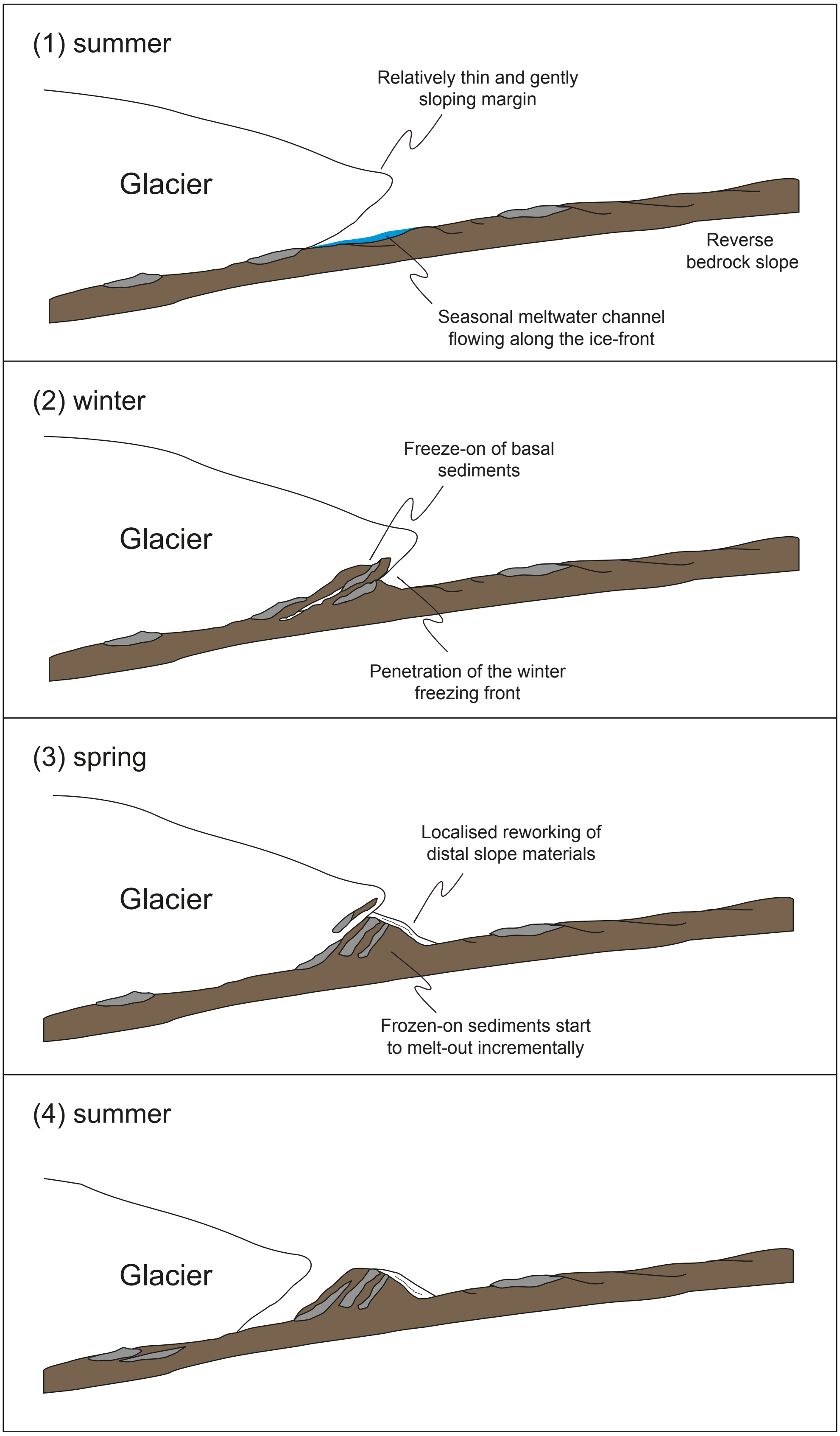

Figure 7.5: Schematic model of annual moraine genesis through emplacement of frozen-on subglacial sediment slabs, as reconstructed from a representative section (SKA-11) on the glacier foreland. For a detailed explanation see §7.1.3.

7.2 Influences on annual moraine geomorphology

Annual moraines on the foreland of Skálafellsjökull display a distinctive *sawtooth* or crenulate planform geometry, similar to that previously identified elsewhere (e.g. Andrews and Smithson, 1966; Price; 1970; Matthews *et al*., 1979; Evans and Twigg, 2002; Bradwell, 2004a; Burki *et al*., 2009). This sawtooth planform geometry has previously been interpreted as reflecting formation along a glacier snout strongly indented by closely-spaced, longitudinal crevasses, giving rise to closely spaced re-entrants or pecten (Price, 1970; Matthews *et al*., 1979; Sharp, 1984; Burki *et al*., 2009; Evans *et al*., submitted). Given that it has been established that annual moraines at Skálafellsjökull form through a range of ice-marginal genetic processes, and predominantly through push/squeeze mechanisms, it suggested that the sawtooth planform of the moraines represents the intricacies of the ice-margin. Further support for this is provided by remote sensing observations, with annual moraines appearing to closely reflect ice-margin morphology. Thus, the geomorphology of annual moraines at Skálafellsjökull is strongly influenced by structural glaciology.

Whilst the geomorphology of the annual moraines is conditioned by ice-margin morphology, it ultimately reflects the interplay of topography and structural glaciology. According to classical theory, crevasses form perpendicular to the principal tensile stress direction (Figure 7.6; Nye, 1952; Hambrey and Lawson, 2000; Benn and Evans, 2010; Cuffey and Paterson, 2010; see also Hopkins, 1844, 1862; van der Ween, 2008). Observations generally support this prevailing theory (e.g. Meier, 1960; Harper *et al*., 1998; but see Hambrey and Müller, 1978). As such, topography exerts a key control on crevasse patterns, with crevasses developing particularly in areas of extensional flow, such as in an icefall or on the outside of a bend (Hambrey and Lawson, 2000). Skálafellsjökull flows down from a high-elevation plateau, through a valley and out onto an unconfined, low-elevation coastal plain, where the glacier splays out to form a piedmont lobe. The down-ice changes in hypsometry, from a topographically-confined icefall to an unconfined foreland, result in changes in transverse tensional stress of the glacier surface layers and corresponding changes in the crevasse pattern. As the glacier flows out onto the unconfined plain there is a reduction in transverse stress, with lateral extension of the ice and longitudinal compressive flow occurring (Nye, 1952; Benn and Evans, 2010; Cuffey and Paterson, 2010). This change in the glacier stress field leads to the development of radial crevasses at the glacier snout, and hence the development of a pecten (Nye, 1952; Matthews *et al*., 1979; Burki *et al*., 2009; Benn and Evans, 2010; Cuffey and Paterson, 2010; Johnson *et al*., 2014). The distinctive sawtooth moraines at Skálafellsjökull therefore integrate the effects of both structural glaciology and topography (Figure 7.6). A similar process-form regime has been identified at Fláajökull (Evans *et al*., submitted), with sawtooth push/squeeze moraines on the foreland recording the development of strong longitudinal crevassing and concomitant well-developed ice-marginal pecten during historical glacier recession.

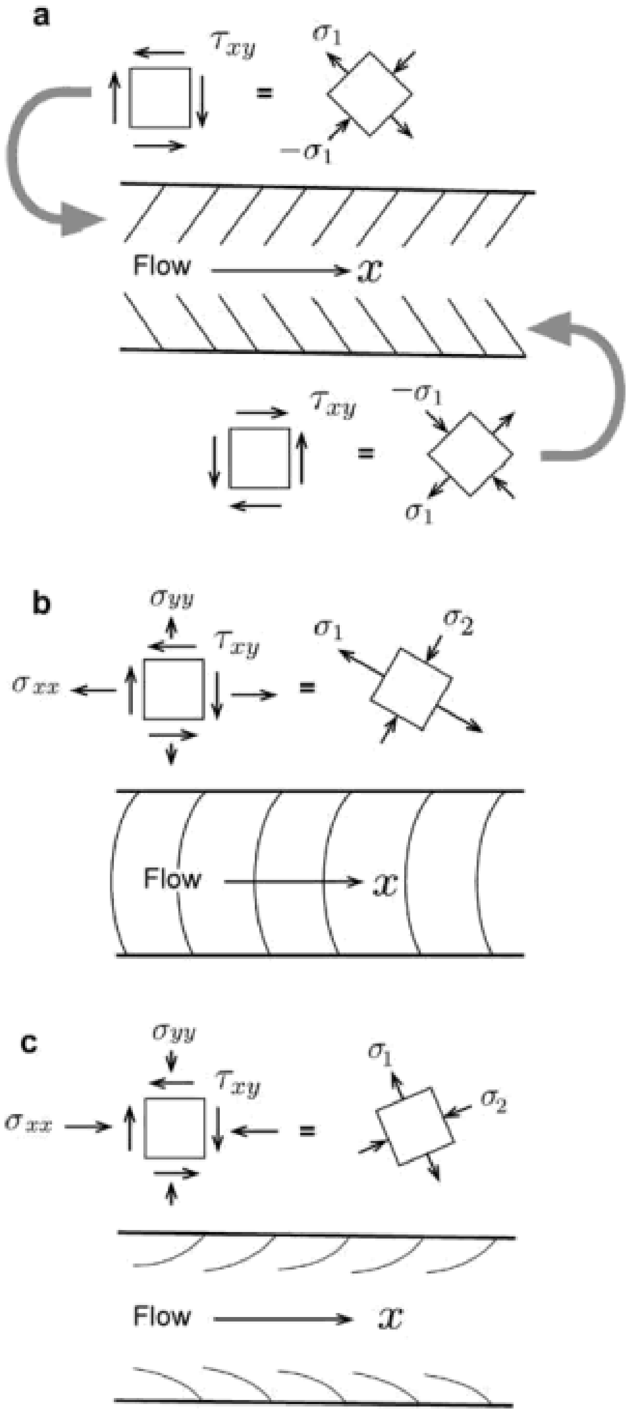

Figure 7.6: Crevasse patterns in a valley glacier. The diagrams at the top of each panel show shear stresses and normal stresses at the glacier surface near the upper margin (left) and the associated principal stresses (right). (a) Chevron crevasses resulting from lateral shear stresses at the margins. (b) Curved transverse stresses resulting from a combination of lateral shear stresses and longitudinal tensile stress (extending flow). (c) Splaying crevasses due to a combination of lateral shear stresses and longitudinal compressive stress (compressive flow). Modified from Nye (1952).

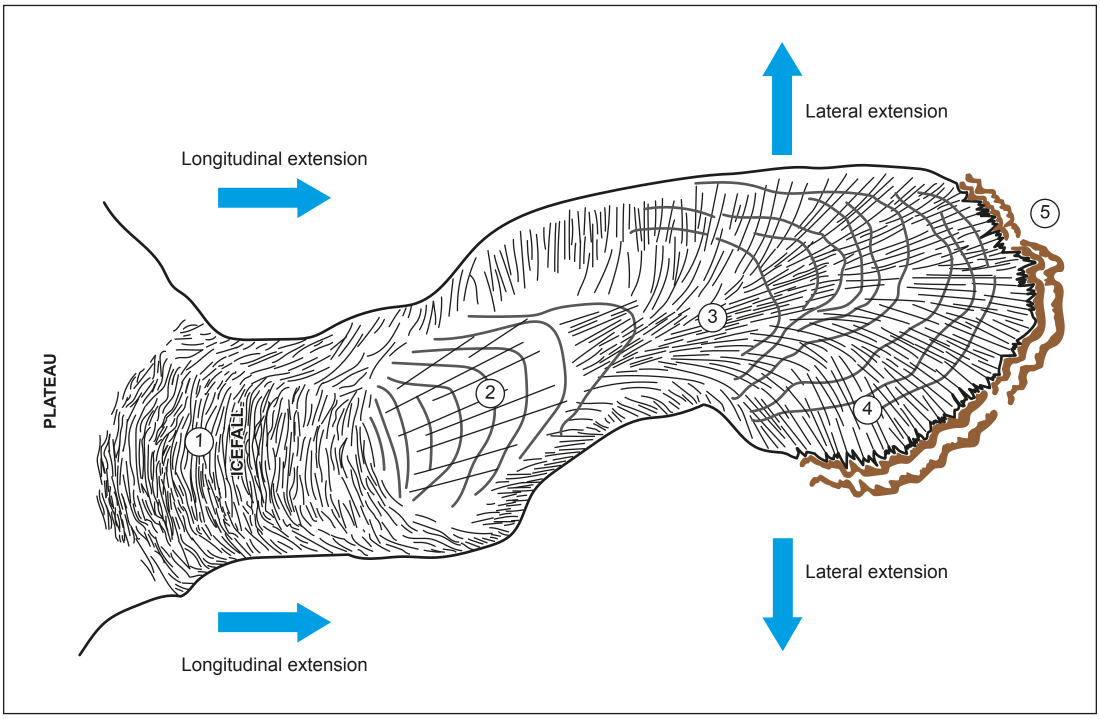

Figure 7.7: Simple schematic diagram showing an idealised piedmont outlet lobe and structures on the glacier surface. (1) Crevasses formed in longitudinal extension; (2) longitudinal compression at the foot of the icefall produces transverse foliation; (3) crevasses formed as a result of longitudinal compressive flow; (4) radial crevasses develop at the glacier snout due to lateral extension and longitudinal compressive flow; and (5) planform geometry of annual moraines, formed through a combination of squeeze and push processes, reflects the ice margin morphology and structure. Diagram not to scale.

Previously it has been demonstrated that sawtooth moraines at Bødalsbreen, southern Norway exhibit statistically significant differences in the morphological characteristics of teeth and notches (Matthews *et al.*, 1979). However, no statistically significant differences were identified in the height and width of moraines at Skálafellsjökull (see §5.1.1), despite the moraine geomorphology at both sites being strongly influenced by structural glaciology and topography (*cf.* Matthews *et al.*, 1979; Burki *et al.*, 2009). The greater height of notches at Bødalsbreen was argued to reflect the accumulation of bulldozed debris in the recesses formed by radial crevasses at the glacier snout, while the lower height of teeth was explained by debris spreading around the advancing protuberances of ice (Matthews *et al.*, 1979). This mechanism does not, however, explain the morphology of the Skálafellsjökull annual moraines. The differences between Skálafellsjökull and Bødalsbreen may reflect the following: (1) a difference in moraine genetic processes, with the Skálafellsjökull moraines predominantly being formed by bulldozing of extruded submarginal sediments (see §7.1) rather than bulldozing of proglacial material; (2) Skálafellsjökull may be a less effective bulldozer of material than Bødalsbreen; (3) differences in glacier dynamics, with Skálafellsjökull being a piedmont lobe rather than a valley glacier; and/or (4) the duration of moraine construction, with the moraines at Skálafellsjökull being formed during a single winter/spring re-advance rather than over a number of seasonal cycles. The difference in moraine genesis (1) is likely to exert a particularly important control, with the regular heights of annual moraines at Skálafellsjökull reflecting the amount of saturated subglacial sediment available for squeezing. Nonetheless, it is likely that the morphological differences reflect a combination of these intimately linked factors.

7.3 Patterns, rates and drivers of recent ice-marginal retreat

7.3.1 Patterns and rates of recent ice-marginal retreat

Annual ice-margin retreat rates (IMRRs), equivalent to annual moraine crest-to-crest spacing (*cf*. Bradwell, 2004a; Lukas, 2012), have been calculated for the periods 1936 – 1964, 1969 – 1974 and 2006 – 2011. Annual moraine spacing was calculated along representative transects through the annual moraine sequences, selected to capture the most complete sequence of ice-marginal fluctuations and avoiding areas with evidence for overriding/superimposition of moraines. The crest-to-crest spacing was extracted using *ArcMap*, providing a consistent method for the calculations. As such, IMRRs were only calculated for the period covered by remote sensing data (up to June 2012). Furthermore, IMRRs have only been calculated based on annual moraine sequences from the central and northern parts of the Skálafellsjökull, due to: (1) difficulties in ascribing dates of formation to moraines at the southeastern margin (see §5.2); and (2) the presence of a reverse bedrock slope which may control and/or modulate the rate of ice-marginal fluctuations at this part of the margin, superimposing another signal on the moraine sequence (Lukas, 2012). The IMRRs for the abovementioned periods are illustrated in Figure 7.8.

Annual moraine spacing (IMRRs) indicates that Skálafellsjökull experienced ice-marginal retreat in every year between 1936 and 1964 (average: 25.6 m a^{-1}), representing the longest sustained period of glacier recession during the ~80 year period examined. Similarly, the ice-front measurement record exhibits net glacier recession in every year during the period 1932 – 1957, with a paucity of data during the 1960s (e.g. Sigurðsson, 1998). Ice-front retreat was particularly rapid during the late 1930s and early 1940s, before a reduction of IMRR values in the latter part of the 1940s (Figure 7.8). More pronounced glacier recession again occurred during the mid-1950s, before rates of ice-margin retreat slowed in early 1960s. Remote sensing observations, based on an archive of aerial photographs, suggests Skálafellsjökull subsequently re-advanced sometime during 1964 – 1969 (see §5.2.1). The reversal in the trend of ice-marginal retreat during the 1960s appears to be a common pattern across all Icelandic non-surge-type glaciers, with many of them advancing to varying degrees during this period (*cf.* Sigurðsson and Jónsson, 1995; Sigurðsson, 1998; Sigurðsson *et al.*, 2007). A short period of annual moraine formation occurred at the northeastern margin of Skálafellsjökull between 1969 and 1974, with IMRRs averaging 9.9 m a^{-1}. Following this period, annual moraine formation ceased at the ice-margin. Remote sensing observations indicate the glacier was relatively stable between 1975 and 1989 (see §5.2.1). Unfortunately there is a lack of ice-front measurements to corroborate these observations between the 1970s and 1990s, though the record does reveal the ice-margin re-advanced in 1992, 1993 and 1995 (e.g. Sigurðsson, 1998). However, observations at other Icelandic non-surge-type glaciers indicate many of them re-advanced between the 1970s and 1990s (e.g. Sigurðsson and Jónsson, 1995; Sigurðsson, 1998; Sigurðsson *et al.*, 2007). Annual moraine formation recommenced at the northeastern Skálafellsjökull margin during winter 2005/2006, with ice-front recession continuing to the end of imagery archive (June 2012).

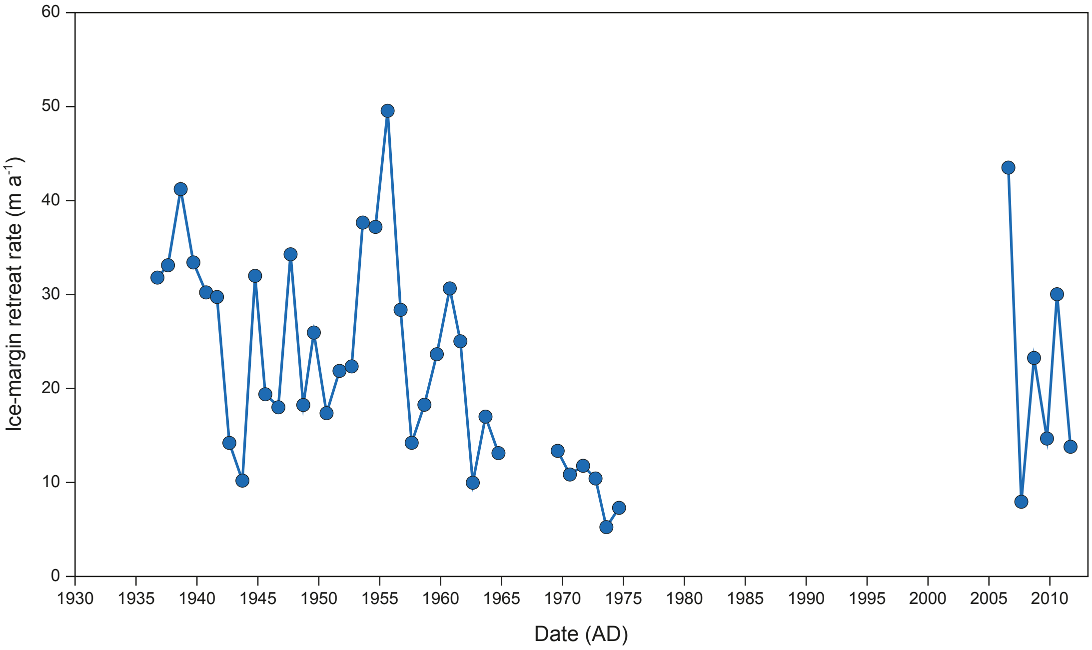

Figure 7.8: Annual ice-margin retreat rates (IMRRs) of Skálafellsjökull calculated from annual moraine crest-to-crest spacing.

Based on the calculated IMRRs two key 6-year periods (1936 – 1941 and 1951 – 1956) of ice-marginal retreat have been identified for comparison with the most recent phase of retreat (2006 – 2011). During the most recent period, the Skálafellsjökull ice margin retreated 133.7 m, with an average IMRR of ~22.3 m a^{-1} (σ = 13.0 m) and a median value of ~19.0 m a^{-1}. However, the two earlier periods identified exhibited more pronounced glacier recession. A total glacier recession distance of 200.0 m occurred between 1936 and 1941, at an average of ~33.3 m a^{-1} (median: ~32 m a^{-1}). Similarly, the period 1951 – 1956 displayed ice-marginal retreat totalling ~197 m, at an average of ~32.9 m a^{-1} (median: ~33.0 m a^{-1}). Moreover, the greatest ice-front recession in any given year occurs in 1953 (~49.7 m). In order to assess the statistical significance of the differences between these periods of glacier recession, unpaired Wilcoxon rank-sum (or Mann Whitney U) tests have been applied (Table 7.1; *cf.* Miles *et al.*, 2013). The statistical analysis indicates no statistically significant differences exist between the three key periods of ice-marginal retreat identified. Thus, glacier recession during these 6-year periods was comparable both in style and magnitude.

Table 7.1: Comparison of three prominent periods of ice-marginal retreat at Skálafellsjökull.

Period	Minimum IMRR (m a^{-1})	Maximum IMRR (m a^{-1})	Average IMRR (m a^{-1})	Wilcoxon rank-sum test		
				1936 – 1941	1951 – 1956	2006 – 2011
1936 – 1941	29.9	41.3	33.3	-	ns	ns
1951 – 1956	21.9	49.7	32.9	ns	-	ns
2006 – 2011	8.1	43.7	22.3	ns	ns	-

The calculated IMRRs for Skálafellsjökull are comparable to retreat rates calculated from annual moraine spacing at other Icelandic outlet glaciers (Bradwell, 2004a; Bradwell *et al.*, 2013). For the period 1936 – 1941, Lambatungnajökull underwent the same amount of glacier recession as Skálafellsjökull: the ice-front retreated 200 m, at an average of ~33 m a^{-1} (*cf.* Bradwell, 2004a). Meanwhile, the Falljökull ice-margin retreated a distance of 310 m during the period 1935 – 1945, at an average of ~28 m a^{-1} (Bradwell *et al.*, 2013). Comparable IMRRs were displayed by Skálafellsjökull during the 1930s and 1940s, with the ice-margin retreating 276.5 m between 1936 and 1945 (average: ~27.7 m a^{-1}). This demonstrates that the glaciers underwent similar change during the 20th Century, and is supported by ice-front measurements from all non-surge-type outlet glaciers in Iceland (*cf.* Sigurðsson *et al.*, 2007). More recently, Falljökull underwent ~230 m of recession during the period 2005 – 2011 (average: ~33 m a^{-1}), representing a significant increase in the rate of frontal retreat (Bradwell *et al.*, 2013). Conversely, the Skálafellsjökull ice-margin retreated by 133.7 m between 2006 and 2011, with other 6-year periods undergoing greater glacier recession (see above). The differences evident between Falljökull and Skálafellsjökull are likely to reflect site specific conditions, with the more rapid IMRRs and change in dynamics at Falljökull (*cf.* Bradwell *et al.*, 2013; Phillips *et al.*, 2013, 2014) a consequence of the smaller, steeper nature of the glacier and the influence of an overdeepening at the base of the icefall.

Recently, Bjørk *et al.* (2012) examined the ice-frontal behaviour of 132 outlet glaciers in SE Greenland using an inventory of aerial photographs and satellite imagery spanning 1931 – 2010. The study revealed a regional response to some external forcing mechanism, regardless of glacier type, terminal environment and size. Two pronounced recessional periods were identified in the record, occurring between 1933 and 1943, and during 2000 – 2010 (Bjørk *et al*., 2012; see also Howat *et al*., 2008; Thomas *et al*., 2009; Howat and Eddy, 2011; Mernild *et al*., 2012). Interestingly, these prominent periods of ice-front recession coincide with the periods of rapid Icelandic glacier retreat identified above (see also Bradwell, 2004a; Sigurðsson *et al*., 2007; Bradwell *et al*., 2013). This implies that glaciers in the North Atlantic region may be responding to a regional external forcing mechanism, rather than local drivers. However, it should be recognised that comparisons between Icelandic and Greenlandic outlet glaciers are somewhat complicated by differences in both size and terminal environment, with many Greenlandic glaciers terminating in a marine environment (*cf*. Bjørk *et al*., 2012). Furthermore, it has been demonstrated that the response of marine-terminating glaciers to forcing may be strongly influenced by topography and bathymetry (e.g. Howat *et al*., 2008; Thomas *et al*., 2009; Carr *et al*., 2013, 2014, in press).

7.3.2 Drivers of recent ice-marginal retreat

Previous studies which have examined ice-marginal retreat through the application of annual moraine spacing, both in Iceland and elsewhere, have demonstrated a temporal coincidence between IMRRs and air temperature anomalies (Boulton, 1986; Krüger, 1995; Bradwell, 2004a; Beedle *et al*., 2009; Bradwell *et al*., 2013). However, such studies have undertaken limited statistical treatment of other climate variables (e.g. precipitation, sea surface temperature). Presently, only two studies have examined the influence of precipitation on IMRRs calculated from annual moraine spacing (Beedle *et al*., 2009; Lukas, 2012). Furthermore, remote sensing studies of ice-frontal retreat frequently present limited statistical analysis of driving mechanisms, often restricted to visual comparisons of time-series plots (e.g. Bjørk *et al*., 2012; Carr *et al*., 2013; Miles *et al*., 2013; Stokes *et al*., 2013a). Statistical analysis of a wider array of climate variables (see Chapter 6) is presented herein, building on previous studies of annual moraine spacing (e.g. Bradwell, 2004a; Beedle *et al*., 2009; Lukas, 2012).

Visual comparison of time-series plots for IMRR and the key climate variables identified in Chapter 6 (air temperature, sea surface temperature, precipitation and the North Atlantic Oscillation) appear to show that periods of glacier recession (and annual moraine formation) are associated with elevated air temperature and sea surface temperature (Figure 7.9). This is particularly apparent in the late 1930s and early 1940s, when IMRRs of ~33 m a^{-1} were associated with ambient air temperature (AAT) anomalies averaging +0.65 °C between 1936 and 1941. Meanwhile, the most recent period of glacier recession (2006 – 2011), is associated with average AAT and sea surface temperature (SST) anomalies of +0.91 °C and +0.85 °C, respectively. Conversely, periods where no annual moraines formed coincide with pronounced phases of negative (1977 – 1981) and positive (1989 – 1994) annual NAO index values. The period of marked positive NAO (average: +2.42) is believed to correspond with a period of re-advance at Skálafellsjökull (e.g. Sigurðsson, 1998).

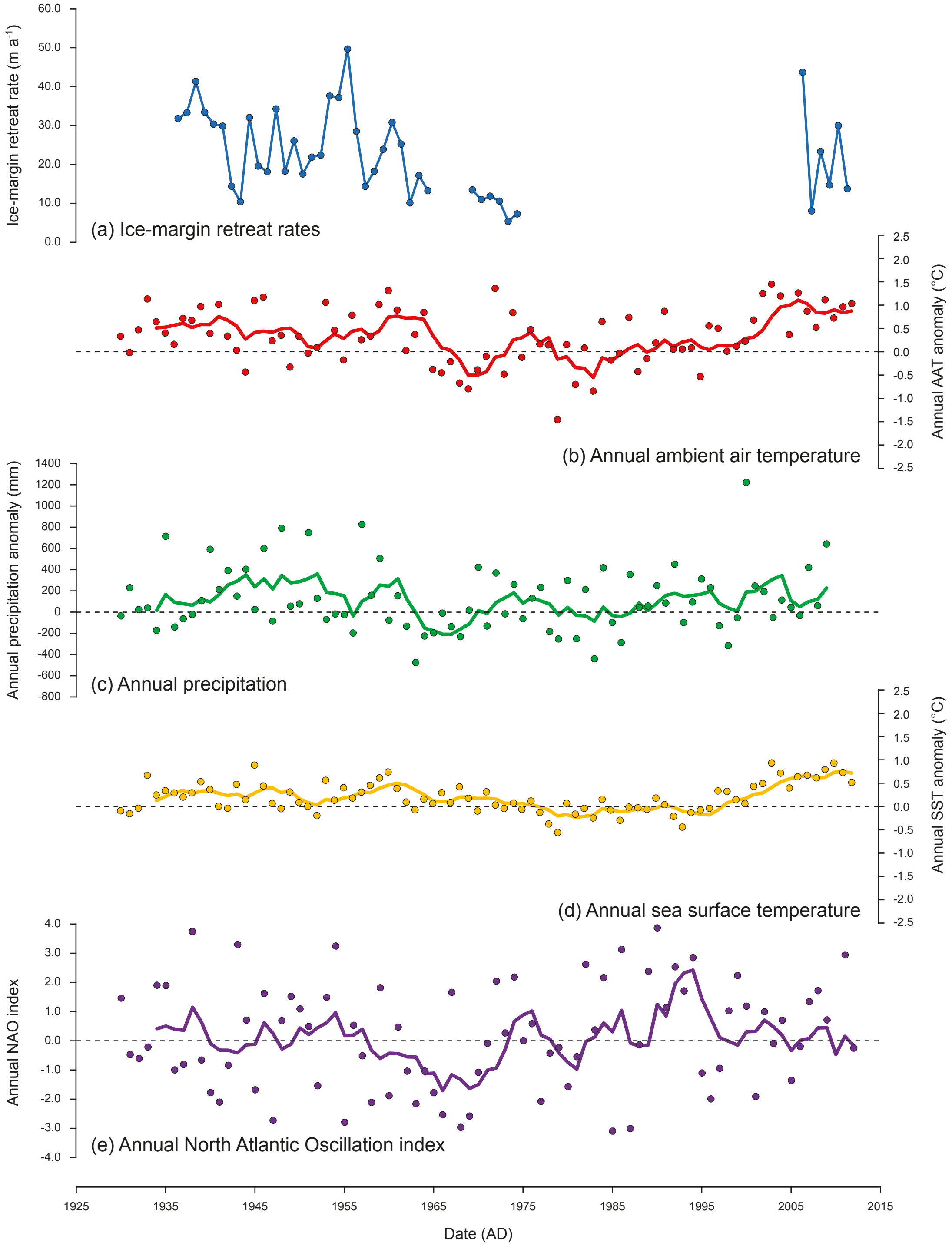

Figure 7.9: Annual ice-margin retreat rates (IMRRs) at Skálafellsjökull (a) compared with inter-annual variability in key climate variables. Solid lines in (b) – (e) show 5-year moving averages. Climate variables in (b) – (d) are reported as deviations from the respective 1961 – 1990 averages.

Icelandic glaciers are thought to be particularly sensitive to variations in summer temperature (e.g. Bradwell, 2004a; Sigurðsson *et al*., 2007; Bradwell *et al*., 2013), whilst accumulation season (winter) precipitation and NAO are believed to be important controls on glacier mass balance in the wider North Atlantic region (e.g. Nesje *et al*., 2000; Laumann and Nesje, 2009; Winkler *et al*., 2009; Marzeion and Nesje, 2012; Mernild *et al*., 2014). Furthermore, it has been established that annual moraines at Skálafellsjökull are formed during the course of a winter re-advance. Thus, winter anomalies in the aforementioned climate variables could have an important influence on the magnitude of the winter re-advance and annual moraine formation, which will in turn partly influence the moraine record. Given the potential importance of these seasonal signals, further detailed comparison of the winter and summer seasonal climate signatures with IMRRs will be undertaken herein. Covariance analysis of the spring and autumn signatures indicated no statistically significant relationships existed between any of the abovementioned climate variables and IMRRs. As such, the winter and summer signatures are the principal focus of this section and are discussed in further detail below.

Although periods of ice-frontal retreat appear to be associated with periods of elevated AAT, a covariance plot of annual AAT anomalies and IMRRs appears to show no visual correlation (Figure 7.10a). This is confirmed by least squares regression analysis, with there being no statistically significant correlation between the data (r^2 = 0.0262, p = 0.3119). Similarly, covariance analysis of winter AAT anomalies and IMRRs (Figure 7.10b) shows no statistically significant relationship between the two variables (r^2 = 0.0242, p = 0.3340). However, comparison of summer AAT anomalies and IMRRs shows a visual positive correlation (Figure 7.10c). Moreover, least squares regression analysis reveals the regression line is a very highly statistically significant fit to the data (r^2 = 0.3464, $p < 0.0001$). This data implies that summer AAT variability may exert an important control on ice-frontal retreat at Skálafellsjökull. Furthermore, the temporal coincidence of summer AAT anomalies and IMRRs suggests that the glacier may have a very rapid *reaction time* (*cf*. Sigurðsson *et al*., 2007; Benn and Evans, 2010; Bradwell *et al*., 2013), reacting to summer AAT fluctuations at a sub-annual timescale (*cf*. Bradwell *et al*., 2013).

A similar pattern is observed from the covariance plots of SST anomalies and IMRRs (Figure 7.11). As with the AAT anomalies, no statistically significant relationships were established for IMRRs and the annual (r^2 = 0.0433, p = 0.8378, Figure 7.11a) and winter (r^2 = 0.0012, p = 0.8300, Figure 7.11b) signals. However, linear regression analysis identified a very highly statistically significant relationship between summer SST anomalies and IMRRs (r^2 = 0.1623, p = 0.0010, Figure 7.11c). Nevertheless, the relatively low coefficient of determination

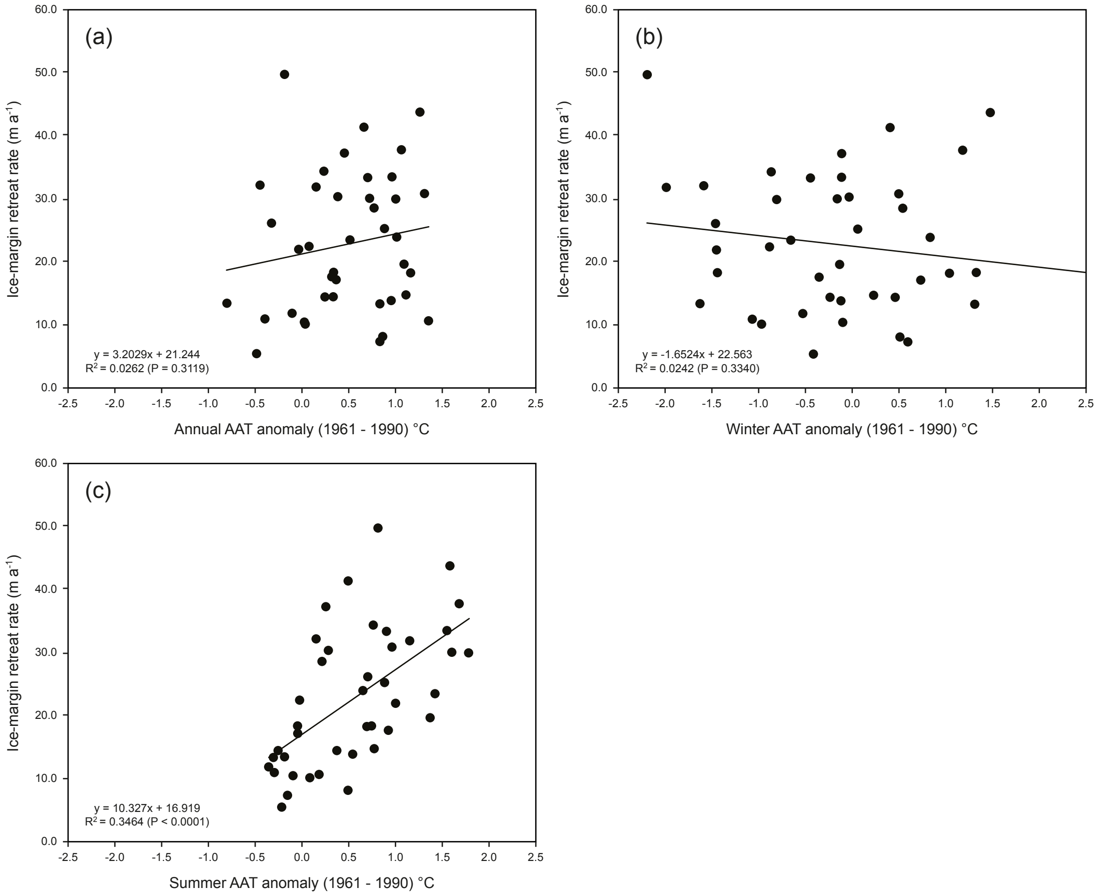

Figure 7.10: Covariance plots of seasonal variations in ambient air temperature (AAT) and annual ice-margin retreat rates (IMRRs). AAT values are expressed as deviations from the 1961 – 1990 average at Hólar í Hornafirði.

indicates a somewhat weak relationship. Thus, summer SST variability may influence IMRRs at Skálafellsjökull to some extent, but to a lesser degree than fluctuations in summer AAT appear to (Figure 7.10c).

In contrast to AAT and SST anomalies, no apparent relationships were evident between deviations in the seasonal average precipitation values and IMRRs (Figure 7.12). Furthermore, linear regression analysis indicates no statistically significant relationships in all cases ($p > 0.05$), with r^2 values ranging between 0.0004 and 0.0552. Thus, the analysis conducted in this study implies precipitation is not an important factor influencing ice-frontal retreat at an inter-annual timescale. To some extent this is not entirely unexpected, as Icelandic precipitation values have shown no apparent trend during the observational period (e.g. Sigurðsson and Jónsson, 1995; Hanna *et al.*, 2004). Moreover, the annual moraines at Skálafellsjökull reflect seasonally-driven submarginal processes active in a given year, such as a spring/summer increase in melt/porewater pressures in the subglacial sediments and winter re-advance due to reduced melting in the ablation zone (*cf.* Price, 1970; Sharp, 1984; Evans and Twigg, 2002; Evans and Hiemstra, 2005). Indeed, annual moraines should more appropriately be referred to

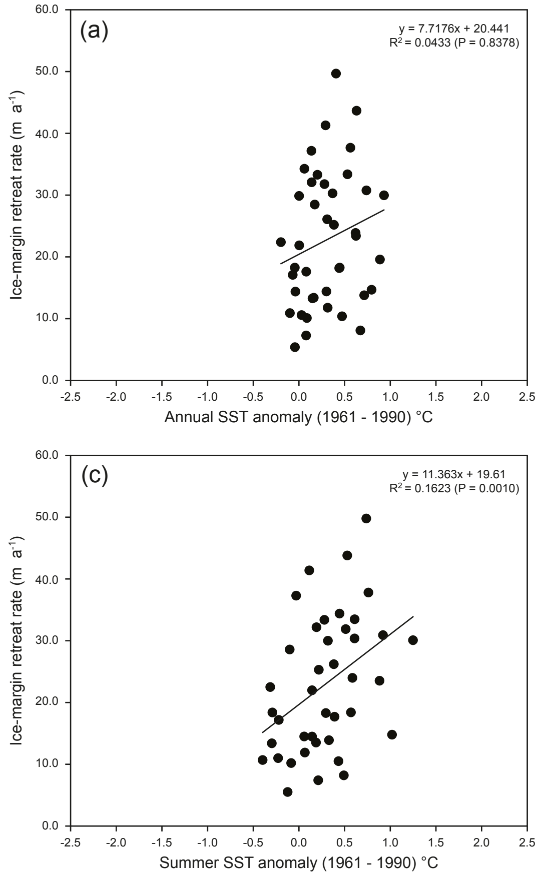

Figure 7.11: Covariance plots of seasonal variations in sea surface temperature (SST) and annual ice-margin retreat rates (IMRRs). SST anomalies are based on the average of values in a grid array covering latitudes 57.5 – 67.5°N and longitudes 7.5 – 17.5°W. Values from 1945 are excluded from the data analysis owing to a lack of SST data. SST data has been extracted from the HadSST2 dataset (Rayner *et al.*, 2006).

as *seasonal process-form regimes*. As such, processes in the accumulation zone (influence of precipitation) do not directly impact moraine construction and are, therefore, not reflected in the annual/seasonal signal recorded by the moraines.

Finally, covariance analysis of variations in average NAO index values and IMRRs reveal patterns similar to those previously described for AAT and SST anomalies (Figure 7.13). No statistically significant relationships were evident between IMRRs and the annual ($r^2 = 0.0011$, $p = 0.8378$, Figure 7.13a) and winter ($r^2 = 0.0633$, $p = 0.1125$, Figure 7.13b) signals. In contrast, linear regression analysis established a highly statistically significant relationship between average summer NAO index values and IMRRs ($r^2 = 0.1310$, $p = 0.0201$, Figure 7.13c). This statistical analysis suggests that summer variations in the NAO may exert a limited influence on ice-marginal retreat Skálafellsjökull, though the relationship is somewhat weak.

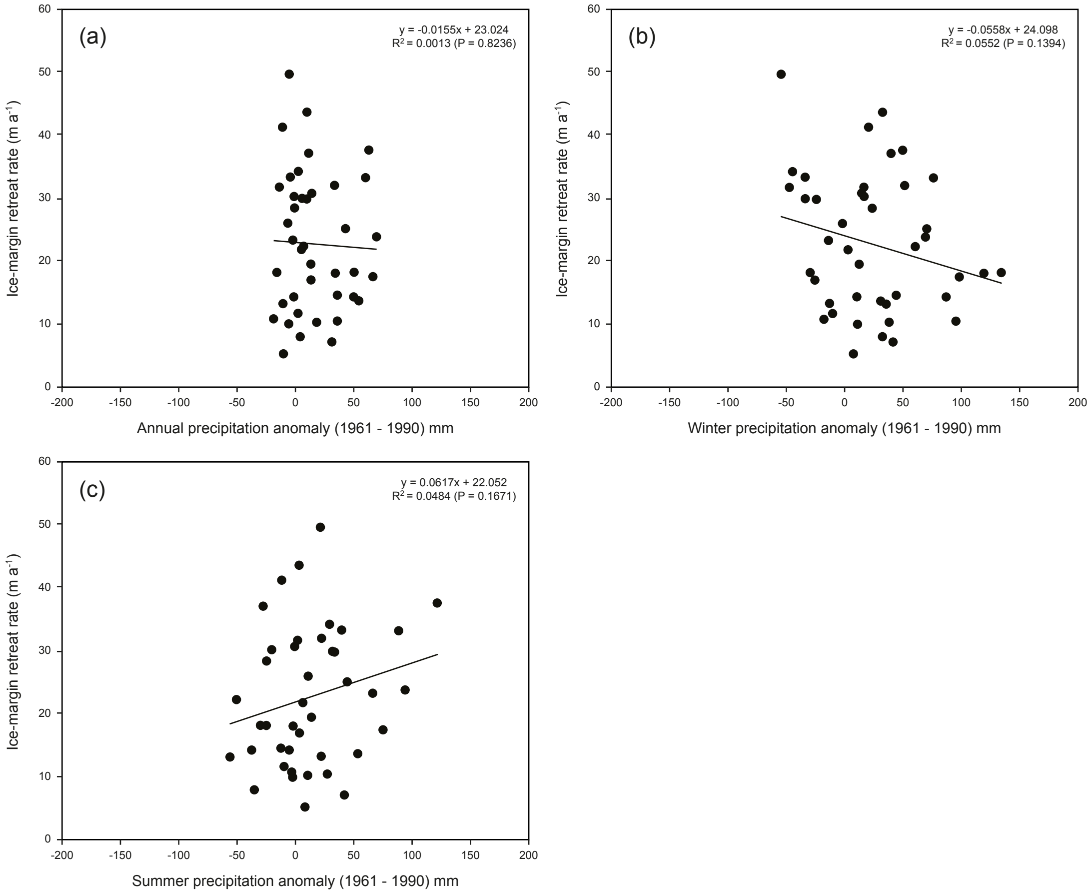

Figure 7.12: Covariance plots of seasonal variations in average precipitation anomalies and annual ice-margin retreat rates (IMRRs). Precipitation values are expressed as deviations from the 1961 – 1990 average at Hólar í Hornafirði. Note that precipitation anomalies are based on monthly averages rather total precipitation.

Based on the analysis presented herein, it appears that Skálafellsjökull is most sensitive to inter-annual variations in summer AAT. This finding is in accordance with previous studies of Icelandic glaciers (e.g. Boulton, 1986; Krüger, 1995; Bradwell, 2004a; Sigurðsson *et al.*, 2007; Bradwell *et al.*, 2013). Variability in summer SST and the NAO also appear to have some influence on IMRRs, though to a lesser degree. Statistically significant relationships between SST and Icelandic termini variations have not hitherto been identified, though it has been identified as a driver of glacier change in SE Greenland (Bjørk *et al.*, 2012). Interestingly, the positive correlation identified between summer NAO and IMRRs is the opposite of that demonstrated in Norway (Nesje *et al.*, 2000), where positive NAO leads to overall increase in glacier mass. This is in agreement with general comparisons presented by Bradwell *et al.* (2006) from elsewhere in SE Iceland.

Although statistically significant relationships have been identified, it should be recognised that SE Iceland climate is highly complex. As demonstrated in Chapter 6, the atmospheric and oceanic climate variables are intimately linked, with AAT in particular appearing to be

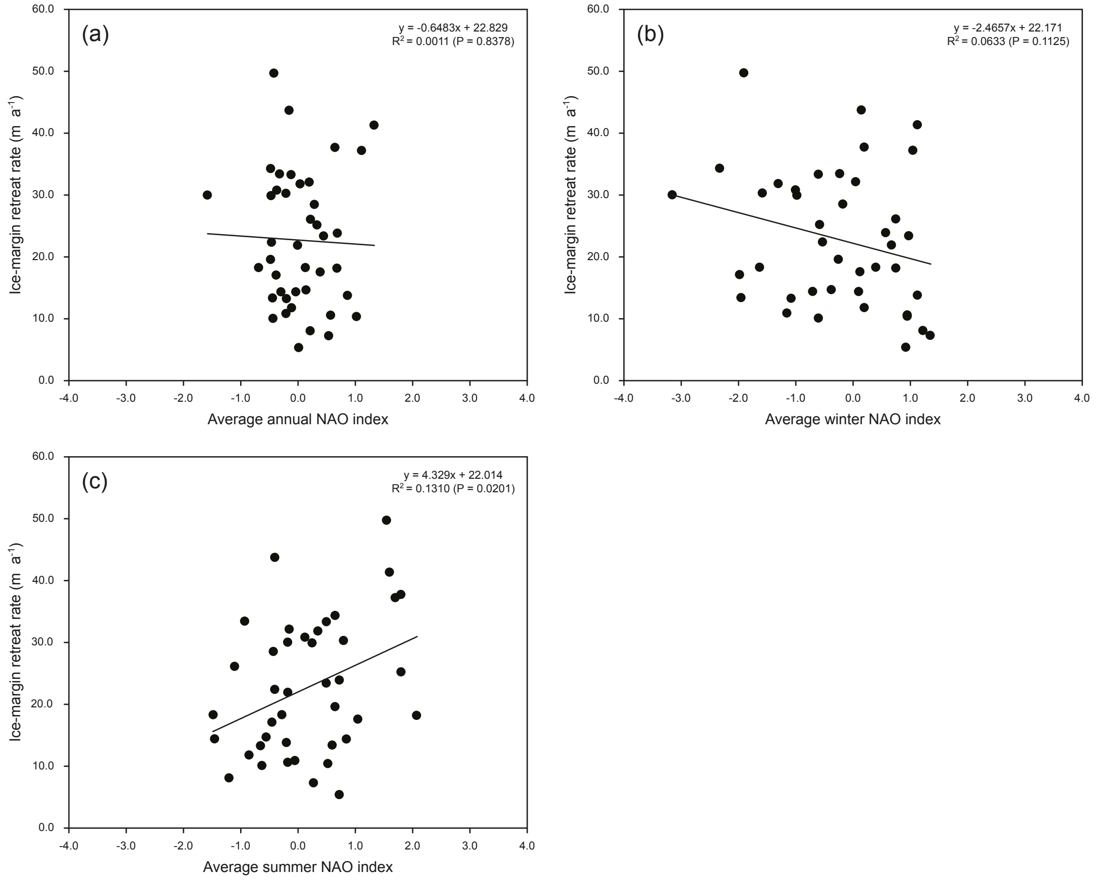

Figure 7.13: Covariance plots of seasonal variations in average North Atlantic Oscillation (NAO) index values and annual ice-margin retreat rates (IMRRs). NAO index values were obtained from the station-based Hurrell NAO database (Hurrell and NCAR Staff, 2014).

strongly influenced by SST at an inter-annual timescale (see §6.2.1). Consequently, it may be difficult to unravel the influence of individual climate variables on ice-frontal variations. For example, the AAT signal may include inherent SST and NAO signals. Conversely, the lack of a strong correlation between the NAO and IMRRs may be a reflection of the importance of seasonal temperature variations and ablation season duration, over winter precipitation, in controlling glacier change in SE Iceland (Ahlmann and Thórarinsson, 1937; Johannesson, 1997; Bradwell *et al*., 2006). In addition to these interactions, there may be underlying longer-term (decadal to multi-decadal) climate signals, with multiple periodicities reinforcing or modulating each other. As such, unravelling the composite climate signal recorded in the Skálafellsjökull moraine record, and establishing the principal drivers of ice-marginal retreat, is not entirely straightforward (*cf.* Kirkbride and Brazier, 1998; Kirkbride and Winkler, 2012, and references therein). Further potential confounding factors in extracting a climate signal from the annual moraine record at Skálafellsjökull relate to internal glacier dynamics, structural glaciology and the presence of the reverse bedrock slope in the southern part of the foreland, which are difficult to quantify. On the basis of remote sensing observations, the southeastern ice-margin retreated up to ~240 m during 2006 – 2011, compared with 134 m of glacier recession calculated from the moraine record. Thus, the reverse bedrock slope appears to have some influence on glacier response to external forcing, but it is difficult to establish how this topographic factor influences ice-marginal response as a whole.

Although there are potential difficulties in distinguishing between both internal and external drivers of ice-marginal retreat at Skálafellsjökull, the coincidence of periods of pronounced glacier recession at the study site with those at glaciers across Iceland (e.g. Sigurðsson, 1998; Bradwell, 2004a; Sigurðsson *et al*., 2007; Bradwell *et al*., 2013) implies glacier change forced by a common, regional mechanism. Furthermore, annual moraine spacing (IMRRs) and ice-front measurements have been shown to correspond to periods of elevated summer temperature elsewhere in Iceland (Boulton, 1986; Krüger, 1995; Sigurðsson and Jónsson, 1995; Bradwell, 2004a; Sigurðsson *et al*., 2007; Bradwell *et al*., 2013). Thus, despite the aforementioned issues, summer AAT variability is considered an important driver of IMRRs at Skálafellsjökull. Moreover, the coincidence of the periods of Icelandic glacier recession and pronounced Greenlandic ice-frontal retreat (*cf*. Bjørk *et al*., 2012) suggests there may be a common mechanism in the North Atlantic region. It is hypothesised that the mutual driver could be SST variability, with SSTs driving AAT change, which in turn forces IMRRs. Evidence which appears to support a link between SSTs and AATs was presented in Chapter 6 (see §6.2.1). It does, however, seem unlikely that there is a direct link between SST variability and IMRRs at Skálafellsjökull given the low coefficient of determination ($r^2 = 0.1623$, $p = 0.0010$).

Since the mid-1990s the upper 1,000 m of the subpolar North Atlantic has undergone unprecedented warming, in the context of the instrumental record (*cf*. Häkkinen *et al*., 2013; Straneo and Heimbach, 2013; Williams *et al*., 2014; Barrier *et al*., 2015, and references therein). During the measurement period, comparable warming only occurred during the 1930s (*cf*. Polyakov *et al*., 2005; Reverdin, 2010; Andresen *et al*., 2012). This warming of the subpolar North Atlantic has been associated with a weakening and shrinking of the subpolar gyre (Häkkinen and Rhines, 2004; Hátún *et al*., 2005; Lohmann *et al*., 2008; Bersch *et al*., 2007; Robson *et al*., 2012). Weakening of the North Atlantic subpolar gyre to the west of the Reykjanes Ridge (the western subpolar gyre) is believed to be a decadal, baroclinic ocean response to positive NAO conditions from 1988 to 1995 (see §6.1.3; Barrier *et al*., 2015). Meanwhile, concomitant changes in the eastern sub-region were induced by an inter-annual, barotropic adjustment of the gyre circulation to an abrupt switch from positive NAO conditions in winter 1995 to negative NAO conditions in winter 1996 (see §6.1.3; Barrier *et al*., 2015). Thus, this atmospheric-driven weakening of the subpolar gyre may ultimately be the driving mechanism of recent ice-marginal retreat in the North Atlantic region, and has previously been implicated in forcing contemporary Greenlandic glacier change (Straneo and Heimbach, 2013). Nevertheless, further evidence from Icelandic glaciers is required to test the links between SST, AAT and IMRRs.

Based on the climate variables analysed in this study and the associated r^2 values, a sensitivity ranking has been developed for Skálafellsjökull (Table 7.2) which could be applied in the examination of ice-frontal retreat at other Icelandic glaciers. The variables with the highest ranking could be tested initially, before further statistical analysis is undertaken. Applying similar approaches to those used in this study, which integrates multiple methods at a range of spatial and temporal scales, combined with a systematic approach to IMRR analysis at other Icelandic glaciers would provide valuable data to test the hypothesis that glacier fluctuations in the North Atlantic region are driven by a common forcing mechanism.

Table 7.2: Sensitivity ranking for Skálafellsjökull, SE Iceland. The ranking is based on the r^2 values for each of the linear regression models.

Climate variable	Annual		Spring		Summer		Autumn		Winter	
	r^2 value	Rank	r^2 value	Rank	r^2 value	Rank	r^2 value	Rank	r^2 value	Rank
AAT	0.0262	11	0.0024	14	0.3464	1	0.0284	10	0.0242	12
Precipitation	0.0013	17	0.0004	20	0.0484	6	0.0014	16	0.0552	5
SST	0.0433	8	0.0177	13	0.1623	2	0.0355	9	0.0012	18
NAO	0.0011	19	0.0452	7	0.1310	3	0.0018	15	0.0633	4

7.4 Applicability of annual moraines as climate indicators

This study has applied annual moraines to examine patterns, rates and drivers at Skálafellsjökull, building on the work of previous studies which have employed annual moraines, and expanded the range of climate variables analysed (*cf*. Boulton, 1986; Krüger, 1995; Bradwell, 2004a; Beedle *et al*., 2009; Lukas, 2012; Bradwell *et al*., 2013). It is, however, worth considering the concept of "annual" moraines and their wider applicability as climatic indicators. Important issues which may affect the climatic integrity and chronological robustness (*sensu* Kirkbride and Winkler, 2012) of the moraine sequences are considered below.

A principal issue with utilising "annual" moraines to examine IMRRs and extract climate signals is establishing a chronological framework for these geomorphological features. Previous studies have employed lichenometric dating to establish the timing of moraine abandonment (e.g. Bradwell, 2004a; Bradwell *et al*., 2013), whilst many accept the features as "annual" moraines without chronological data (e.g. Beedle *et al*., 2009; Lukas, 2012;

Reinardy *et al*., 2013). In this study, moraine chronology was examined through the integration of remote sensing observations, ice-front measurements and lichenometry (see §5.2; Bradwell *et al*., 2013). This approach is effective where the data from each of these techniques overlaps, and particularly during time periods with a high frequency of imagery. However, problems may arise when attempting to establish the date of formation for moraines older than the earliest aerial photograph. Lichenometric dating at Skálafellsjökull focused on a subset of the minor moraines on the foreland (*cf*. Bradwell, 2004a; Bradwell *et al*., 2013), some of which were known to have formed prior to the earliest aerial photograph (1945). For this sequence of 15 minor moraines, a range of dates spanning 1920 – 1965 (i.e. 46 years) were obtained based on the lichenometric dating curves employed in this study (see §5.2.2). Considering only the Bradwell (2001a, b) *age-size* dating curve, which has been employed in recent studies of purported annual moraines in Iceland, yields a range of values spanning 1933 – 1965 (i.e. 33 years). Based on cross-correlation with the imagery archive, combined with observations from the rest of the foreland, annual formation was ascribed to this sequence with reasonable confidence. However, the range of dates presents a potential issue and may influence the analysis of patterns, rates and drivers of ice-marginal retreat. Examination of ice-frontal fluctuations (and annual moraines) in Iceland benefits from the availability of a vast inventory of historical maps and documents, imagery and ice-front measurements (*cf*. Thórarinsson, 1943; Boulton, 1986; Bradwell, 2004a; Sigurðsson, 2005; Sigurðsson *et al*., 2007; Bradwell *et al*., 2013; Hannesdóttir *et al*., 2014, and references therein). Elsewhere such data may not be available, presenting a potential problem when attempting to establish a chronological framework for annual moraines: even the most well-calibrated lichenometric dating has an optimum precision of only 5 – 10% (Innes, 1988; Noller and Locke, 2000).

Further complicating attempts to establish the chronology of purported annual moraines is the possibility that moraines may form on a sub-annual basis. At Skálafellsjökull it has been established that minor moraines are forming on a sub-annual timescale in the southern part of the glacier foreland, with multiple moraines forming per year during the period 2006 – 2011 (see §5.2.1). This implies that *annual moraine couplets* may be a more appropriate classification in some instances. It is suggested that annual moraine couplets may form where submarginal seasonal processes are recorded as dual moraines, rather than a single composite squeeze/push moraine (*cf*. Evans and Hiemstra, 2005). The recognition of annual moraine couplets challenges the concept of "annual" moraines, and brings into question whether moraines elsewhere on the foreland are truly formed annually. Even where the number of moraines formed in a given time period is equivalent to the time elapsed, some of these features may have formed in the same year, whilst no winter re-advance moraine was formed in the previous/subsequent year. Evidently, this would introduce errors into the calculations of IMRRs and the subsequent analysis of driving mechanisms. Without the availability of remotely-sensed data at numerous intervals throughout each year during the period of minor moraine formation, it is difficult to establish definitively whether or not these features are annual moraines.

It has previously been argued that annual moraine sequences in the geological record, once identified, could be employed to extract high-resolution palaeoclimatic information (Bradwell, 2004a). However, given the difficulties in establishing the chronology of "annual" moraines formed during historical times, it seems highly unlikely that moraines could be identified as "annual" features in the geological record and subsequently used to make palaeoclimatic inferences. Indeed, the range of geochronological techniques typically employed in a palaeoglaciological context are frequently associated with substantial errors (e.g. Lukas *et al*., 2007; Fuchs and Owen, 2008; Balco, 2011, Ballantyne, 2012; Small *et al*., 2012) and age estimates may contradict the geomorphological evidence (e.g. Boston *et al*., 2013, 2015; *cf*. Gheorghiu *et al*., 2012; Gheorghiu and Fabel, 2013). The resolution and errors associated with these geochronological techniques would preclude the dating of "annual" moraines. In addition to the difficulties in providing chronological constraint, "annual" moraines typically have a low preservation potential and are often situated in some of the most inimical proglacial environments for moraine preservation (Kirkbride and Winkler, 2012; Bradwell *et al*., 2013). Given these potential issues, it is argued here that it is unlikely "annual" moraines could reliably be employed in a high resolution palaeoclimatic context (*cf*. Boulton, 1986; Krüger, 1995).

Aside from issues relating to the chronological robustness of "annual" moraine sequences, there are other factors that may affect the integrity of the sequences and in turn introduce errors in analysis of IMRRs. In particular, eradication of the sediment-landform evidence (erosional censoring) may occur, reducing the climatic representativeness of the annual moraine record (*cf*. Gibbons *et al*., 1984; Kirkbride and Brazier, 1998; Kirkbride and Winkler, 2012; Barr and Lovell, 2014). Both self-censoring and external censoring processes (*sensu* Kirkbride and Winkler, 2012) are important in the context of annual moraine sequences. At Skálafellsjökull, evidence of obliterative overlap (*sensu* Kirkbride and Winkler, 2012) has been identified, with localised glacier overriding and superimposition of moraines (see also Sharp, 1984; Evans and Orton, 2014). Whilst attempts have been made to utilise representative transects with no evidence of obliterative overlap in the calculation of IMRRs, the variable behaviour along the ice-front may have introduced errors and bias into the analysis of patterns, rates and drivers of ice-marginal retreat. Obliterative overlap has also been identified in other ostensible "annual" moraine sequences (e.g. Price, 1970; Evans and Twigg, 2002) and could introduce uncertainties in the examination of IMRRs using annual moraine spacing elsewhere. Self-censoring of the moraine record may also occur through melting of debris-covered ice in ice-cored moraines (*cf*. Schomacker and Kjær, 2007, 2008; Schomacker, 2008; Lukas, 2011; Kirkbride and Winkler, 2012, and references therein). Ice-cored moraines have hitherto been identified at Skálafellsjökull (*cf*. Sharp, 1984) and may have affected the integrity of the moraine sequence. Elsewhere, the presence of buried ice within moraines is thought to be an important factor influencing annual moraine preservation (e.g. Andersen and Sollid, 1971; Lukas, 2012; Reinardy *et al*., 2013). The prominence of glaciofluvial activity in active temperate glacial landsystems (*cf*. Evans and Twigg, 2002; Evans, 2003a, 2005; Evans and Orton, 2014) also means that annual moraines are located in some of the most unfavourable proglacial environments for moraine preservation, with annual moraine sequences subject to external censoring by glaciofluvial processes. The efficacy of these self-censoring and external censoring processes can have important implications for the integrity of annual moraine sequences and, consequently, their climatic representativeness.

Despite the highlighted issues and the difficulties in quantifying the effects of internal glacial dynamics, annual moraine sequences do afford a valuable tool for examining ice-frontal retreat in contemporary glacial environments (*cf*. Bradwell, 2004a; Beedle *et al*., 2009; Lukas, 2012; Bradwell *et al*., 2013). Provided that issues relating to the integrity of the sequences can be minimised, and annual formation can confidently be ascribed, “annual” moraines can provide valuable insights into patterns, rates and drivers of ice-marginal retreat. Whilst the statistical approaches employed in this study are relatively simplistic, caution should be attached to applying more complex analyses (e.g. multivariate analysis or spectral analysis). Given the issues highlighted, introducing greater complexity to the analysis may be extending annual moraine archives beyond their limitations.

7.5 Summary

This chapter synthesised the data presented in Chapters 5 and 6, and provided discussion of the main findings of this research. Based on the sediment composition and structure of the annual moraines on the Skálafellsjökull foreland, the following categories of moraine-forming processes have been distinguished: (1) submarginal deformation and subsequent bulldozing of the extruded sediments; (2) efficient bulldozing of pre-existing proglacial material; and (3) emplacement of frozen-on submarginal sediment slabs. This range of genetic processes is similar to that previously identified at other Icelandic outlet glaciers (Price, 1970; Sharp, 1984; Krüger, 1993, 1994, 1995, 1996; Evans and Twigg, 2002; Evans and Hiemstra, 2005). Topographic, glaciological and climatic factors play an important role in these moraine-forming processes, with the presence of a reverse bedrock slope in the southern part of the foreland having a particularly important influence. The characteristic *sawtooth* planform geometry of annual moraines at Skálafellsjökull is argued to reflect the interplay of glaciological and topographic factors (*cf.* Price, 1970; Matthews *et al.*, 1979; Sharp, 1984; Burki *et al.*, 2009). The development radial crevasses and a pecten at the glacier snout reflect topographically induced down-ice changes in the stress field (*cf.* Nye, 1952; Benn and Evans, 2010; Cuffey and Paterson, 2010). The formation of annual moraines through push/squeeze processes results in the inheritance of this pecten in their planform.

Calculation of annual ice-margin retreat rates (IMRRs) for periods of known annual moraine formation indicates Skálafellsjökull experienced ice-frontal retreat in every year between 1936 and 1964 (average: 25.6 m a^{-1}). Subsequently, a short period of annual moraine formation occurred at the northeastern margin of Skálafellsjökull between 1969 and 1974, with IMRRs averaging 9.9 m a^{-1}. During the most recent period (2006 – 2011), the ice margin retreated 133.7 m (average: ~22.3 m a^{-1}). Comparison of the record of IMRRs at Skálafellsjökull with other Icelandic glaciers shows that the timing and rate of glacier recession was similar across Iceland (*cf.* Bradwell, 2004a; Sigurðsson *et al.*, 2007; Bradwell *et al.*, 2013, and references therein). Furthermore, the pronounced periods of ice-frontal retreat at Skálafellsjökull coincide with those of Greenlandic outlet glaciers (*cf.* Bjørk *et al.*, 2012).

On the basis of covariance analysis, summer variations in ambient air temperature (AAT), sea surface temperature (SST) and the North Atlantic Oscillation (NAO) are thought to have an important influence on IMRRs at Skálafellsjökull. The glacier appears most sensitive to summer temperature variability, with the temporal coincidence of IMRRs and summer temperature anomalies implying rapid reaction times (*cf.* Bradwell *et al.*, 2013). It is hypothesised that SST variability in the North Atlantic region may be forcing AAT, which in turn drives IMRRs. The variations in SST may reflect subpolar gyre dynamics, with warming in the North Atlantic since the mid-1990s resulting from a weakening of the subpolar gyre (*cf.* Häkkinen and Rhines, 2004; Hátún *et al.*, 2005; Lohmann *et al.*, 2008; Bersch *et al.*, 2007; Robson *et al.*, 2012; Häkkinen *et al.*, 2013). However, a range of potential confounding factors have been discussed that complicate the relationship between IMRRs and climate. In particular, the recognition that minor moraines on the Skálafellsjökull foreland may form as *annual moraine couplets*, rather a single, composite annual moraine, introduces uncertainty in the IMRR calculations. As such, caution should be attached to these interpretations.

CHAPTER 8

Conclusions

This research aimed to use the characteristics of recessional ("annual") moraines and complementary climate data to arrive at a holistic understanding of recent patterns and rates of ice-marginal retreat at Skálafellsjökull, wherein the potential factors controlling ice-marginal fluctuations were assessed. In order to meet this overarching aim, a variety of techniques incorporating different spatial and temporal scales have been integrated, including remote sensing and GIS, field-based geomorphological investigations, sedimentology and lichenometry. Additionally, these approaches have been combined with statistical analysis of instrumental data. The following section summarises the main findings of this thesis, and explores the following themes: (1) production of geomorphological maps and examination of moraine geomorphology; (2) establishment of a moraine chronology at Skálafellsjökull; (3) development of conceptual models of annual moraine formation; (4) patterns, rates and drivers of recent ice-marginal retreat at Skálafellsjökull; and (5) limitations and applicability of annual moraines as climatic indicators. Scope for further research is subsequently discussed in Section 8.2.

8.1 Conclusions

(1) Production of geomorphological maps and examination of moraine geomorphology

Summary

Geomorphological mapping in this study, through a combination of desk- and field-based mapping, has resulted in the production of detailed, high-resolution glacial geomorphological maps showing the distribution of annual moraines and associated geomorphological features on the Skálafellsjökull foreland (Appendix I and II). Moreover, the desk-based mapping integrated remotely-sensed data (aerial photographs, satellite imagery and Digital Elevation Models) spanning a range of spatial and temporal scales, allowing examination of glacier foreland evolution. The geomorphological mapping conducted in this study builds on the previous small-scale landsystem mapping undertaken by Evans and Orton (2014).

The geomorphological mapping and associated field investigations revealed a series of *minor moraines* on the Skálafellsjökull foreland, with long sequences of moraines occurring on the northern and central parts of the glacier foreland. These minor moraines display distinctive *sawtooth* or crenulate planform geometries (*cf*. Price, 1970; Matthews *et al*., 1979; Bradwell, 2004a; Burki *et al*., 2009). Complexities in the general pattern occur locally, with individual moraines exhibiting bifurcations and cross-cutting patterns. Morphometric analyses of the mapped minor moraines indicated that they typically comprise chains of smaller moraine fragments, though moraines may extend up to several hundreds of metres in length. Moreover, moraines typically display widths between 3 m and 8 m, with an average width of 5.74 m.

Implications

The glacial geomorphological mapping conducted in this research has revealed an abundance of *minor moraines* distributed across the Skálafellsjökull foreland. Furthermore, the inventory of maps produced in this study provides the most detailed mapping of these moraines to date (*cf*. Sharp, 1984; Evans and Orton, 2014). The geomorphological maps provide a framework for subsequently exploring the chronology and formation of moraines at Skálafellsjökull. Moreover, the mapped moraine record documents fluctuations of the ice-margin and allows glacier recession at Skálafellsjökull to be explored.

(2) Establishment of a moraine chronology at Skálafellsjökull

Summary

A chronological framework for the mapped moraines has been established through the integration of remote sensing observations and lichenometry (*cf*. Bradwell, 2004a; Bradwell *et al*., 2013). For comparative purposes, a variety of lichenometric dating techniques used previously in SE Iceland were employed (Gordon and Sharp, 1983; Bradwell, 2001a, b, 2004b). The dates derived from the lichenometric analyses, combined with remote sensing observations, suggest minor moraines on the northern and central parts of the Skálafellsjökull foreland formed annually. Furthermore, the geomorphological characteristics of the moraines are similar to other features interpreted as annual moraines (e.g. Boulton, 1986; Krüger, 1995; Bradwell, 2004a; Lukas, 2012; Bradwell *et al*., 2013). Thus, these minor moraines have been interpreted as *annual moraines* with some confidence. Based on bracketing ages established from remote sensing observations and lichenometry, annual moraine formation occurred during the periods 1936 – 1964, 1969 – 1974, and from 2006 onwards. Age estimates could not be confidently ascribed to moraines on the southern part of the Skálafellsjökull foreland due to a paucity of data (remote sensing and ice-front measurements). Moreover, minor moraines in this area of the foreland appear to have formed sub-annually, with more moraines identified than the number years elapsed.

Implications

According to previous studies, *annual moraines* are formed by short-lived seasonal re-advances at the margins of active temperate glaciers during a period of overall retreat (e.g. Price, 1970; Sharp, 1984; Boulton, 1986; Krüger, 1995; Evans and Twigg, 2002; Bradwell *et al*., 2004a; Bradwell *et al*., 2013). Thus, the identification of annual moraine formation during 1936 – 1964, 1969 – 1974, and from 2006 onwards indicates that Skálafellsjökull has undergone active, oscillatory retreat during these time periods. Provided that these annual moraines are formed by a range of ice-marginal genetic processes, the geomorphological maps and established moraine chronology provide a framework for assessing patterns and rates of ice-marginal retreat at Skálafellsjökull. However, the identification of sub-annual moraines on parts of glacier foreland indicates that *annual moraine couplets* could be a more appropriate classification in some settings. Further consideration of the concept of "annual" moraines and their wider applicability is given below.

(3) Development of conceptual models of annual moraine formation

Summary

Based on the sediment composition and structure of the annual moraines, the following categories of moraine-forming processes have been distinguished at Skálafellsjökull: (1) submarginal deformation and subsequent bulldozing of the extruded sediments; (2) efficient bulldozing (*sensu* Lukas, 2012) of pre-existing proglacial material; and (3) emplacement of frozen-on submarginal sediment slabs. The identification of these genetic processes has allowed the development of conceptual models for annual moraine formation at Skálafellsjökull (see §7.1). The range of moraine-forming processes identified at the study site is similar to those previously recognised at other Icelandic outlet glaciers (*cf*. Price, 1970; Sharp, 1984; Krüger, 1993, 1994, 1995, 1996; Evans and Twigg, 2002; Evans and Hiemstra, 2005). Important differences identified between the genetic processes identified in this research and previous models of annual moraine formation are as follows: (1) no evidence was found for snow-cover having a significant role in annual moraine formation (Price, 1970; Birnie, 1977; Sharp, 1984); (2) dead-ice incorporation was not apparent, with no ice-cored moraines identified (Sharp, 1984; Lukas, 2012); and (3) terrestrial ice-contact fans were not evident at Skálafellsjökull. Of the moraine-forming processes previously identified at the study site (Sharp, 1984), only push/squeeze moraines (Type A) were evident during field investigations conducted as part of this research.

Implications

The range of moraine-forming processes identified at Skálafellsjökull indicates site-specific conditions, including topographic, glaciological and climatic factors, have an important role in annual moraine formation. In particular, the reverse basalt bedrock slope in the southern part of the glacier foreland has an important influence on moraine formation at this part of the ice-margin. The presence of this impermeable reverse bedrock slope generates an aquiclude, resulting in surface waters flowing back down the slope and accumulating at the ice-front. This combination of topographic and geological factors results in highly saturated subglacial sediments and high pore-water pressures. As a consequence of these conditions, submarginal deformation and ice-marginal squeezing occurs (*cf*. Price, 1970; Boulton *et al*., 1974, 2001; Sharp, 1984; Evans and Twigg, 2002; Evans and Hiemstra, 2005, and references therein). Topographic, glaciological and climatic factors also have an important influence on the incidence of subglacial freeze-on (*sensu* Krüger, 1994, 1995) at the ice-margin. In places, the meltwater flows along the southeastern Skálafellsjökull margin and undercuts the ice-front. This undercutting, combined with a relatively thin, gently-sloping margin, allows the penetration of the winter freezing front and subsequent freeze-on of basal sediments. Moreover, the occurrence of subglacial freeze-on appears to be associated with unusually cold winter conditions.

The dominance of push/squeeze moraine formation mechanisms at Skálafellsjökull and the distinctive *sawtooth* planform geometry of the annual moraines strongly suggest that annual moraine geomorphology is influenced by structural glaciology, with the sawtooth pattern reflecting ice-margin morphology and structure (*cf*. Price, 1970; Matthews *et al*., 1979; Sharp, 1984; Burki *et al*., 2009). Ultimately, the development of radial crevasses and a pecten at the Skálafellsjökull ice-margin reflects topographically induced down-ice changes in the stress field (*cf*. Nye, 1952; Benn and Evans, 2010; Cuffey and Paterson, 2010). The formation of annual moraines through push/squeeze processes results in the inheritance of this pecten in their planform.

The geomorphological, chronological and sedimentological data presented and discussed in this thesis indicate suites of annual moraines, formed through a combination of ice-marginal processes, exist on the Skálafellsjökull. Moreover, these annual moraines can be interpreted as representing successive ice-frontal positions, with the annual moraine record documenting ice-marginal fluctuations at Skálafellsjökull over the past ~80 years. Thus, these annual moraines can be employed as a geomorphological proxy for patterns and rates of ice-marginal retreat at Skálafellsjökull.

(4) Patterns, rates and drivers of recent ice-marginal retreat at Skálafellsjökull

Summary

Annual ice-margin retreat rates (IMRRs), equivalent to annual moraine spacing, have been calculated for known periods of annual moraine formation. The record of IMRRs indicates Skálafellsjökull experienced net glacier recession in every year between 1936 and 1964 (average: 25.6 m a^{-1}). A subsequent short period of annual moraine formation occurred during 1969 – 1974, with IMRRs averaging 9.9 m a^{-1}. During the most recent period (2006 – 2011) of ice-marginal retreat, the glacier receded 133.7 m (average: ~22.3 m a^{-1}). Comparison of this period of retreat with other pronounced 6-year periods of ice-frontal retreat (1936 – 1941 and 1951 – 1956) indicates Skálafellsjökull has previously exhibited more rapid IMRRs and, therefore, the current phase of glacier recession is not unusual in the context of the ~80 year period examined in this research. Comparison of the record of IMRRs at Skálafellsjökull with other Icelandic glaciers shows that the timing, magnitude and rate of glacier retreat was similar across Iceland (*cf*. Bradwell, 2004a; Sigurðsson *et al*., 2007; Bradwell *et al*., 2013, and references therein). Furthermore, the pronounced periods of ice-frontal retreat at Skálafellsjökull coincide with those of SE Greenland outlet glaciers (*cf*. Bjørk *et al*., 2012).

This study builds on previous work which has employed annual moraine spacing to explore ice-marginal retreat, exploring a wider array of climate variables (*cf*. Bradwell, 2004a; Beedle *et* al., 2009; Lukas, 2012). Statistical analysis of potential drivers of recent ice-marginal retreat at Skálafellsjökull reveals statistically significant relationships between summer variations in air temperature ($r^2 = 0.3464$, $p < 0.0001$), sea surface temperature ($r^2 = 0.1623$, $p = 0.0010$) and the North Atlantic Oscillation ($r^2 = 0.1310$, $p = 0.0201$). No statistically significant relationships were identified between IMRRs and the other climate variables examined in this research. Skálafellsjökull therefore appears to be most sensitive to summer air temperature variations, and this appears to be an important control on ice-frontal retreat.

Implications

The prominent periods of ice-marginal retreat recorded in the annual moraine sequences at Skálafellsjökull are coincident with periods of rapid glacier recession elsewhere in Iceland (e.g. Sigurðsson, 1998; Bradwell, 2004a; Sigurðsson *et al*., 2007; Bradwell *et al*., 2013), implying a common driving mechanism. Annual moraine spacing (IMRRs) and ice-front measurements have been shown to correspond to periods of elevation summer air temperature elsewhere at other Icelandic outlet glaciers (Boulton, 1986; Krüger, 1995; Sigurðsson and Jónsson, 1995; Bradwell, 2004a; Sigurðsson *et al*., 2007; Bradwell *et al*., 2013). Thus, summer air temperature variability appears to exert an important control on ice-frontal retreat throughout SE Iceland. Furthermore, the temporal coincidence of IMRRs and summer air temperature variability implies that Skálafellsjökull has a very rapid *reaction time* (*sensu* Benn and Evans, 2010), responding to summer air temperature fluctuations at a sub-annual timescale. The pronounced periods of ice-frontal retreat at the study site also coincide with prominent phases of glacier recession at Greenlandic outlet glaciers (*cf*. Bjørk *et al*., 2012), suggesting there may be a common forcing mechanism in the North Atlantic region. Analysis of climate variability in SE Iceland conducted in this study has demonstrated that sea surface temperature (SST) exerts on important influence on air temperature. Based on this, it is hypothesised in this study that sea surface temperature could be the mutual driver, with SST forcing air temperature, which in turn drives IMRRs. The most recent period of warming SST may result from a weakening of the North Atlantic subpolar gyre, reflecting decadal and annual scale responses of the subpolar gyre to fluctuations in the NAO (*cf*. Häkkinen and Rhines, 2004; Hátún *et al*., 2005; Lohmann *et al*., 2008; Bersch *et al*., 2007; Robson *et al*., 2012; Häkkinen *et al*., 2013; Barrier *et al*., 2015). This has previously been suggested as a mechanism forcing Greenlandic glacier change (Straneo and Heimbach, 2013). Further evidence is, however, required to test the links between SST, AAT and ice-frontal retreat of Icelandic glaciers. A sensitivity ranking of climate variables has been developed for Skálafellsjökull which could be applied in the analysis of drivers at other glaciers in the North Atlantic region. This would provide a systematic approach to the analysis of drivers of ice-marginal retreat.

(5) Limitations and applicability of annual moraines as climatic indicators

Summary

During the course of this research a number of potential issues with applying “annual” moraines as climatic indicators have been identified. In particular, there are issues relating to the chronological robustness and climatic integrity of annual moraine sequences (*cf*. Kirkbride and Winkler, 2012). Confidently establishing a chronological framework is currently limited by errors and uncertainties associated with the range of dating techniques typically employed. For example, even the most well-calibrated lichenometric dating has an optimum precision of only 5 – 10% (Innes, 1988; Noller and Locke, 2000). Further complicating moraine chronology is the recognition that moraines may form on a sub-annual basis (annual moraine couplets), challenging the concept of "annual" moraines. Even where the number of moraines formed in a given time period is equivalent to the time elapsed, some of these features may have formed in the same year, whilst no winter re-advance moraine was formed in the previous/subsequent year. Aside from issues relating to the chronological robustness of annual moraine sequences, the integrity of moraine records may be affected by erosional censoring (*cf*. Gibbons *et al*., 1984; Kirkbride and Brazier, 1998; Kirkbride and Winkler, 2012; Barr and Lovell, 2014). Such erosional censoring may occur through both self-censoring and external censoring processes (*cf*. Kirkbride and Winkler, 2012; Barr and Lovell, 2014).

Implications

The issues highlighted above can have important implications for the use of annual moraines to examine patterns, rates and drivers of ice-marginal retreat. Uncertainties in chronological techniques can introduce errors into moraine chronologies and, therefore, IMRR calculations. Moreover, the efficacy of the erosional censoring processes can have important implications for the integrity of annual moraine sequences and, consequently, their climatic representativeness. Owing to these limitations, it is argued in this thesis that presently it is unlikely that moraines could be identified as "annual" features in the geological record and subsequently used to make high resolution palaeoclimatic inferences. Despite the highlighted issues, annual moraines do potentially afford a valuable tool for examining ice-frontal retreat in contemporary glacial environments (*cf*. Bradwell, 2004a; Beedle *et al*., 2009; Lukas, 2012). Provided that issues relating to the chronological robustness and integrity of annual moraine sequences can be minimised, annual moraines can give valuable insights into patterns, rates and drivers of ice-marginal retreat.

8.2 Further research

The current research has identified a large scope for further research, both specific to Skálafellsjökull and more widely. In particular these research areas relate to: (1) the influence of structural glaciology on both ice-frontal retreat and annual moraine formation; (2) repeat monitoring of the Skálafellsjökull ice-margin to further explore ice-marginal retreat and proglacial landscape evolution; and (3) patterns, rates and drivers of ice-marginal retreat in the wider North Atlantic region. These themes are discussed in more detail below.

(1) Structural glaciology investigations of Skálafellsjökull

This study has suggested that structural glaciology plays an important role in annual moraine formation and geomorphology. However, the influence of structural glaciology on ice-frontal retreat has yet to be explored. In particular, it would be interesting to explore how transverse glacier structures influence the rate of ice-margin retreat. For example, the presence of transverse structures at the glacier snout may initiate rapid ice-frontal retreat, independent of external forcing. This would in turn influence annual moraine formation and spacing. Thus, it would be fruitful to examine the temporal and spatial evolution of structures on the Skálafellsjökull surface, through a combination of desk-based structural mapping and field-based structural glaciology investigations (e.g. Goodsell *et al*., 2005; Appleby *et al*., 2010; Phillips *et al*., 2013, 2014), in order to further explore the influence of structural glaciology on ice-marginal retreat at Skálafellsjökull. Moreover, these investigations may provide further insights into the role of structural glaciology on annual moraine formation and geomorphology.

(2) Programme of repeat aerial surveying and monitoring at Skálafellsjökull

This research has employed a Digital Elevation Model (DEM) derived from Unmanned Aerial Vehicle (UAV) imagery in the process of geomorphological mapping. So far the application of UAV imagery in glaciology and glacial geomorphology has been limited (e.g. Whitehead *et al*., 2013; Ryan *et al*., 2014; Evans *et al*., submitted). However, UAV imagery potentially represents an effective and low-cost source of high-resolution remotely-sensed data (e.g. d’Oleire-Oltmans *et al*., 2012; Hugenholtz *et al*., 2012, 2013; Lucieer *et al*., 2014) for examining ice-frontal fluctuations and proglacial landscape evolution. It would be fruitful to undertake a programme of repeat aerial surveying and monitoring at Skálafellsjökull in order to attain further insights into annual fluctuations of the ice-margin and its implications for annual moraine formation. In particular, repeat aerial surveying at a high temporal resolution would allow the frequency of moraine formation to be assessed and contribute to debates surrounding the concepts of “annual” moraines or annual moraine couplets.

(3) Patterns, rates and drivers of ice-front retreat in the North Atlantic region

Based on analysis of IMRRs and climate data it has been recognised that summer AAT, SST and the NAO influence IMRRs at Skálafellsjökull. Moreover, the glacier appears most sensitive to inter-annual fluctuations in summer AAT, with a sensitivity ranking having been developed for Skálafellsjökull. Comparison of IMRRs from Skálafellsjökull with those exhibited by glaciers elsewhere in Iceland and the wider North Atlantic region reveals a temporal coincidence in periods of pronounced ice-marginal retreat, suggesting a common, regional driving mechanism. Further research is, however, required to examine the hypothesis that IMRRs are driven by a common forcing mechanism. This could be achieved through investigations of annual moraines, following the approaches used in this research (see also Bradwell, 2004a; Beedle *et al*., 2009; Lukas, 2012; Bradwell *et al*., 2013), and/or through remote sensing studies of ice-frontal retreat (e.g. Bjørk *et al*., 2012; Carr *et al*., 2013, 2014, in press; Miles *et al*., 2013; Stokes *et al*., 2013). Statistical analysis of potential external drivers of ice-margin retreat could employ the sensitivity ranking derived for Skálafellsjökull, providing a systematic approach.

8.3 Summary

This research applied annual moraines, and integrated multiple methods at a range of spatial and temporal scales, to examine patterns, rates and drivers of ice-marginal retreat at Skálafellsjökull. High-resolution glacial geomorphological mapping revealed suites of minor moraines across the glacier foreland, with the features displaying distinctive *sawtooth* or crenulate planform geometries. Chronological investigations of the Skálafellsjökull moraines, which integrated remote sensing observations and lichenometry, indicated that minor moraines on the northern and central parts of the glacier foreland formed on an annual basis. These *annual moraines* are believed to have formed during three key periods: 1936 – 1964; 1969 – 1974; and from 2006 onwards. Sedimentological investigations revealed that annual moraines at Skálafellsjökull form through a range of ice-marginal processes, with push/squeeze mechanisms being dominate. Furthermore, structural glaciology was identified as a key factor in annual moraine formation and geomorphology. The geomorphological, chronological and sedimentological data therefore indicated these moraines represent successive annual ice-frontal positions. Thus, these annual moraines provided a framework for exploring patterns, rates and drivers of ice-marginal retreat at Skálafellsjökull.

Calculation of annual ice-margin retreat rates (IMRRs), on the basis of annual moraine spacing, indicated pronounced glacier recession occurred at Skálafellsjökull in three key periods: 1936 – 1941; 1951 – 1956; and 2006 – 2011. Comparison of these periods of ice-marginal retreat revealed no statistical significant differences, indicating that the most recent period of ice-frontal retreat (2006 – 2011) is not unusual in the context of the ~80 year period examined. These pronounced periods of glacier recession coincide with those exhibited elsewhere in Iceland and the wider North Atlantic region, implying a regional driving mechanism may be forcing IMRRs. Covariance analysis of IMRRs at Skálafellsjökull and climate data suggested summer air temperature, sea surface temperature and North Atlantic Oscillation have an influence on IMRRs, with the glacier appearing to be most sensitive to summer air temperature. Based on the climate data analysis conducted in this research, it has been hypothesised that sea surface temperature may drive air temperature changes in the North Atlantic region, which in turn forces IMRRs. The increase in SST over recent decades may result from an atmospheric-driven weakening in the North Atlantic subpolar gyre. However, further data is required to test the links between SST, AAT and IMRRs.

The current research has identified a large scope for further research, both specific to Skálafellsjökull and more widely. In particular these research areas relate to: (1) the influence of structural glaciology on both ice-frontal retreat and annual moraine formation; (2) repeat monitoring of the Skálafellsjökull ice-margin to further explore ice-marginal retreat and proglacial landscape evolution; and (3) patterns, rates and drivers of ice-marginal retreat in the wider North Atlantic region.

REFERENCES

Aðalgeirsdóttir, G., Jóhannesson, T., Björnsson, H., Pálsson, F., Sigurðsson, O., 2006. Response of Hofsjökull and southern Vatnajökull, Iceland, to climate change. Journal of Geophysical Research 111, F03001, DOI: 10.1029/2005JF000388.

Ahlmann, H.W., Thórarinsson, S., 1937. Vatnajökull. Scientific results of the Swedish - Icelandic investigations. Geografiska Annaler 19, 146–231.

Alexander, M.A., Kilbourne, K.H., Nye, J., 2014. Climate variability during warm and cold phases of the Atlantic Multidecadal Oscillation (AMO) 1871–2008. Journal of Marine Systems 133, 14–26

Alexander, M.J., Worsley, P., 1973. Stratigraphy of a Neoglacial end moraine in Norway. Boreas 2, 117–142.

Alley, R.B., Lawson, D.E., Evenson, E.B., Strasser, J.C., Larson, G.J., 1998. Glaciohydraulic supercooling:a freeze-on mechanism to create stratified, debris-rich basal ice. II. Theory. Journal of Glaciology 44, 563–569.

Alley, R.B., Strasser, J.C., Lawson, D.E., Evenson, E.B., Larson, G.J., 1999. Glaciological and geological implications of basal-ice accretion in overdeepenings. In: Mickelson, D.M., Attig, J.W. (eds.), Glacial Processes: Past and Present. Geological Society of America, Special Paper 337, pp. 1–9.

Andersen, J.L., Sollid, J.L., 1971. Glacial chronology and glacial geomorphology in the marginal zones of the glaciers Midtdalsbreen and Nigardsbreen, south Norway. Norsk Geografisk Tidsskrift 25, 1–38.

Anderson, L.S., Roe, G.H., Anderson, R.S., 2014. The effects of interannual climate variability on the moraine record. Geology 42, 55–58.

Anderson, R.S., Dühnforth, M., Colgan, W., Anderson, L., 2012. Far-flung moraines: exploring the feedback of glacial erosion on the evolution of glacier length. Geomorphology 179, 269–285.

Andresen, C.S., Straneo, F., Ribergaard, M.H., Bjørk, A.A., Andersen, T.J., Kuijpers, A., Nørgaard-Pedersen, N., Kjær, K.H., Schjøth, F., Weckström, K., Ahlstrøm, A.P., 2012. Rapid response of Helheim glacier in Greenland to climate variability over the past century. Nature Geoscience 5, 37–41.

Andrews, D.E., Smithson, B.B., 1966. Till fabric of the cross-valley moraines of north-central Baffin Island, North West Territories, Canada. Geological Society of America Bulletin 77, 271–290.

Armstrong, R.A., 1983. Growth curve of the lichen Rhizocarpon geographicum. New Phytologist 94, 619–622.

Armstrong, R.A., 2015. The Influence of Environmental Factors on the Growth of Lichens in the Field. In: Upreti, D.K., Divakar, P.K., Shukla, V., Bajpai., R. (eds.), Recent Advances in Lichenology. Springer, New Delhi, pp. 1–18.

Bahr, D.B., Dyugerov, M., Meier, M.F., 2009. Sea-level rise from glaciers and ice caps: a lower bound. Geophysical Research Letters 36, DOI: 10.1029/2008GL036309.

Bahr, D.B., Pfeffer, W.T., Sassolas, C., Meier, M.F., 1998. Response time of glaciers as a function of size and mass balance: 1. Theory. Journal of Geophysical Research: Solid Earth 103(B5), 9777–9782.

Balco, G., 2011. Contributions and unrealized potential contributions of cosmogenic-nuclide exposure dating to glacier chronology, 1990–2010. Quaternary Science Reviews 30, 3–27.

Ballantyne, C.K., 2012. Chronology of glaciation and deglaciation during the Loch Lomond (Younger Dryas) Stade in the Scottish Highlands: implications of recalibrated ^{10}Be exposure ages. Boreas 41(4), 513–526.

Barlow, L.K., 2001. The time period A.D. 1400–1980 in central Greenland ice cores in relation to the North Atlantic sector. Climatic Change 48, 101–119.

Barr, I.D., Clark, C.D., 2012. Late Quaternary glaciations in Far NE Russia; combining moraines, topography and chronology to assess regional and global glaciation synchrony. Quaternary Science Reviews 53, 72–87.

Barr, I.D., Lovell, H., 2014. A review of topographic controls on moraine distribution. Geomorphology 226, 44–64.

Barrier, N., Deshayes, J., Treguier, A.-M., Cassou, C., 2015. Heat budget in the North Atlantic subpolar gyre: Impacts of atmospheric weather regimes on the 1995 warming event. Progress in Oceanography 130, 75–90.

Battisti, D.S., Bhatt, U.S., Alexander, M.A., 1995. A modeling study of the interannual variability in the wintertime North Atlantic Ocean. Journal of Climate 8, 3067–3083.

Bárðarson, G., 1934. Islands Gletscher: Beiträge zur Kenntnis der Gletscherbewegungen und Schwankungen auf Grund alter Quellenschriften und neuester Forschung: nachgelassenes Manuskript. Rit Vísindafélags Íslendinga 16, 60.

Beedle, M.J., Menounos, B., Luckman, B.H., Wheate, R., 2009. Annual push moraines as climate proxy. Geophysical Research Letters 36, L20501, DOI: 10.1029/2009GL039533.

Benedict, J.B., 1967. Recent glacial history of an alpine area in the Colorado Front Range, USA. I. Establishing a lichen growth curve. Journal of Glaciology 6, 817–832.

Benedict, J.B., 1985. Arapaho Pass. Glacial geology and archaeology at the crest of the Colorado Front Range. Centre for Mountain Archaeology Research Report No. 3. Ward, Colorado.

Benedict J.B., 1990. Experiments on lichen growth. I. Seasonal patterns and environmental controls. Arctic and Alpine Research 22(3), 244–254.

Benediktsson, Í.Ö., Ingólfsson, Ó., Schomacker, A., Kjær, K.H., 2009. Formation of submarginal and proglacial end moraines: implications of ice-flow mechanism during the 1963–64 surge of Brúarjökull, Iceland. Boreas 38(3), 440–457.

Benestad R.E., Melsom A., 2002. Is there a link between the unusually wet autumns in southeastern Norway and sea-surface temperature anomalies? Climate Research 23, 67–79.

Benn, D.I., 1992. The genesis and significance of 'hummocky moraine': evidence from the Isle of Skye, Scotland. Quaternary Science Reviews 11, 781–99.

Benn, D.I., 1994. Fluted moraine formation and till genesis below a temperate glacier: Slettmarkbreen, Jotunheimen, Norway. Sedimentology 41, 279–292.

Benn, D.I., 1995. Fabric signature of subglacial till deformation, Breiðamerkurjökull, Iceland. Sedimentology 42, 735–747.

Benn, D.I., 2004. Clast morphology. In: Evans, D.J.A., Benn, D.I. (eds.), 2004. A Practical Guide to the Study of Glacial Sediments. Arnold, London, pp. 78–92.

Benn, D.I., Ballantyne, C.K., 1993. The description and representation of particle shape. Earth Surface Processes and Landforms 18, 665–72.

Benn, D.I., Ballantyne, C.K., 1994. Reconstructing the transport history of glacigenic sediments: a new approach based on the co-variance of clast shape indices. Sedimentary Geology 91, 215–27.

Benn, D.I., Evans, D.J.A., 1996. The interpretation and classification of subglacially deformed materials. Quaternary Science Reviews 15, 23–52.

Benn, D.I., Evans, D.J.A., 1998. Glaciers and Glaciation (First Edition). Arnold, London, 734 pp.

Benn, D.I., Evans, D.J.A., 2010. Glaciers and Glaciation (Second Edition). Hodder Education, London, 802 pp.

Benn, D.I., Lukas, S., 2006. Younger Dryas glacial landsystems in North West Scotland: an assessment of modern analogues and palaeoclimatic implications. Quaternary Science Reviews 25, 2390–2408.

Bennett, G.L., Evans, D.J.A., Carbonneau, P., Twigg, D.R., 2010. Evolution of a debris-charged glacier landsystem, Kvíárjökull, Iceland. Journal of Maps 6(1), 40–67.

Bennett, M.R., 2001. The morphology, structural evolution and significance of push moraines. Earth-Science Reviews 53, 197–236.

Bennett, M.R., Huddart, D., Waller, R.I., 2000. Glaciofluvial crevasse and conduit fills as indicators of supraglacial dewatering during a surge, Skeiðarárjökull, Iceland. Journal of Glaciology 46, 25–34.

Bersch, M., Yashayaev, I., Koltermann, K.P., 2007. Recent changes of the thermohaline circulation in the subpolar North Atlantic. Ocean Dynamics 57, 223–235.

Beschel, R.E., 1950. Flechten als Altersmasstab Rezenter Moränen. Zeitschrift für Gletscherkunde und Glazialgeologie 1(2), 152–161.

Beschel, R.E., 1961. Dating rock surfaces by lichen growth and its application to glaciology and physiography (lichenometry). In: Raasch, G.O. (ed.), Geology of the Arctic Vol. 2. University of Toronto Press, Toronto, pp. 1044–1062.

Birnie, R.V., 1977. A snow-bank push mechanism for the formation of some “annual” moraine ridges. Journal of Glaciology 18, 77–85.

Bjerknes, J., 1964. Atlantic air–sea interaction. Advances in Geophysics 10, 1–82.

Bjørk, A.A., Kjær, K.H., Korsgaard, N.J., Khan, S.A., Kjeldsen, K.K., Andresen, C.S., Box, J.E., Larsen, N.K., Funder, S., 2012. An aerial view of 80 years of climate-related glacier fluctuations in southeast Greenland. Nature Geoscience 5, 427–432.

Björnsson, F., 1998. Samtíningur um jökla milli Fells og Stadherfjalls. Jökull 46, 49–61.

Björnsson, H., 1971. Bægisárjökull, North-Iceland. Results of glaciological investigations 1967–1968. Part I. Mass balance and general meteorology. Jökull 21, 1–23.

Björnsson, H., 1979. Glaciers in Iceland. Jökull 29, 74–80.

Björnsson, H., 1988. Hydrology of Ice Caps in Volcanic Regions. Societas Scientarium Islandica, University of Iceland, Reykjavík, Rit 45, 139 pp.

Björnsson, H., 1996. Scales and rates of glacial sediment removal: a 20km long, 300m deep trench created beneath Breiðamerkurjökull during the little ice age. Annals of Glaciology 22, 141–146.

Björnsson, H., 2002. Subglacial lakes and jökulhlaups in Iceland. Global and Planetary Change 35, 255–271.

Björnsson, H., Pálsson, F., 2008. Icelandic glaciers. Jökull 58, 365–386.

Björnsson, H., Pálsson, F., Guðmundsson, M.T., Haraldsson, H., 1998. Mass balance of western and northern Vatnajökull, Iceland, 1991–1995. Jökull 45, 35–58.

Björnsson, H., Pálsson, F., Guðmundsson, S., 2001. Jökulsárlón at Breiðamerkursandur, Vatnajökull, Iceland: 20th century changes and future outlook. Jökull 50, 1–18.

Björnsson, H., Pálsson, F., Guðmundsson, S., Magnússon, E., Adalgeirsdóttir, G., Jóhannesson, T., Berthier, E., Sigurðsson, O., Thorsteinsson, T., 2013. Contribution of Icelandic ice caps to sea level rise: Trends and variability since the Little Ice Age. Geophysical Research Letters 40, 1546–1550.

Björnsson, H., Pálsson, F., Haraldsson, H., 2002. Mass balance of Vatnajökull (1991–2001) and Langjökull (1996–2001), Iceland. Jökull 51, 75–78.

Black, T.A., 1990. The Holocene fluctuation of the Kvíárjökull Glacier, southeastern Iceland. Unpublished MA thesis, University of Colorado, USA.

Blair, R., Higgins, J.T., 1980. A comparison of the power of Wilcoxon’s rank-sum statistic to that of the Student’s t statistic under various non-normal distributions. Journal of Educational Statistics 5(4), 309–335.

Boston, C.M. 2012a. A Lateglacial plateau icefield in the Monadhliath Mountains, Scotland: reconstruction, dynamics and palaeoclimatic implications. Unpublished PhD thesis, Queen Mary University of London, UK, 295 pp.

Boston, C.M., 2012b. A glacial geomorphological map of the Monadhliath Mountains, Central Scottish Highlands. Journal of Maps 8(4), 437–444.

Boston, C.M., Lukas, S., Carr, S.J., 2015. A Younger Dryas plateau icefield in the Monadhliath, Scotland, and implications for regional palaeoclimate. Quaternary Science Reviews 108, 139–162.

Boston, C.M., Lukas, S., Merritt, J.W. (eds.), 2013. The Quaternary of the Monadhliath Mountains and the Great Glen: Field Guide. Quaternary Research Association, London, 230 pp.

Boulton, G.S., 1976. The origin of glacially fluted surfaces: observations and theory. Journal of Glaciology 17, 287–309.

Boulton, G.S., 1978. Boulder shapes and grain-size distributions of debris as indicators of transport paths through a glacier and till genesis. Sedimentology 25(6), 773–799.

Boulton, G.S., 1979. Processes of glacier erosion on different substrata. Journal of Glaciology 23, 15–38.

Boulton, G.S., 1986. Push moraines and glacier-contact fans in marine and terrestrial environments. Sedimentology 33, 677–698.

Boulton, G.S., 1987. A theory of drumlin formation by subglacial sediment deformation. In: Menzies, J., Rose, J. (eds.), Drumlin Symposium. Balkema, Rotterdam, pp. 25–80.

Boulton, G.S., Dent, D.L., 1974. The nature and rates of postdepositional changes in recently deposited till from south-east Iceland. Geografiska Annaler 56A, 121–134.

Boulton, G.S., Dent, D.L., Morris, E.M., 1974. Subglacial shearing and crushing, and the role of water pressures in tills from southeast Iceland. Geografiska Annaler 56A, 135–145.

Boulton, G.S., Dobbie, K.E., 1998. Slow flow of granular aggregates: the deformation of sediments beneath glaciers. Philosophical Transactions of the Royal Society of London A 356(1747), 2713–2745.

Boulton, G.S., Dobbie, K.E., Zatsepin, S., 2001. Sediment deformation beneath glaciers and its coupling to the subglacial hydraulic system. Quaternary International 86, 3–28.

Boulton, G.S., Harris, P.W.V., Jarvis, J., 1982. Stratigraphy and structure of a coastal sediment wedge of glacial origin inferred from sparker measurements in glacial Lake Jökulsárlón in southeastern Iceland. Jökull 32, 37–47.

Boulton, G.S., Hindmarsh, R.C.A., 1987. Sediment deformation beneath glaciers: rheology and sedimentological consequences. Journal of Geophysical Research: Solid Earth 92, 9059–9082.

Bradwell, T. 2001a. A new lichenometric dating curve for southeast Iceland. Geografiska Annaler 83A, 91–101.

Bradwell, T., 2001b. Glacier Fluctuations, Lichenometry and Climatic Change in Iceland. Unpublished PhD thesis, University of Edinburgh, UK, 374 pp.

Bradwell, T., 2004a. Annual moraines and summer temperatures at Lambatungnajökull, Iceland. Arctic, Antarctic, and Alpine Research 36, 502–508.

Bradwell, T., 2004b. Lichenometric dating in southeast Iceland: the size-frequency approach. Geografiska Annaler 86A, 31–41.

Bradwell, T., 2009. Lichenometric dating: a commentary, in the light of some recent statistical studies. Geografiska Annaler 91A(2), 61–69.

Bradwell, T., Armstrong, R.A., 2007. Growth rates of Rhizocarpon geographicum: a review with new data from Iceland. Journal of Quaternary Science 22, 311–320.

Bradwell, T., Dugmore, D.J., Sugden, D.E., 2006. The Little Ice Age glacier maximum in Iceland and the North Atlantic Oscillation: evidence from Lambatungnajökull, southeast Iceland. Boreas 35, 61–80.

Bradwell, T., Sigurðsson, O., Everest, J., 2013. Recent, very rapid retreat of a temperate glacier in SE Iceland. Boreas 42, 959–973.

Brook, M.S., Lukas, S., 2012. A revised approach to discriminating sediment transport histories in glacigenic sediments in a temperate alpine environment: a case study from Fox Glacier, New Zealand. Earth Surface Processes and Landforms 37, 895–900.

Brown, V.H., Evans, D.J.A., Evans, I.S., 2011. The Glacial Geomorphology and Surficial Geology of the South-West English Lake District. Journal of Maps 7(1), 221–243.

Brynjólfsson, S., Schomacker, A., Ingólfsson, Ó., 2014. Geomorphology and the Little Ice Age extent of the Drangajökull ice cap, NW Iceland, with focus on its three surge-type outlets. Geomorphology 213, 292–304.

Bull, W.B., Brandon, M.T., 1998. Lichen dating of earthquake-generated regional rockfall events, Southern Alps, New Zealand. Geological Society of America Bulletin 110(1), 60–84.

Burki, V., Larsen, E., Fredin, O., Margreth, A., 2009. The formation of sawtooth moraine ridges in Bødalen, western Norway. Geomorphology 105, 182–192.

Campbell, J.B., Wynne, R.H., 2011. Introduction to remote sensing (Fifth Edition). Taylor and Francis, London, 667 pp.

Carr J.R., Stokes C.R., Vieli A., 2014. Recent retreat of major outlet glaciers on Novaya Zemlya, Russian Arctic, influenced by fjord geometry and sea-ice conditions. Journal of Glaciology 60(219), 155–170.

Carr J.R., Vieli A., Stokes C.R., 2013. Climatic, oceanic and topographic controls on marine-terminating outlet glacier behavior in north-west Greenland at seasonal to interannual timescales. Journal of Geophysical Research 118(3), 1210–1226.

Carr J.R., Vieli A., Stokes C.R., Jamieson S.S.R., Palmer S.J., Christoffersen P., Dowdeswell J.A., Nick F.M., Blankenship D.D., Young D.A., in press. Basal topographic controls on rapid retreat of Humboldt Glacier, northern Greenland. Journal of Glaciology.

Caseldine, C.J., 1983. Resurvey of the margins of Gljúfurárjökull and the chronology of recent deglaciation. Jökull 33, 111–118.

Caseldine, C.J., 1985. Survey of Gljúfurárjökull and features associated with a glacier burst in Gljúfurárdalur. Jökull 35, 61–68.

Caseldine, C.J., 1987. Neoglacial Glacier Variation in Northern Iceland. Examples from the Eyjafjördur area. Arctic and Alpine Research 19, 296–304.

Caseldine, C.J., 1990. A review of dating methods and their applications in the development of chronology of Holocene glacier Variation in Northern Iceland. In: Caseldine, C.J., Häberle, T., Kugelmann, O., Munzer, U., Stötter, J., Wilhelm, F. (eds.), Geomoprhologische und landschaftsgeschichtliche Untersuchungen in Nordisland. Munchen Geogr. Abl. B8, pp. 59–82.

Caseldine, C.J., 1991. Lichenometric dating, lichen population studies and Holocene glacial history in Tröllaskagi, northern Iceland. In: Maizels, J.K. and Caseldine, C. (eds.), Environmental Change in Iceland: Past and Present. Glaciology and Quaternary Geology. Kluwer Academic Publishers. Dordrecht pp. 219–233.

Caseldine, C.J. and Baker, A., 1998: Frequency distribution of Rhizocarpon geographicum s.l., modeling, and climate variation in Tröllaskagi, northern Iceland. Arctic and Alpine Research 30(2), 175–183.

Caseldine, C.J., Stötter, J., 1993. ''Little Ice Age'' glaciation of Trollaskagi peninsula, northern Iceland: climatic implications for reconstructed equilibrium line altitudes (ELAs). The Holocene 3, 357–366.

Casely, A.F., Dugmore, A.J., 2004. Climate change and 'anomalous' glacier fluctuations: the southwest outlets of Mýrdalsjökull, Iceland. Boreas 33, 108–122.

Cayan D.R., 1992a. Latent and sensible heat flux anomalies over the northern oceans: the connection to monthly atmospheric circulation. Journal of Climate 5, 354–369.

Cayan, D.R., 1992b. Latent and sensible heat flux anomalies over the northern oceans, driving the sea surface temperature. Journal of Physical Oceanography 22, 859–881.

Cernohorský, Z., 1977. Rhizocarpon Ram. em. Th. Fr. subgen. Rhizocarpon. In: Poelt, J., Vezda, A., (eds.), Bestimmungsschlüssel Europäischer Flechten, Ergänzungsheft 1. Vaduz, pp. 217–231.

Chen, C., Rose, J., 2008. Assessment of remote sensed imagery on the analysis of landforms in Glen Roy. In: Palmer, A.P., Lowe, J.J., Rose, J. (eds.), The Quaternary of Glen Roy and vicinity: Field guide. Quaternary Research Association, London, pp. 36–45.

Chenet, M., Roussel, E., Jomelli, V., Grancher, D., 2010. Asynchronous Little Ice Age glacial maximum extent in southeast Iceland. Geomorphology 114(3), 253–260.

Chenet, M., Roussel, E., Jomelli, V., Grancher, D., Cooley, D., 2011. A response to the commentary of M. Dąbski about the paper 'Asynchronous Little Ice Age glacial maximum extent in southeast Iceland' (Geomorphology (2010), 114, 253–260). Geomorphology 128(1–2), 103–104.

Church, J.A., White, N.J., Konikow, L.F., Domingues, C.M., Cogley, J.G., Rignot, E., Gregory, J.M., van den Broeke, M.R., Monaghan, A.J., Velicogna, I., 2011. Revisiting the Earth's sea-level and energy budgets from 1961 to 2008. Geophysical Research Letters 38, L18601, DOI: 10.1029/2011GL048794.

Clark, C.D., Hughes, A.L.C., Greenwood, S.L., Spagnolo, M., Ng, F.S.L., 2009. Size and shape characteristics of drumlins, derived from a large sample, and associated scaling laws. Quaternary Science Reviews 28, 677–692.

Clayton, A.I., 2011. Remote sensing of subglacial bedforms from the British Ice Sheet using an Unmanned Aerial System (UAS): Problems and Potential. Unpublished MSc thesis, University of Durham, UK, 117 pp.

Cogley, J.G., 2009. Geodetic and direct mass-balance measurements: comparison and joint analysis. Annals of Glaciology 50(50), 96–100.

Colman A.W., 1997. Prediction of summer central England temperature from preceding north Atlantic winter sea surface temperature. International Journal of Climatology 17, 1285–1300.

Colman A.W., Davey M.K., 1999. Prediction of summer temperature, rainfall and pressure in Europe from preceding winter North Atlantic ocean temperature. International Journal of Climatology 19, 513–536.

Cook-Talbot, J.D., 1991. Sorted circles, relative-age dating and palaeo-environmental reconstruction in an alpine periglacial environment, eastern Jotunheim, Norway: Lichenometric and weathering-based approaches. The Holocene 1, 128–141.

Cooley, D., Naveau, P., Jomelli, V., Rabatel, A., Grancher, D., 2006. A Bayesian hierarchical extreme value model for lichenometry. Environmetrics 17, 555–574.

Cuffey, K.M., Clow, G.D., 1997. Temperature, accumulation and ice sheet elevation in central Greenland through the last deglacial transition. Journal of Geophysical Research 102(C12), 26,383–26,396.

Cuffey, K.M., Paterson, W.S.B., 2010. The Physics of Glaciers (Fourth Edition). Butterworth-Heinemann, Burlington, MA, USA and Kidlington, Oxford, UK, 693 pp.

Danish General Staff, 1904. Sheet 96-NA, 1:50.000. The topographic department of the Danish General Staff, Copenhagen.

Darvill, C.M., Stokes, C.R., Bentley, M.R., Lovell, H., 2014. A glacial geomorphological map of the southernmost ice lobes of Patagonia: the Bahía Inútil – San Sebastián, Magellan, Otway, Skyring and Río Gallegos lobes. Journal of Maps 10(3), 500–520.

Davis, P.T., Briner, J.P., Coulthard, R.D., Finkel, R.W., Miller, G.H., 2006. Preservation of Arctic landscapes overridden by cold-based ice sheets. Quaternary Research 65, 156–163.

Dąbski, M., 2010. A commentary to 'Asynchronous Little Ice Age glacial maximum extent in southeast Iceland' by Chenet et al. (Geomorphology 114 (2010) 253–260); a case of Fláajökull. Geomorphology 120(3–4), 365–367.

Delworth, T.L., 1996. North Atlantic interannual variability in a coupled ocean–atmosphere model. Journal of Climate 9, 2356–2375.

Denton, G.H., Karlén, W., 1973. Lichenometry: its application to holocene moraine studies in southern Alaska and Swedish Lapland. Arctic and Alpine Research 5, 347–372.

Deser, C., Timlin, M.S., 1997. Atmosphere–ocean interaction on weekly time scales in the North Atlantic and Pacific. Journal of Climate 10, 393–408.

d'Oleire-Oltmanns, S., Marzolff, I., Peter, K.D., Ries, J.B., 2012. Unmanned Aerial Vehicle (UAV) for monitoring soil erosion in Morocco. Remote Sensing 4, 3390–3416.

Dowdeswell, J.A., Sharp, M.J., 1986. Characterization of pebble fabrics in modern terrestrial glacigenic sediments. Sedimentology 33, 699–710.

Drinkwater, K.F., Miles, M., Medhaug, I., Otterå. O.H., Kristiansen, T., Sundby, S., Gao, Y., 2014. The Atlantic Multidecadal Oscillation: Its manifestations and impacts with special emphasis on the Atlantic region north of 60°N. Journal of Marine Systems 133, 117–130.

Dugmore, A.J., 1987. Holocene glacier fluctuation around Eyjafjallajökull, South Iceland. Unpublished PhD thesis, University of Aberdeen, UK, 114 pp.

Dugmore, A.J., 1989. Tephrochronological studies of Holocene glacier fluctuations in south Iceland. In: Oerlemans, J. (ed.), Glacier fluctuations and climate change. Dordrecht, Kluwer Academic Publishers, pp. 37–55.

Dugmore, A.J., Sugden, D.S., 1991. Do the anomalous fluctuation of Sólheimajökull reflect ice-divide migration? Boreas 20, 105–113.

Einarsson, M.A., 1984. Climate of Iceland. In: van Loon, H. (ed.), World Survey of climatology 15, Climates of the Oceans. Elsevier, Amsterdam, pp. 673–697.

Einarsson, Þ., 1963. Pollen analytical studies on the vegetation and climate history of Iceland in Late and Postglacial times. In: Löve, A., Löve, D. (eds.), North Atlantic Biota and Their History. Pergamon Press, Oxford, pp. 355–365.

Eiríksson, H.H., 1931. Observations and Measurements of some Glaciers in Austur-Skaftafellssýla. Visindaf61ag Islendinga XII. Societas Scientiarum Islandica, University of Iceland, Reykjavík, 35 pp.

Evans, D.J.A., 2000. A gravel outwash/deformation till continuum, Skalafellsjokull, Iceland. Geografiska Annaler 82A(4), 499–512.

Evans, D.J.A., 2003a. Ice-Marginal Terrestrial Landsystems: Active Temperate Glacier Margins. In: Evans, D.J.A. (ed.), Glacial Landsystems. Arnold, London, pp. 12–43.

Evans, D.J.A. (ed.), 2003b. Glacial Landsystems. Arnold, London, 532 pp.

Evans, D.J.A., 2005. The glacier-marginal landsystems of Iceland. In: Caseldine, C., Russell, A., Harðardóttir, J., Knudsen, Ó. (eds.), Iceland – Modern Processes and Past Environments. Developments in Quaternary Sciences 5, 93–126.

Evans, D.J.A., 2009a. Controlled moraines: origins, characteristics and palaeoglaciological implications. Quaternary Science Reviews 28, 183–208.

Evans, D.J.A., 2009b. Special theme: Modern analogues in Quaternary palaeoglaciological reconstruction. Quaternary Science Reviews 28, 181–182.

Evans, D.J.A., 2013. The glacial and periglacial research – geomorphology and retreating glaciers. In: Shroder, J., Giardino, R., Harbor, J. (eds.), Treatise on Geomorphology 8, Glacial and Periglacial Geomorphology. Academic Press, San Diego, CA, pp. 460–478.

Evans, D.J.A., Archer, S., Wilson, D.J.H. 1999a. A comparison of the lichenometric and Schmidt hammer dating techniques based on data from the proglacial areas of some Icelandic glaciers. Quaternary Science Reviews 18, 13–41.

Evans, D.J.A., Benn, D.I. (eds.), 2004. A Practical Guide to the Study of Glacial Sediments. Arnold, London, 266 pp.

Evans, D.J.A., Ewertowski, M., Orton, C., submitted. Fláajökull (north lobe), Iceland: active temperate piedmont lobe glacial landsystem. Journal of Maps.

Evans, D.J.A., Hiemstra, J.F., 2005. Till deposition by glacier submarginal, incremental thickening. Earth Surface Processes and Landforms 30, 1633–1662.

Evans, D.J.A., Lemmen, D.S., Rea, B.R., 1999b. Glacial landsystems of the southwest Laurentide Ice Sheet: modern Icelandic analogues. Journal of Quaternary Science 14, 673–691.

Evans, D.J.A., Orton, C., 2014. Heinabergsjökull and Skalafellsjökull, Iceland: Active Temperate Piedmont Lobe and Outwash Head Glacial Landsystem. Journal of Maps, DOI: 10.1080/17445647.2014.919617.

Evans D.J.A., Phillips E.R., Hiemstra J.F., Auton C.A., 2006. Subglacial till: Formation, sedimentary characteristics and classification. Earth-Science Reviews 78(1–2), 115–176.

Evans, D.J.A., Shulmeister, J., Hyatt, O., 2010. Sedimentology of latero-frontal moraines and fans on the west coast of South Island, New Zealand. Quaternary Science Reviews 29(27–28), 3790–3811.

Evans, D.J.A., Twigg, D.R., 2000. Breiðamerkurjökull 1998. 1:30,000 Scale Map. University of Glasgow and Loughborough University.

Evans, D.J.A., Twigg, D.R., 2002. The active temperate glacial landsystem: a model based on Breiðamerkurjökull and Fjallsjökull, Iceland. Quaternary Science Reviews 21, 2143–2177.

Evans, D.J.A., Rea, B.R., 1999. Geomorphology and sedimentology of surging glaciers: a land-systems approach. Annals of Glaciology 28, 75–82.

Evans, D.J.A., Rea, B.R., Benn, D.I., 1998. Subglacial deformation and bedrock plucking in areas of hard bedrock. Glacial Geology and Geomorphology (rp04/1998—http://ggg.qub.ac.uk/ggg/papers/full/1998/rp041998/rp04.html).

Evans, D.J.A., Young, N.J.P., Ó Cofaigh, C., 2014. Glacial geomorphology of terrestrial-terminating fast flow lobes/ice stream margins in the southwest Laurentide Ice Sheet. Geomorphology 204, 86–113.

Eyþórsson, J. 1931. On the present position of the glaciers in Iceland: some preliminary studies and investigations in the summer 1930. Vísindafélag Isl. Rit. 10.

Eyþórsson, J. 1935. On the variations of glaciers in Iceland. Some studies made in 1931. Geografiska Annaler 17, 121–137.

Eyþórsson, J. 1963. Variation of Iceland glaciers 1931–1960. Jökull 13, 31–33.

Eyþórsson, J. 1962–1966: Jöklabreytingar (Glacier variations in metres). Jökull 12, 37–39; 13, 29–30; 14, 97–99; 15, 148–150.

Fay, H., 2002. Formation of ice block obstacle marks during the November 1996 glacier-outburst flood (jökulhlaup), Skeiðarársandur, southern Iceland. In: Martini, I.P., Baker, V.R., Garzon, G. (eds.), Flood and Megaflood Deposits: Recent and Ancient. Special Publication of the International Association of Sedimentologists.

Fay, M.P., Proschan, M.A., 2010. Wilcoxon-Mann-Whitney or *t*-test? On assumptions for hypothesis tests and multiple interpretations of decision rules. Statistics Surveys 4, 1–39.

Flowers, G.E., Björnsson, H., Geirsdóttir, Á., Miller, G.H., Black, J.L., Clarke, G.K.C., 2008. Holocene climate conditions and glacier variation in central Iceland from physical modeling and empirical evidence. Quaternary Science Reviews 27, 797–813.

Flowers, G.E., Marshall, S.J., Björnsson, H., Clarke, G.K.C., 2005. Sensitivity of Vatnajökull ice cap hydrology and dynamics to climate warming over the next 2 centuries, Journal of Geophysical Research 110, F02011, DOI: 10.1029/2004JF000200.

Forman, S.L., Mann, D.H., Miller, G.H., 1987. Late Weichselian and Holocene relative sea level history of Broggerhalvoya, Spitsbergen. Quaternary Research 27, 41–50.

Fuchs, M., Owen, L.A., 2008. Luminescence dating of glacial and associated sediments: review, recommendations and future directions. Boreas 37, 636–659.

Funder, S., 1972. Deglaciation of the Scoresby Sund fjord region, North-East Greenland. In: Price, R.J., Sugden, D.E. (eds.), Polar Geomorphology, IBG Special Publication No. 4, pp. 33–41.

Funder, S., 1989. Quaternary geology of the ice-free areas and adjacent shelves of Greenland. In: Fulton, R.J. (ed.), Quaternary Geology of Canada and Greenland (Geology of Canada). Geological Society of America, Boulder, CO, pp. 741–792.

Gardner, A.S., Moholdt, G., Cogley, J.G., Wouters, B., Arendt, A.A., Wahr, J., Berthier, E., Hock, R., Pfeffer, W.T., Kaser, G., Ligtenberg, S.R.M., Bolch, T., Sharp, M.J., Hagen, J.O., van den Broeke, M.R., Paul, F., 2013. A reconciled estimate of glacier contributions to sea level rise: 2003 to 2009. Science 340, 852–857.

Geirsdóttir, A., Miller, G.H., Axford, Y., Olafsdottir, S., 2009. Holocene and latest Pleistocene climate and glacier fluctuations in Iceland. Quaternary Science Reviews 28, 2107–2118.

Gheorghiu, D.M., Fabel, D., 2013. Revised surface exposure ages in the southeast part of the Monadhliath Mountains, Scotland. In: Boston, C.M., Lukas, S., Merritt, J.W. (eds.), The Quaternary of the Monadhliath Mountains and the Great Glen: Field Guide. Quaternary Research Association, London, pp. 183–189.

Gheorgiu, D.M., Fabel, D., Hansom, J.D., Xu, S., 2012. Lateglacial surface exposure dating in the Monadhliath Mountains, Central Highlands, Scotland. Quaternary Science Reviews 41, 132–146.

Gibbons, A.B., Megeath, J.D., Pierce, K.L., 1984. Probability of moraine survival in a succession of glacial advances. Geology 12, 327–330.

Gordon, J. E., Sharp, M. 1983. Lichenometry in dating recent glacial landforms and deposits, southeast Iceland. Boreas 12, 191–200.

Graham, D.J., Midgley, N.G., 2000. Graphical representation of particle shape using triangular diagrams: an Excel spreadsheet method. Earth Surface Processes and Landforms 25, 1473–1477.

Grove, J.M., 1988. The Little Ice Age (First Edition). Methuen, London, 498 pp.

Grove, J.M., 2001. The initiation of the ‘Little Ice Age’ in regions round the North Atlantic. Climatic Change 48, 53–82.

Grove, J.M., 2004. Little ice ages: ancient and modern. Volume 1 (Second Edition). Routledge, London, 432 pp.

Guðmundsson, H.J., 1997. A review of the Holocene environmental history of Iceland. Quaternary Science Reviews 16, 81–92.

Guðmundsson, H.J., 1998a. Holocene glacier fluctuations and tephrochronology of the Öræfi district, Iceland. Unpublished PhD thesis, University of Edinburgh, UK.

Guðmundsson, H.J., 1998b. Holocene glacier fluctuations of the Eiríksjökull ice cap, west central Iceland. Jökull 46, 17–28.

Guðmundsson, M.T., 2000. Mass balance and precipitation on the summit plateau of Öræfajökull, SE Iceland. Jökull 48, 49–54.

Guðmundsson, S., Björnsson, H., Magnússon, E., Berthier, E., Pálsson, F., Guðmundsson, M.T., Högnaðóttir, T., Dall, J., 2011. Response of Eyjafjallajökull, Torfajökull and Tindfjallajökull ice caps in Iceland to regional warming, deduced by remote sensing. Polar Research 30, 72–82

Haeberli, W. 1995. Glacier fluctuations and climate change detection: operational elements of a worldwide monitoring strategy. WMO Bulletin 44(1), 23–31.

Haeberli, W., J. Noetzli, M. Zemp, S. Baumann, R. Frauenfelder and M. Hoelzle, (eds.)., 2005. Glacier Mass Balance Bulletin No. 8 (2002–2003). IUGG (CCS) / UNEP / UNESCO / WMO, World Glacier Monitoring Service, Zurich, Switzerland, 100 pp.

Haeberli, W., Zemp, M. and Hoelzle, M. (eds.), 2007. Glacier Mass Balance Bulletin No. 9 (2004-2005). ICSU (FAGS) / IUGG (IACS) / UNEP / UNESCO / WMO, World Glacier Monitoring Service, Zurich, Switzerland, 100 pp.

Haeberli, W., Gärtner-Roer, I., Hoelzle, M., Paul, F. and Zemp, M. (eds.), 2009. Glacier Mass Balance Bulletin No. 10 (2006-2007). ICSU (WDS) / IUGG (IACS) / UNEP / UNESCO / WMO, World Glacier Monitoring Service, Zurich, Switzerland, 96 pp.

Hambrey, M.J., Lawson, W., 2000. Structural styles and deformation fields in glaciers: a review. In: Maltman, A.J., Hubbard, B., Hambrey, M.J. (eds.), Deformation of glacial materials. Geological Society of London Special Publication 176, pp. 321–336.

Hambrey, M.J., Müller, F., 1978. Structure and ice deformation in the White Glacier, Axel Heiberg Island, Northwest Territories, Canada. Journal of Glaciology 20, 41–66.

Hanna, E., Cappelen, J., 2003. Recent cooling in coastal southern Greenland and relation with the North Atlantic Oscillation. Geophysical Research Letters 30(3), 1132, DOI: 10.1029/2002GL015797.

Hanna, E., Cappelen, J., Allan, R., Jónsson, T., le Blancq, F., Lillington, T., Hickey, K., 2008. New insights into North European and North Atlantic surface pressure variability, storminess and related climatic change since 1830. Journal of Climate 21, 6739–6766.

Hanna, E., Jónsson, T., Box, J.E., 2004. An analysis of Icelandic climate since the nineteenth century. International Journal of Climatology 24, 1193–1210.

Hannesdóttir, H., Björnsson, H., Pálsson, F., Aðalgeirsdóttir, G., Guðmundsson, S., 2014. Variations of southeast Vatnajökull ice cap (Iceland) 1650–1900 and reconstruction of the glacier surface geometry at the Little Ice Age maximum. Geografiska Annaler: Series A, Physical Geography, DOI: 10.1111/geoa.12064.

Harper, J.T., Humphrey, N.F., Pfeffer, W.T., 1998. Crevasse patterns and the strain-rate tensor: A high-resolution comparison. Journal of Glaciology 44, 68–76.

Harris, C., Bothamley, K. 1984. Englacial deltaic sediments as evidence for basal freezing and marginal shearing, Leirbreen, southern Norway. Journal of Glaciology 30, 30–34.

Hart, J.K., 1995. Subglacial erosion, deposition and deformation associated with deformable beds. Progress in Physical Geography 19(2), 173–191.

Hattestrand, C., Stroeven, A.P., 2002. A relict landscape in the centre of Fennoscandian glaciation: geomorphological evidence of minimal Quaternary glacial erosion. Geomorphology 44, 127–143.

Häberle, T., 1991. Holocene glacial history of the Horgardalur area, Trollaskagi, northern Iceland. In: Maizels, J.K., Caseldine, C.J. (eds.), Environmental Change in Iceland: Past and Present. Kluwer, Dordrecht, pp. 193–202.

Häberle, T., 1994. Glacial, Late glacial and Holocene history of the Hiirgardalur area, Trollaskagi, Northern Iceland. In: Stötter, J., Wilhelm, F. (eds.), Environmental Change in Iceland. Munchener Geog. Abl. B12, 41–63.

Häkkinen, S., Rhines, P.B., 2004. Decline of subpolar North Atlantic circulation during the 1990s. Science 304, 555–559,

Häkkinen, S., Rhines, P.B., Worthen, D.L., 2013. Northern North Atlantic sea surface height and ocean heat content variability. Journal of Geophysical Research: Oceans 118, 3670–3678.

Hátún, H., Sandø, A.B., Drange, H., Hansen, B., Valdimarsson, H., 2005. Influence of the Atlantic subpolar gyre on the thermohaline circulation. Science 309, 1841–1844.

Heikinnen, O., 1994. Using dendrochronology for the dating of land surfaces. In: Beck, C. (ed.), Dating in surface context. New Mexico University Press, pp. 213–230.

Helland, A. 1882. Islædingen Sveinn Pálssons beskrivelser of islandke vulkaner og bræer. Den Norske Turisforensing, Årbog.

Henderson, E., 1819. Iceland: or the Journal of a Residence in that Island, during the Years 1814 and 1815. Wayward Innes, Edinburgh.

Hicock, S.R., 1992. Lobal interactions and rheologic superposition in subglacial till near Bradtville, Ontario, Canada. Boreas 21, 73–88.

Hicock, S.R., Dreimanis, A., 1989. Sunnybrook drift indicates a grounded early Wisconsin glacier in the Lake Ontario basin. Geology 17, 169–172.

Hicock, S.R., Dreimanis, A., 1992a. Sunnybrook drift in the Toronto area, Canada: reinvestigation and reinterpretation. In: Clark, P.U., Lea, P.D. (eds.), The Last Interglacial–Glacial Transition in North America. Geological Society of America Special Paper, vol. 270, pp. 139–161.

Hicock, S.R., Dreimanis, A., 1992b. Deformation till in the Great Lakes region: implications for rapid flow along the south-central margin of the Laurentide Ice Sheet. Canadian Journal of Earth Sciences 29, 1565–1579.

Hicock, S.R., Fuller, E.A., 1995. Lobal interactions, rheologic superposition, and implications for a Pleistocene ice stream on the continental shelf of British Columbia. Geomorphology 14, 167–184.

Hirabayashi, Y., Zhang, Y., Watanabe, S., Koirala, S., Kanae, S., 2013. Projection of glacier mass changes under a high-emission climate scenario using the global glacier model HYOGA2. Hydrological Research Letters 7, 6–11.

Hjört, C., Ingolfsson, Ó., Norðdahl, H., 1985. Late Quatemary Geology and Glacial history of Homstrandir. Northwest Iceland. A reconnaissance study. Jökull 35, 9–29.

Hopkins, W., 1844. On the motion of glaciers. Transactions of the Cambridge Philosophical Society 8, 50–74.

Hopkins, W., 1862. On the theory of the motion of glaciers. Philosophical Transactions of the Royal Society of London 152, 677–745.

Hoppe, G., 1952. Hummocky moraine regions, with special reference to the interior of Norrbotten. Geografiska Annaler 34, 1–72.

Howarth, P.J., 1968. Geomorphological and Glaciological Studies, Eastern Breiðamerkurjökull, Iceland. Unpublished PhD thesis, University of Glasgow, UK.

Howarth, P.J., 1971. Investigations of two eskers at eastern Breiðamerkurjökull, Iceland. Arctic and Alpine Research 3, 305–318.

Howarth, P.J., Price, R.J., 1969. The proglacial lakes of Breiðamerkurjökull and Fjallsjökull, Iceland. Geographical Journal 135, 573–581.

Howat, I.M., Eddy, A., 2011. Multi-decadal retreat of Greenland's marine-terminating glaciers. Journal of Glaciology 57(203), 389–396.

Howat, I.M., Joughin, I., Fahnestock, M., Smith, B.E., Scambos, T.A., 2008. Synchronous retreat and acceleration of southeast Greenland outlet glaciers 2000–06: ice dynamics and coupling to climate. Journal of Glaciology 54(187), 646–660.

Hubbard, A., Bradwell, T., Golledge, N., Hall, A., Patton, H., Sugden, D., Cooper, R., Stoker, M., 2009. Dynamic cycles, ice-streams and their impact on the extent, chronology and deglaciation of the British–Irish Ice Sheet. Quaternary Science Reviews 28, 758–776.

Hubbard, B., Glasser, N.F., 2005. Field techniques in glaciology and glacial geomorphology. John Wiley and Sons, Chichester, 400 pp.

Hubbard, B., Sharp, M.J., 1989. Basal ice formation and deformation: a review. Progress in Physical Geography 13, 529–558.

Hubbard, B., Sharp, M.J., 1993. Weertman regelation, multiple refreezing effects and the isotopic evolution of the basal ice layer. Journal of Glaciology 39, 275–291.

Hugenholtz, C.H., Levin, N., Barchyn, T.E., Baddock, M.C., 2012. Remote sensing and spatial analysis of aeolian sand dunes: a review and outlook. Earth-Science Reviews 111, 319–334.

Hugenholtz, C.H., Whitehead, K., Brown, O.W., Barchyn, T.E., Moorman, B.J., LeClair, A., Riddell, K., Hamilton, T., 2013. Geomorphological mapping with a small unmanned aircraft system (sUAS): feature detection and accuracy assessment of a photogrammetrically-derived digital terrain model. Geomorphology 194, 16–24.

Hughes, A.L.C., Clark, C.D., Jordan, C.J., 2010. Subglacial bedforms of the last British Ice Sheet. Journal of Maps 2010, 543–563.

Humlum, O., 1985. Genesis of an imbricate push moraine, Hofdabrekkujokull, Iceland. Journal of Geology 93, 185–195.

Hurrell, J.W., 1995. Decadal trends in the North Atlantic Oscillation regional temperatures and precipitation. Science 269, 676–679.

Hurrell, J.W., 1996. Influence of variations in extratropical wintertime teleconnections on Northern Hemisphere temperature. Geophysical Research Letters 23, 665–668.

Hurrell, J.W., Deser, C., 2009. North Atlantic climate variability: The role of the North Atlantic Oscillation. Journal of Marine Systems 78, 28–41.

Hurrell, J.W., Kushnir, Y., Ottersen, G., Visbeck, M., 2003. An overview of the North Atlantic Oscillation. Geophysical Monograph 134, 1–35.

Hurrell, J.W., NCAR Staff [National Center for Atmospheric Research Staff], 2014. Hurrell North Atlantic Oscillation (NAO) Index (station-based). Available at: https://climatedataguide.ucar.edu/climate-data/hurrell-north-atlantic-oscillation-nao-index-station-based.

Hurrell, J.W., van Loon, H., 1997. Decadal variations in climate associated with the North Atlantic Oscillation. Climate Change 36, 301–326

Ingólfsson, Ó., Norðdahl, H., Schomacker, A., 2010. Deglaciation and Holocene Glacial History of Iceland. In: Schomacker, A., Krüger, J., Kjær, K. (eds.), The Mýrdalsjökull Ice Cap, Iceland. Glacial processes, sediments and landforms on active volcano. Developments in Quaternary Sciences 13, 51–68.

Innes, J.L., 1982. Lichenometric use of an aggregated Rhizocarpon 'species'. Boreas 11, 53–57.

Innes, J.L., 1983. Development of lichenometric dating curves for Highland Scotland. Transactions of the Royal Society of Edinburgh, Earth Sciences 74, 23–32.

Innes, J.L., 1985. Lichenometry. Progress in Physical Geography 9(2), 187–254.

Innes, J.L., 1986. The size-frequency distributions of the lichens time at Storbreen, south-west Norway. Journal of Biogeography 13, 283–291.

Innes, J.L., 1988. The use of lichens in dating. In: Galun, M. (ed.), CRC Handbook of Lichenology, Volume III. CRC Press, Boca Raton, pp. 75–91.

IPCC, 2007. Climate Change 2007: The Physical Science Basis. Contribution of Working Group I to the Fourth Assessment Report of the Intergovernmental Panel on Climate Change [Solomon, S., Qin, D., Manning, M., Chen, Z., Marquis, M., Averyt, K.B., Tignor, M., Miller, H.L. (eds.)]. Cambridge University Press, Cambridge, United Kingdom and New York, NY, USA, 996 pp.

IPCC, 2013. Climate Change 2013: The Physical Science Basis. Contribution of Working Group I to the Fifth Assessment Report of the Intergovernmental Panel on Climate Change [Stocker, T.F., Qin, D., Plattner, G.-K., Tignor, M., Allen, S.K., Boschung, J., Nauels, A., Xia, Y., Bex, V., Midgley, P.M. (eds.)]. Cambridge University Press, Cambridge, United Kingdom and New York, NY, USA, 1535 pp.

Jacob, T., Wahr, J., Pfeffer, W.T., Swenson, S., 2012. Recent contributions of glaciers and ice caps to sea level rise. Nature 482, 514–518.

Jaksch, K., 1970. Beobachtung in den Gletschervorfelden des Sóolheima- und Sídujökull im Sommer 1970. Jökull 20, 45–49.

Jaksch, K., 1975. Das Gletschervorfeld des Sólheimajökull. Jökull, 25, 34–38.

Johnson, M.D., Schomacker, A., Benediktsson, I.Ö., Geiger, A.J., Ferguson, A., Ingólfsson, Ó., 2010. Active drumlin field revealed at the margin of Múlajökull, Iceland: a surge-type glacier. Geology 38, 943–946.

Johnson, W.H., Hansel, A.K., 1999. Wisconsin episode glacial landscape of central Illinois: a product of subglacial deformation processes? In: Mickelson, D.M., Attig, J.W. (eds.), Glacial Processes: Past and Present. Geological Society of America Special Paper 337, pp. 121–135.

Jomelli, V., Grancher, D., Naveau, P., Cooley, D., Brunstein, D., 2007. Assessment study of lichenometric methods for dating surfaces. Geomorphology 86, 131–143.

Jomelli, V., Grancher, D., Brunstein, D., Solomina, O., 2008. Recalibration of the yellow Rhizocarpon growth curve in the Cordillera Blanca (Peru) and implications for LIA chronology. Geomorphology 93, 201–212.

Jóhannesson, T., 1986. The response time of glaciers in Iceland to changes in climate. Annals of Glaciology 8, 100–101.

Jóhannesson, T., 1997. The response of two Icelandic glaciers to climatic warming computed with degree-day mass balance model coupled to a dynamic glacier model. Journal of Glaciology 43, 321–327.

Jóhannesson, T., Björnsson, H., Magnússon, E., Guðmundsson, S., Pálsson, F., Sigurðsson, O., Torsteinsson, T., Berthier, E., 2013. Ice-volume changes, bias-estimation of mass-balance measurements and changes in subglacial lakes derived by LiDAR-mapping of the surface of Icelandic glaciers, Annals of Glaciology 54, 63–74.

Jóhannesson, T., Björnsson, H., Pálsson, F., Sigurðsson, O., Þorsteinsson, Þ., 2011. LiDAR mapping of the Snæfellsjökull ice cap, western Iceland. Jökull 61, 19–32.

Jóhannesson, T., Raymond, C., Waddington, E., 1989. Time-scale for adjustment of glaciers to changes in mass balance. Journal of Glaciology 35(121), 355–369.

Jóhannesson, T., Sigurðsson, O., 1998. Interpretation of glacier variations in Iceland 1930–1995. Jökull 45, 27–33.

Jónsson, S.A., Schomacker, A., Benediktsson, Í.Ö., Ingólfsson, Ó., Johnson, M.D., 2014. The drumlin field and the geomorphology of the Múlajökull surge-type glacier, central Iceland. Geomorphology 207, 213–220.

Kaplan, M.R., Hein, A.S., Hubbard, A., Lax, S.M., 2009. Can glacial erosion limit the extent of glaciation? Geomorphology 103(2), 172–179.

Kaser, G., Cogley, J.G., Dyurgerov, M.B., Meier, M.F., Ohmura, A., 2006. Mass balance of glaciers and ice caps: consensus estimates for 1961–2004. Geophysical Research Letters 33, DOI: 10.1029/2006GL027511.

Kerr, R.A., 2000. North Atlantic climate pacemaker for centuries. Science 288(5473), 1984–1985.

Kessler, M.A., Anderson, R.S., Stock, G.M., 2006. Modeling topographic and climatic control of east–west asymmetry in Sierra Nevada glacier length during the Last Glacial Maximum. Journal of Geophysical Research 111(F2), F02002, DOI: 10.1029/2005JF000365

Kirkbride, M.P. 2002. Icelandic climate and glacier fluctuations through the termination of the ‘Little Ice Age’. Polar Geography 26(2), 116–133.

Kirkbride, M.P., Brazier, V., 1998. A critical evaluation of the use of glacier chronologies in climatic reconstruction, with reference to New Zealand. In: Owen, L.A. (ed.), Mountain Glaciation. Quaternary Proceedings N6, Supplement 1 to Journal of Quaternary Science Volume 13. Wiley, Chichester, pp. 55–64.

Kirkbride, M.J., Deline, P., 2013. The formation of supraglacial debris covers by primary dispersal from transverse englacial debris bands. Earth Surface Processes and Landforms 38(15), 1779–1792.

Kirkbride, M.J., Dugmore, A.J., 2001a. Can lichenometry be used to date the 'Little Ice Age' maximum in Iceland? Climatic Change 48, 151–167.

Kirkbride, M.P., Dugmore, A.J., 2001b. Timing and significance of mid-Holocene glacier advances in northern and central Iceland. Journal of Quaternary Science 16, 145–153.

Kirkbride, M.P., Dugmore, A.J., 2006. Responses of mountain ice caps in central Iceland to Holocene climate change. Quaternary Science Reviews 25, 1692–1707.

Kirkbride, M.P., Dugmore, A.J., 2008. Two millennia of glacier advances from southern Iceland dated by tephrochronology. Quaternary Research 70, 398–411.

Kirkbride, M.P., Winkler, S., 2012. Correlation of Late Quaternary moraines: impact of climate variability, glacier response, and chronological resolution. Quaternary Science Reviews 46, 1–29.

Kjær, K.H., Krüger, J., 2001. The final phase of dead-ice development: processes and sediment architecture, Kötlujökull, Iceland. Sedimentology 48, 935–952.

Kjær, K.H., Sultan, L., Krüger, J., Schomacker, A., 2004. Architecture and sedimentation of outwash fans in front of the Mýrdalsjökull ice cap, Iceland. Sedimentary Geology 172, 139–163.

Klok, E.J., Oerlemans, J., 2003. Deriving historical equilibrium-line altitudes from a glacier length record by linear inverse modelling. The Holocene 13, 343–351.

Kruger, J., 1985. Formation of a push moraine at the margin of Hofjabrekkujökull, south Iceland. Geografiska Annaler 67A, 199–212.

Kruger, J., 1987. Traek af et glaciallandskabs udvikling ved nordranden af Myrdalsjökull, Iceland. Dansk Geologisk Foreningens Arsskrift for 1986, 49–65.

Kruger, J., 1993. Moraine ridge formation along a stationary ice front in Iceland. Boreas 22, 101–109.

Krüger, J., 1994. Glacial processes, sediments, landforms and stratigraphy in the terminus region of Mýrdalsjökull, Iceland. Folia Geographica Danica 21, 1–233.

Krüger, J., 1995. Origin, chronology and climatological significance of annual moraine ridges at Mýrdalsjökull, Iceland. The Holocene 5, 420–427.

Kruger, J., 1996. Moraine ridges formed from subglacial frozen-on sediment slabs and their differentiation from push moraines. Boreas 25, 57–63.

Kruger, J., 1997. Development of minor outwash fans at Kotlujökull, Iceland. Quaternary Science Reviews 16, 649–659.

Krüger, J., Aber, J.S., 1999. Formation of supraglacial sediment accumulations on Kötlujökull, Iceland. Journal of Glaciology 45, 400–402.

Krüger, J., Schomacker, A., Benediktsson, Í.Ö., 2010. Ice-marginal environments: geomorphic and structural genesis of marginal moraines at Mýrdalsjökull. In: Schomacker, A., Krüger, J., Kjær, K. (eds.), The Mýrdalsjökull Ice Cap, Iceland. Glacial processes, sediments and landforms on active volcano. Developments in Quaternary Sciences 13, pp. 79–104.

Kruger, J., Thomsen, H.H., 1984. Morphology, stratigraphy and genesis of small drumlins in front of the glacier Mýrdalsjökull, south Iceland. Journal of Glaciology 30, 94–105.

Knight, J.R., Allan, R.J., Folland, C.K., Vellinga, M., Mann, M.E., 2005. A signature of persistent natural thermohaline circulation cycles in observed climate. Geophysical Research Letters 32, L20708, DOI: 10.1029/2005GL024233.

Krzyszkowski, D., 2002. Sedimentary successions in ice-marginal fans of the Late Saalian glaciation, southwestern Poland. Sedimentary Geology 149, 93–109.

Krzyszkowski, D., Zielinski, T., 2002. The Pleistocene end moraine fans: controls on their sedimentation and location. Sedimentary Geology 149, 73–92.

Kugelman, O., 1990. Datierung neuzeitlicher Gletschervorstöße im Svarfadardalur/Skídadalur (Nordisland) mit einer neu erstallten Flechtenwachstumskurve. Münchener Geog. Abl. B8, 36–59.

Kugelman, O., 1991. Dating recent glacier advances in the Svarfadardalur/Skídadalur area of northern Iceland by means of a new lichen curve. In: Maizels, J.K., Caseldine, C.J. (eds.), Environmental Change in Iceland: Past and Present. Kluwer, Dordrecht, pp. 203–217

Kuhn, M., 1985. Fluctuations of climate and mass balance: different responses of two adjacent glaciers. Zeitschrift für Gletscherkunde und Glazialgeologie 21, 409–416.

Landvik, J.Y., Ingolfsson, O., Mienert, J., Lehman, S.J., Solheim, A., Elverhoi, A., Ottesen, D., 2005. Rethinking Late Weichselian ice sheet dynamics in coastal NW Svalbard. Boreas 34, 7–24.

Larsen, D.J., Miller, G.H., Geirsdóttir, Á., Thordarson, T., 2011. A 3000-year varved record of glacier activity and climate change from the proglacial lake Hvítárvatn, Iceland. Quaternary Science Reviews 30, 2715–2731.

Laumann, T., Nesje, A., 2009. A simple method of simulating the future frontal position of Briksdalsbreen, western Norway. The Holocene 19, 221–228.

Lawson, D.E., 1982. Mobilization, movement and deposition of active subaerial sediment flows, Matanuska Glacier, Alaska. Journal of Geology 90, 279–300.

Lawson, D.E., Strasser, J.C., Evenson, E.B., Alley, R.B., Larson, G.J., Arcone, S.A., 1998. Glaciohydraulic supercooling:a freeze-on mechanism to create stratified, debris-rich basal ice. I. Field evidence. Journal of Glaciology 44, 547–562.

Leclercq, P.W., Oerlemans, J., Cogley, J.G., 2011. Estimating the glacier contribution to sea-level rise for the period 1800–2005. Surveys in Geophysics, 32, 519–535.

Lillesand, T.M., Kiefer, R.W., Chipman, J.W., 2008. Remote sensing and image interpretation (Sixth Edition). John Wiley & Sons, Hoboken, 804 pp.

Locke, W.W., Andrews, J.T., Webber, P.J., 1979. A manual for lichenometry. British Geomorphological Research Group, Technical Bulletin 26, 1–47.

Lohmann, K., Drange, H., Bentsen, M., 2008. Response of the North Atlantic subpolar gyre to persistent North Atlantic oscillation like forcing. Climate Dynamics 32, 273–285.

Lucieer, A., Turner, D., King, D.H., Robinson, S.A., 2014. Using an unmanned aerial vehicle (UAV) to capture micro-topography of Antarctic moss beds. International Journal of Applied Earth Observation and Geoinformation 27, 53–62.

Lukas S. 2005a. A test of the englacial thrusting hypothesis of 'hummocky' moraine formation – case studies from the north-west Highlands, Scotland. Boreas 34, 287–307.

Lukas, S., 2005b. Younger Dryas moraines in the NW Highlands of Scotland: genesis, significance and potential modern analogues. Unpublished PhD thesis, University of St Andrews, UK.

Lukas, S. 2007a. Englacial thrusting and (hummocky) moraine formation: a reply to comments by Graham et al. (2007). Boreas 36, 108–113.

Lukas, S., 2007b. Early-Holocene glacier fluctuations in Krundalen, south central Norway: palaeo-glacier dynamics and palaeoclimate. The Holocene 17, 585–598.

Lukas, S., 2011. Ice-cored Moraines. In: In: Singh, V., Singh, P., Haritashya, U.K. (eds.), Encyclopaedia of Snow, Ice and Glaciers. Springer, Heidelberg, pp. 616–618.

Lukas, S., 2012. Processes of annual moraine formation at a temperate alpine valley glacier: insights into glacier dynamics and climatic controls. Boreas 41, 463–480.

Lukas, S., Benn, D.I., Boston, C.M., Brook, M.S., Coray, S., Evans, D.J.A., Graf, A., Kellerer-Pirklbauer-Eulenstein, A., Kirkbride, M.P., Krabbendam, M., Lovell, H., Machiedo, M., Mills, S.C., Nye, K., Reinardy, B.T.I., Ross, F.H., Signer, M., 2013. Clast shape analysis and clast transport paths in glacial environments: A critical review of methods and the role of lithology. Earth-Science Reviews 121, 96–116.

Lukas, S., Graf, A., Coray, S., Schlüchter, C., in press. The influence of clast lithology and fluvial reworking on the reliability of clast shape measurements in glacial environments – a case study from a temperate Alpine glacier. In: Bridgland, D.R.

(ed.), Clast Lithological Analysis. Technical Guide. Quaternary Research Association, London.

Lukas, S., Lukas, T., 2006. A glacial geological and geomorphological map of the far NW Highlands, Scotland. Parts 1 and 2. Journal of Maps 2006, 43–56, 56–58.

Lukas, S., Nicholson, L.I., Ross, F.H., Humlum, O., 2005. Formation, meltout processes and landscape alteration of high-arctic ice-cored moraines: examples from Nordenskiöld Land, central Spitsbergen. Polar Geography 29, 157–187.

Lukas, S., Spencer, J.Q.G., Robinson, R.A.J., Benn, D.I., 2007. Problems associated with luminescence dating of Late Quaternary glacial sediments in the NW Scottish Highlands. Quaternary Geochronology 2, 243–248.

Magnússon, Á., 1953. Chorographica islandic. In: Lárusson, Ó. (ed.), Safn til sögu Íslands og íslenskra bókmennta, annar flokkur I, 2. [The Story of Iceland and the Icelandic literature in the past and at present]. Hið íslenzka bókmenntafélag, Reykjavík [Written in 1702 – 1714].

Magnússon, Á., Vídalín, P., 1980. Jarðabók Árna Magnússonar og Páls Vídalín. [Farm account by Árni Magnússon and Páll Vídalín, information gather in 1702 – 1714]. Volume 1 – 13, Second Edition. Hið íslenzka fræðafélag, Reykjavík.

Magnússon, E., Björnsson, H., Dall, J., Pálsson, F., 2005. The 20th century retreat of ice caps in Iceland derived from airborne SAR: W-Vatnajökull and N-Mýrdalsjökull. Earth and Planetary Science Letters 237, 508–515.

Maizels, J., 1997. Jokulhlaup deposits in proglacial areas. Quaternary Science Reviews 16, 793–819.

Maizels, J.K., Dugmore, A.J., 1985. Lichenometric dating and tephrochronology of sandur deposits, Sólheimajökull area, southern Iceland. Jökull 35, 69–77.

Mann, H.B., Whitney, D.R., 1947. On a Test of Whether one of Two Random Variables is Stochastically Larger than the Other. Annals of Mathematical Statistics 18(1), 50–60.

Marshall, J., Kushnir, Y., Battisti, D., Chang, P., Czaja, A., Dickson, R., Hurrell, J., McCartney, M., Saravanan, R., Visbeck, M., 2001. North Atlantic climate variability, phenomena, impacts and mechanisms. International Journal of Climatology 21, 1863–1898.

Marzeion, B., Jarosch, A.H., Hofer, M., 2012. Past and future sea-level change from the surface mass balance of glaciers. Cryosphere 6, 1295–1322.

Marzeion, B., Nesje, A., 2012. Spatial patterns of North Atlantic oscillation influence on mass balance variability of European glaciers. The Cryosphere 6, 661–673.

Matthews, J.A., 1975. Experiments on the reproducability and reliability of lichenometric dates, Storbreen gletschervorfeld, southern Norway. Norsk Geografisk Tidsskrift 29, 97–109.

Matthews, J.A., 1980. Some problems and implications of ^{14}C dates from a podzol buried beneath an end moraine at Haugabreen, southern Norway. Geografiska Annaler 62A, 185–208.

Matthews, J.A., Cornish, R., Shakesby, R.A., 1979. “Saw-tooth” moraines in front of Bødalsbreen, southern Norway. Journal of Glaciology 88, 535–546.

Matthews, J.A., McCarroll, D., Shakesby, R.A., 1995. Contemporary terminal-moraine ridge formation at a temperate glacier: Styggedalsbreen, Jotunheimen, southern Norway. Boreas 24, 129–139.

McCarroll, D., 1991. The Schmidt hammer, weathering and rock surface roughness. Earth Surface Process and Landform 16, 474–480.

McCarroll, D., 2006. Average glacial conditions and the landscape of Snowdonia. In: Knight, P.G. (ed.), Glacier science and environmental change. Blackwell, Oxford, pp. 266–268.

McKinzey, K.M., Orwin, J.F., Bradwell, T., 2004. Re-dating the moraines at Skálafellsjökull and Heinabergsjökull using different lichenometric methods: implications for the timing of the Icelandic Little Ice Age maximum. Geografiska Annaler 86A, 319–355.

McKinzey, K.M., Orwin, J.F., Bradwell, T., 2005. A revised chronology of key Vatnajökull (Iceland) outlet glaciers during the Little Ice Age. Annals of Glaciology 42, 171–179.

Mehta, V., Suarez, M., Manganello, J., Delworth, T., 2000. Oceanic influence on the North Atlantic Oscillation and associated northern hemisphere climate variations: 1959–1993. Geophysical Research Letters 27, 121–124.

Meier, M.F., 1960. Mode of Flow of Saskatchewan Glacier, Alberta, Canada. US Geological Survey Professional Paper 351. US Geological Survey, Washington DC, 70 pp.

Meier, M.F., Dyurgerov, M.B., Rick, U.K., O'Neel, S., Pfeffer, W.T., Anderson, R.S., Anderson, S.P., Glazovsky, A.F., 2007. Glaciers dominate eustatic sea level rise in the 21st Century. Science 317, 1064–1067.

Mercer, J.H., 1961. The response of fjord glaciers to changes in the firn limit. Journal of Glaciology 3, 850–858.

Mernild, S.H., Hanna, E., Yde, J.C., Seidenkrantz, M.-S., Wilson, R., Knudsen, N.T., 2014. Atmospheric and oceanic influence on mass balance of northern North Atlantic region land-terminating glaciers. Geografiska Annaler 96A(4), 561–577.

Mernild, S.H., Malmros, J.K., Yde, J.C., Knudsen, N.T., 2012. Multi-decadal marine and land-terminating glacier retreat in Ammassalik region, Southeast Greenland. The Cryosphere 6, 625–639.

Miles, B.W.J., Stokes, C.R., Vieli, A., Cox, N.J., 2013. Rapid, climate-driven changes in outlet glaciers on the Pacific coast of East Antarctica. Nature 500, 563–566.

Naveau, P., Nogaja, M., Ammann, C., Yiou, P., Cooley, D., Jomelli, V., 2005. Statistical methods for the analysis of geophysical extreme events. Comptes Rendus de l'Académie des Sciences 337, 1013–1022.

Naveau, P., Jomelli, V., Cooley, D. and Rabatel, A., 2007. Modeling uncertainties in lichenometry studies with an application: the Tropical Andes (Charquini Glacier in Bolivia). Arctic, Antarctic, and Alpine Research 39, 277–285.

Nesje, A., Lie, Ø., Dahl, S.O., 2000. Is the North Atlantic Oscillation reflected in Scandinavian glacier mass balance records? Journal of Quaternary Science 15, 587–601.

NGRIP (North Greenland Ice Core Project) members, 2004. High-resolution record of Northern Hemisphere climate extending into the last interglacial period. Nature 431, 147–151.

Nick, F.M., van der Kwast, J., Oerlemans, J., 2007. Simulation of the evolution of Breidamerkurjökull in the late Holocene. Journal of Geophysical Research: Solid Earth 112(B1), B01103, DOI: 10.1029/2006JB004358.

Noller, J.S., Locke, W.W., 2000. Lichenometry. In: Noller, J.S., Sowers, J.M., Lettis, W.R. (eds.), Quaternary Geochronology: Methods and Applications. American Geophysical Union, Washington DC, pp. 261–272.

Nye, J.F., 1952. The mechanics of glacier flow. Journal of Glaciology 2(12), 82–93.

Nye, J.F., 1965. The frequency response of glaciers. Journal of Glaciology 5, 567–587.

Oerlemans, J., 1989. On the response of valley glaciers to climatic change. In: Oerlemans, J. (ed.), Glacier Fluctuations and Climatic Change. Kluwer Academic Press, Dordrecht, pp. 353–371.

Oerlemans, J., 2007. Estimating response times of Vadret da Morteratsch, Vadret da Palü, Briksdalsbreen and Nigardsbreen from their length record. Journal of Glaciology 53, 357–362.

Oerlemans, J., Anderson, V., Hubbard, A., Huybrechts, P., Jóhannesson, T., Knap, W.H., Schmeits, M., Stroeven, A.P., van de Wal, R.S.W., Wallinga, J., Zuo, Z., 1998. Modelling the response of glaciers to climate warming. Climate Dynamics 14, 267–274.

Ogilvie, A.E.J., 1984. The past climate and sea-ice record from Iceland, Part 1: Data to AD 1780. Climatic Change 6, 131–152.

Ogilvie, A.E.J., 1992. Documentary evidence for changes in the climate of Iceland, AD1500 to 1800. In: Bradley, R.S., Jones, P.D. (eds.), Climate Since AD1500. Routledge, New York, pp. 93–117.

Ogilvie, A.E.J., Jónsson, T., 2001. "Little Ice Age" Research: a perspective from Iceland. Climate Change 48, 9–52.

Olsen, J., Anderson, N.J., Knudsen, M.S., 2012. Variability of the North Atlantic oscillation over the past 5,200 years. Nature Geoscience 5, 808–812.

Orwin, J.F., McKinzey, K.M., Stephens, M.A., Dugmore, A.J., 2008. Identifying moraine surfaces with similar histories using lichen size distributions and the U^2 statistic, southeast Iceland. Geografiska Annaler 90A, 151–164.

Ó Cofaigh, C., Evans, D.J.A., Hiemstra, J.F., 2011. Formation of a stratified subglacial 'till' assemblage by ice-marginal thrusting and glacier overriding. Boreas 40(1), 1–14.

Ólafsdóttir, K.B., Geirsdóttir, Á., Miller, G.H., Larsen, D.J., 2013. Evolution of NAO and AMO strength and cyclicity derived from a 3-ka varve-thickness record from Iceland. Quaternary Science Reviews 69, 142–154.

Ólafsson, E., Pálsson, B. 1975, Travels in Iceland 1752 – 1756. Revised English Edition [originally published in 1772]. Bókaútgáfan Örn og Örlygur, Reykjavík, 186 pp.

Park, W., Latif, M., 2005. Ocean Dynamics and the Nature of Air-Sea Interactions over the North Atlantic. Journal of Climate 18(7), 982–995.

Pálsson, F., Guðmundsson, S., Björnsson, H., Berthier, E., Magnússon, E., Guðmundsson, S., Haraldsson, H.H., 2012. Mass and volume changes of Langjökull ice cap, Iceland, ~1890 to 2009, deduced from old maps, satellite images and in situ mass balance measurements. Jökull 62, 81–96.

Pálsson, S., 1945. Ferðabók Sveins Pálssonar. Dagbækur og ritgerðir 1791–1794 [The Travel Book of Sveinn Pálsson. Dairies and Essays 1791–1794]. Snælandsútgáfan, Reykjavík.

Pálsson, S., 2004. Draft of a physical, geographical and historical description of Icelandic ice mountains on the basis of a journey to the most prominent of them in 1792–1794 with four maps and eight perspective drawings. The Icelandic Literary Society, Reykjavík.

Pearce, D., Rea, B.R., Bradwell, T., McDougall, D., 2014. Glacial geomorphology of the Tweedsmuir Hills, Central Southern Uplands, Scotland. Journal of Maps 10(3), 457–465.

Pfeffer, W.T., Harper, J.T., O'Neel, S., 2008. Kinematic constraints on glacier contributions to 21st century sea level rise. Science 321, 1340–1343.

Pfeffer, W.T., Arendt, A.A., Bliss, A., Bolch, T., Cogley, J.G., Gardner, A.S., Hagen, J.-O., Hock, R., Kaser, G., Kienholz, C., Miles, E.S., Moholdt, G., Mölg, N., Paul, F., Radić, V., Rastner, P., Raup, B.H., Rich, J., Sharp, M.J., The Randolph Consortium., 2014. The Randolph Glacier Inventory: a globally complete inventory of glaciers. Journal of Glaciology 60, 537–552.

Phillips, E., Finlayson, A., Bradwell, T., Everest, J., Jones, L., 2014. Structural evolution triggers a dynamic reduction in active glacier length during rapid retreat: Evidence from Falljökull, SE Iceland. Journal of Geophysical Research: Earth Surface 119, 2194–2208.

Phillips, E., Finlayson, A., Jones, L., 2013. Fracturing, block faulting, and moulin development associated with progressive collapse and retreat of a maritime glacier: Falljökull, SE Iceland. Journal of Geophysical Research: Earth Surface 118, 1–17.

Phillips I.D., McGregor G.R., 2002. The relationship between monthly and seasonal south-west England rainfall anomalies and concurrent North Atlantic sea surface temperatures. International Journal of Climatology 22, 197–217.

Phillips, I.D., Thorpe, J., 2006. Icelandic precipitation – North Atlantic sea-surface temperature associations. International Journal of Climatology 26, 1201–1221.

Poelt, J., 1988. Rhizocarpon Ram. em. Th. Fr. Subgen. Rhizocarpon in Europe. Arctic and Alpine Research 20, 292–298.

Polyakov, I.V., Bhatt, U.S., Simmons, H.L., Walsh, D., Walsh, J.E., Zhang, X., 2005. Multidecadal variability of North Atlantic temperature and salinity during the twentieth century. Journal of Climate 18, 4562–4581.

Porter, S.C., 1989. Some geological implications of average Quaternary glacial conditions. Quaternary Research 32, 245–261.

Pratt-Sitaula, B., Burbank, D.W., Heimsath, A.M., Humphrey, N.F., Oskin, M., Putkonen, J., 2011. Topographic control of asynchronous glacial advances: a case study from

Annapurna, Nepal. Geophysical Research Letters 38(24), L24502, DOI: 10.1029/2011GL049940.

Price, R.J., 1966. Eskers near the Casement Glacier, Alaska. Geografiska Annaler 48, 111–125.

Price, R.J., 1969. Moraines, sandar, kames and eskers near Breiðamerkurjökull, Iceland. Transactions of the Institute of British Geographers 46, 17–43.

Price, R.J., 1970. Moraines at Fjallsjökull, Iceland. Arctic and Alpine Research 2, 27–42.

Price, R.J., 1971. The development and destruction of a sandur, Breiðamerkurjökull, Iceland. Arctic and Alpine Research 3, 225–237.

Price, R.J., 1973. Glacial and Fluvioglacial Landforms. Longman, London, 242 pp.

Price, R.J., 1982. Changes in the proglacial area of Breiðamerkurjökull, southeastern Iceland: 1890–1980. Jökull 32, 29–35.

Principato, S., 2008. Geomorphic evidence for Holocene glacial advances and sea level fluctuations on eastern Vestfirðir, northwest Iceland. Boreas 37, 132–145.

Punkari, M., 1980. The ice lobes of the Scandinavian ice sheet during the deglaciation in Finland. Boreas 9(4), 307–310.

Putkonen, J., O'Neal, M., 2006. Degradation of unconsolidated Quaternary landforms in the western North America. Geomorphology 75(3), 408–419.

Radić, V., Hock, R., 2011. Regionally differentiated contribution of mountain glaciers and ice caps to future sea-level rise. Nature Geoscience 4(2), 91–94.

Ran, L., Jiang, H., Knudsen, K.L., Eiríksson, J., 2008. A high-resolution Holocene diatom record from the North Icelandic shelf. Boreas 37, 399–413.

Randolph Glacier Inventory, 2014. The Randolph Glacier Inventory Version 4.0 [released on 1st December 2014]. Available at: http://www.glims.org/RGI/.

Rayner, N.A., Brohan, P., Parker, D.E., Folland, C.K., Kennedy, J.J., Vanicek, M., Ansell, T.J., Tett, S.F.B., 2006. Improved Analyses of Changes and Uncertainties in Sea Surface Temperature Measured In Situ since the Mid-Nineteenth Century: The HadSST2 Dataset. Journal of Climate 19, 446–469.

Reinardy, B.T.I., Leighton, I., Marx, P.J., 2013. Glacier thermal regime linked to processes of annual moraine formation at Midtdalsbreen, southern Norway. Boreas 42, 896–911.

Rennen, M., 2004. Cocodat^{i}: Coordinate Conversion and Datum Transformation in Iceland Version 1.3. Online Software - Manual and Technical Reference. Landmælíngar Íslands, Iceland, 28 pp. Available at: http://cocodati.lmi.is/cocodati/cocodati-manual.pdf.

Reverdin, G., 2010. North Atlantic subpolar gyre surface variability (1895–2009). Journal of Climate 23, 4571–4584.

Rignot, E., Velicogna, I., van den Broeke, M.R., Monaghan, A., Lenaerts, J., 2011. Acceleration of the contribution of the Greenland and Antarctic ice sheets to sea level rise. Geophysical Research Letters 38, L05503, DOI: 10.1029/2011GL046583.

Rist, S. 1967–1987. Jöklabreytingar (Glacier variations in metres). Jökull 17, 321–325; 18, 401–405; 20, 83–87; 21, 73–77; 22, 89–95; 23, 61–66; 24, 77–82; 25, 73–79; 26, 69–74; 27, 88–93; 28, 61–65; 31, 37–46; 32, 121–125; 33, 141–144; 34, 173–179; 35, 111–119; 36, 83–90; 37, 85–90.

Roberts, B., Beckett, J.A., Lewis, W.V., Anderson, F.W., Fleming, W.L.S., Falk, P., 1933. The Cambridge Expedition to Vatnajökull, 1932. The Geographical Journal 81(4), 289–308.

Roberts, D.H., Hart, J.K., 2005. The deforming bed characteristics of a stratified till assemblage in north East Anglia, UK: investigating controls on sediment rheology and strain signatures. Quaternary Science Reviews 24, 123–140.

Robertson, A., Mechoso, C., Kim, Y.-J., 2000. The influence of Atlantic sea surface temperature anomalies on the North Atlantic Oscillation. Journal of Climate 13, 122–138.

Robson, J., Sutton, R., Lohmann, K., Smith, D., Palmer, M.D., 2012. Causes of the rapid warming of the North Atlantic Ocean in the mid-1990s. Journal of Climate 25, 4116–4134.

Rogers, J.C., 1984. The Association between the North Atlantic Oscillation and the Southern Oscillation in the Northern Hemisphere. Monthly Weather Review 112, 1999–2015.

Rogerson, R.J., Batterson, M.J., 1982. Contemporary push-moraine formation in the Yoho valley, B.C. In: Davidson-Arnott, R., Nickling, W., Fahey, B.D. (eds.), Research in Glacial, Glacio-Fluvial and Glaciolacustrine Systems. Geobooks, Norwich, pp. 71–90.

Rose, J., Whiteman, C.A., Lee, J., Branch, N.P., Harkness, D.D., Walden, J., 1997. Mid- and late-Holocene vegetation, surface weathering and glaciations, Fjallsjökull, southeast Iceland. The Holocene 7, 457–471.

Rosqvist, G., Østrem, G., 1989. The sensitivity of a small ice-cap to climatic fluctuations. Geografiska Annaler 71A, 99–103.

Rothwell, M.J., Folland, C.K., 2002. Atlantic air–sea interaction and seasonal predictability. Quarterly Journal of the Royal Meteorological Society 128(583), 1413–1443.

Rowntree, P., 1976. Response of the atmosphere to a tropical Atlantic ocean temperature anomaly. Quarterly Journal of the Royal Meteorological Society 102(433), 607–625.

Runemark, H., 1956. Studies in Rhizocarpon, I. Taxonomy of the yellow species in Europe. Opera Botanica 2, 1–152.

Russell, A.J., Knudsen, O., 1999. Controls on the sedimentology of the November 1996 jokulhlaup deposits, Skeidararsandur, Iceland. In: Smith, N.D., Rogers, J., Plint, A.G. (eds.), Advances in Fluvial Sedimentology. International Association of Sedimentologists, Special Publication 28, 315–329.

Ryan, J.C., Hubbard, A.L., Todd, J., Carr, J.R., Box, J.E., Christoffersen, P., Holt, T.O., Snooke, N., 2014. Repeat UAV photogrammetry to assess calving front dynamics at a large outlet glacier draining the Greenland Ice Sheet. The Cryosphere Discussions 8, 2243–2275.

Saemundsson, K., 1979. Outline of the geology of Iceland. Jökull 29, 7–28.

Salinger, M.J., Heine, M.J., Burrows, C.J., 1983. Variations of the Stocking (Te Wae Wae) Glacier, Mount Cook, and climatic relationships. New Zealand Journal of Science 26, 321– 338.

Schomacker, A., 2008. What controls dead-ice melting under different climate conditions? A discussion. Earth-Science Reviews 90(3–4), 103–113.

Schomacker, A., 2010. Expansion of ice-marginal lakes at the Vatnajökull ice cap, Iceland, from 1999 to 2009. Geomorphology 119, 232–236.

Schomacker A., Kjær K.H., 2007. Origin and de-icing of multiple generations of ice-cored moraines at Brúarjökull, Iceland. Boreas 36, 411–425.

Schomacker A., Kjær K.H., 2008. Quantification of dead-ice melting in ice-cored moraines at the high-Arctic glacier Holmströmbreen, Svalbard. Boreas 37, 211–225.

Schomacker, A., Krüger, J., Larsen, G., 2003. An extensive late Holocene glacier advance of Kötlujökull, central south Iceland. Quaternary Science Reviews 22, 1427–1434.

Sharp, M.J., 1982a. Modification of clasts in lodgement tills by glacial erosion. Journal of Glaciology 28, 475–481.

Sharp, M.J., 1982b. A comparison of the landforms and sedimentary sequences produced by surging and non-surging glaciers in Iceland. Unpublished PhD thesis, University of Aberdeen, UK, 598 pp.

Sharp, M.J., 1984. Annual moraine ridges at Skálafellsjökull, southeast Iceland. Journal of Glaciology 30, 82–93.

Sharp, M.J., 1985a. “Crevasse-fill” ridges: a landform type characteristic of surging glaciers? Geografiska Annaler 67A, 213–220.

Sharp, M.J., 1985b. Sedimentation and stratigraphy at Eyjabakkajökull—an Icelandic surging glacier. Quaternary Research 24, 268–284.

Sharp, M.J., 1988. Surging glaciers: geomorphic effects. Progress in Physical Geography 12, 533–559.

Sharp, M.J., Dugmore, A.J., 1985. Holocene glacier fluctuations in eastern Iceland. Zeitschrift für Gletscherkunde und Glazialgeologie 21, 341–349.

Shaw, J., 1977. Sedimentation in an alpine lake during deglaciation, Okanagan Valley, British Columbia, Canada. Geografiska Annaler 59A, 221–240.

Siegel, S., 1956. Non-parametric statistics for the behavioral sciences. McGraw-Hill, New York, 312 pp.

Sigurðsson, O., 1992. Jöklabreytingar 1930–1960, 1960–1990 og 1990–1991. Jökull 42, 81–87.

Sigurðsson, O., 1998. Glacier variations in Iceland 1930–1995: from the database of the Iceland Glaciological Society. Jökull 45, 3–25.

Sigurðsson, O., 2005a. Variations of termini of glaciers in Iceland in recent centuries and their connection with climate. In: Caseldine, C., Russell, A., Harðardóttir, J., Knudsen, Ó. (eds.), Iceland – Modern Processes and Past Environments. Developments in Quaternary Sciences 5, 241–255.

Sigurðsson, O. 2005b. Jöklabreytingar 1930–1960, 1960–1990 og 2003–2004. Jökull 55, 163–170.

Sigurðsson, O., Jónsson, T. 1995. Relation of glacier variations to climate changes in Iceland. Annals of Glaciology 21, 263–270.

Sigurðsson, O., Jónsson, T., Jóhannesson, T., 2007. Relation between glacier-termini variations and summer temperatures in Iceland since 1930. Annals of Glaciology 42, 395–401.

Sigurðsson, O., Sigurðsson, Ó.J., 1998. Afkoma nokkurra jökla á Íslandi 1992–1997. (Mass balance of a number of Icelandic glaciers 1992–1997). Rep. OS-98082 (in Icelandic), National Energy Authority, Reykjavík.

Sigurðsson, O., Thorsteinsson, Th., Ágústsson, S.M., Einarsson, B., 2004. Afkoma Hofsjökuls 1997–2004. (Mass balance of Hofsjökull 1997–2004). Rep. OS-2004/029, National Energy Authority, Reykjavík.

Sigurðsson, O., Williams, R.S., 2008. Geographic names of Icelandic glaciers: historic and modern. US Geological Survey Professional Paper 1746, 225 pp.

Small, D., Rinterknecht, V., Austin, W., Fabel, D., Miguens-Rodriguez, M., Xu, S., 2012. In situ cosmogenic exposure ages from the Isle of Skye, northwest Scotland: implications for the timing of deglaciation and readvance from 15 to 11 ka. Journal of Quaternary Science 27(2), 150–158.

Smith, M.J., Clark, C.D., 2005. Methods and visualization of digital elevation models for landform mapping. Earth Surface Processes and Landforms 30, 885–900.

Snavely, N., 2008. Scene reconstruction and visualization from Internet photo collections. Unpublished PhD thesis, University of Washington, USA.

Snorrason, S., 1984. Myrarjöklar og Vatnsdalur. Unpubl. Cand. Real. thesis. University of Oslo, Norway.

Sodemann, H., Masson-Delmotte, V., Schwierz, C., Vinther, B.M., Wernli, H., 2008. Interannual variability of Greenland winter precipitation sources: 2. Effects of North Atlantic Oscillation variability on stable isotopes in precipitation. Journal of Geophysical Research: Atmospheres 113(D12), DOI: 10.1029/2007JD009416.

Spagnolo, M., Clark, C.D., Ely, J.C., Stokes, C.R., Anderson, J.B., Andreassen, K., Graham, A.G.C., King, E.C., 2014. Size, shape and spatial arrangement of megascale glacial lineations from a large and diverse dataset. Earth Surface Processes and Landforms 39, 1432–1448.

Spagnolo, M., Clark, C.D., Hughes, A.L.C., Dunlop, P., Stokes, C.R., 2010. The planar shape of drumlins. Sedimentary Geology 232, 119–129.

Stefánsson, U., 1969. Sjávarhiti og selta á nokkrum stöðum við strendur landsins á ratuginn 1960–1969. Hafrannsóknir 1969, 9–22.

Stokes, C.R., Shahgedanova, M., Evans, I.S., Popovin, V.V., 2013a. Accelerated loss of alpine glaciers in the Kodar Mountains, south-eastern Siberia. Global and Planetary Change 101, 82–96.

Stokes, C.R., Spagnolo, M., Clark, C.D., O'Cofaigh, C., Lian, O.B., Dunstone, R.B., 2013b. Formation of mega-scale glacial lineations on the Dubawnt Lake Ice Stream bed: 1.

size, shape and spacing from a large remote sensing dataset. Quaternary Science Reviews 77, 190–209.

Storrar, R.D., 2013. Reconstructing subglacial meltwater dynamics from the spatial and temporal variation in the form and pattern of eskers. Unpublished PhD thesis, University of Durham, UK, 256 pp.

Storrar, R.D., Evans, D.J.A., Stokes, C.R., submitted. Controls on the formation of complex esker systems at decadal timescales, Breiðamerkurjökull, SE Iceland. Earth Surface Processes and Landforms.

Storrar, R.D., Stokes, C.R., Evans, D.J.A., 2014. Morphometry and pattern of a large sample (>20,000) of Canadian eskers and implications for subglacial drainage beneath ice sheets. Quaternary Science Reviews 105, 1–25.

Stötter, J., 1990. Beobachtungen und Uberlegungen zur postglazialen Landschaftsgeschichte Islands am Beispiel des Svarfadar-Skídadals. Munchener Geogr. Abh. B8, 83–104.

Stötter, J., 1991. New observations on the postglacial glacier history of Trollaskagi, northern Iceland. In: Maizels, J.K., Caseldine, C.J. (eds.), Environmental Change in Iceland: Past and Present. Kluwer, Dordrecht, pp. 181–192.

Stötter, J., 1994. Changing the Holocene record – A call for International Interdisciplinary co-oporation. Munchener Geogr. Abl. B12, 257–273

Stötter, J., Wastl, M., Caseldine, C., Háberle, T., 1999. Holocene palaeoclimatic reconstruction in northern Iceland: approaches and results. Quaternary Science Reviews 18, 457–474.

Straneo, F., Heimbach, P., 2013. North Atlantic warming and the retreat of Greenland’s outlet glaciers. Nature 504, 36–43.

Sutton, R., Norton, W., Jewson, S., 2000. The North Atlantic Oscillation—what role for the ocean? Atmospheric Science Letters 1(2), 89–100.

Teller, J.T., 2003. Subaquatic Landsystems: Large Proglacial Lakes. In: Evans, D.J.A. (ed.), Glacial Landsystems. Arnold, London, pp. 348–371.

Thomas, R., Frederick, E., Krabill, W., Manizade, S., Martin, C., 2009. Recent changes on Greenland outlet glaciers. Journal of Glaciology 55(189), 147–162.

Thompson, A., 1988. Historical development of the proglacial landforms of Svinafellsjökull and Skaftafellsjökull, southeast Iceland. Jökull 38, 17–30.

Thompson, A., Jones, A., 1986. Rates and causes of proglacial river terrace formation in southeast Iceland: an application of lichenometric dating techniques. Boreas 15, 231–246.

Thordarson, T., Höskuldsson, Á., 2002. Iceland. Classic Geology in Europe 4. Terra Publishing, Edinburgh, 224 pp.

Thórarinsson, S., 1939. Vatnajökull. The scientific results of the Swedish-Icelandic investigations 1936-37-38. Chapter IX. The ice dammed lakes of Iceland with particular reference to their values as indicators of glacier oscillations. Geografiska Annaler 21, 216–242.

Thórarinsson, S., 1943. Oscillations of the Icelandic glaciers in the last 250 years. Geografiska Annaler 25, 1–54.

Thórarinsson, S., 1949. Some tephrochronological contributions to the volcanology and Glaciology of Iceland. Geografska Annaler 21, 239–256.

Thórarinsson, S., 1955. Öskufall svo sporrækt vard og Kötlugosið 1721. Náttúrufrædingurinn 20, 113–133.

Thórarinsson, S., 1956. On the variations of Svínafellsjökull, Skaftafellsjökull and Kvíárjökull in Öræfi. Jökull 6, 1–15.

Thórarinsson, S., 1958. The Öræfajökull eruption of 1362. Acta Naturalia Islandica 2, 1–100.

Thórarinsson, S., 1964. On the age of the terminal moraines of Brúárjökull and Hálsajökull. Jökull 14, 67–75.

Thórarinsson, S., 1966. The age of the maximum postglacial advance of Hagafellsjökull eystri. A tephrochronological study. Jökull 16, 207–210.

Thórarinsson, S., 1967. Washboard moraines in front of Skeiðarárjökull. Jökull 17, 311–312.

Thoroddsen, Þ., 1911. Lýsing Íslands 11 [Description of Iceland II]. Hið íslenska bókmenntafélag, Kaupmannahöfn.

Thoroddsen, Þ., 1931–1935. Lýsing Íslands [Description of Iceland]. Sjóður Þorvaldar Thoroddsen, Reykjavík.

Thoroddsen, Þ., 1958. Ferðabók. Skýrslur og rannsóknir á Íslandi 1882–1898 [Travel Book. Reports and Research from Iceland 1882–1898]. Snæbjörn Jónasson, Reykjavík.

Trouet, V., Esper, J., Graham, N.E., Baker, A., Scourse, J.D., Frank, D.C., 2009. Persistent positive North Atlantic oscillation mode dominated the medieval climate anomaly. Science 324, 78–80.

Trouet, V., Scourse, J.D., Raible, C.C., 2011. North Atlantic storminess and Atlantic meridional overturning circulation during the last millennium: reconciling contradictory proxy records of NAO variability. Global and Planetary Change 84, 48–55.

van der Meer, J.J.M., 1997. Short-lived streamlined bedforms (annual small flutes) formed under clean ice, Turtman Glacier, Switzerland. Sedimentary Geology 111, 107–118.

van der Ween, C.J., 2008. Crevasses on glaciers. Polar Geography 23(3), 213–245.

Visbeck, M., Chassignet, E.P., Curry, R.G., Delworth, T.L., Dickson, R.R., Krahmann, G., 2003. The ocean's response to North Atlantic Oscillation variability. In: Hurrell, J.W., Kushnir, Y., Ottersen, G., Visbeck, M. (eds.), The North Atlantic Oscillation, Climatic Significance and Environmental Impact. AGU Geophysical Monograph 134, pp. 113–146.

Wadell, H., 1920: Vatnajökull. Some studies and observations from the greatest glacial area in Island. Geografiska Annaler 4, 300–323.

Walker, G.P.L., 1964. Geological investigations in eastern Iceland. Bulletin Volcanologique 27(1), 351–63.

Walker, G.T., Bliss, E.W., 1932. World Weather V. Memoirs of the Royal Meteorological Society Vol. IV (36), 53–84.

Walter K., Graf H.F., 2002. On the changing nature of the regional connection between the North Atlantic oscillation and sea surface temperatures. Journal of Geophysical Research: Atmospheres 107(D17), ACL 7-1–ACL 7-13, DOI: 10.1029/2001JD000850.

Wanner, H., Holzhauser, H., Pfister, C., Zumbühl, H., 2000. Interannual to century scale climate variability in the European Alps. Erkunde 54, 62–69.

Warren, C.R., 1991. Terminal environment, topographic control and fluctuations of West Greenland glaciers. Boreas 20(1), 1–15.

Warren, C.R., Hulton, N.R.J., 1990. Topographic and glaciological controls on Holocene ice-sheet margin dynamics, central West Greenland. Annals of Glaciology 14, 307–310.

Watson, G.S., 1961. Goodness-of-fit tests on a circle. Biometrika 48, 109–114.

Welch, R., 1967. The Application of Aerial Photography to the Study of a Glacial Area. Breidamerkur, Iceland. Unpublished PhD thesis, University of Glasgow, UK.

Westoby, M.J., Brasington, J., Glasser, N.F., Hambrey, M.J., Reynolds, J.M., 2012. ‘Structure-from-Motion’ photogrammetry: A low-cost, effective tool for geoscience applications. Geomorphology 179, 300–314.

Whitehead, K., Moorman, B.J., Hugenholtz, C.H., 2013. Brief Communication: Low-cost, ondemand aerial photogrammetry for glaciological measurement. The Cryosphere, 7, 1879–1884.

Williams, R.G., Roussenov, V., Smith, D., Lozier, S., 2014. Decadal evolution of ocean thermal anomalies 1 in the North Atlantic: the effect of Ekman, overturning and horizontal transport. Journal of Climate 27(2), 698–719.

Winkler, S., Chinn, T., Gärtner-Roer, I., Nussbaumer, S.U., Zemp, M., Zumbühl, H.J., 2010. An introduction to mountain glaciers as climate indicators with spatial and temporal diversity. Erdkunde 64, 97–118.

Winkler, S., Elvehøy, H., A. Nesje, A., 2009. Glacier fluctuations of Jostedalsbreen, western Norway, during the past 20 years: The sensitive response to maritime mountains glaciers. The Holocene 19, 395–414.

Worsley, P., 1974. Recent "annual" moraine ridges at Austre Okstindbreen, Okstindan, north Norway. Journal of Glaciology 13(68), 265–277.

Zemp, M., Hoelzle, M., Haerberli, W., 2009. Six decades of glacier mass-balance observations: a review of the worldwide monitoring network. Annals of Glaciology 50(50), 101–111.

Zemp, M., Nussbaumer, S.U., Gärtner-Roer, I., Hoelzle, M., Paul, F. and Haeberli, W. (eds.), 2011. Glacier Mass Balance Bulletin No. 11 (2008-2009). ICSU (WDS) / IUGG (IACS) / UNEP / UNESCO / WMO, World Glacier Monitoring Service, Zurich, Switzerland, 102 pp.

Zemp, M., Nussbaumer, S.U., Naegeli, K., Gärtner-Roer, I., Paul, F., Hoelzle, M. and Haeberli, W. (eds.), 2013. Glacier Mass Balance Bulletin No. 12 (2010-2011). ICSU (WDS) / IUGG (IACS) / UNEP / UNESCO / WMO, World Glacier Monitoring Service, Zurich, Switzerland, 106 pp.

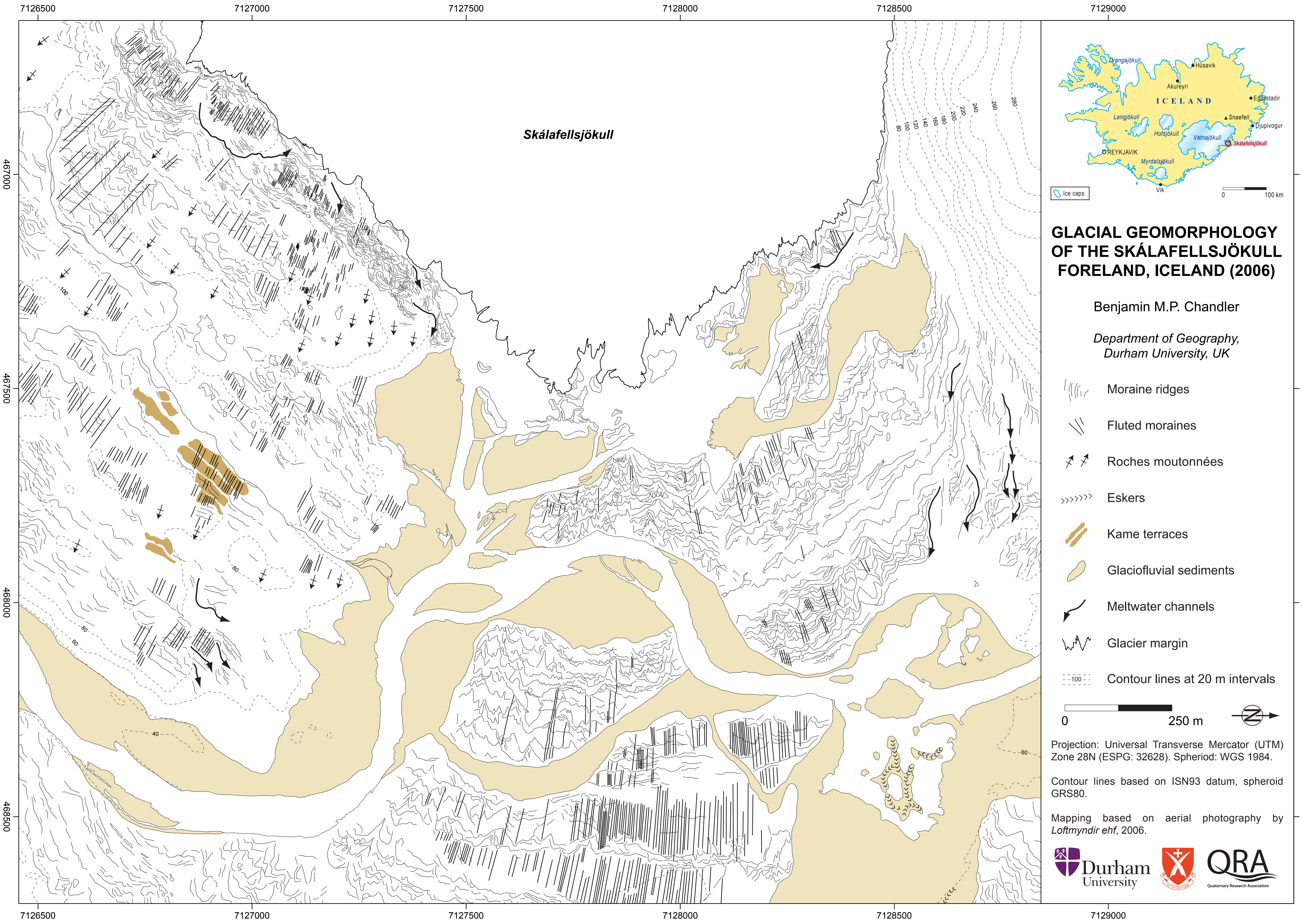

GLACIAL GEOMORPHOLOGY OF THE SKÁLAFELLSJÖKULL FORELAND, ICELAND (2006)

Benjamin M.P. Chandler

Department of Geography,
Durham University, UK

Projection: Universal Transverse Mercator (UTM) Zone 28N (ESPG: 32628). Spheriod: WGS 1984.

Contour lines based on ISN93 datum, spheroid GRS80.

Mapping based on aerial photography by *Loftmyndir ehf*, 2006.

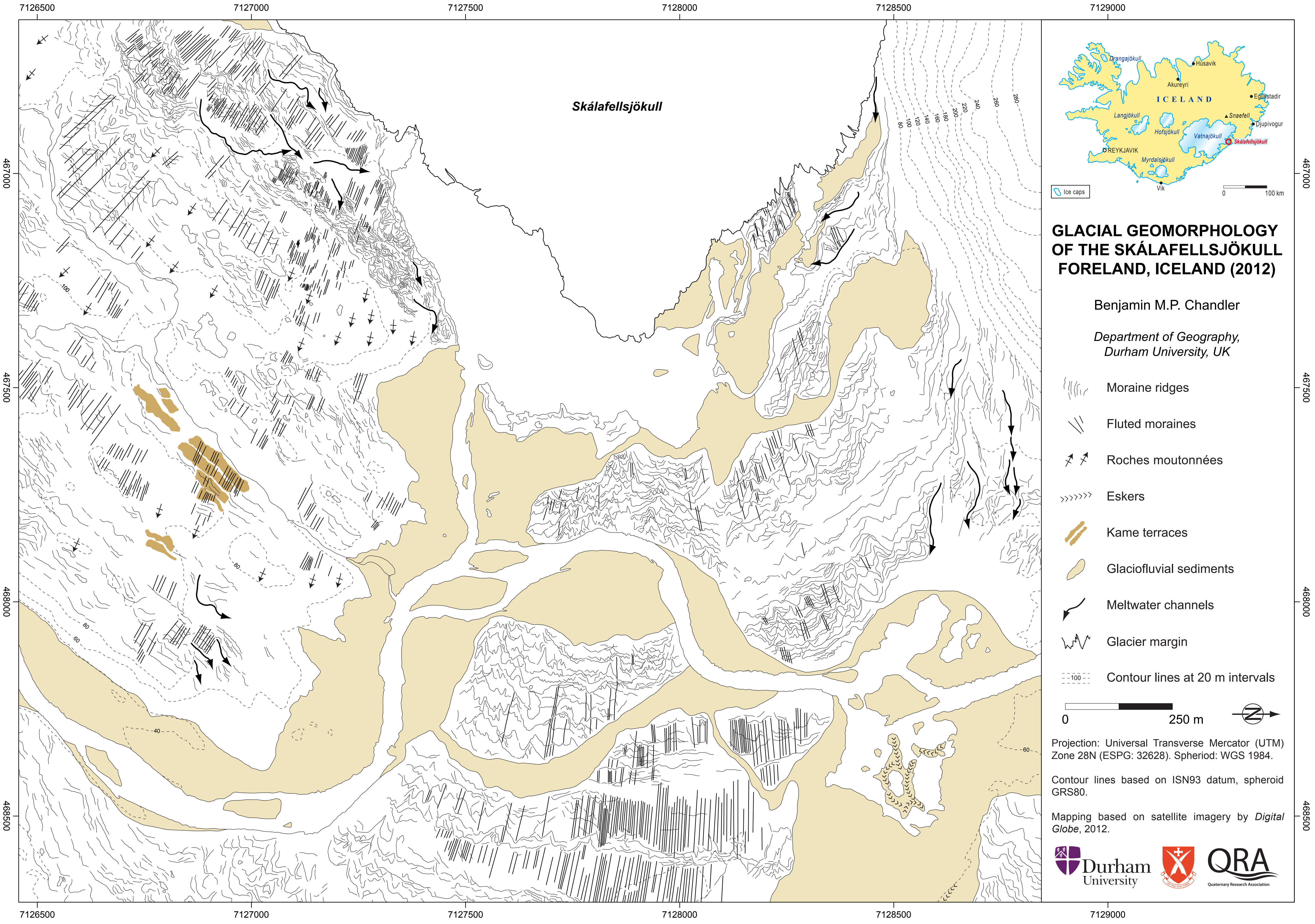

GLACIAL GEOMORPHOLOGY OF THE SKÁLAFELLSJÖKULL FORELAND, ICELAND (2012)

Benjamin M.P. Chandler

Department of Geography,
Durham University, UK

- Moraine ridges
- Fluted moraines
- Roches moutonnées
- Eskers
- Kame terraces
- Glaciofluvial sediments
- Meltwater channels
- Glacier margin
- Contour lines at 20 m intervals

Projection: Universal Transverse Mercator (UTM) Zone 28N (ESPG: 32628). Spheriod: WGS 1984.

Contour lines based on ISN93 datum, spheroid GRS80.

Mapping based on satellite imagery by *Digital Globe*, 2012.